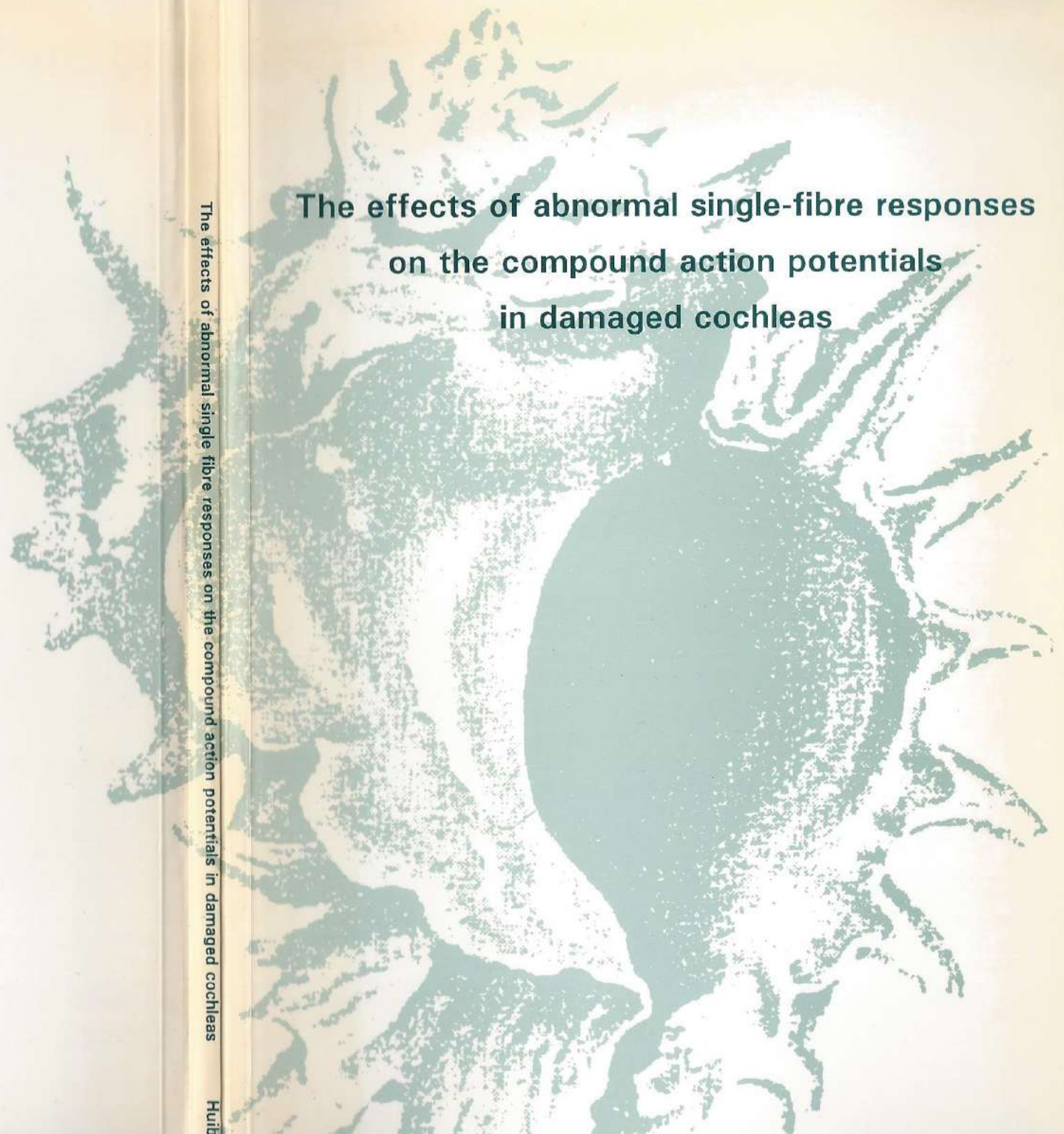


**The effects of abnormal single-fibre responses
on the compound action potentials
in damaged cochleas**

The effects of abnormal single fibre responses on the compound action potentials in damaged cochleas

Hult



THE EFFECTS OF ABNORMAL SINGLE-FIBRE RESPONSES
ON THE COMPOUND ACTION POTENTIAL IN DAMAGED COCHLEAS

Proefschrift
ter verkrijging van de graad van Doctor
aan de Rijksuniversiteit te Leiden,
op gezag van de Rector Magnificus Dr. L. Leertouwer,
hoogleraar in de faculteit der Godgeleerdheid,
volgens besluit van het college van dekanen
te verdedigen op
dinsdag 12 oktober 1993 te klokke 14.15 uur

door

Huibert Versnel

geboren te Waalre in 1962

Promotiecommissie:

Promotores: Prof. dr. P.H. Schmidt
Prof. dr. E. de Boer (Universiteit van Amsterdam)
Co-promotor: Dr. V.F. Prijs
Referent: Prof. dr. J.J. Eggermont (University of Calgary)
Overige leden: Prof. dr. J.J. Grote
Prof. dr. H.A.C. Kamphuisen
Prof. dr. ir. H.P. Wit (Rijksuniversiteit Groningen)

Wie oren heeft om te horen, die hore!
(Marcus 4: 9)

*Voor papa en mama,
m'n ware supporters*

Preface

This Ph.D. thesis on a subject in hearing research is basically a compilation of 5 papers published or submitted to the scientific journal *Hearing Research* and 1 paper published in proceedings of an international symposium. These 6 papers are presented as separate chapters, introduced and concluded by two short additional chapters. The essence of the thesis, reflected in the title, is explained in the first chapter, which includes brief introductions to the hearing organ and electrocochleography. The main results of the research project are reviewed in the final chapter. For the Dutch reader: *Een samenvatting in de Nederlandse taal is toegevoegd. Hierin heb ik geprobeerd, ter wille van degenen die niet thuis zijn in wetenschappelijke verhandelingen, de taal iets eenvoudiger te laten klinken.*

The thesis project was proposed by Vera Prijs, head of the experimental audiology lab of the E.N.T. department of the University Hospital in Leiden, The Netherlands. The project was approved and financially supported by the Netherlands organization for scientific research (N.W.O.) via the Foundation for Biophysics. Other financial support was granted by the Heinsius Houbolt Fund. The E.N.T. department of Prof. dr. P.H. Schmidt and Prof. dr. J.J. Grote provided facilities for the experiments and data analysis. From October 1986 till June 1991, I worked in the audiology lab in Leiden. Finally, a great part of the actual writing of this thesis is done in the Neural Systems Lab of the University of Maryland in College Park, U.S.A. Vera Prijs and Ruurd Schoonhoven were greatly involved in this project, as, among so many other things, in co-authoring the publications. An important role of persistent and patient advisor has been played by Prof. dr. E. de Boer.

At various meetings, including 5 international ones, I have presented data described in this thesis. Furthermore, work forthcoming from this thesis is presented by Ruurd Schoonhoven and Vera Prijs. It is worth mentioning a paper by Ruurd (submitted to J.A.S.A.) which is dedicated to the modelling of single-fibre data, and as such is an extension of Chapter VI, and a paper by Vera (submitted to *Hearing Research*) which describes neural refractory properties on the basis of single-fibre activity taped along with my data collections.

Many colleagues and friends contributed to this thesis, in one way or the other. I am very grateful to them.

Many thanks to Aart, Bart, Pim, and Victor, and to Jan (K.) and Dr. van der Velde; special thanks to Paul, Alan, Bill and Ian; extra thanks to Shihab; and my very special thanks to Friedo, Jan (van #35), Anne, and Gavin.

Huib

Contents

<i>Preface</i>		5
Chapter I	General introduction	9
Chapter II	Single-fibre responses to clicks in relationship to the compound action potential in the guinea pig. Co-authors: Vera Prijs and Ruurd Schoonhoven. Hearing Research 46: 147-160 (1990).	21
Chapter III	Single-fibre and whole-nerve responses to clicks as a function of sound intensity in the guinea pig. Co-authors: Ruurd Schoonhoven and Vera Prijs. Hearing Research 59: 138-156 (1992).	37
Chapter IV	Round-window recorded potential of single-fibre discharge (unit response) in normal and noise-damaged cochleas. Co-authors: Vera Prijs and Ruurd Schoonhoven. Hearing Research 59: 157-170 (1992).	57
Chapter V	Click responses in noise-damaged guinea-pig cochleas. I. Abnormal single-fibre responses. Co-authors: Vera Prijs and Ruurd Schoonhoven. Submitted to Hearing Research (1993).	73
Chapter VI	Aberrant temporal discharge patterns in noise-damaged guinea-pig cochleas. Co-authors: Ruurd Schoonhoven and Vera Prijs. In: Y. Cazals, L. Demany and K.C. Horner (Eds.), Auditory Physiology and Perception, Advances in the Biosciences, Pergamon Press, Oxford, Vol. 83: 607-615 (1992).	105
Chapter VII	Click responses in noise-damaged guinea-pig cochleas. II. Sensorineural causes of deviations in the compound action potential. Co-authors: Vera Prijs and Ruurd Schoonhoven. Submitted to Hearing Research (1993).	115
Chapter VIII	Summary and conclusions.	149
Samenvatting		155
Curriculum vitae		164

Chapter I

General introduction

Electrocochleography, the recording of evoked potentials from a site close to the cochlea or auditory nerve, provides an opportunity to assess the physiological condition of the cochlea. This technique has been developed with respect to clinical use by Yoshie et al. (1967) and Portmann et al. (1967). The main component in the recorded cochlear potentials is the compound action potential (CAP). The interpretation of this waveform is mainly based on large sets of phenomenological data in man and animal. In order to refine the analysis of the CAP many studies have been done involving modelling of CAPs using response characteristics of single auditory-nerve fibres as have been observed in experimental studies in animals. Little work has been done on modelling CAPs in pathological cochleas.

This thesis presents a study of single-fibre discharge patterns underlying abnormal CAPs in pathological cochleas. We recorded simultaneously the single-fibre responses and CAPs in normal as well as in acoustically traumatized guinea pigs. For analysis we developed a phenomenological CAP model which was fully based on single-fibre data from one species (guinea pig). This PhD work is done at the ENT department in Leiden, The Netherlands, where electrocochleography (ECoG) was clinically applied since 1971 (Eggermont et al., 1974). This thesis can be considered a follow-up of PhD work by Eggermont (1972) and Prijs (1980).

The following sections give brief overviews of the morphology and physiology of the cochlea, and of the technique of electrocochleography. Subsequently, CAPs are discussed in the context of damaged cochleas.

Cochlea and auditory nerve

First, we give a brief introduction on a very delicate and complicated system which challenged scientists of different backgrounds (physics, biology, electro engineering, medicine), the cochlea. After sound enters the cochlea via outer ear canal, tympanic membrane and middle-ear ossicles, the cochlea transfers the mechanical vibrations to electro-chemical activity of the nerve, i.e. the generation and propagation of action potentials along the fibres. The various aspects of sound (frequency spectrum, intensity) are encoded by a distribution of action potentials over the fibre population of the nerve and over time.

Figure 1A shows the basic anatomy of the cochlea and surrounding structures of

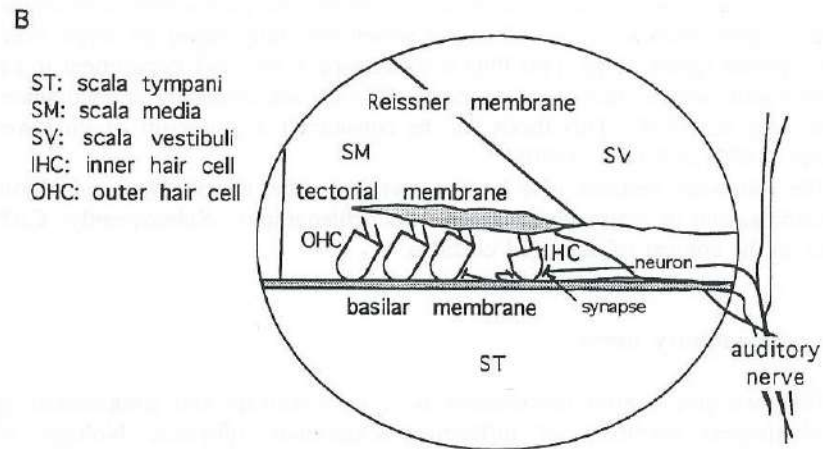
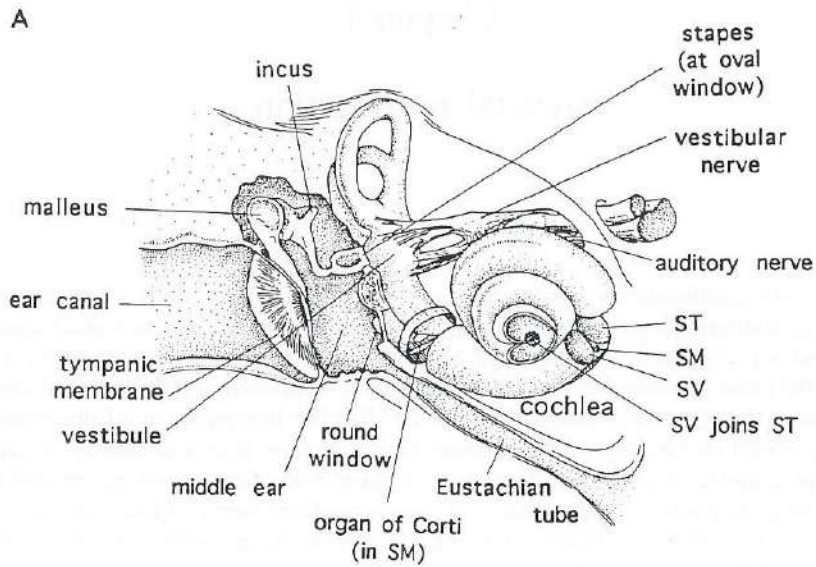


Fig. 1. (A) The cochlea and surrounding structures of the ear (from W.A. Yost and D.W. Nielsen, *Fundamentals of hearing*, Holt Rinehart and Winston, New York, 1985). (B) Schematic drawing of cross section of the cochlear canal showing the most relevant structures.

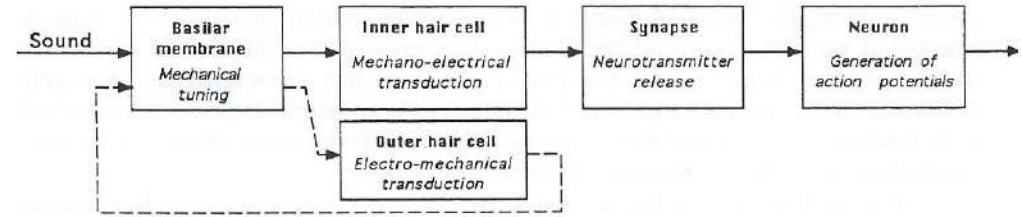


Fig. 2. Block diagram of cochlea showing transducer functions in various cochlear structures.

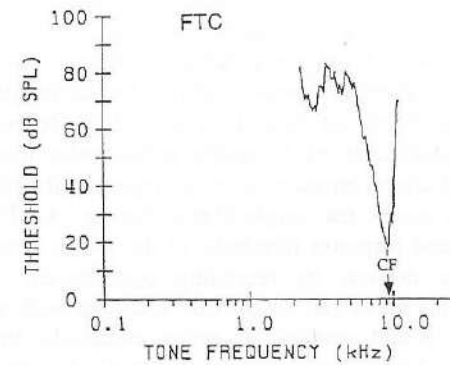


Fig. 3. Example of frequency threshold curve (FTC) recorded from a single fibre. In our experiments the FTC is determined with a threshold tracking algorithm, sweeping frequencies from high to low, and using a threshold criterion of an increase of typically 1 spike above spontaneous discharge rate per tone burst of 50 ms duration. In this example the CF is 9.2 kHz and the minimum threshold is 18 dB SPL.

the ear. The cochlea resembles a coiled tube and has 2.5 (human) to 4 windings (guinea pig). In a cross section of the cochlear canal, as schematically presented in Fig. 1B, the relevant structures can be distinguished. The cochlea has three compartments which are filled with lymph and separated by Reissner's membrane and basilar membrane. The sensory system, the organ of Corti, is located on the basilar membrane. A large dc potential is maintained, like a battery, across the apical pole of the hair cell where the cilia are located. Two types of hair cells are distinguished, inner and outer hair cells (IHCs and OHCs, respectively), which differ distinctly in morphological respect as well as in function. The vast majority of the total 40,000 afferent nerve fibres (which carry information to the brain) innervate the inner hair cells.

The block diagram in Fig. 2 reflects a model view of the cochlea with its various structures as links in a transduction chain. The first link is the basilar membrane which vibrates in response to stapes oscillation. The basilar membrane is tonotopically organized: basal locations are sensitive to high sound frequencies, the apical part responds best to low frequencies. Vibration of basilar and tectorial membrane and lymph triggers displacement of the cilia of the hair cells. Subsequently, this cilia motion induces opening (and closing) of ion channels, and, thus, a change in membrane conductivity, which leads to a change in electric potential inside the hair cells, which in turn gives rise to release of synaptic neurotransmitter. Finally, at the nerve fibre terminals across the synapse, action potentials are generated. The role of IHCs in the transduction chain can be considered as a pure mechano-electrical one, the OHCs are believed to act as electro motors which give positive mechanical feedback in order to increase detection sensitivity and quality of frequency tuning.

Response behaviour of the auditory nerve reflects cochlear (dys)functioning. For instance, the frequency tuning of given locations along the basilar membrane is reflected by the tuning of auditory-nerve fibres (cf. Sellick et al., 1982). Responses from fibres can be measured in animal experiments by recording action potentials of single fibres with micro electrodes. Figure 3 shows an example of a frequency threshold curve (FTC) which is usually measured to assess the single-fibre's tuning. An FTC provides the characteristic frequency (CF) and response threshold of the fibre. Temporal patterns of single-fibre responses can be derived by recording poststimulus time histograms (PSTHs). Also, the activity of the nerve can be globally recorded with a macro electrode close to the nerve, e.g. at the round window. If action potentials are simultaneously evoked in a sufficient number of fibres the resulting potential change at the site of the electrode is measurable; and it is termed the compound action potential (CAP). The method to record the CAP is known as electrocochleography (ECoG), and can be applied both in animals and man. In the next section we will address the CAP in mathematical terms.

An illustrated summary of above described cochlear anatomy and physiological recording methods is presented in Fig. 4.

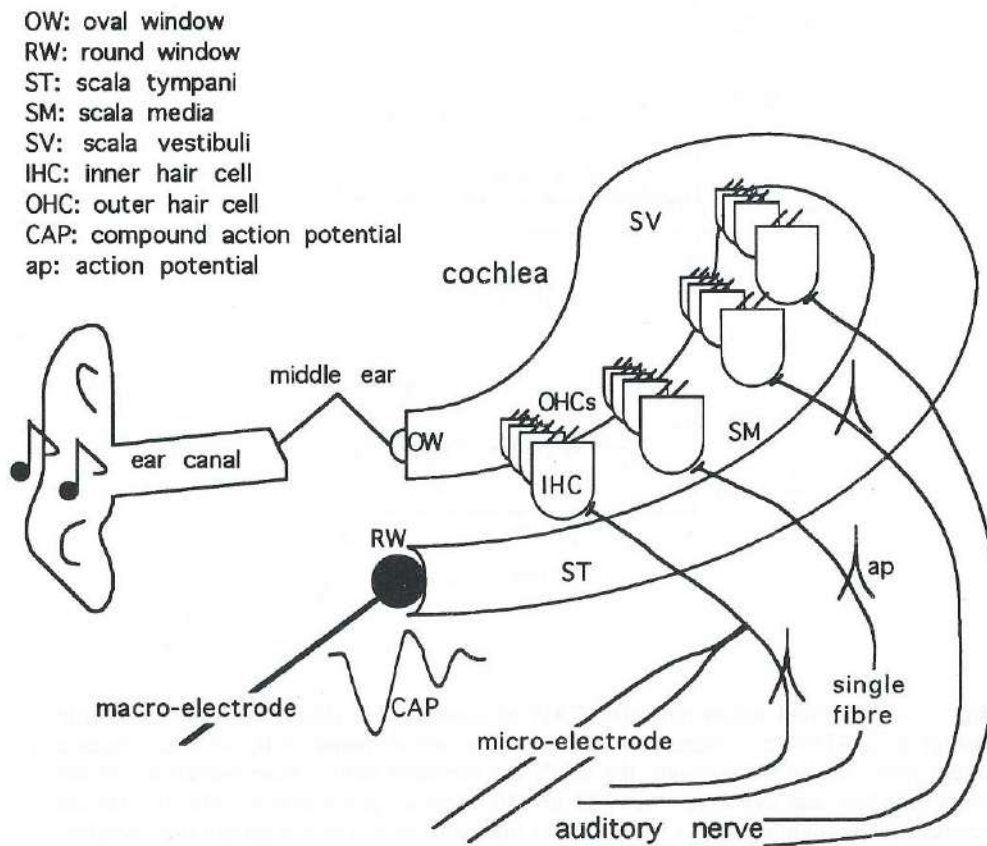


Fig. 4. Schematic view of cochlea in uncoiled configuration with electrode positions. The single-fibre action potentials are recorded with glass micropipette filled with a conductive medium, the CAPs are recorded with silver wire electrode.

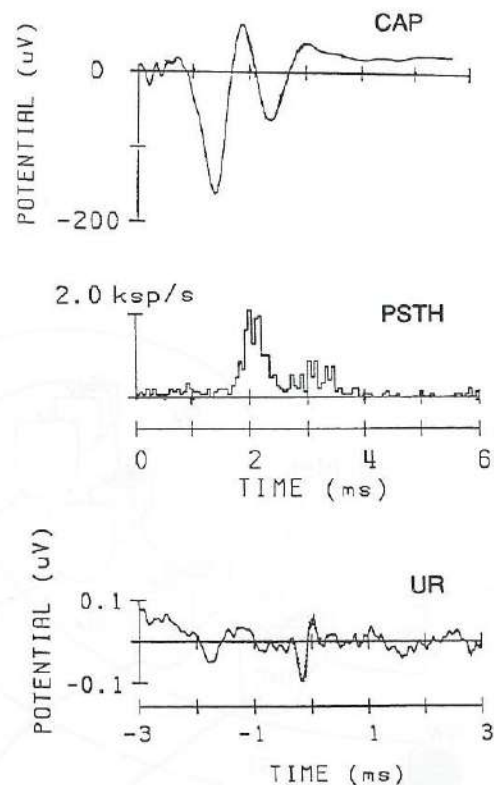


Fig. 5. A compound action potential (CAP) to condensation clicks, a poststimulus time histogram (PSTH) to condensation clicks and a unit response (UR) recorded from a single fibre. In our experiments the CAPs are recorded with a macro-electrode at the round window and averaged over 128 or 256 stimulus presentations. The PSTHs are determined by counting spikes in small time intervals (60 μ s) over a certain time window (6 or 12 ms) directly after the stimulus presentation. Typically, 256 iterations are applied and the total spike count fairly represents the discharge probability function of the fibre. The PSTH is normalized to a density function by dividing the spike count per bin by the number of iterations and by the bin width. The UR is the round window recorded potential which results from a single action potential. It is measured by the method of spike-triggered averaging, i.e., the spike recorded with the micro-electrode functions as a trigger for averaging of the round-window signal recorded with the macro-electrode.

Compound action potential in mathematical description

The CAP represents the summation of electric potential variations at an extra-cochlear recording site resulting from discharges of individual nerve fibres responding to an acoustic stimulus. The relationship between the CAP and the underlying single-fibre responses is expressed by a theorem of Goldstein and Kiang (1958) which has formed a basis for CAP modelling (e.g. de Boer, 1975; Elberling, 1976; Wang, 1979; Bappert et al., 1980; Dolan et al., 1983). The CAP is considered the convolution of the sum of discharge probability densities of the single fibres with the unit response (UR), the latter being the potential at the CAP-recording site that is induced by a fibre discharge. The discharge probabilities are usually estimated on the basis of PSTHs. Figure 5 shows examples of a CAP and PSTH to a click stimulus, and a UR that is experimentally derived by spike-triggered averaging. Since action potentials are basically equal for all auditory-nerve fibres the UR is expected not to vary significantly across fibres, which is indicated by a few known experiments (Kiang et al., 1976; Wang, 1979; Prijs, 1986). The UR is an entity independent of the stimulus. The PSTH varies across fibres and depends on the stimulus. The convolution formula of the CAP can be put as follows:

$$C(t) = \int_{-\infty}^t \left\{ \sum_{i=1}^N p_i(\tau) \right\} U(t-\tau) d\tau \quad (1)$$

in which N is the number of fibres, $C(t)$ is the CAP, $p_i(t)$ the discharge probability of the i^{th} fibre, and $U(t)$ the UR. The expression in Eqn. (1) holds under conditions that UR is identical across fibres, that discharges of the individual fibres are mutually independent and that the single-fibre contributions add linearly.

Damaged cochleas

Electrocochleography is applied for diagnosis of hearing disorders since CAPs recorded from pathological ears reveal significant deviations from normal. Phenomenological relationships are found between deviations in CAPs and specific pathologies which are usually of cochlear origin (Eggermont, 1976). However, these relations are obscured by large statistical interindividual variations and they are not always well understood. Model analysis of abnormal CAPs with use of the convolution equation have rarely been done. After applying such a model Elberling and Salomon (1976) could predict click evoked CAPs for various types of abnormal tone audiograms. However, their assumptions on UR and especially on PSTHs of fibres in hearing loss areas were indirectly based on experimental data without any evidence for their accuracy. Since then much more has become known about the auditory physiology in cochlear pathology. Very recently, cochlear modelling is being applied to pathology,

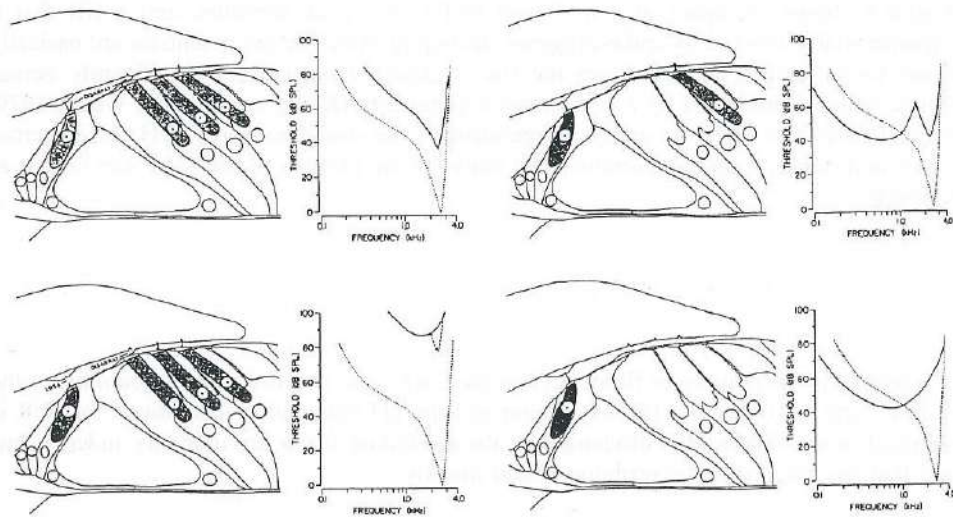


Fig. 6. Scheme by Liberman and Dodds (Fig. 14; 1984) based on their combined morphological and physiological experiments in cats. The plots show cross sections of the cochlea with four different stages of hair cell damage and the corresponding type of abnormal FTC. Upper left: disarray of cilia in inner hair cell (IHC) and outer hair cell (OHC). Upper right: Partial loss of OHCs. Bottom left: loss of IHC cilia, disarray of OHC cilia. Bottom right: total loss of OHCs. The dotted line in the FTC plots represents the normal tuning curve.

which can offer a better understanding of cochlear dysfunction.

In cochlear pathology most commonly the hair cells are damaged, and early damage of hair cells is usually at the cilia. Such lesions will affect the transduction process in the hair cell, and consequently (cf. Fig. 2), the responses of auditory-nerve fibres. Phenomenological indications for direct relationships between different hair cell lesions and tuning and sensitivity of nerve fibres were given by Liberman and Dodds (1984). Figure 6 shows a schematic plot by these authors in which they associate various stages of hair cell lesions with various abnormal types of single-fibre FTCs. Globally, their findings are supported (e.g. Schmiedt et al., 1980; Geisler, 1991; Patuzzi, 1992) and can be described as follows. In the case of damage to IHCs, the functional effects vary from threshold elevation to complete non-responding. In the case of OHC damage, sensitivity and frequency tuning are affected (usually deteriorated).

Evidently, CAPs will change if a group of fibres has elevated response thresholds (at low stimulus levels: effectively a change of N in Eqn. (1)). Also changes in temporal response patterns of single fibres might occur at high stimulus levels and especially in those cases where the tuning is affected. Some examples of such changes are found by Salvi et al. (1979). Such changes, in addition to threshold elevations, might have a large impact on CAPs (change of $p_1(t)$ in Eqn. (1)).

Preview of thesis

The goal of the experimental research discussed in this thesis is to provide a basis for interpretation of CAPs recorded in abnormal cochleas in terms of single-fibre responses. Several questions will be addressed. First, how are click PSTHs of single fibres from hearing loss regions in abnormal cochleas affected, and are their abnormal features related to abnormal FTCs? If abnormal FTCs are uniquely reflected by abnormal click PSTHs these might be associated to specific types of morphological damage. Second, does the UR significantly change as a result of cochlear damage? If not, then interpretation of CAPs is simplified and deviations in CAPs can be ascribed only to changes in PSTHs (in $p_1(t)$ in Eqn. (1)). Third, are CAP deviations only determined by a reduction of contributions as given by threshold elevations and if not, to what extent are abnormal single-fibre responses also responsible for deviations in CAPs? Finally, we examine in view of diagnosis purposes whether it is possible to derive from click CAPs the response properties at the single-fibre level.

These questions are addressed in the following experiments. Single-fibre responses, represented by PSTHs, and CAPs at the round window were simultaneously recorded in normal as well as in acoustically traumatized guinea pigs. The acoustic stimuli were condensation and rarefaction clicks of various intensities. Furthermore, in the same animals we determined the spike-triggered average of the round-window potential as an accurate estimate of the UR. Two sorts of model analysis were applied on the experimental data. Simulations of different abnormal types of abnormal FTCs and click PSTHs were performed using a theoretical model of the cochlea. This cochlear

model, developed by co-workers and in upgraded version published in Schoonhoven et al. (—), considers the cochlea as a unidirectional sequence of four transducers as schematically represented in Fig. 2. Furthermore, a phenomenological CAP model is developed following the convolution theorem as given in Eqn. (1). Here, $p_i(t)$ is described according to the recorded click PSTHs as a function of fibres variables CF and spontaneous discharge rate (SR) and click stimulus variables level (L) and polarity (m). A model waveform for $U(t)$ was based on an average of experimentally found URs. The CAP modelling was applied to both normal and pathological cochleas.

Chapters II and III provide a normal reference of click PSTHs and click CAPs. A preliminary version of the empirical CAP model is presented for normal cochleas. Chapter IV presents UR recordings in normal and noise-traumatized cochleas. A generalized UR is proposed for CAP model purposes. Chapter V describes click PSTHs in fibres with various types of abnormal FTCs. Chapter VI is dedicated to cochlear model analysis of some striking examples of abnormal PSTHs. Finally, chapter VII gives a single-fibre based analysis of click CAPs for different types of abnormal threshold audiograms. The CAP model is adapted to abnormal cochleas and is as such based on click PSTHs described in chapter V and on the UR discussed in chapter IV.

References

- Bappert, E., Hoke, M., Lütkenhöner, B. and Niestroj, B. (1980) Intensity dependence of the compound action potential and the deconvolution technique. In: M. Hoke, G. Kaufmann and E. Bappert (Eds.), *Scand. Audiol. Suppl.* 11, 45-58.
- de Boer, E. (1975) Synthetic whole-nerve action potentials for the cat. *J. Acoust. Soc. Am.* 58, 1030-1045.
- Dolan, D. F., Teas, D. C. and Walton, J. P. (1983) Relation between discharges in auditory nerve fibres and the whole-nerve response shown by forward masking: an empirical model for the AP. *J. Acoust. Soc. Am.* 73, 580-591.
- Eggermont, J.J. (1972) Tijdsafhankelijke eigenschappen van cochleaire actiepotentialen bij de cavia. Ph. D. thesis, University of Leiden.
- Eggermont, J.J. (1976) Electrocochleography. In: W.D. Keidel and W.D. Neff (Eds.), *Handbook of sensory physiology*, Springer Verlag, Berlin, Heidelberg, New York, Vol. V, pp. 626-705.
- Eggermont, J.J., Odenthal, D.W., Schmidt, P.H. and Spoor, A. (1974) Electrocochleography, basic principles and clinical application. *Acta Oto-Laryngol. Suppl.* 316.
- Elberling, C. (1976) Simulation of cochlear action potentials recorded from the ear canal in man. In: R. Ruben, C. Elberling and G. Salomon (Eds.), *Electrocochleography*, University Park Press, Baltimore, pp. 151-168.
- Elberling, C. and Salomon, G. (1976) Action potentials from pathological ears compared to potentials generated by a computer model. In: R. Ruben, C. Elberling and G. Salomon (Eds.), *Electrocochleography*. University Park Press, Baltimore, pp. 439-455.
- Geisler, C.D. (1991) A cochlear model using feedback from motile outer hair cells. *Hear. Res.* 54, 105-117.
- Goldstein, M.H. and Kiang N.Y.S. (1958) Synchrony of neural activity in electric responses evoked by transient acoustic stimuli. *J. Acoust. Soc. Am.* 30, 107-114.
- Kiang, N.Y.S., Moxon, E.C. and Kahn, A.R. (1976) The relationship of gross potentials recorded from the cochlea to single unit activity in the auditory nerve. In: R.J. Ruben, C. Elberling and G. Salomon (Eds.), *Electrocochleography*, University Park Press, Baltimore, pp. 95-115.
- Lieberman, M.C. and Dodds, L.W. (1984) Single-neuron labeling and chronic cochlear pathology. III. Stereocilia damage and alterations of threshold tuning curves. *Hear. Res.* 16, 55-74.
- Patuzzi, R.B. (1992) Effect of noise on auditory nerve responses. In: A.L. Dancer, D. Henderson, R.J. Salvi and R.P. Hamernik (Eds.), *Noise-induced hearing loss*, Mosby Year Book, StLouis, pp 45-59.
- Portmann, M., Le Bert, G. and Aran, J.-M. (1967) Potentiels cochléaires obtenus chez l'homme en dehors de toute intervention chirurgicale. *Rev. de Laryng. (Bordeaux)* 88, 157-164.
- Prijs, V.F. (1980) The single-fibre representation in the compound action potential of the auditory nerve. Ph.D. thesis, University of Nijmegen.
- Prijs, V.F. (1986) Single-unit response at the round window of the guinea pig. *Hear. Res.* 21, 127-133.
- Salvi, R.J., Henderson, D. and Hamernik, R.P. (1979) Single auditory nerve fiber and action potential latencies in normal and noise-treated chinchillas. *Hear. Res.* 1, 237-251.
- Schmiedt, R.A., Zwislocki, J.J. and Hamernik, R.P. (1980) Effects of hair cell lesions on responses of cochlear nerve fibers. I. Lesions, tuning curves, two-tone inhibition, and responses to trapezoidal-wave patterns. *J. Neurophysiol.* 43, 1367-1389.
- Schoonhoven, R., Keijzer, J., Versnel H. and Prijs, V.F. (—) A dual resonance model describing single-fiber responses to clicks in the normal and noise-damaged cochlea. Submitted to *J. Acoust. Soc. Am.*
- Sellick, P. M., Patuzzi, R. B. and Johnstone, B. M. (1982) Measurement of basilar membrane motion in the guinea pig using the Mössbauer technique. *J. Acoust. Soc. Am.* 72, 131-141.
- Wang, B. (1979) The relation between the compound action potential and unit discharges in the auditory nerve. Doctoral dissertation, Dept. of Electrical Engineering and computer sciences, M.I.T.
- Yoshie, N., Ohashi, T. and Suzuki, T. (1967) Nonsurgical recording of auditory nerve action potentials in man. *Laryngoscope* 77, 76-85.

Chapter II

Single-fibre responses to clicks in relationship to the compound action potential in the guinea pig

Huib Versnel, Vera F. Prijs and Ruurd Schoonhoven

Summary

Poststimulus time histograms (PSTHs) to clicks of standard level were measured in eighth-nerve fibres of normal-hearing guinea pigs. In the context of studying the fibres' contribution to the compound action potential (CAP), the PSTHs are described with the parameters latency (t_p), amplitude (A_p) and synchronization (S_p) of the dominant PSTH peak. These parameters are considered in relation to characteristic frequency (CF) and spontaneous rate (SR). An adequate description for t_p is one in which t_p is constant for non-phase-locking fibres (CF above 3 kHz) and it is an exponential function of CF for phase-following fibres. The low-SR fibres (SR below 5 spikes/s) had smaller amplitudes and longer latencies than the other ones. The variations of A_p with CF can be explained by the varying synchronization of the response.

Key words: Poststimulus time histogram; Click; Characteristic frequency; Spontaneous rate; Compound action potential; Guinea pig.

This chapter has been published in *Hearing Research*, 46: 147-160 (1990). Preliminary results were presented at the XXVth Workshop on Inner Ear Biology, London, September 1988.

Single-fibre responses to clicks in relationship to the compound action potential in the guinea pig *

Huib Versnel, Vera F. Prijs and Ruurd Schoonhoven

ENT Department, University Hospital, Leiden, The Netherlands

(Received 2 September 1989; accepted 17 January 1990)

Poststimulus time histograms (PSTHs) to clicks of standard level were measured in eighth-nerve fibres of normal-hearing guinea pigs. In the context of studying the fibres' contribution to the compound action potential (CAP), the PSTHs are described with the parameters latency (t_p), amplitude (A_p) and synchronization (S_p) of the dominant PSTH peak. These parameters are considered in relation to characteristic frequency (CF) and spontaneous rate (SR). An adequate description for t_p is one in which t_p is constant for non-phase-locking fibres (CF above 3 kHz) and it is an exponential function of CF for phase-following fibres. The low-SR fibres (SR below 5 spikes/s) had smaller amplitudes and longer latencies than the other ones. The variations of A_p with CF can be explained by the varying synchronization of the response.

Poststimulus time histogram; Click; Characteristic frequency; Spontaneous rate; Compound action potential; Guinea pig

Introduction

The compound action potential (CAP) recorded by electrocochleography gives useful information for the assessment of cochlear condition. The interpretation of the CAP is mainly based on clinical experiments (Eggermont, 1976) and on single-fibre measurements in normal and pathological cochleas (e.g. Kiang et al. (1976a) and Harrison and Prijs (1984)). Since single-fibre responses give information about the local cochlear transduction process, the translation of the CAP in terms of cochlear functioning can be obtained from the single-fibre responses and their relation-

ship with the CAP. For examination of that relationship, simultaneous measurements of both responses, as performed e.g. in cats by Antoli-Candela and Kiang (1978), Wang (1979) and Dolan et al. (1983), are required.

The fibre responses to a stimulus can be characterized by poststimulus time histograms (PSTHs) which are estimates of discharge probability density functions. As introduced by Goldstein and Kiang (1958), the CAP can be written by a convolution as:

$$C(t) = \sum_{i=1}^N \int_{-\infty}^t p_i(\tau) U_i(t-\tau) d\tau \quad (1)$$

in which N is the number of fibres, $C(t)$ is the CAP, $p_i(t)$ the discharge probability density function of the i^{th} fibre, and $U_i(t)$ the unit response (UR) of the i^{th} fibre at the CAP-recording site. On the basis of this mathematical concept many studies have been made to understand the relative contribution of the fibres to the CAP (see e.g. de Boer, 1975; Kiang et al., 1976b; Elberling, 1976a; Wang, 1979; Prijs, 1980; Charlet de Sauvage et al., 1987). However, several manifestations of the CAP

are still to be clarified, in particular those concerning abnormal cochleas.

Our final goal is to explain the CAP for pathological cochleas on the basis of the fibres' contributions. We started our study in normal hearing subjects and performed simultaneous measurements of PSTHs and CAPs. We also determined URs in the same preparations.

Reports on measurements of the UR at the round window (Kiang et al., 1976b; Prijs, 1986) lead to the assumption that in normal hearing condition the UR is equal for all fibres in one individual animal. Then, the relation between whole-nerve and single-fibre responses can be expressed as (Elberling, 1976b):

$$C(t) = \int_{-\infty}^t \left\{ \sum_{i=1}^N P_i(\tau) \right\} U(t-\tau) d\tau \quad (2)$$

with $P_i(t)$ the PSTH of the i^{th} fibre and $U(t)$ the universal UR. Once the UR is known, modelling the CAP reduces to modelling PSTHs of all fibres. In this report we describe measured PSTHs in relation to various fibre properties. For simplification we focus our attention on click stimuli at a fixed intensity. This leaves polarity as the only stimulus variable. As already reported by Peake and Kiang (1962), condensation and rarefaction clicks evoke different nerve responses (except at low intensities).

We characterize fibre properties by characteristic frequency (CF) and spontaneous discharge rate (SR). The CF reflects the location along the length of the cochlea. As a consequence, the latency of the click response decreases with increasing CF (e.g. Kiang et al., 1965; Evans, 1972). SR is correlated with morphological properties of the fibre and its corresponding synapse (Lieberman, 1982; Liberman and Oliver, 1984). It has been reported that magnitude and latency of the click response vary systematically with SR (Antoli-Candela and Kiang, 1978; Wang, 1979), which could be attributed to the sensitivity that is found to be related to the SR (Lieberman, 1978).

PSTH parameters

As parameters of the measured PSTH we take the latency, the amplitude and the degree of syn-

chronization of the dominant peak, to be denoted by t_p , A_p and S_p , respectively. (The latency is determined at the top of the peak.) These parameters are presumed to be the most important ones with respect to the description of the fibres' contributions to the CAP.

For analysis of t_p we make the following assumptions. Three main processes in the cochlea contribute to the latency of the fibre's response: cochlear mechanics causes a CF-related delay; the synaptic mechanisms cause an SR-related delay; and there is a neural conduction time which is in first approximation equal for all fibres. In this context t_p can be written as:

$$t_p(f_c, r_s) = t_1(f_c) + t_2(r_s) \quad (3)$$

with f_c and r_s representing characteristic frequency (CF) and spontaneous rate (SR), respectively. The neural conduction time is included in the second term.

The amplitude is defined as the ratio of the average number of spikes per stimulus presentation and the bin width (and thus, A_p is expressed in spikes/s). In order to derive a measure of synchronization and to analyse A_p , we consider the average number of discharges per stimulus presentation which occur over the period of the dominant peak, to be denoted by p_p (p_p actually is the area of the PSTH peak; it is expressed in spikes). We define the synchronization index of the click response (S_p) as the ratio of A_p and p_p so that

$$A_p = S_p p_p \quad (4)$$

This equation shows that A_p is determined by two quantities, of which S_p reflects the inverse of the PSTH-peak width.

Methods

The experiments were performed in 12 healthy female albino guinea pigs weighing 200-800 g. Premedications were atropine sulphate (25 μ g/kg) and Thalamonal (1.6 cc/kg). Anaesthesia was obtained with Nembutal^R (27 mg/kg), and was maintained during the experiment by adding doses of Thalamonal (or Fentanyl) and Nembutal (about each hour 100% and 10%, respectively). A

* Preliminary results were presented at the XXVth Workshop on Inner Ear Biology, London, September 1988.

Abbreviations: C(t): compound action potential (CAP); N_1 : first peak of CAP; P(t): poststimulus time histogram (PSTH); U(t): unit response (UR); t_p : latency of PSTH peak; A_p : amplitude of PSTH peak; S_p : synchronization of PSTH peak; p_p : total peak rate; r_s : spontaneous rate (SR); f_c : characteristic frequency (CF).

Correspondence to: H. Versnel, ENT Department, University Hospital, P.O. Box 9600, 2300 RC Leiden, The Netherlands.

tracheotomy was performed and body temperature was maintained at 37–38°C by means of a heating pad (Searle Instruments). A silver ball electrode was positioned at the round window and sealed into the bulla. The cochlear nerve was approached as described by Evans (1979). The single-fibre recordings were made with (mostly beveled) glass micropipettes filled with 2.7 M KCl or 0.5 M KCl/0.1 M Tris buffer (in situ resistance 15–30 MΩ and 30–60 MΩ, respectively). Advance of the microelectrode (minimal steps of 2–3 μm) was controlled by a home-made hydraulic micro-manipulator.

Sound was presented by a dynamic earphone (Standard Telephones and Cables 4026A) to the animal in a sound-proof room. The sound pressure level at the ear canal was measured by means of a half-inch condenser microphone (Brüel and Kjaer 4134) via a narrow tube. The frequency characteristic of the earphone was flat within 10 dB up to 10 kHz, where it fell off at a rate of about 50 dB/octave. Frequency and intensity of the stimuli were controlled by a DEC PDP 11/10 computer connected to an oscillator (Krohn-Hite 4140R) and a set of programmable attenuators (Grason Stadler model 1284). The threshold audiogram of the averaged CAP was determined using tone bursts with 4 ms plateaux and 2 cycles of rise-fall time. For click stimuli, rectangular pulses of 100 μs were delivered by a pulse generator (Devices type 2521) at an interstimulus interval of 128 ms. The spectrum of the click was similar to that of the earphone, apart from a smooth fall-off to 10 kHz which is inherent to a pulse of 100 μs. The amplitude of the standard click was equivalent to the peak-to-peak amplitude of a sinusoidal tone of 92 dB SPL; the level was 51 dB above the CAP threshold for click stimuli averaged over all animals.

Single-fibre responses were recorded via a microprobe amplifier (5x, WPI-M707-A) and were presented to both an FM magnetic taperecorder (TEAC XR-510WB) using a recording bandwidth of 6.25 kHz and a spike discriminator (Mentor N-750) from which spike-triggered pulses were delivered to the computer. Simultaneously, the round-window signals were amplified (5000 × – 25000 ×) and recorded on tape. Bursts of broadband noise were used as search stimuli. For each

fibre the frequency threshold curve (FTC) was determined with a threshold tracking algorithm (Evans, 1979). The rate-increase criterion was 1 spike in a 50 ms burst, except for fibres with very high spontaneous activity (above about 100 spikes/s) for which it was 2 spikes. The SR was determined from the silent parts of the FTC procedure. Subsequently, standard condensation and rarefaction clicks were presented (256 sweeps).

The PSTHs were determined on-line using a bin width of 60 μs (or 100 μs for 3 animals) and the averaged CAP was determined off-line. The PSTH parameters t_p , A_p and S_p were calculated after slight smoothing of the PSTH. The timing of PSTHs and CAPs was referred to the start of cochlear microphonics. We used multiple regression analysis to examine the relationship of t_p to CF and SR.

The first criterion of normal hearing was based on the CAP-threshold audiogram. An animal's hearing was considered normal if the tone thresholds were not raised by more than 2 S.D. (corresponding to about 15 dB) from the mean values determined from an extensive sample of 35 healthy animals. These normal tone-audiogram values were in the range of commonly-found CAP thresholds (e.g. Aran et al., 1985; Johnstone et al., 1979; Syka and Popelář, 1980); the mean audiogram of the present sample is given in Fig. 1. The criterion for preservation of normal hearing during the experiment was based on the CAP threshold for clicks determined during the single-fibre measurement. Only thresholds below 15 dB nSL were permitted. Moreover, when using the standard click the N_1 latency changed by more than 0.15 ms or the N_1 amplitude by more than 50%, the data were discarded.

Results

The frequency threshold curve and the spontaneous rate were determined for 116 fibres in 12 guinea pigs. In 80 of these fibres a PSTH for condensation clicks of standard level (51 dB nSL) was measured, and this was done for rarefaction clicks in 71 fibres.

Spontaneous rate and threshold at CF

In Fig. 2 the distribution of the spontaneous rate is shown. It had two distinct maxima: one at

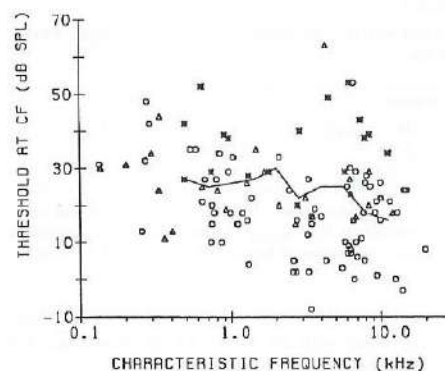


Fig. 1. Threshold at CF versus CF for 116 fibres. Circles represent high-SR fibres (SR above 30 sp/s), triangles medium-SR fibres (SR between 5 and 30 sp/s) and asterisks low-SR fibres (SR below 5 sp/s). The solid line represents the CAP thresholds for tones averaged over the corresponding sample of 12 guinea pigs.

the first bin of 0–5 spikes/s and the other at about 70–90 spikes/s. By analogy with cat data (e.g. Liberman, 1978), we divide the fibres in guinea pigs in three groups with respect to their SR. As points of distinction between the low-, medium- and high-SR fibres we take 5 spikes/s (upper limit of first bin of the histogram) and 30 spikes/s (the minimum of the distribution of SR). The small peak for SR above 110 spikes/s is assumed not to reflect a separate group, it is too

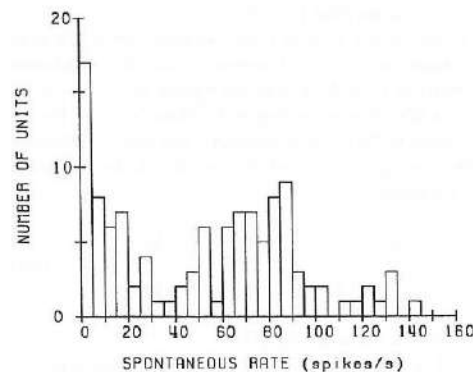


Fig. 2. Distribution of spontaneous discharge rate for the same sample of units as shown in Fig. 1 ($N=116$). Bin width is 5 spikes/s.

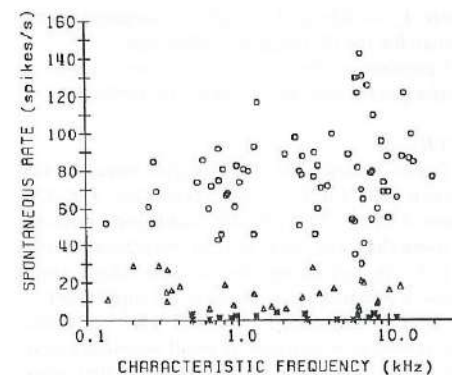


Fig. 3. SR versus CF for the same sample of units as shown in Fig. 1. Circles: high SR; triangles: medium SR; asterisks: low SR.

little pronounced. We found that 15% of the fibres had a low SR, 23% had a medium SR and 62% had a high SR.

The fibres' thresholds at CF are plotted versus CF in Fig. 1. Except for a few fibres, for each individual animal the fibres' thresholds were within 20 dB from the CAP threshold. On average the threshold at CF was highest for fibres with low SR. Medium-SR fibres had intermediate thresholds. The threshold differences were largest for fibres with a CF above 3 kHz, as shown in Fig. 1. The thresholds in that CF-range were 41 ± 8 , 25 ± 13 and 15 ± 11 dB SPL for low, medium- and high-SR fibres, respectively.

The distribution of SR with CF is shown in Fig. 3. The data indicate that the maximum values for SR were larger for higher CF. As a consequence of this, there was a weak (but significant; see Table I) correlation between SR and CF. All SR subgroups were represented along the entire CF-range.

Tuning

The tuning quality defined as the ratio of CF to the bandwidth at 10 dB above the minimum threshold, the Q_{10dB} , is plotted against CF in Fig. 4 for the investigated fibres. Q_{10dB} increased significantly ($P < 0.001$) with CF. The regression of Q_{10dB} with CF is given by:

$$Q_{10dB} = 2.70f_c^{0.28} \quad (5)$$

where f_c is CF in kHz. Q_{10dB} appeared to be similar for the different SR subgroups.

Correlations between the different fibre response parameters are compiled in Table I.

PSTHS

Figure 5 shows PSTHS of various fibres for two animals and for both click polarities. For CFs below 3 kHz, fibres showed phase lock reflected by more than one peak with an inter-peak interval of $1/f_c$ (or $2/f_c$ when the response which would follow a previous peak seems to be suppressed — see Figs. 5A and 5B). Above 3 kHz no phase-locked response occurred. A small secondary peak, which followed about 1 ms after the first peak, sometimes appeared in high-CF fibre's responses (e.g. unit with CF of 6.84 kHz in Figs. 5C and 5D). In further analysis of the PSTHS the high- and low-CF fibres are considered separately, with 3 kHz as the point of distinction.

Latency of the PSTH-peak

The latency of the dominant peak (t_p) for high-CF units was as short as the N_1 latency; t_p increased with decreasing CF for low-CF fibres for both condensation and rarefaction clicks, as clearly demonstrated in Figs. 5A and 5B. Comparing fibres with similar CF it appears that the low-SR fibre (the fibre with an SR of 0 sp/s in

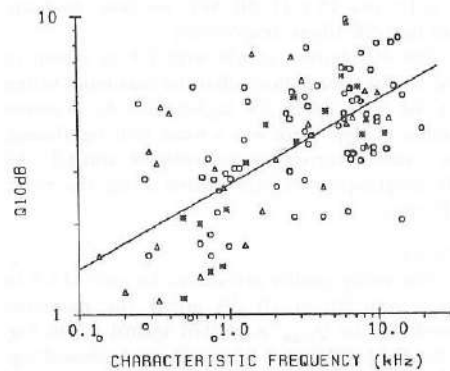


Fig. 4. Q_{10dB} versus CF for the same fibres as in Fig. 1. The drawn line represents the linear regression: $Q_{10dB} = 2.70f_c^{0.28}$, f_c in kHz; $r = 0.64$. Circles: high SR; triangles: medium SR; asterisks: low SR.

TABLE I

CORRELATIONS BETWEEN FIBRE RESPONSE PROPERTIES

Correlation	r	N
$r_s = 46 + 16 \log f_c$	0.23	116 *
$Q_{10dB} = 2.70f_c^{0.28}$	0.64	116 ***
$\theta_{cf} = 30 - 0.15r_s$	-0.43	116 ***

Symbols: f_c : characteristic frequency; r_s : spontaneous rate; θ_{cf} : threshold at CF; Q_{10dB} : tuning quality; r: correlation coefficient; N: number of fibres. * $P < 0.05$; *** $P < 0.001$.

Figs. 5C and 5D) and some of medium-SR fibres (e.g. the fibre with an SR of 14 sp/s in Figs. 5A and 5B) had longer peak latencies.

Components of t_p can be determined on the basis of Eqn. (3). Firstly we assume that t_2 does not vary with SR, in order to determine the CF-dependence of t_1 . An appropriate estimate of t_2 is given by a minimal response onset. This was obtained from rarefaction-click responses of fibres with a CF between 6 and 12 kHz, for which responses were the shortest. The mean value was 1.01 ± 0.16 ms ($N = 24$). Hence t_1 can be estimated by subtracting 1.01 from t_p . Figure 6 shows t_p minus 1.01 versus CF for condensation clicks. A straight line fits the data well. The regression line, shown by the solid line in Fig. 6, corresponds with:

$$t_p - 1.01 = 1.40f_c^{-0.66} \quad (6a)$$

with t in ms and f in kHz.

If the high-CF, non-phase-locking fibres are considered separately it appears that the correlation between t_p and CF was not significant ($r = -0.28$, $N = 42$). Thus for high-CF fibres t_p can be assumed to be CF-independent. For the responses to the condensation click this results in the following expression for t_p :

$$t_p - 1.01 = 1.22f_c^{-0.92} \quad \text{for } f_c \leq 3 \text{ kHz} \\ = 0.44 \quad \text{for } f_c > 3 \text{ kHz} \quad (6b)$$

with t in ms and f in kHz.

In Fig. 6 Eqn. (6b) is shown by a dashed line.

So far t_2 has been assumed to be constant. However, multiple linear regression analysis shows

that the latencies differed significantly ($P < 0.05$) for the three SR groups. For both click polarities the low-SR fibres had longer latencies than the others, while the medium-SR fibres had intermediate latencies. For condensation clicks the latency difference between the low-SR and the other fibres was significant ($P < 0.05$), and for rarefaction clicks this level of significance applied

to the difference between the high-SR and the other fibres.

Let us therefore consider Eqn. (3) with t_2 being SR-dependent. Estimates of t_2 for the three SR groups, obtained again from the minimum response onset, are 0.95 ± 0.14 ms for high-SR, 1.07 ± 0.09 ms for medium-SR and 1.20 ± 0.13 ms for low-SR fibres. Substitution of these values gives

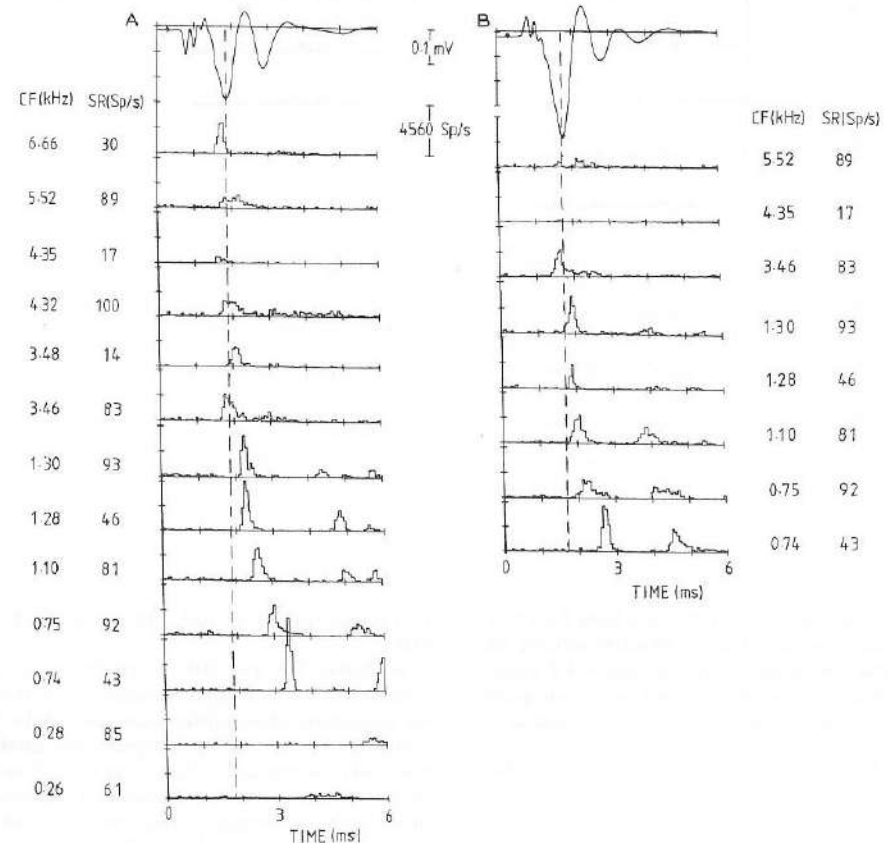


Fig. 5. (A) PSTHS for different fibres and the CAP, to condensation clicks at the standard level 51 dB nSL, for animal GP115. The plotted CAP is one of the compound responses measured simultaneously with one of the plotted PSTHS. The PSTHS are arranged in order of descending CF in one column. Bin width is 60 μ s. The timing of the CAP has been adjusted to allow comparison with the PSTHS. The ordinate represents the ratio of average number of spikes and the bin width. The dashed line is aligned with the N_1 latency in order to compare conveniently with the PSTH latencies. (B) As Fig. 5A, but concerning responses to rarefaction clicks. (C) As Fig. 5A, but concerning animal GP117. (D) As Fig. 5B, but concerning animal GP117.

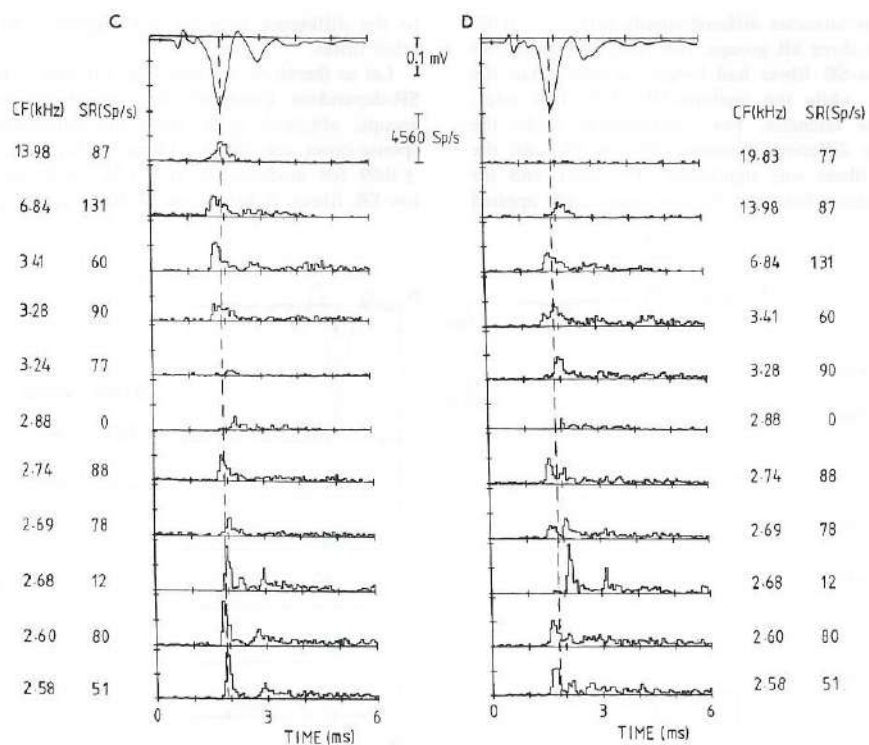


Fig. 5 (continued).

for each SR-group new regression lines for $t_1(f_c)$. It appears now that $t_1(f_c)$ is indistinguishable for the three SR-groups over the entire CF-range. Thus Eqn. (3) can be retained as an adequate description of t_p , and t_p can now be written as:

$$t_p = 1.41f_c^{-0.65} + t_2(r_s) \quad (7a)$$

or

$$t_p = 1.23f_c^{-0.91} + t_2(r_s) \quad \text{for } f_c \leq 3 \text{ kHz} \quad (7b)$$

$$t_p = 0.45 + t_2(r_s) \quad \text{for } f_c > 3 \text{ kHz}$$

with $t_2(r_s) = 0.95$ for high-, 1.07 for medium and

1.20 for low-SR fibres and with t in ms and f in kHz.

In Tables IIA and IIB the results for t_p are summarized for both click polarities. The results for rarefaction clicks differ from the results for condensation clicks in some aspects. For rarefaction clicks the regression lines fit less well than for the opposite polarity. The latencies for rarefaction clicks were on average shorter over the whole frequency range except for a CF above 12 kHz (for this CF range, t_p of the rarefaction click response increases slightly with CF, therefore, these responses have been excluded from the regression analysis). As shown in Fig. 7, it appears that the absolute difference between the latency

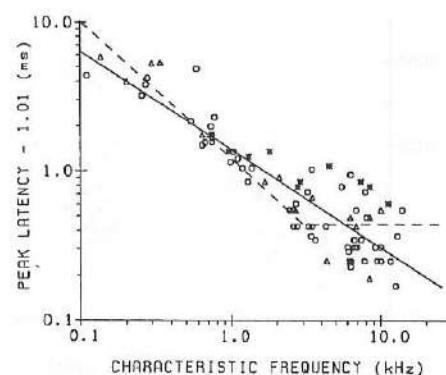


Fig. 6. PSTH-peak latency versus CF. The synaptoneuronal delay (assumed to be 1.01 ms) has been subtracted. The responses to the standard condensation clicks are from 80 fibres in 12 animals. The solid line represents the calculated linear regression: $t_p - 1.01 = 1.40f_c^{-0.66}$, t in ms, f_c in kHz; $r = -0.89$. The dashed line represents the regression line with t_p constant for a CF above 3 kHz. Circles: high SR; triangles: medium SR; asterisks: low SR.

for condensation clicks and that for rarefaction clicks largely followed $0.5/f_c$, except for CFs below 0.5 kHz where the latency difference was smaller and for CFs above 7 kHz where it increased with CF.

TABLE II
LATENCIES OF DOMINANT PSTH PEAK

Latency of dominant PSTH peak, $t_p = t_1(f_c) + t_2(r_s)$, for condensation and rarefaction clicks of standard level (51 dB nSL)

Click polarity	f_c	$t_1(f_c)$	r	N
Condensation	all	$1.41f_c^{-0.65}$	-0.88	80 ***
	≤ 3 kHz	$1.23f_c^{-0.91}$	-0.88	38 ***
	> 3 kHz	0.45		42
Rarefaction	all	$1.02f_c^{-0.65}$	-0.84	67 ***
	≤ 3 kHz	$0.88f_c^{-0.89}$	-0.82	35 ***
	> 3 kHz	0.34		32

TABLE IIB

r_s	t_2	SD	N
all	1.01	0.16	24
< 5 sp/s	1.20	0.13	3
5-30 sp/s	1.07	0.09	5
≥ 30 sp/s	0.95	0.14	16

Regression lines for $t_1(f_c)$ were computed by linear regression applied to logarithms of the variables with t_2 varying with SR (Table IIA). For rarefaction clicks the data for CFs above 12 kHz were excluded. For fibres with a CF between 6 and 12 kHz, t_2 was estimated from onset latencies of PSTHs for rarefaction clicks (Table IIB). t in ms, f in kHz; N : number of fibres, S.D.: standard deviation, r : correlation coefficient. *** $P < 0.001$.

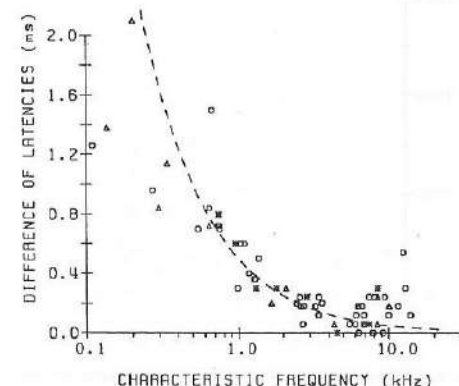


Fig. 7. Absolute difference between latencies for condensation (C) and rarefaction (R) click at standard level (51 dB nSL), $|t_p(f_c, C) - t_p(f_c, R)|$, versus CF ($N = 68$). The dashed line represents the theoretical latency difference: $|t_p(f_c, C) - t_p(f_c, R)| = 0.5f_c^{-1}$. Circles: high SR; triangles: medium SR; asterisks: low SR.

Amplitude and synchronization of the PSTH peak

In Fig. 8 the amplitude of the dominant peak, A_p , is shown as a function of CF for the same PSTHs (for condensation clicks) as in Fig. 6. The

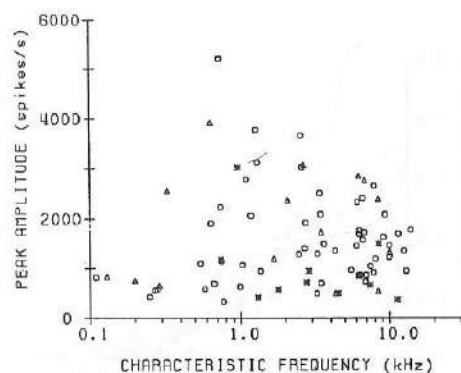


Fig. 8. PSTH-peak amplitude versus CF, concerning for the same responses as in Fig. 6. Circles: high SR; triangles: medium SR; asterisks: low SR.

amplitudes vary from 400 sp/s up to 4–6 ksp/s. Maximal values were found around 1 kHz. For CFs below 0.5 kHz, A_p tended to be small. It appears that low-SR fibres had smaller amplitudes than medium- and high-SR fibres.

The results concerning A_p for both click polarities are summarized in Table III. For high CFs, A_p tended to be larger for condensation clicks

TABLE III
AMPLITUDES OF DOMINANT PSTH PEAK

Amplitude of dominant PSTH peak, A_p , for different groups of fibres, click stimuli at standard level (51 dB nSL)

Condensation click		mean A_p	SD	N
f_c	r_s			
≤ 3 kHz	< 5 sp/s	1.1	0.9	6
≤ 3 kHz	5–30 sp/s	1.9	1.2	8
≤ 3 kHz	≥ 30 sp/s	1.7	1.3	24
> 3 kHz	< 5 sp/s	0.8	0.4	5
> 3 kHz	5–30 sp/s	1.7	0.9	7
> 3 kHz	≥ 30 sp/s	1.5	0.5	30

Rarefaction click		mean A_p	SD	N
f_c	r_s			
≤ 3 kHz	< 5 sp/s	1.2	1.0	5
≤ 3 kHz	5–30 sp/s	2.0	1.1	8
≤ 3 kHz	≥ 30 sp/s	1.6	0.8	22
> 3 kHz	< 5 sp/s	0.4	0.1	4
> 3 kHz	5–30 sp/s	1.2	0.8	6
> 3 kHz	≥ 30 sp/s	1.2	0.6	25

For further explanation see Table II. In contrast to Table II, rarefaction data cover the whole CF range. A_p in kspikes/s.

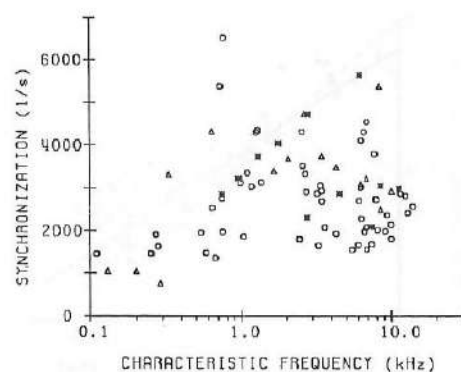


Fig. 9. Synchronization of the click response versus CF. Sample of fibres as in Fig. 6. Circles: high SR; triangles: medium SR; asterisks: low SR

than for rarefaction clicks; for low CFs such differences did not appear. For rarefaction clicks the tendency for a decrease of A_p with CF above 12 kHz was larger.

For both click polarities we found that the total discharge rate, p_p , did not vary with CF. For both medium- and high-SR fibres p_p had a mean value of 0.6 of a spike, which was significantly larger than that for low-SR fibres (about 0.3 of a spike). In Fig. 9 the variation of the synchronization with CF is shown. In the phase-locking range S_p increased with CF and for CFs above 3 kHz it appeared to be CF-invariant. Therefore, for non-phase-locking fibres the peak width, which is the inverse of S_p , was independent of CF. For high CFs the mean S_p was significantly ($P < 0.05$) larger for medium- than for high-SR fibres (low-SR values were intermediate). Table IV shows the results for S_p , which are similar for both click polarities.

Discussion

In describing the PSTH we use latency, amplitude and synchronization of the dominant peak as parameters. These parameters are found to depend on fibre discharge properties as CF, SR, Q_{10dB} and threshold. Since threshold at CF was related to SR and Q_{10dB} was related to CF, we have decided to describe t_p and A_p as functions of CF and SR only. The low-SR fibres had signifi-

TABLE IV
SYNCHRONIZATION OF DOMINANT PSTH PEAK

Synchronization of dominant PSTH peak, S_p , for different groups of fibres, click stimuli at standard level (51 dB nSL)

Condensation click		$S_p(f_c)$ or mean S_p	r	SD	N
f_c	r_s				
≤ 3 kHz	< 5 sp/s	$3.2 + 0.9 \log f_c$	0.28		6
≤ 3 kHz	5–30 sp/s	$3.3 + 2.5 \log f_c$	0.81		8 **
≤ 3 kHz	≥ 30 sp/s	$3.0 + 1.6 \log f_c$	0.43		24 *
> 3 kHz	< 5 sp/s	3.2		1.1	5
> 3 kHz	5–30 sp/s	3.4		0.7	7
> 3 kHz	≥ 30 sp/s	2.5		0.8	30

Rarefaction click		$S_p(f_c)$ or mean S_p	r	SD	N
f_c	r_s				
≤ 3 kHz	< 5 sp/s	$3.0 + 5.3 \log f_c$	0.95		5 ***
≤ 3 kHz	5–30 sp/s	$3.6 + 2.4 \log f_c$	0.83		8 **
≤ 3 kHz	≥ 30 sp/s	$2.7 + 2.0 \log f_c$	0.61		22 **
> 3 kHz	< 5 sp/s	2.6		0.5	4
> 3 kHz	5–30 sp/s	4.0		1.7	6
> 3 kHz	≥ 30 sp/s	2.4		0.7	25

For further explanation see table II. As in table III, rarefaction data cover the whole CF range. S_p in $(\text{ms})^{-1}$; f_c in kHz. * $P < 0.05$; ** $P < 0.01$; *** $P < 0.001$.

cantly higher thresholds than the other fibres; the medium-SR fibres had intermediate thresholds which is in accordance to fibre behaviour in cats (Lieberman, 1978). The bimodal distribution of SR agrees with distribution histograms reported for guinea pigs (Manley and Robertson, 1976) and cats (Lieberman, 1978). The Q_{10dB} values were in the same range of values as found by Evans (1972). PSTHs to clicks have two shapes: low-CF fibres show multiple peaks and high-CF fibres show single peaks (apart from a small secondary peak). The point of distinction between both groups is 3 kHz, which agrees with the findings on phase-lock behaviour in guinea pigs by Palmer and Russell (1986).

Latency of the PSTH peak

We have hypothesized a description of t_p according to Eqn. (3). This description, t_p as a sum of two independent terms, is based on the presupposition that the CF- and SR-related delay components are the result of two independent mechanisms: the mechanics of the cochlea and the mechanism which causes the spontaneous activity, respectively. According to Manley and Robertson (1976), the latter is of presynaptic origin. Their

arguments are supported by the evidence that fibres of different SR innervate one inner hair cell (Lieberman, 1982). The finding that the difference between latencies for both click polarities was similar for all SR groups (see Fig. 7) supports the assumption that the SR-related delay is not mechanically induced. We neglect a possible third latency term dependent on both CF and SR. This omission is justified because multiple linear regression analysis applied to the logarithms of t_p and CF do not reject Eqn. (3).

As an estimate of t_2 we used the minimum onset latency of the PSTHs. This choice is based on the assumptions that the rise time of the PSTH is mainly determined by the mechanical process and that the travelling wave time is negligibly small for high CFs. The onset values, obtained for rarefaction click responses, agree with data of Palmer and Russell (1986). As reviewed by Smolders and Klinke (1986), in other vertebrates the synapto-neural delay lies in a similar range.

Regression analysis shows that the low-SR fibres had longer latencies than the other ones while medium-SR fibres had intermediate latencies. The phenomenon of SR-dependency has been reported for the cat. Wang (1979) found that

medium-SR fibres (in his report: SR between 0.5 and 18 spikes/s) had longer latencies than high-SR fibres. In contrast, Antoli-Candela and Kiang (1978) found that only fibres with an SR below 0.5 spikes/s had longer latencies. The latency differences reported in both papers were of the same order as in our findings (0.15 ms). For the guinea pig, Evans (1972) commented that latencies for two populations of fibres with different SR (SR below 20 sp/s and SR above 80 sp/s) were similar. The discrepancies of the data illustrate that the effect is small and difficult to distinguish from statistical scatter. Differences between the data could be due to different stimulus intensities being used.

The SR dependence of the latency will have its origin in the synaptic structures and in the neural conduction. The latter can be excluded because the diameters of the groups of fibres as measured by Liberman and Oliver (1984) imply conduction times which are very similar (assuming a length of 3 mm and a conduction velocity of 5 m/s per μm diameter the conduction times differ by 0.02 ms). A larger sensitivity and a shorter click latency follow for higher-SR fibres if it is supposed that a higher SR is caused by a larger spontaneous release of transmitter substance (Manley and Robertson, 1976). Then, as a consequence, the mean of the spontaneous generator potential is larger, which means that the excitation threshold can be reached easier and thus, assuming a certain build-up time of the generator potential, earlier.

In the literature, latencies have mostly been described in a single relation to only CF, as in Eqn. (6a), without division in any subgroups. The exponent of $t_1(f_c)$ as given in Eqn. (6a) is comparable to the value of -0.725 found by Anderson (1971) for the group delay in the squirrel monkey, the value of -0.5 reported by Goldstein et al. (1971) for group delay and click latency data in the cat, and the slope of -0.77 for narrow-band AP latencies in man (Eggermont, 1979).

The exponents in Eqns. (6) and (7) can be explained when cochlear mechanics is described in terms of filters. The filter response time depends on the cycle ($1/f_c$) duration and on the number of cycles before the maximum is reached. The latter factor is related to the sharpness of the filter. Calculations of Goldstein et al. (1971) and Eggermont (1979) show that for a linear filter the number of cycles, N , is almost directly proportional with $Q_{10\text{dB}}$. We found that $Q_{10\text{dB}}$ is proportional to $f_c^{0.28}$ (see Eqn. (5)), which in approximation should lead to a filter delay which amounts to $N/f_c = \text{const. } f_c^{-0.72}$. The exponent is similar to those in Eqns. (6) and (7). We examined whether the variation of latency within the high-CF group is due to different tuning qualities. We, however, found no correlation between t_p and $Q_{10\text{dB}}$.

The guinea-pig data of Evans (1972) support the assumption that for the non-phase-locking fibres the latency is independent of CF. In cats, the high-CF plateau is even more pronounced (Antoli-Candela and Kiang, 1978; Wang, 1979; Dolan, 1983). Data of squirrel monkeys (Anderson et al., 1971) and man (narrow-band AP data; Eggermont, 1979) do not reveal the latency plateau. A plateau could be caused by several factors. The increasing length of the axons with increasing CF for high CF (Liberman and Oliver, 1984) could partly compensate the mechanically induced decrease of latency (but not more than 0.1 ms). Another compensating factor could be the frequency spectrum of the acoustic click, which has a low-pass character. The relatively lower effective intensity for high CFs may induce an increase of latency (0.1–0.2 ms; own results concerning intensity dependence, to be published). As shown by Fig. 4, the plateau is not caused by a larger increase of $Q_{10\text{dB}}$ with CF for high CFs.

In conclusion, for empirical description of PSTH-peak latencies, Eqns. (7) are more accurate than Eqns. (6); no preference appears for Eqn. (7a) or (7b) on the basis of data fitting.

Amplitude and synchronization of the PSTH peak

The amplitude of the PSTH peak, A_p , is determined by the (time-integrated) discharge probability and by the degree of synchronization of discharges. We describe this relationship by Eqn. (4). With t_p and A_p , the synchronization, S_p , is an important parameter in view of modelling PSTHs, since it reflects the inverse of the effective peak width.

The average peak rate, p_p , which reflects the discharge probability, did not vary with CF. Minimal and maximal values were 0.1 and 1.0 of a spike, respectively. Because of refractoriness p_p

cannot exceed 1; second discharges will form a distinct peak (Lütkenhöner et al., 1980). Since p_p was CF-invariant, the variation of A_p with CF can be accounted for by the behaviour of S_p ; this is illustrated by comparing Fig. 8 with Fig. 9. The increase of S_p with CF for low-CF fibres can be understood as the decrease of the peak width with CF. This indicates that the fibre responses largely follow the excitatory half of the filter response cycle.

For high CFs the filter impulse response would have its maximum at later cycles and thus the fibre response, which does not follow the cycles, would show up as one broad peak. This explains why the S_p and, consequently, the A_p of the high-CF fibres were not as large as for several low-CF fibres (see Figs. 8 and 9, and Table III). The decrease of A_p for CF above 12 kHz can be explained by the frequency spectrum of the acoustic click, which contains few frequencies above 12 kHz.

Our results of A_p in relationship to SR agree with reports on cats: fibres with an SR below 0.5 spikes/s have small click responses at moderate level and there is no difference between peak amplitudes of medium- and high-SR fibres (Antoli-Candela and Kiang, 1978).

According to the explanation of t_p in relationship with SR (see previous section), smaller discharge rates as expressed by p_p are consistent with longer latencies for fibres with lower SR. Indeed, we found a significantly smaller p_p and, in accordance with Eqn. (4), a smaller A_p for low-SR fibres than for the other ones. For high CFs there is a slight tendency that high-SR fibres have a larger p_p than the medium-SR fibres. The difference of synchronization seems to compensate that effect such that the amplitudes for medium- and high-SR fibres are similar.

It can be concluded that, to a first approximation, A_p in relationship to CF is determined by variations of S_p with CF and A_p in relationship to SR is determined by variations of p_p with SR.

CAP

In order to estimate which fibres contribute to the N_1 component of the CAP, without actually executing convolution computations, we make the following assumptions. The measured unit re-

sponse in the guinea pig has a diphasic waveform and a width of about 0.6 ms (see Prijs, 1986; Charlet de Sauvage et al., 1987). From Eqn. (2) we see that if UR is narrow compared with the sum of discharge probability functions (expressed by sum of PSTHs) it can be approximated by the derivative of the mathematical δ -function (apart from a conversion factor). Using Eqn. (2) we obtain for the CAP:

$$C(t) = \frac{d \left(\sum_{i=1}^N P_i(t) \right)}{dt} \quad (8a)$$

Wang (1979) demonstrated the utility of this approximation by showing that the sum of PSTHs agreed well, at least for the part which corresponds to the N_1 , with the integral of the CAP. If UR is broad compared to the sum of PSTHs, the latter can be approximated by the δ -function, $\delta(t - t_p)$, which gives for the CAP:

$$C(t) = U(t - t_p) \sum_{i=1}^N p_i \quad (8b)$$

with t_p being the latency of the sum of PSTHs and p_i being the discharge probability of the i^{th} fibre (dimensionless form of p_p).

The best description probably is one between both limits. According to Eqn. (8a) a rapid increase of the number of responding fibres at the N_1 -peak latency, t_{N_1} , accounts for the N_1 , as well as fibres that have an abrupt rise of response at t_{N_1} . Hence, fibres with t_p somewhat longer than t_{N_1} (i.e. between t_{N_1} and the zero-crossing of the CAP) will contribute to the N_1 . According to Eqn. (8b), that corresponds to the other limit, fibres with a t_p equal to t_{N_1} contribute to N_1 .

The values of t_{N_1} were on average 1.35 and 1.25 ms for condensation and rarefaction clicks, respectively. Applying Eqn. (7b) and the above-mentioned assumptions, and taking a neural conduction time of 0.2 ms into account, we obtain a reasonable estimate of the fibres that contribute to the N_1 . Evidently, the contribution to the CAP applies mainly to the medium- and high-SR fibres. Of these, most high-CF fibres (at least for CF below 12 kHz) will contribute to the N_1 , and a fair

proportion of the low-CF fibres could have a considerable contribution to the N_1 , moreover in view of their large A_p . The lower CF boundary would be about 1.3 kHz for condensation clicks and about 1.0 kHz for rarefaction clicks.

We conclude that the parameters t_p , A_p and S_p are useful to understand the contribution of the different fibres to the N_1 . Also, these parameters (with $1/S_p$ as peak width) can be applied to make up a sum of PSTHs, that has to be used in convolution computations. Analysis of the parameters for other click intensities will be discussed in a forthcoming paper.

Acknowledgements

This study was supported by the Netherlands Organization for Scientific Research (NWO) and by the Heinsius Houbolt Fund. Constructive comments on the manuscript were given by E. de Boer (ENT Dept., University of Amsterdam) and P.J. Kolston (ENT Dept., Utrecht University). Assistance concerning the statistical analysis was given by E.A. van der Velde (Dept. of Medical Statistics, Leiden University).

References

- Anderson, D.J., Rose, J.E., Hind, J.E. and Brugge, J.F. (1971) Temporal position of discharges in single auditory nerve fibers with the cycle of a sine-wave stimulus: frequency and intensity effects. *J. Acoust. Soc. Am.* 49, 1131-1139.
- Antoli-Candela, F. Jr. and Kiang, N.Y.S. (1978) Unit activity underlying the N_1 potential. In: R.F. Naunton and C. Fernandez (Eds.), *Evoked electrical activity in the auditory nervous system*, Academic Press, New York, pp. 165-189.
- Aran, J.-M., Erre, J.-P. and Charlet de Sauvage, R. (1985) Derived evoked potentials for continuous tones using a hybrid electrical-acoustical stimulation. *Hear. Res.* 20, 289-293.
- de Boer, E. (1975) Synthetic whole-nerve action potentials for the cat. *J. Acoust. Soc. Am.* 58, 1030-1045.
- Charlet de Sauvage, R., Aran, J.-M. and Erre, J.-P. (1987) Mathematical analysis of VIIIth nerve cap with a linearly-fitted experimental unit response. *Hear. Res.* 29, 105-115.
- Dolan, D.F., Teas, D.C. and Walton, J.P. (1983) Relation between discharges in auditory nerve fibres and the whole-nerve response shown by forward masking: an empirical model for the AP. *J. Acoust. Soc. Am.* 73, 580-591.
- Eggermont, J.J. (1976) Electrocochleography. In: W.D. Keidel and W.D. Neff (Eds.), *Handbook of Sensory Physiology*. Springer Verlag, Berlin, Heidelberg, New York, Vol. V, pp. 626-705.
- Eggermont, J.J. (1979) Narrow-band AP latencies in normal and recruiting human ears. *J. Acoust. Soc. Am.* 65, 463-470.
- Elberling, C. (1976a) Simulation of cochlear action potentials recorded from the ear canal in man. In: R. Ruben, C. Elberling and G. Salomon (Eds.), *Electrocochleography*, University Park Press, Baltimore, pp. 151-168.
- Elberling, C. (1976b) Deconvolution of action potentials recorded from the ear canal in man. In: S.D.G. Stephens (Ed.), *Disorders of auditory function II*, Academic Press, London, pp. 109-117.
- Evans, E.F. (1972) The frequency response and other properties of single fibres in the guinea pig cochlear nerve. *J. Physiol.* 226, 263-287.
- Evans, E.F. (1979) Single-unit studies of mammalian cochlear nerve. In: H.A. Beagley (Ed.), *Auditory investigation: The technological and scientific basis*, Clarendon Press, Oxford, pp. 324-367.
- Goldstein, J.L., Baer, T. and Kiang, N.Y.S. (1971) A theoretical treatment of latency, group delay, and tuning characteristics for auditory nerve responses to clicks and tones. In: H.A. Beagley (Ed.), *Physiology of the auditory system*, National educational consultants, Baltimore, pp. 133-141.
- Goldstein, M.H. and Kiang, N.Y.S. (1958) Synchrony of neural activity in electric responses evoked by transient acoustic stimuli. *J. Acoust. Soc. Am.* 30, 107-114.
- Harrison, R.V. and Prijs, V.F. (1984) Single cochlear fibre responses in guinea pigs with long-term endolymphatic hydrops. *Hear. Res.* 14, 79-84.
- Johnstone, J.R., Alder, V.A., Johnstone, B.M., Robertson, D., Yates, G.K. (1979) Cochlear action potential threshold and single unit thresholds. *J. Acoust. Soc. Am.* 65, 254-257.
- Kiang, N.Y.S., Watanabe, T., Thomas, E.C. and Clark, L.F. (1965) Discharge patterns of single fibers in the cat's auditory nerve. M.I.T. Research Monograph No 35, M.I.T. Press, Cambridge Massachusetts.
- Kiang, N.Y.S., Liberman, M.C. and Levine, R.A. (1976a) Auditory-nerve activity in cats exposed to ototoxic drugs and high-intensity sounds. *Ann. Otol. Rhinol. Laryngol.* 85, 752-786.
- Kiang, N.Y.S., Moxon, E.C. and Kahn, A.R. (1976b) The relationship of gross potentials recorded from the cochlea to single unit activity in the auditory nerve. In: R.J. Ruben, C. Elberling and G. Salomon (Eds.), *Electrocochleography*, University Park Press, Baltimore, pp. 95-115.
- Liberman, M.C. (1978) Auditory-nerve response from cats raised in a low-noise chamber. *J. Acoust. Soc. Am.* 63, 442-455.
- Liberman, M.C. (1982) Single-neuron labelling in the cat auditory nerve. *Science* 216, 1239-1241.
- Liberman, M.C. and Oliver, M.E. (1984) Morphometry of intracellularly labeled neurons of the auditory nerve: correlations with functional properties. *J. Comp. Neurol.* 223, 163-176.
- Lütkenhöner, B., Hoke, M. and Bappert, E. (1980) Effect of varying properties of the discharge pattern of auditory nerve fibres. In: M. Hoke, G. Bappert and E. Bappert (Eds.), *Cochlear and Brainstem Evoked Response Audiometry and Electrical Stimulation of the VIIIth Nerve*. *Scand. Audiol. Suppl.* 11, 25-43.
- Manley, G.A. and Robertson, D. (1976) Analysis of spontaneous activity of auditory neurones in the spiral ganglion of the guinea pig cochlea. *J. Physiol.* 258, 323-336.
- Palmer, A.R. and Russell, I.J. (1986) Phase-locking in the cochlear nerve of the guinea-pig and its relation to the receptor potential of inner hair-cells. *Hear. Res.* 24, 1-15.
- Peake, W.T. and Kiang, N.Y.S. (1962) Cochlear responses to condensation and rarefaction clicks. *Biophys. J.* 2, 23-34.
- Prijs, V.F. (1980) The single-fibre representation in the compound action potential of the auditory nerve. Ph.D. thesis, University of Nijmegen.
- Prijs, V.F. (1986) Single-unit response at the round window of the guinea pig. *Hear. Res.* 21, 127-133.
- Smolders, J.W.T. and Klinke, R. (1986) Synchronized responses of primary auditory fibre-populations in *Caiman crocodilus* (L.) to single tones and clicks. *Hear. Res.* 24, 89-103.
- Syka, J. and Popelář, J. (1980) Hearing threshold shifts from prolonged exposure to noise in guinea pigs. *Hear. Res.* 3, 205-213.
- Wang, B. (1979) The relation between the compound action potential and unit discharges in the auditory nerve. Doctoral dissertation, Dept. of Electrical Engineering and computer sciences, M.I.T.

Chapter III

Single-fibre and whole-nerve responses to clicks as a function of sound intensity in the guinea pig

Huib Versnel, Ruurd Schoonhoven and Vera F. Prijs

Summary

This paper describes a study of the intensity dependence of click-evoked responses of auditory-nerve fibres in relation to the simultaneously recorded compound action potential (CAP). Condensation and rarefaction clicks were presented to normal hearing guinea pigs over an intensity range of 60 dB. The recorded poststimulus time histograms (PSTHs) were characterized by the latency (t_p), amplitude (A_p) and synchronization (S_p) of their dominant peak, parameters that are particularly important for the understanding of the CAP. For all fibres t_p decreased monotonically with increasing intensity, in a continuous way for fibres with high characteristic frequency ($CF > 3$ kHz), and in discrete steps of one CF-cycle for low-CF ($CF \leq 3$ kHz) fibres. An additional analysis of PSTH envelopes revealed that average latency shifts with intensity are similar for all CFs above 2 kHz. For all fibres A_p increased monotonically with intensity; the increase was stronger and maximum values were larger for low-CF than for high-CF fibres. A schematic model PSTH was then formulated on the basis of the experimental data. A sum of these model PSTHs from a hypothesized fibre population was convolved with an elemental unit response (Versnel et al., 1992) in order to simulate the compound action potential. Synthesized CAPs agreed with experimental CAPs in their main aspects.

Key words: Poststimulus time histogram; Intensity; Click; Compound action potential; Convolution; Guinea Pig

This chapter has been published in *Hearing Research*, 59: 138-156 (1992).

Preliminary results were presented at the 2nd International Symposium on Cochlear Mechanics and Otoacoustic Emissions, Rome, March 1989.

Single-fibre and whole-nerve responses to clicks as a function of sound intensity in the guinea pig¹

Huib Versnel, Ruurd Schoonhoven and Vera F. Prijs

ENT Department, University Hospital, Leiden, The Netherlands

(Received 11 February 1991; accepted 19 December 1991)

This paper describes a study of the intensity dependence of click-evoked responses of auditory-nerve fibres in relation to the simultaneously recorded compound action potential (CAP). Condensation and rarefaction clicks were presented to normal hearing guinea pigs over an intensity range of 60 dB. The recorded poststimulus time histograms (PSTHs) were characterized by the latency (t_p), amplitude (A_p) and synchronization (S_p) of their dominant peak, parameters that are particularly important for the understanding of the CAP. For all fibres t_p decreased monotonically with increasing intensity, in a continuous way for fibres with high characteristic frequency (CF > 3 kHz), and in discrete steps of one CF-cycle for low-CF (CF ≤ 3 kHz) fibres. An additional analysis of PSTH envelopes revealed that average latency shifts with intensity are similar for all CFs above 2 kHz. For all fibres A_p increased monotonically with intensity; the increase was stronger and maximum values were larger for low-CF than for high-CF fibres. A schematic model PSTH was then formulated on the basis of the experimental data. A sum of these model PSTHs from a hypothesized fibre population was convolved with an elemental unit response (Versnel et al., 1992) in order to simulate the compound action potential. Synthesized CAPs agreed with experimental CAPs in their main aspects.

Poststimulus time histogram; Intensity; Click; Compound action potential; Convolution; Guinea Pig

Introduction

The compound action potential (CAP) as recorded by electrocochleography in human subjects or animals strongly depends on the intensity of the acoustic stimulus. Both for tonal and click stimuli the amplitude of the CAP increases and its latency decreases with increasing intensity (e.g. Peake and Kiang, 1962; Eggermont, 1976; Elberling, 1976; Salvi et al., 1979; Prijs and Eggermont, 1980; Møller, 1986). The CAP represents the summation of electric potential variations at the recording site (e.g. the round window) induced by discharges of the responding afferent fibres. If the unit response (UR) associated with a single discharge is identical across fibres of different CF and SR (cf. Kiang et al., 1976; Prijs, 1986; Versnel et al., 1992), if discharges of the individual fibres are mutually independent and if the single-fibre contributions add linearly, then the relation between whole-nerve and sin-

gle-fibre responses can be expressed by a convolution as (Goldstein and Kiang, 1958):

$$C(t) = \int_{-\infty}^t \left\{ \sum_{i=1}^N P_i(\tau) \right\} U(t-\tau) d\tau \\ = \int_{-\infty}^t S(t)U(t-\tau) d\tau \quad (1)$$

in which N is the number of fibres, $C(t)$ is the CAP, $U(t)$ is the unit response (UR), $P_i(t)$ is the PSTH of the i th fibre as the experimental estimate of its discharge probability density function, and $S(t)$ the compound or whole-nerve discharge latency distribution, i.e. the sum of P_i 's.

Several studies have been reported on the relation between the CAP and the underlying single-fibre discharge patterns using the convolution description (e.g. de Boer, 1975; Elberling, 1976; Wang, 1979; Bappert et al., 1980; Dolan et al., 1983; Versnel et al., 1990). De Boer (1975) modelled CAPs to tone bursts in cat applying a theoretical model in which the parameter choice for the $P_i(t)$ constituting $S(t)$ was based on reverse-correlation data for the cochlear filter combined with an empirical description of the inner hair

cell (IHC) and synaptic transduction, and on a unit response waveform which was mathematically postulated. CAPs could be simulated realistically for low intensities but the results on CAP amplitude, in particular, were not satisfactory for high intensities. Elberling (1976) and Bappert et al. (1980) simulated click CAPs in humans. Their models generated an $S(t)$ function by combining click PSTH data in cat (Kiang et al., 1965) and an excitation pattern derived by matching simulated narrow-band CAPs to the experimental CAP data. As UR waveform they used a high-frequency derived narrow-band CAP. In their results the CAP amplitude versus intensity profile was reproduced correctly. In order to relate experimental CAP and single-fibre data Dolan et al. (1983) applied a model in which they constructed $S(t)$ on the basis of experimental PSTH data. They selected UR parameters on the basis of data of Kiang et al. (1976) such that the modelled CAP N_1 component matched the experimental N_1 . To simulate a proper N_2 component second PSTH peaks in high-CF fibres had to be included in the model. Wang (1979) developed an empirical CAP model on the basis of URs and PSTHs experimentally determined in the same animal. Within individual cats he generally found a reasonable agreement for the N_1 latency and a small discrepancy in amplitude. In a qualitative study of CAPs and PSTHs for various click intensities in cats Antoli-Candela and Kiang (1978) concluded that the main contributions to the N_1 component of the CAP are due to the high-CF fibres.

In the present paper experimentally recorded single-fibre responses to clicks at various intensities and of both polarities are analysed in the context of their contribution to the compound action potential. To that end, a schematic model PSTH is formulated based on the experimental single-fibre data. Using this PSTH model, CAPs are simulated on the basis of Eqn. (1) and compared to CAPs that were recorded simultaneously during the single-fibre experiments. An evaluation of the experimentally derived UR is the subject of the companion paper (Versnel et al., 1992). Our PSTH model formulation is intended to establish a basis for the study of changes in the CAP in cochlear pathology as will be the subject of forthcoming papers. Our study is comparable to Wang's (1979) work and it contrasts to other CAP studies mentioned above in that we have directly measured both the single-fibre responses $P_i(t)$, the whole-nerve CAP and the unit response $U(t)$ in the same guinea pigs. This paper forms an extension of a previous paper (Versnel et al., 1990) where single-fibre responses were discussed for only one click intensity and where they were related qualitatively to CAPs.

The most commonly studied N_1 component of the CAP is supposed to be largely determined by the dominant peaks of the PSTHs. Therefore we concentrate on an investigation of latency, amplitude and

degree of synchronization of the dominant peak of our click PSTHs. We indicate these parameters, denoted as t_p , A_p and S_p , respectively, as P(peak)-parameters. Following a previous paper (Versnel et al., 1990) we distinguish three groups of spontaneous rates SR (in mathematical expressions denoted as r_c): low, medium and high SR, with 5 and 30 spikes/s as boundaries, and two groups of characteristic frequencies CF (mathematically denoted as f_c): low and high CF with 3 kHz as a boundary. The distinction of different SR subgroups is made because of the SR dependence of e.g. thresholds and rate-intensity functions (Lieberman, 1978; Winter et al., 1990; Versnel et al., 1990). The subdivision according to CF is motivated by the fact that click PSTHs of low-CF fibres have the well-known multiple-peaked character and click polarity dependence, while click PSTHs of high-CF fibres are basically single-peaked and virtually independent of click polarity (e.g. Kiang et al., 1965). In order to compare latency changes with intensity across the entire CF range we present an investigation of the latency of the PSTH envelope. It is based on a parameterization of the PSTH envelope by a function which has earlier been used to describe the envelope of the reverse correlation function that approximates the cochlear filter impulse response that underlies the neural click response (Grashuis, 1974; de Boer, 1975).

Finally, a model PSTH is formulated based on the relation of the PSTH parameters t_p , A_p and S_p with the fibre parameters CF and SR, and with the stimulus variables intensity and polarity. In combination with a postulated fibre population this model is used to synthesize a compound discharge latency distribution function $S(t)$ for clicks of different intensities and both polarities. This function is convolved with an estimate of UR described in the accompanying paper (Versnel et al., 1992). Simulated compound action potentials resulting from the model are then compared to CAPs recorded experimentally in the same population of animals.

Methods

Physiological experiments

Acute experiments were performed on 14 healthy female albino guinea pigs weighing 200-800 g. Details of the animal preparation and of the equipment for sound stimulation and signal recording have been described in a previous paper (Versnel et al., 1990). The main points are given below.

Premedication consisted of Atropine Sulphate (25 μ g/kg) and Thalamonal (1.6 ml/kg) and anaesthesia was obtained with Nembutal® (27 mg/kg). A silver ball electrode was positioned on the round window for the whole-nerve recordings. The CAP tone threshold au-

Correspondence to: H. Versnel, (Present address) Systems Research Center, University of Maryland, College Park, MD 20742, USA. Fax: (301)314-9920.

¹ Preliminary results were presented at the 2nd International Symposium on Cochlear Mechanics and Otoacoustic Emissions, Rome, March 1989.

diagram was used to assess the condition of the cochlea. The cochlear nerve was approached intracranially (Evans, 1979); during the preparation the condition of the cochlea was monitored by continuously recording the click CAP. Single-fibre responses were recorded using micropipettes filled with 2.7 M KCl or 0.5 M KCl/0.1 M TRIS buffer.

Sound was presented to the animal, placed in a sound proof room, by a dynamic earphone (Standard Telephones and Cables 4026A) and closed coupler system. A pulse generator (Devices type 2521) delivered 100 μ s pulses for click stimuli with an interstimulus interval of 128 ms. The spectrum of the acoustic click is shown in Fig. 1A: it was flat within 10 dB up to about 8–9 kHz where it fell off rapidly. The intensity was set by attenuators (Grason-Stadler model 1284) which were controlled by a DEC PDP 11/10 computer. Single-fibre signals were recorded via a microprobe amplifier (5 \times , WPI-M707-A), passed to the PDP-11/10 via a spike discriminator (Mentor N-750) and also stored on magnetic tape (datarecorder TEAC XR-510WB, recording bandwidth 0–6.25 kHz). The simultaneously generated round-window responses were amplified (5,000 \times –25,000 \times) and stored on the same tape.

For each fibre a frequency threshold curve (FTC) was determined using a threshold tracking algorithm (Evans, 1979), and the spontaneous rate (SR) was determined during silent intervals in this tracking procedure. First, condensation and rarefaction clicks were presented at an intensity level of 51 dB nSL (normal sensation level, i.e. re: mean CAP threshold at 1 μ V criterion over a population of normal animals; cf. Versnel et al., 1990). Then, clicks were presented at intensities varied in 10 dB steps above and below this level. PSTHs were recorded on-line using 256 sweeps and a bin width of 60 μ s, and were normalized to a discharge

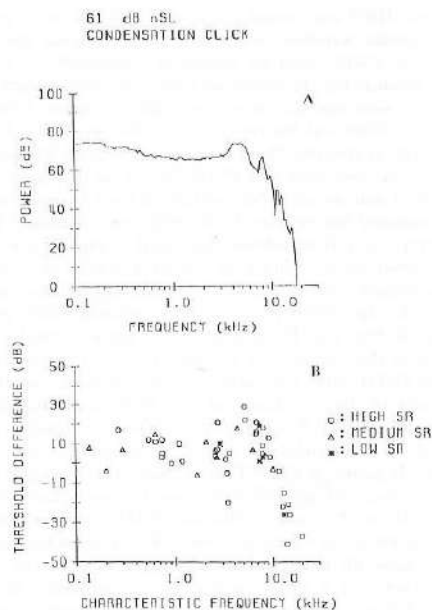


Fig. 1. (A) Spectrum of the acoustic click (condensation polarity; 61 dB nSL). (B) Difference between CF-tone threshold and click threshold, $\theta_{cf} - \theta_{click}$, versus CF. θ_{cf} is expressed in dB SPL, θ_{click} in dB nSL. Asterisks represent low-SR fibres (SR below 5 sp/s), triangles medium-SR fibres (SR between 5 and 30 sp/s) and circles high-SR fibres (SR above 30 sp/s).

probability density by dividing the total number of spikes per bin by the number of sweeps and by the bin width. For glossary of abbreviations see Table 1.

TABLE 1
GLOSSARY OF ABBREVIATIONS, SYMBOLS AND DEFINITIONS

FTC: frequency threshold curve	t_p : latency of dominant PSTH peak
CF, f_c : characteristic frequency (frequency of minimal threshold)	A_p : amplitude of dominant PSTH peak
θ_{cf} : pure tone threshold at CF	S_p : synchronization of dominant PSTH peak
Q_{10dB} : tuning quality, ratio of CF and bandwidth 10 dB above θ_{cf} , derived from FTC	p_p : area of dominant PSTH peak (expected number of spikes occurring during this peak)
SR, r_s : spontaneous rate	$g(t)$: gamma distribution function used to describe PSTH envelope
L_c : click intensity (dB nSL)	t_γ : latency of PSTH envelope as described by $g(t)$
nSL: dB scale for click intensity relative to the average CAP threshold in normal guinea pigs	BF: best frequency, frequency where difference PSTH power spectrum is maximum
L: effective stimulus level in the CAP model, including corrections e.g. for SR	CAP, C(t): compound action potential
PSTH, P(t): poststimulus time histogram, normalized to a discharge probability density function	S(t): compound discharge latency distribution function
compound PSTH: presentation of PSTHs to both click polarities plotted upward and downward, respectively	UR, U(t): unit response, contribution of individual fibre discharge to the CAP
difference PSTH: difference of PSTHs to both click polarities	$N_{(2)}$: first (second) negative peak of CAP
	t_{N1} : latency of CAP N_1
	A_{N1} : amplitude of CAP N_1

Data analysis

The PSTHs were slightly smoothed using a three-point (1/4, 1/2, 1/4) window. Then the latency t_p , the amplitude A_p and the synchronization S_p of the dominant PSTH peak were determined. These measures will be referred to as P-parameters. Latency was referred to the start of the cochlear microphonic in order to eliminate the acoustic and middle-ear delays. The synchronization S_p is defined as the ratio of amplitude A_p and area p_p of the PSTH peak (cf. Versnel et al., 1990)

$$S_p = A_p/p_p \quad (2)$$

Since the peak area p_p is the expected number of spikes over the duration of the dominant peak (typically between 0 and 1 spike) and A_p is in spikes/s, S_p has the dimension of s^{-1} .

A second latency parameterization is based on PSTH envelopes. We will assume that the PSTH envelope can be described by the function

$$g(t) = \begin{cases} ((t - \alpha)/\beta)^{\gamma-1} \exp\{-(t - \alpha)/\beta\} & \text{for } t \geq \alpha \\ 0 & \text{for } t < \alpha \end{cases} \quad (3)$$

This function was fitted to the PSTH envelopes by a least-squares curve fitting procedure (Bevington, 1969). For the high-CF fibres (CF above 3 kHz) we fitted $g(t)$ to the amplitude values in the (typically 20) individual bins of the dominant PSTH peak; the procedure is applied for each click polarity separately. For the low-CF fibres (CFs below 3 kHz), which show multiple-peaked responses, we fitted $g(t)$ to the set of peak maxima combining the (together typically 10–15) peaks of rarefaction and condensation click PSTHs. The latency t_γ of the maximum of the thus fitted PSTH envelope is given by

$$t_\gamma = \alpha + \beta(\gamma - 1) \quad (4)$$

The indication γ is because the function $g(t)$ is related to the gamma distribution (de Boer, 1975).

Additionally, an analysis was made of the multiple peak patterns of the PSTHs of low-CF fibres by a spectral analysis of the difference PSTH, that is defined as the condensation-click PSTH minus the rarefaction-click PSTH (cf. Pfeiffer and Kim, 1972). In particular we study the frequency where the power spectrum of the difference PSTH has its maximum, indicated as the best frequency (BF) following Eggermont et al. (1983).

CAP model

The empirical CAP model is based on the convolution formalism of Eqn. (1). A compound discharge

latency distribution $S(t)$ is simulated by adding a set of model PSTHs from a hypothetical population of individual fibres. The CAP is then calculated by convolving $S(t)$ with an elemental unit response UR. A detailed description of how the model PSTH is defined on the basis of the P-parameters, how the fibre population is generated and which UR is used is given in the Appendix.

Results

For 95 fibres in 14 guinea pigs a PSTH was determined for condensation clicks at the starting intensity level of 51 dB nSL. For 33 of these fibres, series of PSTHs for at least four intensities were determined for the two click polarities.

From the amplitude-intensity curves the fibre's click threshold, θ_{click} (dB nSL), was estimated. This was compared to the fibre's CF-tone thresholds, θ_{cf} (dB SPL), by considering the threshold difference, $\theta_{cf} - \theta_{click}$ (dB), as a function of CF. Fig. 1B shows that this threshold difference largely followed the spectrum of the acoustic click (Fig. 1A). We found no effect of SR on this relationship. The similarity between the click spectrum and the difference of CF-tone threshold and click threshold allows a prediction of θ_{click} from click spectrum and threshold at CF.

Compound PSTHs

Fig. 2 shows five representative series of PSTHs measured at various intensities in fibres with CFs in the range of 0.7 to 8 kHz. The data are given as compound PSTHs with responses to condensation clicks are plotted upwards and responses to rarefaction clicks plotted downwards. In addition, the frequency threshold curves (FTCs) of the fibres are given.

For two high-CF fibres (CF about 7 kHz) with a high SR and a low SR PSTHs are shown in Fig. 2A and B, respectively. For both fibres the responses to opposite click polarities were basically identical at low and intermediate stimulus intensities. The PSTHs consist of a single dominant peak with, for the high-SR fibre, a small secondary peak at an interpeak time of about 1 ms for intermediate intensities. The rise time of the dominant PSTH peak decreases with increasing intensity. At high intensities the PSTHs to both polarities are increasingly different from each other, in that the large dominant peak in the rarefaction click PSTH appears with a shorter latency than that in the condensation click PSTH (e.g. Fig. 2A,B upper trace). In addition, multiple small late peaks occur producing a low-frequency oscillatory pattern (Fig. 2A, upper trace). The PSTH patterns shown in Fig. 2A,B are representative for fibres with CFs above 3 kHz.

Fig. 2C,D show compound PSTHs of low-CF fibres with CFs of approximately 2.6 kHz and high and medium SR respectively, while Fig. 2E represents a 0.74 kHz, high SR fibre. These PSTHs have multiple peaks which approximate a modulated sinusoid of characteristic period $1/f_c$, particularly for low intensities (10–20 dB nSL). A comparison between the PSTHs of the 2.6 kHz fibres suggests that the medium-SR fibre (D) responded with a pattern like that of the high-SR fibre (C) at a 10 dB lower click level. For the 0.7 kHz fibre the interpeak intervals in the early part

of the PSTH increase for high-intensity stimuli, and the peaks do not interleave exactly between the peaks of responses to clicks of opposite polarity (Fig. 2E, upper two traces). The patterns shown for the 0.7 kHz fibre are typical for the fibres with CFs between 0.5 and 1.5 kHz.

P-parameters

In Fig. 3 the P-parameters latency, amplitude and synchronization of the dominant peak are shown for

fibres from three CF ranges (0.5–1, 2–3 and 6–12 kHz). Other CF ranges are not included because too little data were available in those ranges. The P-parameters for fibres in the CF range 6–12 kHz (Fig. 3A,B) have been averaged over each SR subgroup. The high-SR group, however, was further subdivided into two parts, one containing two fibres with extremely low thresholds (squares), the other containing the other high-SR fibres (circles), in order to preserve the individual character of the response behaviour of the two subgroups. The parameters for fibres of the other CF ranges are plotted individually, because of the larger spread of these data (e.g. the strong CF dependent latency).

Latency of the dominant PSTH peak

Fig. 3A,B show that for the 6–12 kHz fibres the latency of the dominant PSTH peak decreases monotonically with intensity. With t_p being longer for low-SR fibres, the low- and high-SR fibres have t_p curves that run parallel to each other; the medium-SR latencies run in between. The average shift of t_p over the 60 dB intensity range is about 20 μ s/dB. There is a small polarity dependence of t_p , particularly in that t_p is shorter for rarefaction clicks at high intensities.

In the 2–3 kHz CF range the latencies of individual PSTH peaks are virtually independent of intensity as illustrated in Fig. 2C,D. However, with increasing intensity earlier peaks become dominant and thus t_p

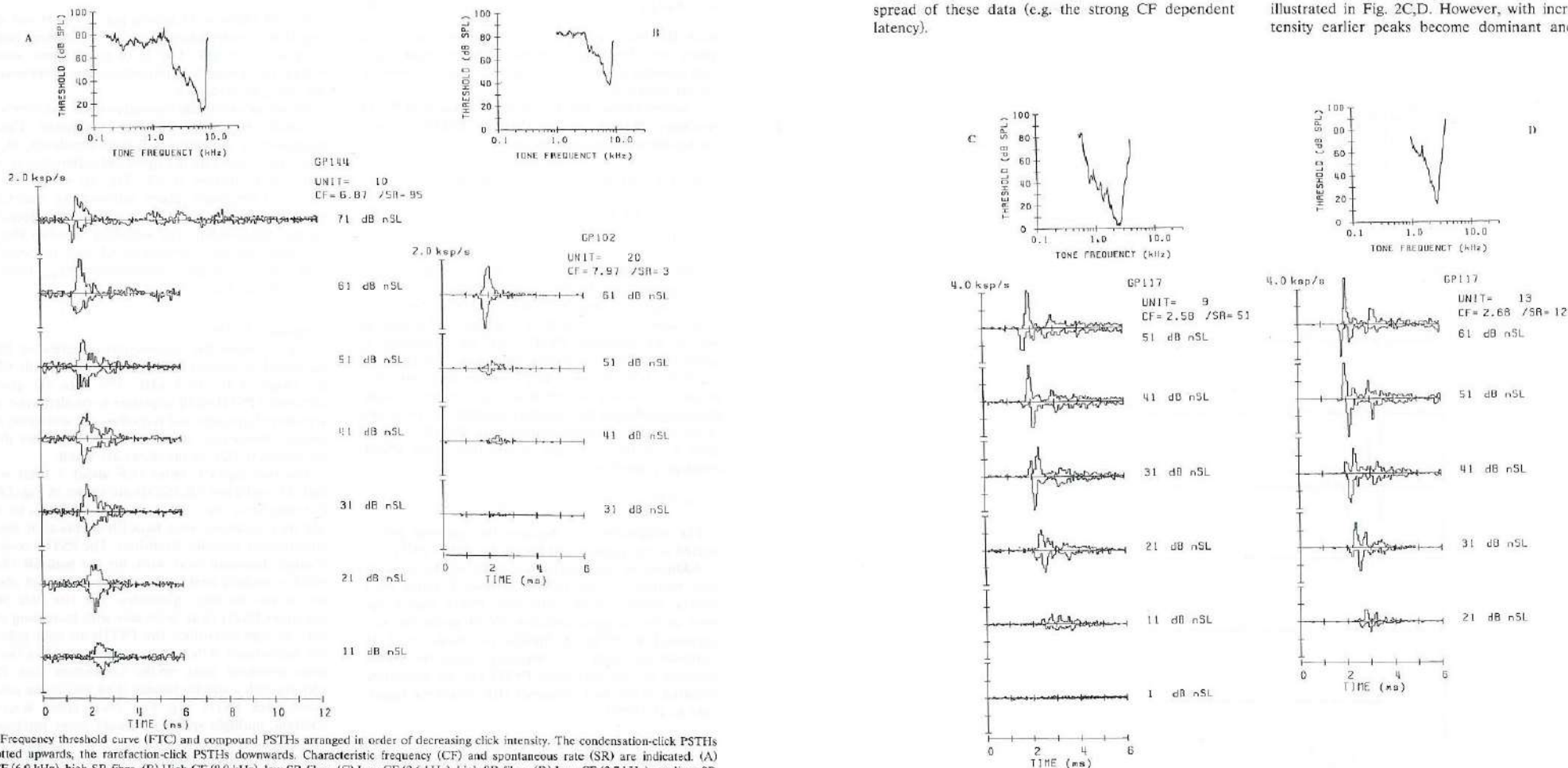


Fig. 2. Frequency threshold curve (FTC) and compound PSTHs arranged in order of decreasing click intensity. The condensation-click PSTHs are plotted upwards, the rarefaction-click PSTHs downwards. Characteristic frequency (CF) and spontaneous rate (SR) are indicated. (A) High-CF (6.9 kHz), high-SR fibre. (B) High-CF (8.0 kHz), low-SR fibre. (C) Low-CF (2.6 kHz), high-SR fibre. (D) Low-CF (2.7 kHz), medium-SR fibre. (E) Low-CF (0.7 kHz), high-SR fibre. Note the differences in ordinate scales between panels A/B, C/D and E.

Fig. 2. (continued).

peak (cf. Fig. 2C,D,E). On the basis of the curve fits the latency t_p of the maximum of the PSTH envelope (Eqn. (4)) was determined. Fig. 5 shows t_p versus click intensity for the same groups of PSTHs as described in Fig. 3.

For the 6–12 kHz fibres the shift of t_p with intensity over the 0–60 dB intensity range is, on average, about 20 μ s/dB (Fig. 5A), in agreement with the shift of t_p (Fig. 3A,B). As expected, for low-CF fibres t_p shifts gradually with intensity in contrast to t_p that shifts in discrete steps (Fig. 3C,D). For the 2–3 kHz fibres (Fig. 5B) t_p decreases by about 20 μ s/dB on average. Note that for the 0.5–1 kHz range (Fig. 5C) t_p decreases at about the same rate for low intensities, but reaches a minimum at an intermediate level and tends to increase for higher intensities.

Fourier analysis of difference PSTHs

In Fig. 6 intensity series of Fourier power spectra of difference PSTHs are shown corresponding to the PSTHs of Fig. 2C,E. Near threshold the best frequency (BF) of the difference PSTH power spectrum corre-

sponded with the CF as derived from the FTC. For 13 of 16 fibres, with a CF between 0.5 and 3 kHz, the BF decreased with intensity. This shift could increase to one octave. However, the power spectra generally preserved a local maximum at CF (e.g. Fig. 6B). Commonly, concomitant with the decrease of BF, the power spectra showed a broadening with increasing intensity (Fig. 6). In contrast to the observations in the 0.5–3 kHz CF range, in all 3 fibres with a CF below 0.5 kHz, in which a series of difference PSTHs could be determined, BF increased with intensity.

Sum of PSTHs and CAP

As an illustrative application of the empirical model, CAPs were simulated in response to rarefaction and condensation clicks of different intensities. Fig. 7 shows the synthesized compound discharge latency distributions $S(t)$, based on 4000 fibres per octave over the 0.5 to 24 kHz frequency range, with appropriate SR distribution. These functions $S(t)$ are very similar for the two polarities, but show small intensity dependent differences e.g. in peak latency and rise time.

Fig. 8A shows a representative example of round-window recorded CAPs. The latency of the N_1 component of the CAP, t_{N1} , decreased monotonically with increasing intensity at an average rate of 15 μ s/dB, and the amplitude of N_1 , A_{N1} , increased to 100–150 μ V from threshold to 30 dB nSL. In most animals there was a second, large amplitude increase for intensities above 50 dB nSL. Below 40 dB nSL the experimental CAPs were similar for both click polarities; above that level, however, t_{N1} was shorter by 0.1–0.2 ms and A_{N1} was generally larger by a factor of 1.5 to 2 for rarefaction than for condensation clicks. In Fig. 8B we show a series of model generated CAPs, based on the $S(t)$ of Fig. 7. The global waveform of the simulated CAP N_1 component is very similar to that of the experimental data. The model CAPs do not show the pronounced N_2 component present in the experimental data. More detailed observation reveals that the simulated N_1 waves are slightly broader and their onset latencies are slightly smaller than those of the experimental data.

Amplitude and latency input-output functions of averaged experimental data and model-generated CAPs are compared in Fig. 9. CAP latency and its intensity dependence are reproduced correctly by the model. The same applies to the crossing-over of the t_{N1} of condensation clicks with that of rarefaction clicks at intermediate intensity. The model predicts absolute CAP amplitudes within the range observed in normal animals, but it does not adequately reproduce the increase of A_{N1} for intensities above 50 dB nSL, nor the divergence of rarefaction and condensation click amplitude curves.

Discussion

PSTHs for high-CF fibres

The PSTHs of high-CF fibres show a large dominant peak followed by a smaller secondary peak with a delay of about 1.0 ms, presumably reflecting repetitive discharges after the refractory period (Kiang et al., 1965;

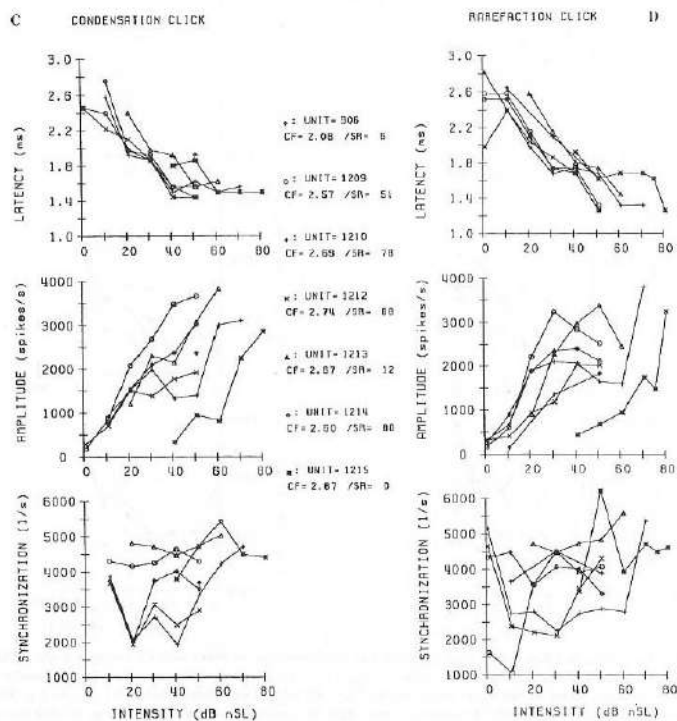


Fig. 3. (continued).

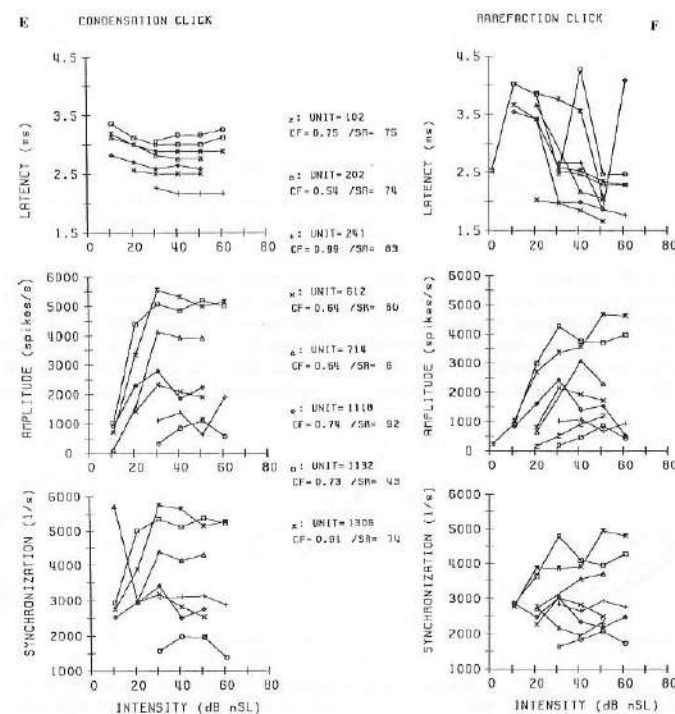


Fig. 3. (continued).

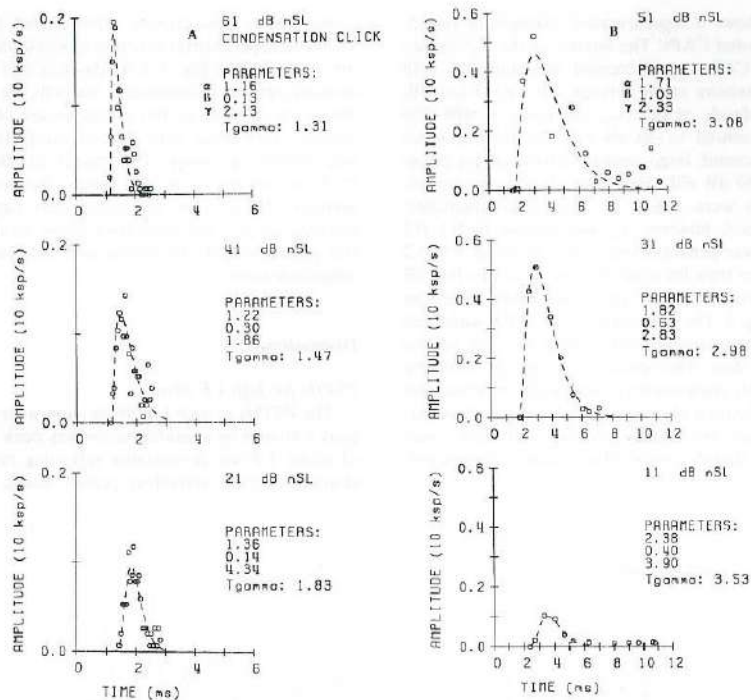


Fig. 4. Fits of the function $g(t)$ (Eqn. (3)) to the PSTH envelopes. Fitted curves are represented by dashed lines; the PSTH envelope data points are represented by circles. Values of the parameters α , β , and γ are shown with the corresponding t_γ (Eqn. (4)) beside each plot. (A) Fits for single PSTHs from Fig. 2B for various intensities of condensation clicks. The data points represent PSTH amplitudes in individual bins. (B) Fits for compound PSTHs from Fig. 2E for various intensities. The data points reflect the various PSTH peak maxima.

Lütkenhöner et al., 1980; Dolan et al., 1983). At high intensities the similarity between rarefaction and condensation click responses, as observed at low and moderate intensities, is lost. A clear latency difference between the dominant peaks of rarefaction and condensation click PSTHs emerges, and in addition sev-

eral smaller peaks at larger latency are observed, interleaving for the two click polarities (Fig. 2A). Similar high-intensity phenomena can also be observed in cat (Kiang et al., 1965; Antoli-Candela and Kiang, 1978). In our data, the dissimilarity between rarefaction and condensation click responses occurs at a click level of

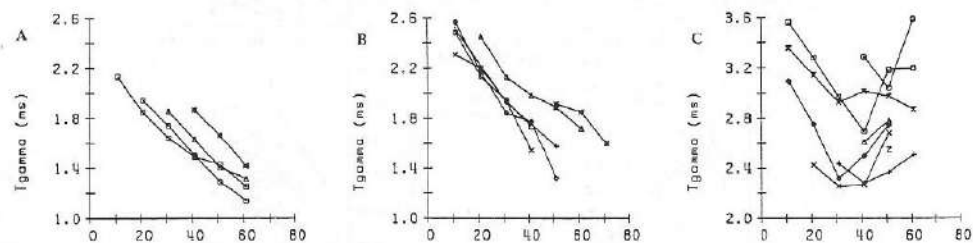


Fig. 5. The PSTH envelope latency t_γ (Eqn. (4)) as a function of intensity for different CF groups and with symbols as in Fig. 3. (A) Mean values of t_γ for fibres with CF between 6 and 12 kHz, values for condensation and rarefaction clicks are averaged. (B) Parameters determined from envelopes of compound PSTHs, for fibres with CF between 2 and 3 kHz. (C) As panel B, but for fibres with CFs of 0.5–1 kHz.

50–60 dB above the fibre's threshold, which just corresponds to the FTC tip-to-tail level difference. Thus, both the temporal response patterns of the PSTH at high click levels and the presence of the tail in the FTC suggest that basally in the cochlea the cochlear parti-

tion has a secondary weak resonance in a frequency range considerably below CF, in addition to the high-frequency resonance constituting the tip of the FTC (cf. Antoli-Candela and Kiang, 1978; Prijs et al., 1990). Note that the latency difference of the dominant PSTH

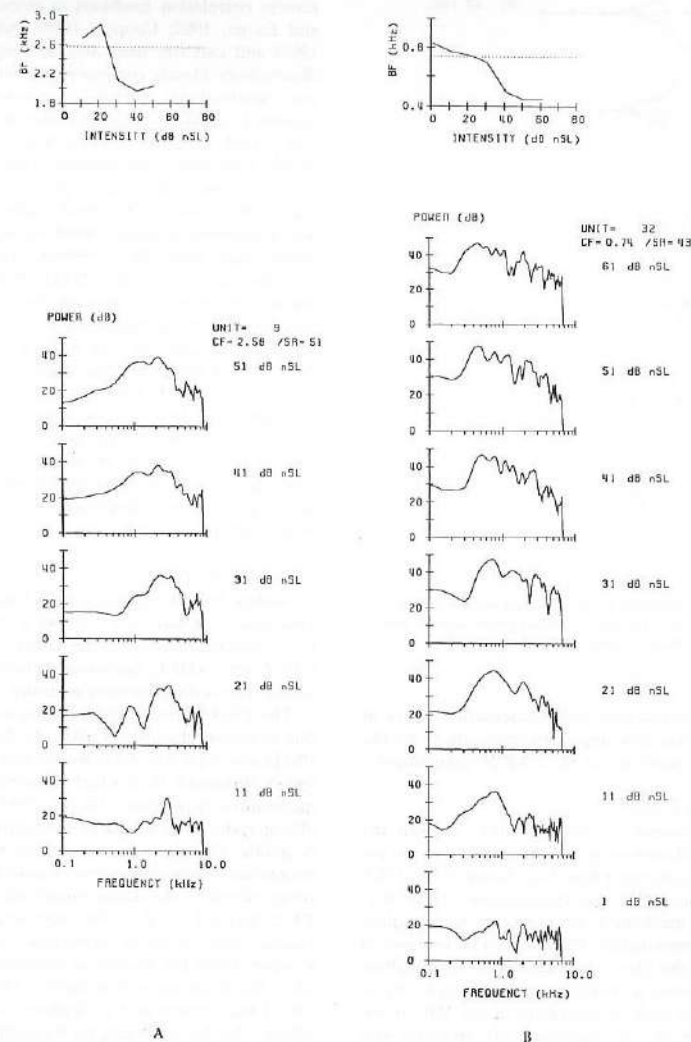


Fig. 6. Power spectra of difference PSTHs at various intensities. In the top panel the best frequency (BF) is plotted versus intensity, the dotted line representing CF determined from the FTC. (A) Fibre with CF of 2.6 kHz and SR of 51 spikes/s (animal GP117) (cf. Fig. 2C). (B) Fibre with CF of 0.7 kHz and SR of 43 spikes/s (animal GP115) (cf. Fig. 2E).

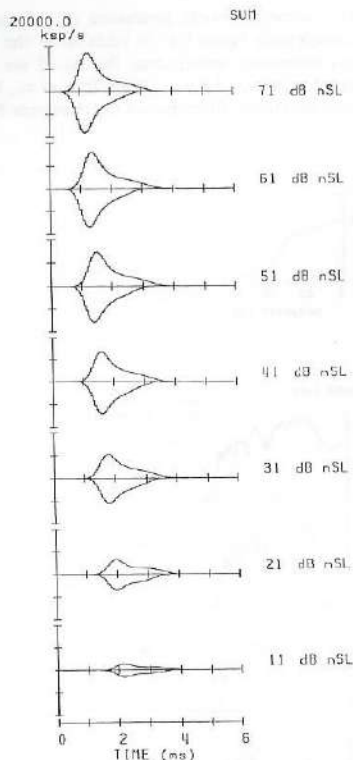


Fig. 7. Synthesized compound discharge latency distributions $S(t)$ for various click intensities. The $S(t)$ to condensation clicks is plotted upwards, that to rarefaction clicks downwards.

peak between rarefaction and condensation clicks at high intensities will have important implications for the click polarity dependence of the CAP N_1 component.

PSTHs for low-CF fibres

The click responses of low-CF fibres showed the well-known oscillatory pattern with multiple peaks occurring in the excitatory phase (e.g. Kiang et al., 1965; Pfeiffer and Kim, 1972). This temporal pattern primarily reflects the mechanical resonance of the cochlear filter. At low intensities the PSTH envelope is expected to approximate the filter envelope, but at intermediate and high intensities it is determined to a large extent by nonlinearities such as saturation of the IHC transduction and neural refractoriness. Concomitantly with the increase of early interpeak intervals in the PSTHs of very low-CF fibres (Fig. 2E), the BF of the difference PSTH power spectra decreased with increasing

intensity for most fibres with CF between 0.5 and 3 kHz (Fig. 6), to a slightly larger extent than e.g. the BF of reverberation functions reported by Harrison and Evans (1982) in the same species. Other eighth-nerve single-fibre data pointing to a downward shift of best frequency with increasing intensity include iso-intensity contours in squirrel monkeys (Rose et al., 1971) and reverse correlation functions in guinea pigs (Harrison and Evans, 1982; Cooper, 1989), rats (Møller, 1977, 1983) and cats (de Boer and de Jongh, 1978). These observations closely correspond to nonlinear phenomena observed in mechanical basilar-membrane responses to clicks of increasing intensities: early oscillation periods increase, resulting in a net downward shift of BF with increasing intensity (Robles et al., 1976, squirrel monkey; Ruggero et al., 1991, chinchilla). Related effects have been demonstrated in basilar-membrane responses to tonal stimuli by Sellick et al. (1982; guinea pig). From these considerations we conclude that the increase of early PSTH interpeak intervals is mainly caused by a downward shift of the resonance frequency of the cochlear filter at large excursions of the basilar membrane. The pattern in the late part of the PSTH, however, has the same resonance frequency and is as regular as the response pattern at low click intensity. Note that in guinea pig the intensity dependence of early inter-peak intervals in click PSTHs is larger than e.g. in cat (cf. Kiang et al., 1965; Antoli-Candela and Kiang, 1978), which may be related with the smaller intensity dependence of tuning in the latter species (Harrison and Evans, 1982).

Latency of the PSTH

Rather than the dominant peak latency t_p , the PSTH envelope peak latency t_e allows a comparison of latency characteristics over the entire CF range. For all CFs above 2 kHz t_e decreased monotonically and with similar rate with increasing intensity.

The PSTH latency shift with intensity is presumably due to two mechanisms. Firstly, the latency of the click PSTH envelope will decrease because the neural excitation threshold is reached in earlier cycles of the mechanical oscillation (Møller, 1985) and refractory effects reduce the discharge probability in later cycles. Secondly, the number of cycles in which the basilar membrane impulse response reaches its maximum is proportional to the tuning quality (cf. Goldstein et al., 1971; Versnel et al., 1990) and since the latter decreases with intensity (Harrison and Evans, 1982; Cooper, 1989) the latency as expressed in the number of cycles decreases with intensity. The dependence on CF of the latency shift is determined by two opposite effects. On the one hand, for a sharply tuned mechanical filter the impulse response will reach its maximum after a large number of cycles (de Boer, 1979), and a shift of the PSTH maximum over many cycles is possi-

ble with increasing intensity. Consequently, the possible latency shift expressed in numbers of cycles will increase with CF, since Q_{10dB} increases with CF (Evans, 1972; Versnel et al., 1990). On the other hand, the cycle duration decreases with CF, which makes the absolute shift per cycle smaller for high-CF fibres, which has an opposite effect on the latency shift. Since our results on t_e show that latency shifts with intensity are basically equal for fibres with CF above 2 kHz we conclude that these two opposite effects largely cancel over that frequency range. Our data further suggest that this conclusion can be extended to the 0.5–1 kHz fibres for low click intensities.

Note that since the decrease of tuning quality with intensity is larger in guinea pigs than in cats (Harrison and Evans, 1982) the above first consideration may explain why for high-CF fibres the latency decrease in the guinea pig ($20 \mu\text{s}/\text{dB}$) is larger than the 5–15 $\mu\text{s}/\text{dB}$ observed in the cat data of Kiang et al. (1965) and Antoli-Candela and Kiang (1978) or in chinchillas (less than 5 $\mu\text{s}/\text{dB}$; Salvi et al., 1979).

Amplitude and synchronization of the PSTH

The dynamic range of the A_p -intensity curves varied from 20 to 50 dB which is similar to that for pure-tone rate-intensity curves (Harrison, 1981; Sachs et al., 1989;

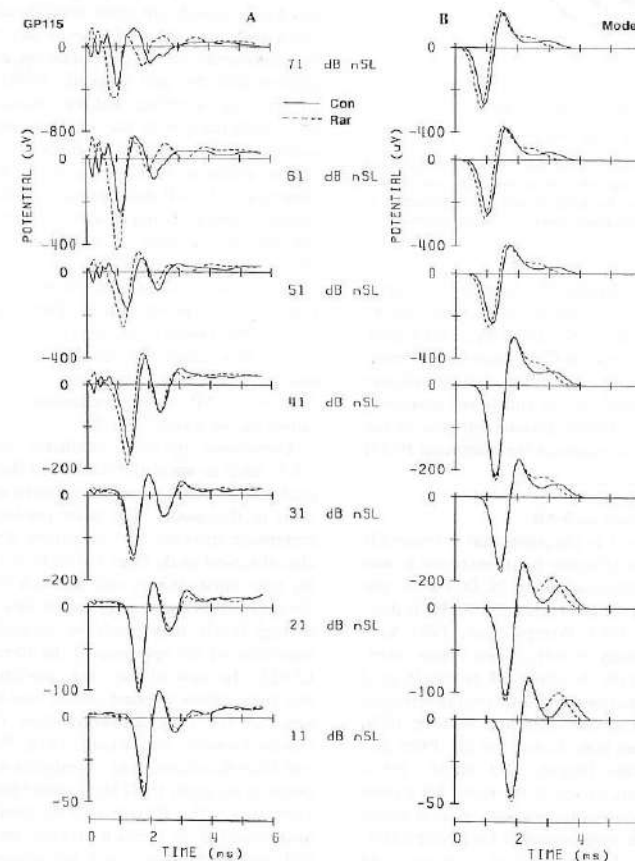


Fig. 8. Compound action potentials (CAPs) to condensation clicks (solid lines) and to rarefaction clicks (dashed lines) for various intensities. (A) CAPs recorded from animal GP115. (B) model simulated CAPs resulting from convolution of the $S(t)$ from Fig. 7 with the elemental unit response.

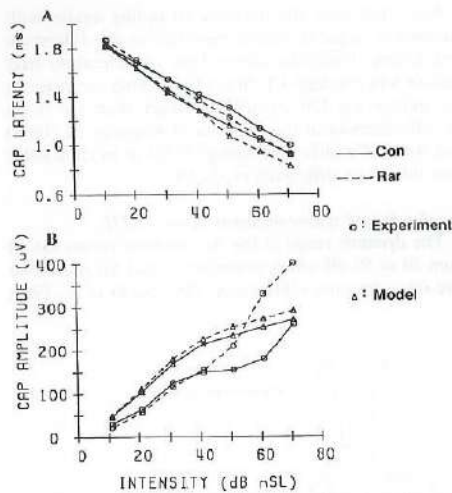


Fig. 9. (A) CAP N_1 latency and (B) amplitude versus intensity curves for experimental data (average over ten guinea pigs; circles) and model simulations (triangles). As in Fig. 8 solid lines correspond to condensation clicks and dashed lines to rarefaction clicks.

Winter et al., 1990). Systematic variations of slopes with SR as reported for such static rate-intensity curves (Sachs et al. 1989; Winter et al., 1990) were not found. In the context of the empirical CAP model it is important to note that the high-CF fibres have shallower slopes of the A_p -intensity curves and lower maximum A_p values than low-CF fibres, presumably due to the relatively small synchronization of the dominant PSTH peaks.

Variations of P-parameters with SR

For various reasons it is plausible that a lower SR corresponds to a lower effective input intensity as was suggested in the presentation of Fig. 2C,D. Firstly, the threshold at CF is inversely correlated with SR (Liberman, 1978; Schmiedt, 1989; Winter et al., 1990; Versnel et al., 1990). Secondly, PSTH latency versus intensity curves run parallel for the three SR groups (Figs. 3 and 5) in a way that is consistent with results reported for a single click level in cats (Kim and Molnar, 1979; Wang, 1979) and guinea pigs (Versnel et al., 1990) and for tone bursts in cats (Rhode and Smith, 1985). Thirdly, the A_p -intensity curves of the three SR groups are shifted along the intensity axis with similar initial slopes (Fig. 3). From a comparison of threshold differences and shifts along the intensity axis of latency and amplitude input-output curves we conclude that the PSTH parameters t_p and A_p show a virtually identical variation with click intensity for all fibres if for low-

and medium-SR fibres the click level is corrected according to their average threshold difference as compared to high-SR fibres.

Sum of PSTHs and CAPs

We have formulated a simple empirical convolution model for the CAP (Eqn. (1)) that is fully based on experimental single-fibre data. The model was based on experimental data of P-parameters available up to 50–60 dB nSL and extrapolated to 70 dB nSL. Cochlear mechanisms that are explicitly or implicitly included in the response behaviour, as reflected by the P-parameters, concern intensity dependent tuning (t_p shift), synaptic mechanisms (SR dependence), IHC saturation and neural refractoriness (t_p shift and limited range for A_p increase). The main simplification of the model concerns the omission of other peaks of the PSTH than the dominant one. In the following discussion we will assume that the unit response (UR) was realistically chosen, and therefore that the extent of agreement of the synthesized with the experimental CAPs is fully accounted for by the PSTH model.

The synthetic CAPs (Figs. 8 and 9) agree with the experimental CAP data in many relevant aspects. The match of absolute amplitudes indicates that (the product of) the estimate of the number of contributing fibres (4000 per octave) and the amplitude of the unit response were realistically chosen. Note that in contrast to other model studies (Elberling, 1976; Bappert et al., 1980; Dolan et al., 1983), but in analogy to Wang (1979), this result was obtained without any a priori matching of model parameters to the CAP amplitude. Also the CAP latency behaviour is correctly reproduced by the model (Fig. 9).

Deviations between synthetic and experimental CAPs such as small differences in the width of the N_1 peak and its onset latency are due to various simplifications in the model. The poor prediction of the CAP amplitude increase for intensities above 50 dB nSL, also observed by de Boer (1975) in his CAP simulations for tone burst stimuli, and the lack of a divergence of the rarefaction and condensation click amplitude curves at high levels, may partly be caused by an incorrect modelling of the response of the fibres with CF above 12 kHz. In view of the click spectrum it is plausible that these fibres respond only to low-frequency components of the click activating their FTC-tail segment (Antoli-Candela and Kiang, 1978; Prijs et al., 1990), and that therefore their thresholds should have been taken at an equal (tail) level rather than monotonically increasing with CF (step v of the model), which would have resulted in a much steeper increase of A_{N1} at high intensities. Since such tail responses strongly depend on the polarity of the click (cf. Fig. 2A) an increased click polarity dependence of the CAP amplitude is then expected as well. Note that the incorpora-

tion in the model of higher thresholds for low-SR fibres in the model, which implies that their dynamic range shifts to higher intensities, appears not to provide a sufficient basis for a large increase of CAP amplitude at high intensities.

The unrealistic reproduction of the N_2 component is primarily due to the omission of secondary peaks in the PSTHs of the high-CF fibres, which appear at a similar time interval after the first peak as the N_2 - N_1 interval (about 1 ms) (Özdamar and Dallos, 1978; Dolan et al., 1983). Additional contributions to the N_2 from the cochlear nucleus cannot fully be excluded (Møller and Jannetta, 1985), but in our view these are unlikely since basically all available unit response data lack an evident N_2 component (Kiang et al., 1976; Prijs, 1986; Charlet de Sauvage et al., 1983; Versnel et al., 1992).

Further exploration of the above discussed aspects and application of the model for the interpretation of click CAPs in noise-damaged cochleas will be the subject of forthcoming studies.

Appendix

In this Appendix details of the phenomenological CAP model are given. The quantities to be described are: 1) model PSTHs that are derived from the P-parameters, 2) the hypothetical fibre distribution, 3) the elemental unit response. The relevant parameters of this model, largely based on the data of Fig. 3, are given in Table II.

Model PSTHs $P(t)$ were generated on the basis of the following assumptions:

TABLE II
PARAMETERS OF THE MODEL PSTH

Parameter	Value	Unit
$c_1(L_0 \leq 45)$	$1.07 + 0.06 m$	ms
$c_1(L_0 > 45)$	$1.09 + 0.15 m$	ms
$c_2(L_0 \leq 45)$	$0.85 + 0.05 m$	
$c_2(L_0 > 45)$	0.90	
c_3	0.014	dB ⁻¹
$t_2(0)$	1.92	ms
$a(f_c \leq 3)$	100	sp/s/dB
$a(f_c > 3)$	40	sp/s/dB
$L_s(f_c \leq 3)$	30	dB
$L_s(f_c > 3)$	40	dB
$b(f_c \leq 3)$	π	(ms) ⁻¹
$b(f_c > 3)$	2.5	(ms) ⁻¹
d	50	dB/octave
σ_r	0.15	ms
$\delta L(r_s \leq 5)$	26	dB
$\delta L(5 < r_s \leq 30)$	10	dB
$\delta L(r_s > 30)$	0	dB

Symbols are explained in the Appendix; $m=1$ for condensation clicks; $m=-1$ for rarefaction clicks; L_0 in dB nSL; parameter values are based on f_c in kHz; r_s in spikes/s.

i) The PSTH of a particular fibre consists of a single peak that is fully determined by the P-parameters t_p , A_p and S_p associated with the characteristic frequency f_c and spontaneous rate r_s of the fibre and with the intensity L_0 and polarity m of the acoustic click stimulus ($m=1$ for condensation, $m=-1$ for rarefaction click).

ii) For a low-CF fibre ($f_c \leq 3$ kHz) $P(t)$ is represented by a half period of a sinusoid, the frequency of which is chosen so as to achieve the correct value for the parameter S_p :

$$P(t_p, A_p, S_p; t) = A_p \cos\{2S_p(t - t_p)\}$$

for $f_c \leq 3$ kHz

with $|t - t_p| \leq \pi/(4S_p)$

For a high-CF fibre a Gaussian probability density function centered around t_p is assumed, which is a simplification (for large γ) of the function $g(t)$ of Eqn. (3):

$$P(t_p, A_p, S_p; t) = A_p \exp\{-\pi S_p^2(t - t_p)^2\}$$

for $f_c > 3$ kHz

iii) The influence of spontaneous rate is incorporated as a virtual shift of effective stimulus level L . Therefore, L is assumed to be different for the three SR groups: $L = L_0 - \delta L(r_s)$. Values of $\delta L(r_s)$ were derived from CF-tone threshold differences between the three SR groups (Versnel et al., 1990).

iv) For the description of the PSTH peak latency t_p as function of CF and SR we use a formulation that was introduced in Versnel et al. (1990):

$$t_p = t_1(f_c; L_0, m) + t_2(r_s; L_0)$$

The first term, depending on CF, is presumed to account for cochlear mechanical delays. The second term, depending on SR, is supposed to reflect synaptic and neural conduction delays. The SR dependence is incorporated by defining the effective stimulus level as described above, thus writing this term as $t_2(r_s; L_0) = t_2(L)$. The magnitude of $t_2(L)$ was taken equal to the PSTH onset delay for 6–12 kHz high-SR fibres for each click intensity, which is supposed to reflect the minimal value for this delay term. Its intensity dependence is described by

$$t_2(L) = t_2(0) \exp(-c_3 L).$$

The term $t_1(f_c; L_0, m)$ was estimated from a regression analysis of $\log(t_p - t_2)$ versus $\log(f_c)$ for $f_c \leq 3$ kHz and was taken constant for $f_c > 3$ kHz, a procedure described in detail in Versnel et al. (1990). This proce-

ture was applied to the data for each click intensity and each polarity separately, and led to a description of the form

$$t_1(f_c, L_0, m) = c_1(L_0, m) f_c^{-c_2(L_0, m)} \quad \text{for } f_c \leq 3 \text{ kHz} \\ = c_1(L_0, m) 3^{-c_2(L_0, m)} \quad \text{for } f_c > 3 \text{ kHz} \\ (\text{constant independent of } f_c)$$

It appeared that changes with intensity of t_1 are relatively small compared to changes in t_2 . Therefore, the constants c_1 and c_2 determining t_1 were pooled over the intensity ranges above and below 45 dB nSL, respectively. Note that the parameterization of latency is the only section of the model where click polarity is explicitly accounted for. For the high-CF fibres, the values of c_1 and c_2 derived from the experimental data imply that below 45 dB t_1 is equal for the two click polarities, for click levels above 45 dB it is 0.1 ms smaller for rarefaction than for condensation clicks.

v) The PSTH peak amplitude A_p is assumed to increase linearly with the effective intensity:

$$A_p(f_c, L) = 0 \quad \text{for } L \leq 0 \\ = a(f_c)L \quad \text{for } 0 \leq L \leq L_s(f_c) \\ = a(f_c)L_s(f_c) \quad \text{for } L > L_s(f_c)$$

with both the increase rate a and saturation intensity L_s varying with CF. Furthermore, A_p is constrained to be smaller than S_p , since the probability of more than one spike in a single PSTH peak is assumed to be zero. L is the effective stimulus level (step iii above). Regarding the prediction of A_p , we made an additional level correction for fibres with $f_c > 12$ kHz to account for the steep click threshold increase (Fig. 1):

$$L = L_0 - \delta L(r_c) - d^2 \log(f_c/12)$$

with d : rate of threshold increase with CF in dB/octave. The frequency bound of 12 kHz rather than 9 kHz, as suggested by the click spectrum (Fig. 1), was chosen because of the relatively low pure-tone thresholds in the 9–12 kHz frequency range; click thresholds actually started increasing at CFs higher than the cut-off frequency in the click spectrum.

vi) S_p is assumed to be invariant with intensity. For CFs below 1 kHz it is described according to Eqn. (5), for low CFs above 1 kHz and for high CFs two constant values are taken that represent the experimental data:

$$S_p(f_c) = \pi f_c \quad \text{for } f_c \leq 1 \text{ kHz} \\ = b(f_c) \quad \text{for } f_c > 1 \text{ kHz}$$

As the next step of the model, summation of model PSTHs over a population of fibres is accomplished to

simulate a compound discharge latency distribution $S(t)$. The fibre population is generated as follows:

vii) There are 100 CF points per octave, logarithmically distributed. We assume that over a characteristic frequency range of 10 octaves there are 2,000 inner hair cells (Burda, 1984) each innervated by 20 afferent fibres (Liberman, 1980). Accordingly, we assume 40 afferent fibres per discrete CF point. For the composition of $S(t)$ the CF range is limited from 0.5 to 24 kHz.

viii) The 40 fibres per CF point are subdivided in high-, medium- and low-SR fibres according to the ratio 25:9:6 (Versnel et al., 1990).

ix) A variability between latencies of different fibres of similar CF and SR is simulated using a Gaussian latency spread with standard deviation σ_t chosen on the basis of standard deviations of t_p for high-CF fibres.

The model PSTHs $P(t)$ of the contributing fibres are added and their sum $S(t)$ is convolved with an elemental unit response (UR) according to Eqn. (1).

x) The UR is defined on the basis of averaged experimental UR data (Versnel et al., 1992):

$$U(t) = U_N/\sigma_N(t-t_0) \exp\left\{\frac{1}{2} - (t-t_0)^2/2\sigma_N^2\right\} \quad \text{for } t < t_0 \\ U(t) = U_P/\sigma_P(t-t_0) \exp\left\{\frac{1}{2} - (t-t_0)^2/2\sigma_P^2\right\} \quad \text{for } t \geq t_0 \quad (6)$$

with the parameter values: $t_0 = -0.06$ ms, $U_N = 0.12$ μ V, $\sigma_N = 0.12$ ms, $U_P = 0.09$ μ V and $\sigma_P = 0.16$ ms.

Acknowledgements

This study was supported by The Netherlands organization for scientific research (NWO) and by the Heinsius Houbolt Fund. The authors thank E. de Boer (ENT Department, University of Amsterdam) for many constructive discussions and comments and A.R. Palmer (Nottingham, U.K.) for valuable suggestions regarding the manuscript.

References

- Antoli-Candela, F.J. and Kiang, N.Y.S. (1978) Unit activity underlying the NI potential. In: R.F. Naunton and C. Fernandez (Eds.), *Evoked electrical activity in the auditory nervous system*, Academic Press, New York, pp. 165–189.
- Bappert, E., Hoke, M., Lütkenhöner, B. and Niestroj, B. (1980) Intensity dependence of the compound action potential and the deconvolution technique. In: M. Hoke, G. Kaufmann and E. Bappert (Eds.), *Scand. Audiol. Suppl.* 11, 45–58.
- Bevington, P.R. (1969) *Data reduction and error analysis for the physical sciences*. McGraw-Hill, New York.

- de Boer, E. (1975) Synthetic whole-nerve action potentials for the cat. *J. Acoust. Soc. Am.* 58, 1030–1045.
- de Boer, E. and de Jongh, H.R. (1978) On cochlear encoding: Potentials and limitations of the reverse-correlation technique. *J. Acoust. Soc. Am.* 63, 115–135.
- de Boer, E. (1979) Travelling waves and cochlear resonance. In: M. Hoke and E. de Boer (Eds.), *Scand. Audiol. Suppl.* 11, 17–33.
- Burda, H. (1984) Guinea pig cochlear hair cell density; its relation to frequency discrimination. *Hear. Res.* 14, 315–317.
- Charlet de Sauvage, R., Cazals, Y. and Aran, J.-M. (1983) Acoustically derived auditory nerve action potentials evoked by electrical stimulation: an estimation of the waveform of single unit contribution. *J. Acoust. Soc. Am.* 73, 616–627.
- Cooper, N.P. (1989) On the peripheral coding of complex auditory stimuli: temporal discharge patterns in guinea-pig cochlear nerve fibres. Ph.D. thesis, University of Keele.
- Dolan, D.F., Teas, D.C. and Walton, J.P. (1983) Relation between discharges in auditory nerve fibres and the whole-nerve response shown by forward masking: an empirical model for the AP. *J. Acoust. Soc. Am.* 73, 580–591.
- Eggermont, J.J. (1976) Electrocochleography. In: W.D. Keidel and W.D. Neff (Eds.), *Handbook of sensory physiology*, Springer Verlag, Berlin, Heidelberg, New York, Vol. V, pp. 626–705.
- Eggermont, J.J., Johannesma, P.I.M. and Aertsen, A.M.H.J. (1983) Reverse-correlation techniques in auditory research. *Quart. Rev. Biophys.* 16, 341–414.
- Elberling, C. (1976) Simulation of cochlear action potentials recorded from the ear canal in man. In: R. Ruben, C. Elberling and G. Salomon (Eds.), *Electrocochleography*, University Park Press, Baltimore, pp. 151–168.
- Evans, E.F. (1972) The frequency response and other properties of single fibres in the guinea pig cochlear nerve. *J. Physiol.* 226, 263–287.
- Evans, E.F. (1979) Single-unit studies of mammalian cochlear nerve. In: H.A. Beagley (Ed.), *Auditory investigation: the technological and scientific basis*, Clarendon Press, Oxford, pp. 324–267.
- Goldstein, M.H. and Kiang, N.Y.S. (1958) Synchrony of neural activity in electric responses evoked by transient acoustic stimuli. *J. Acoust. Soc. Am.* 30, 107–114.
- Goldstein, J.L., Baer, T. and Kiang, N.Y.S. (1971) A theoretical treatment of latency, group delay, and tuning characteristics for auditory nerve responses to clicks and tones. In: M.B. Sachs (Ed.), *Physiology of the auditory system*, National Educational Consultants, Baltimore, 133–141.
- Grashuis, J.L. (1974) The pre-event stimulus ensemble: an analysis of the stimulus-response relation for complex stimuli applied to auditory neurons. Ph.D. thesis, University of Nijmegen.
- Harrison, R.V. (1981) Rate-versus-intensity functions and related AP responses in normal and pathological guinea pig and human cochleas. *J. Acoust. Soc. Am.* 70, 1036–1044.
- Harrison, R.V. and Evans, E.F. (1982) Reverse correlation study of cochlear filtering in normal and pathological guinea pig ears. *Hear. Res.* 6, 303–314.
- Kiang, N.Y.S., Watanabe, T., Thomas, E.C. and Clark, L.F. (1965) Discharge patterns of single fibers in the cat's auditory nerve. M.I.T. Research Monograph No 35, M.I.T. Press, Cambridge Massachusetts.
- Kiang, N.Y.S., Moxon, E.C. and Kahn, A.R. (1976) The relationship of gross potentials recorded from the cochlea to single unit activity of the auditory nerve. In: R. Ruben, C. Elberling, G. Salomon (Eds.), *Electrocochleography*, Baltimore University Park Press, Baltimore, 95–115.
- Kim, D.O. and Molnar, C.E. (1979) A population study of cochlear nerve fibers: comparison of spatial distributions of average-rate and phase-locking measures of responses to tones. *J. Neurophysiol.* 42, 16–30.

- Liberman, M.C. (1978) Auditory-nerve response from cats raised in a low-noise chamber. *J. Acoust. Soc. Am.* 63, 442–455.
- Liberman, M.C. (1980) Morphological differences among radial afferent fibers in the cat cochlea: an electron-microscopic study of serial sections. *Hear. Res.* 3, 45–63.
- Lütkenhöner, B., Hoke, M. and Bappert, E. (1980) Effect of recovery properties on the discharge pattern of auditory nerve fibres. In: M. Hoke, G. Kaufmann and E. Bappert (Eds.), *Cochlear and Brainstem Evoked Response Audiometry and Electrical Stimulation of the VIIIth Nerve*, Scand. Audiol. Suppl. 11, 25–43.
- Møller, A.R. (1977) Frequency selectivity of single auditory nerve fibers in response to broadband noise stimuli. *J. Acoust. Soc. Am.* 62, 135–142.
- Møller, A.R. (1983) Frequency selectivity of phase-locking of complex sounds in the auditory nerve of the rat. *Hear. Res.* 11, 267–284.
- Møller, A.R. (1985) Origin of latency shift of cochlear nerve potentials with sound intensity. *Hear. Res.* 17, 177–189.
- Møller, A.R. (1986) Effect of click spectrum and polarity on round window N_1N_2 response in the rat. *Audiology* 25, 29–43.
- Møller, A.R. and Jannetta, P.J. (1985) Neural generators of the auditory brainstem response. In: J.T. Jacobson (Ed.), *The auditory brainstem response*, Taylor & Francis, London, pp. 13–31.
- Ozdamar, Ö. and Dallos, P. (1978) Synchronous responses of the primary auditory fibers to the onset of tone bursts and their relation to compound action potentials. *Brain Res.* 155, 169–175.
- Peake, W.T. and Kiang, N.Y.S. (1962) Cochlear responses to condensation and rarefaction clicks. *Biophys. J.* 2, 23–34.
- Pfeiffer, R.R. and Kim, D.O. (1972) Response patterns of single cochlear nerve fibers to click stimuli: descriptions for cat. *J. Acoust. Soc. Am.* 52, 1669–1677.
- Prijs, V.F. and Eggermont, J.J. (1980) On peripheral auditory adaptation I. Dependence on the recording site. *Acustica* 44, 283–300.
- Prijs, V.F. (1986) Single-unit response at the round window of the guinea pig. *Hear. Res.* 21, 127–133.
- Prijs, V.F., Keijzer, J., Schoonhoven, R. and Versnel, H. (1990) The sting is in the tail. In: P. Dallos, C.D. Geisler, J.W. Matthews, M.A. Ruggero and C.R. Steeles (Eds.), *The Mechanics and Biophysics of Hearing*, Springer-Verlag, Berlin, Heidelberg, pp. 154–161.
- Rhode, W.S. and Smith, P.H. (1985) Characteristics of tone-pip response patterns in relationship to spontaneous rate in cat auditory nerve fibres. *Hear. Res.* 18, 159–168.
- Robles, L., Rhode, W.S. and Geisler, C.D. (1976) Transient response of the basilar membrane measured in squirrel monkeys using the Mössbauer effect. *J. Acoust. Soc. Am.* 59, 926–939.
- Rose, J.E., Hind, J.E., Anderson, D.J. and Brugge, J.F. (1971) Some effects of stimulus intensity on response of auditory nerve fibers in the squirrel monkey. *J. Neurophysiol.* 34, 685–699.
- Ruggero, M.A., Rich, N.C. and Recio, A. (1991) Basilar membrane responses to clicks. In: Y. Cazals, L. Demany, and K.C. Horner (Eds.), *Auditory Physiology and Perception*, Proc. 9th Int. Symp. Hear., Carcans, France, 1991; 7 pp., in press.
- Sachs, M.B., Winslow, R.L. and Sokolowski, B.E.A. (1989) A computational model for rate-level functions from cat auditory-nerve fibers. *Hear. Res.* 41, 61–70.
- Salvi, R.J., Henderson, D. and Hamernik, R.P. (1979) Single auditory nerve fiber and action potential latencies in normal and noise-treated chinchillas. *Hear. Res.* 1, 237–251.
- Schmiedt, R.A. (1989) Spontaneous rates, thresholds and tuning of auditory-nerve fibers in the gerbil: Comparisons to cat data. *Hear. Res.* 42, 23–36.
- Sellick, P.M., Patuzzi, R.B. and Johnstone, B.M. (1982) Measurement of basilar membrane motion in the guinea pig using the Mössbauer technique. *J. Acoust. Soc. Am.* 72, 131–141.
- Versnel, H., Prijs, V.F. and Schoonhoven, R. (1990) Single-fibre

responses to clicks in relationship to the compound action potential in the guinea pig. *Hear. Res.* 46, 147-160.

Versnel, H., Prijs, V.F. and Schoonhoven, R. (1992) Round-window recorded potential of single-fibre discharge (unit response) in normal and noise-damaged cochleas. *Hear. Res.* 59, 157-170.

Wang, B. (1979) The relation between the compound action poten-

tial and unit discharges of the auditory nerve. Doctoral dissertation, Dept. of Electrical Engineering and Computer Science, M.I.T., Cambridge, MA.

Winter, I.A., Robertson, D. and Yates, G.K. (1990) Diversity of characteristic frequency rate-intensity functions in guinea pig auditory nerve fibres. *Hear. Res.* 45, 191-202.

Chapter IV

Round-window recorded potential of single-fibre discharge (unit response) in normal and noise-damaged cochleas

Huib Versnel, Vera F. Prijs and Ruurd Schoonhoven

Summary

Unit responses (URs) of eighth-nerve fibres have been determined at the round window by spike-triggered averaging in both normal and pathological guinea pig cochleas. The pathology was mainly noise-induced damage. The URs have been analysed with respect to their dependence on the fibre's threshold, characteristic frequency (CF) and spontaneous rate (SR). The results from normal cochleas confirmed earlier data (Prijs, 1986): the UR has a diphasic waveform and the amplitude of its negative first peak is about 0.1 μ V. From the six parameters (amplitude, latency, and width of the two peaks) by which the UR was described only the amplitude of the positive peak showed a significant variation with CF: a small decrease with increasing CF (CF-range 0.1 to 20 kHz). This finding may possibly be caused by oscillations in the spike-triggered average for low CFs. URs for most low- and medium-SR fibres were found to be large (greater than 0.3 μ V). However, this result is interpreted as an artefact caused by synchrony of fibre spontaneous activity. In damaged cochleas only slight changes of the UR were found: the waveform duration became significantly shorter and on some occasions the positive peak increased in amplitude, but latency and amplitude of the negative component of the UR remained unchanged.

Key words: Unit response; Noise trauma; Single fibre; Guinea pig

This chapter has been published in *Hearing Research*, 59: 157-170 (1992).

Round-window recorded potential of single-fibre discharge (unit response) in normal and noise-damaged cochleas

Huib Versnel, Vera F. Prijs and Ruurd Schoonhoven

ENT Department, University Hospital, Leiden, The Netherlands

(Received 11 February 1991; accepted 19 December 1991)

Unit responses (URs) of eighth-nerve fibres have been determined at the round window by spike-triggered averaging in both normal and pathological guinea pig cochleas. The pathology was mainly noise-induced damage. The URs have been analysed with respect to their dependence on the fibre's threshold, characteristic frequency (CF) and spontaneous rate (SR). The results from normal cochleas confirmed earlier data (Prijs, 1986): the UR has a biphasic waveform and the amplitude of its negative first peak is about 0.1 μ V. From the six parameters (amplitude, latency, and width of the two peaks) by which the UR was described only the amplitude of the positive peak showed a significant variation with CF: a small decrease with increasing CF (CF-range 0.1 to 20 kHz). This finding may possibly be caused by oscillations in the spike-triggered average for low CFs. URs for most low- and medium-SR fibres were found to be large (greater than 0.3 μ V). However, this result is interpreted as an artefact caused by synchrony of fibre spontaneous activity. In damaged cochleas only slight changes of the UR were found: the waveform duration became significantly shorter and on some occasions the positive peak increased in amplitude, but latency and amplitude of the negative component of the UR remained unchanged.

Unit response; Noise trauma; Single fibre; Guinea pig

Introduction

Cochlear function in human subjects or animals can be assessed by measuring the compound action potential (CAP) as recorded by electrocochleography. In order to provide a rational basis for the use of the CAP as a diagnostic tool many studies have investigated the mechanism of generation of the CAP (Goldstein and Kiang, 1958; Biondi et al., 1975; de Boer, 1975; Kiang et al., 1976; Hoke et al., 1979; Wang, 1979; Prijs and Eggermont, 1981; Dolan et al., 1983; Charlet de Sauvage et al., 1987). As formulated by Goldstein and Kiang (1958), the CAP can be conceived as resulting from a convolution of a discharge probability distribution function across all fibres in the auditory nerve and a unit response (UR). In this formulation the unit response, being the contribution of one nerve fibre action potential to the CAP, is assumed to be invariant across fibres i.e. invariant with characteristic frequency (CF) and spontaneous rate (SR) of the fibres.

In many simulations of the compound action potential some diphasic UR was proposed (Biondi et al., 1975; de Boer, 1975; Dolan et al., 1983). From experimental data UR can be estimated either directly (Kiang

et al., 1976; Wang, 1979; Prijs, 1986; Evans, 1987) or indirectly (Hoke et al., 1979; Charlet de Sauvage, 1983). From CAP simulations using different UR estimations it appeared that the exact shape of the waveform of the UR is quite critical for the convolution result (Hoke et al., 1979; Schoonhoven et al., 1989), and therefore the estimate of the UR should represent the actual UR as closely as possible.

There have only been a few experimental estimates of the UR. These estimates have been determined directly by spike-triggered averaging of the round window potential (in cats: Kiang et al., 1976; Wang, 1979; Evans, 1987; in guinea pigs: Prijs, 1986) or indirectly by acoustical masking of the whole-nerve response to electrical stimulation (in guinea pigs: Charlet de Sauvage et al., 1983) or acoustical stimulation (in humans: Hoke et al., 1979). For the normal cochlea the directly obtained experimental results revealed a diphasic UR waveform, almost independent of the fibre's CF (Wang, 1979; Prijs, 1986) or fibre's SR (Wang, 1979) and a larger inter-animal than intra-animal variation. Stretching of the nerve induced a change of the UR for some fibres (Prijs, 1986).

We present a study on the influence of cochlear damage on the UR. In addition, we extensively examined the (in)variance of the UR with CF and SR in the guinea pig. Cochlear pathology was induced experimentally by exposure to loud sound. Our determina-

tion of the contribution of a single-fibre discharge to the potential at the round window was performed using the spike-triggered averaging method of Kiang et al. (1976). This method yields a unit response under the assumption that the firings of the individual fibres are independent. Violation of this assumption was found for very sensitive fibres (Evans, 1987) and explained by synchronization of discharges to animal-generated or external noise. Results in this study indicate that this assumption can also be violated for low and medium SR fibres (SR below 30 spikes/s).

In order to study the dependence of the UR on CF, SR and hearing threshold, we define six parameters of the UR: the latency, amplitude and width of the negative first phase and of the positive second phase of the UR. For the benefit of mathematical CAP analyses an elemental unit response, representing the invariant UR, is proposed on the basis of individual URs.

Methods

Physiological experiments

Acute experiments were performed on 20 healthy, female, albino guinea pigs weighing 200–800 g. Nine of these had normal hearing. Seven guinea pigs had been exposed under anaesthesia to a tone of 6 kHz and 121–123 dB SPL for 2 h in a closed sound box with loud speaker (Fane type Classic 10–125T). Four others had been exposed to a tone in the range 1.4–1.7 kHz and 112–122 dB SPL, also for 2 h. Single-fibre experiments were performed on the noise-exposed animals after a survival time of 14–123 days.

Details of the animal preparation and of the equipment for sound stimulation and signal recording have been described in a previous paper (Versnel et al., 1990). The main points of the methods are given briefly here.

Premedication consisted of atropine sulphate (25 μ g/kg) and Thalamonal (1.6 cc/kg) and anaesthesia was obtained with Nembutal® (27 mg/kg). A silver ball electrode was positioned on the round window for the whole-nerve and unit-response recordings. The CAP threshold audiogram, which was used to assess the condition of the cochlea (Versnel et al., 1990), was determined using tone bursts of 4 ms plateau and 2 cycles rise/fall time. The cochlear nerve was approached intracranially (Evans, 1979). During the exposure of the auditory nerve the condition of the cochlea was checked by monitoring the CAP N_1 and N_2 . Single-fibre responses were recorded using micropipettes filled with 2.7 M KCl or 0.5 M KCl/0.1 M TRIS buffer.

The frequency and intensity of the stimuli were controlled by a DEC PDP 11/10 computer, connected to an oscillator (Krohn-Hite 4140R) and programmable

attenuators (Grason-Stadler model 1284). Single-fibre signals were stored on magnetic tape (datarecorder TEAC XR-510WB, recording bandwidth 0–6.25 kHz) and also led to the PDP-11/10 via a spike discriminator (Mentor N-750). The simultaneously generated round-window signals were amplified ($5,000 \times$ – $25,000 \times$) and stored on tape.

After contacting a fibre, a frequency threshold curve (FTC), using a threshold tracking algorithm (Evans, 1979), and its SR were first determined. The unit response at the round window was recovered by spike-triggered averaging (Kiang et al., 1976), i.e. the spike recorded with the microelectrode served as trigger for averaging of the round-window potential registered with the gross electrode. The trigger pulses to the computer were generated by the spike discriminator, initiated when the leading phase of the spike crossed a preset voltage value. The time window of analysis extended 3 ms both before and after the trigger, consisting of 200 sample points. The number of triggers (indicated by K) was usually of the order of 10,000, which were required to obtain a sufficient signal-to-noise ratio; occasionally, fewer spikes were sufficient. The URs were derived on-line as well as off-line from the signal on tape. For the on-line derivations of the URs we used continuous spontaneous activity. For the off-line derivations we not only used sections of tape corresponding to the on-line determination, but also the periods between successive stimuli (here: clicks; cf. Versnel et al., 1992). The analysis periods were separated from those in which spike times were correlated with the stimulus by excluding time windows, 10 ms after the stimulus trigger for high-CF fibres (CFs above 3 kHz) and 20–30 ms for low-CF fibres. Most round-window signals from tape were high-pass filtered (cut-off frequency 170 Hz) in order to eliminate slow potential components.

Data analysis

As parameters of the UR we used the latencies τ_N and τ_P , the amplitudes U_N and U_P , and measures of widths σ_N and σ_P , of the negative (N) and positive (P) wave peaks of the UR. The two latency parameters were referred to the spike-trigger. The latencies and amplitudes were visually determined using a computer-terminal cursor; slight smoothing was sometimes applied to noisy signals. The width parameters were derived by a least-squares fitting procedure (Bevington, 1969). The function used in this fitting procedure was the negative of the first derivative of an asymmetrical distribution function, constructed from two Gaussian distribution functions, with different amplitudes and standard deviations (Schoonhoven et al., 1989).

The fitting function, denoted as $G(t)$, is defined by:

$$G(t) = c(t - t_0) \exp\left\{-\frac{(t - t_0)^2}{2\sigma^2}\right\} \quad (1)$$

Correspondence to: Huib Versnel (Present address) Systems Research Center, University of Maryland, College Park, MD 20742, USA. Fax: 0301/314-9920.

with

$$c = c_N \text{ and } \sigma = \sigma_N \text{ for } t < t_0$$

$$c = c_p \text{ and } \sigma = \sigma_p \text{ for } t \geq t_0$$

The function $G(t)$ contains five fit parameters. Two of these, the standard deviations σ_N and σ_p , serve as measures of peak width. Parameters $c_{N(p)}$ are related to $U_{N(p)}$ as follows: $c_{N(p)} = \sqrt{e} U_{N(p)} / \sigma_{N(p)}$; t_0 is related to $\tau_{N(p)}$ according to: $\sigma_{N(p)} = |\tau_{N(p)} - t_0|$, for a proper fit $\sigma_N + \sigma_p$ should equal $\tau_p - \tau_N$.

The fibres were divided into low-threshold (normal) and high-threshold (abnormal) fibres. Fibres with a threshold at CF raised by more than 2 S.D. from the mean values in an extensive sample of normal-hearing guinea pigs (see Fig. 1 in Versnel et al., 1990) were considered abnormal. In order to analyse the dependence of the UR on cochlear condition, we distinguished three groups of URs, denoted by Roman numerals: URs of low-threshold fibres in normal-hearing animals (group I), URs of low-threshold fibres from hearing-impaired animals (group II) and URs of high-threshold fibres from hearing-impaired animals (group III). In analysing the possible relation of UR with SR, we distinguished, as usual, three SR groups: low, medium and high SR, with boundaries 5 and 30 sp/s chosen according to Versnel et al. (1990).

Results

Unit responses were recorded in 20 guinea pigs; data with an insufficient signal-to-noise ratio, according to criteria given below, were left out from further analysis. The properties of the unit responses as described in this study are based on qualified UR estimates from 114 fibres. In 9 normal-hearing animals we determined unit responses for 20 fibres on-line. By off-line analysis of the tape recordings this number was extended to 33. All fibres of this group (group I) had normal thresholds. In 11 hearing-impaired guinea pigs we determined URs on-line for 30 fibres which by off-line analysis was extended to 81 fibres. From these 81 fibres 35 had a normal threshold (group II) and 46 had a raised threshold (group III). All determinations of URs presented here were based on spontaneous discharges. For some low- or medium-SR fibres we tried to recover a unit response by enhancing the spike rate with a CF tone above threshold. However, these attempts did not succeed since large cochlear microphonics in the averaged round-window potential exceeded the single-fibre response, irrespective of the fibre's CF. As a consequence, a UR could only be determined for few low- or medium-SR fibres; remarkably, in these cases a low number of averages (of the

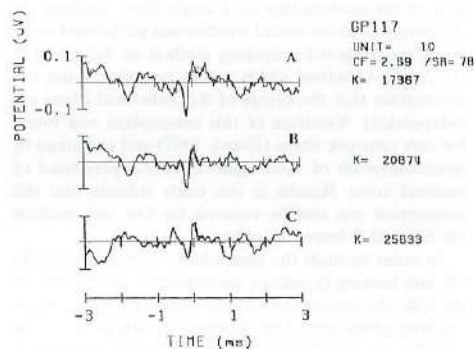


Fig. 1. Unit responses determined on-line (A) and off-line (B-C), and curves fitted to the URs. The fitted curves (dotted lines) are described by Eqn. (1). The abscissa zero corresponds to the spike-trigger time. Numbers of spikes used for the averaging (K) are indicated in the plot. (A) UR determined on-line. (B) UR determined off-line from the tape-recording track that corresponds to the on-line determined UR. (C) UR determined off-line by using sections of the tape recording between click presentations.

order of 1,000) appeared to be sufficient to obtain a fair signal-to-noise ratio. Furthermore, for low-CF fibres we sometimes observed oscillations which disturbed the UR waveform to some degree.

Fig. 1 shows three representative UR estimations for one fibre. The first trace (Fig. 1A) shows the on-line response, the other two (Figs. 1B, C) show off-line responses determined from different sections of tape. Trace B represents the off-line UR determined from the tape recordings of the on-line responses used for the UR in trace A. It appeared that the two UR estimations were similar over the whole time window. The absence of high-frequency components in the off-line signal was due to the limited recording bandwidth (see methods section). The off-line response in trace C, representing the response from inter-stimulus periods, was similar to the other two UR estimations (1A and 1B) with respect to the two main aspects: the diphasic waveform and the magnitude. On the whole, comparison of the UR parameters for the three different UR estimations showed that there were no significant differences between on-line and off-line recording results. In our further analysis we mainly deal with the off-line determined URs.

The function $G(t)$ (see Eqn. (1)) was fitted to each spike-triggered average that we collected. For averages with a fair signal-to-noise ratio (i.e. a ratio greater than 3) satisfactory curve fits could be obtained. A low signal-to-noise ratio was found in cases in which a small number (K) of spikes was available for the averaging process or in which the guinea pig was relatively unstable (e.g. due to extensive respiratory movements).

Fig. 1 shows examples of the fitting procedure (dotted lines). It can be seen that these functions agreed well with the URs, in particular with the negative components. If the fitted function deviated markedly, as judged by eye, the UR estimates were excluded from further analysis. This exclusion affected 22% of the total amount of averages determined with $K \geq 10,000$ and 45% of those determined with $K < 10,000$. For high CFs, where oscillations in the spike-triggered average did not occur, these numbers were more favourable.

Fig. 2 shows examples of URs for different fibres in the normal hearing guinea pig GP117. Most URs had negative peak amplitudes of about $0.1 \mu\text{V}$. Examples of this UR group are plotted in the left panel (Fig. 2A), showing a better signal-to-noise ratio when K was

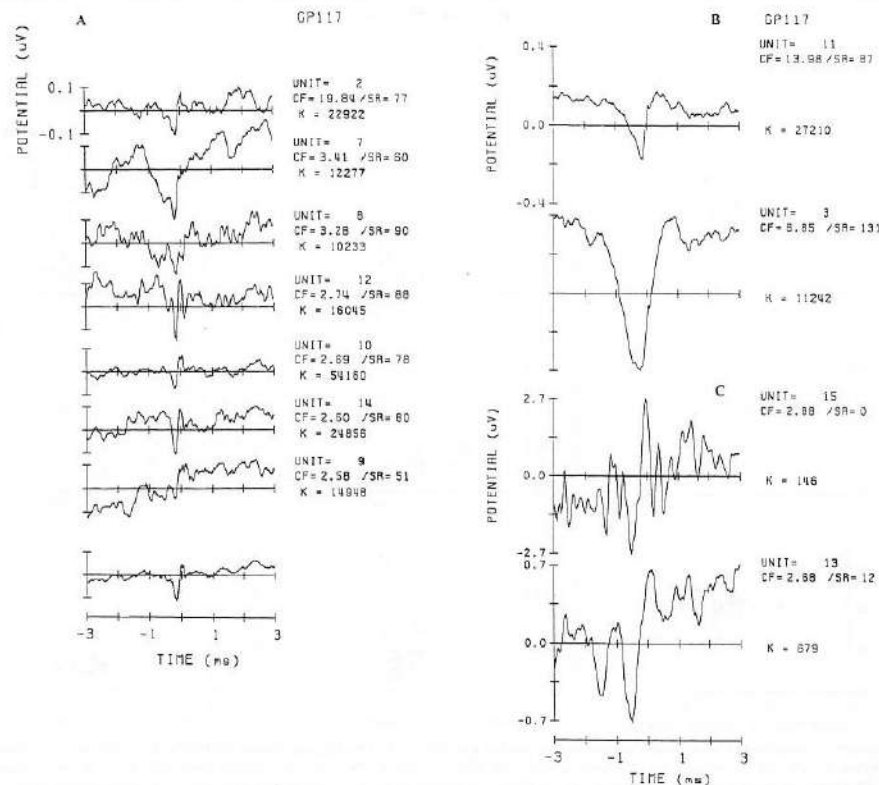


Fig. 2. URs determined in one normal guinea pig. K is the number of spikes used for the averaging. (A) Normal URs. The signal plotted at the bottom reflects the grand average, weighted according to numbers K, of the 7 above-plotted URs. The dotted line represents the fitted curve. (B) Large URs of high-SR fibres. (C) Large URs of low- and medium-SR fibres.

larger. URs of this group clearly show a diphasic waveform; small extra peaks which could point to another waveform are not reproducible. In some low-CF fibres we observed oscillatory patterns (e.g. URs of units 8 and 12 shown in Fig. 2A). Under the assumption that similar URs reflected estimates of one fibre-independent UR, they were averaged in order to obtain an animal-specific UR with a better signal-to-noise ratio. For GP117 this grand average, weighted according to the numbers K involved in the averaging of the individual URs, is shown in the bottom panel of Fig. 2A.

As shown in Fig. 2B and C some fibres had UR negative peak amplitudes (0.3 to $2.5 \mu\text{V}$) which were considerably larger than $0.1 \mu\text{V}$. Large URs were particularly prevalent for high-SR fibres with very low

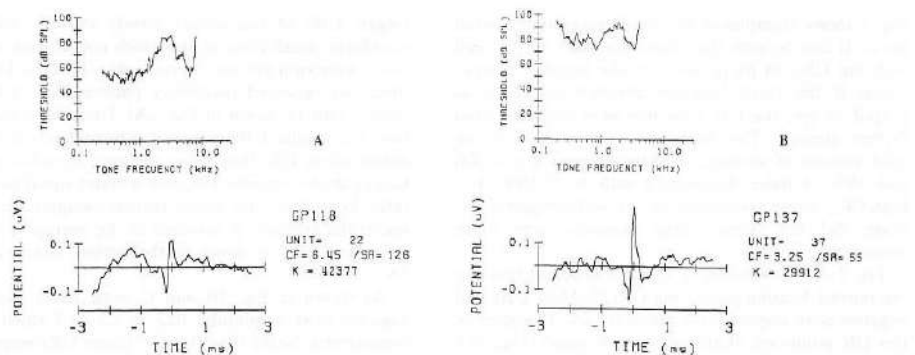


Fig. 3. Unit responses of fibres from noise-damaged cochlear regions, with the associated frequency threshold curves (FTCs) (upper panels). The URs were determined off-line from sections of tape-recording of long silent periods (as in Fig. 1B) and periods between successive click presentations (as in Fig. 1C). K is the number of spikes used for the averaging. (A) UR and FTC of a high-threshold fibre of animal GP118. This animal had been exposed to a 6 kHz, 122 dB SPL tone. (B) UR and FTC of a high-threshold fibre of GP137. This animal had been exposed to a 1.7 kHz, 122 dB SPL tone.

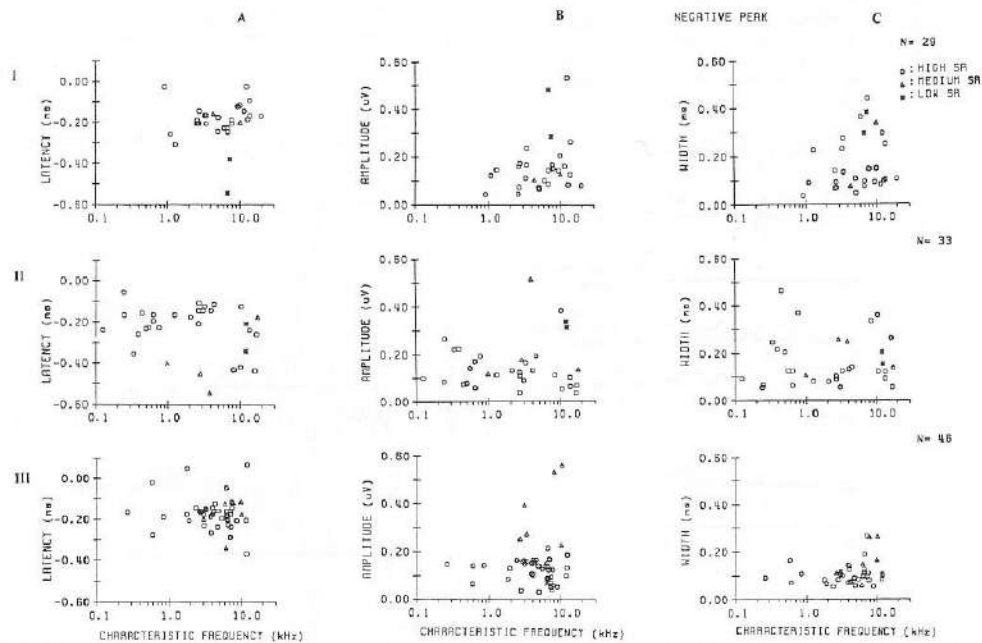


Fig. 4. Latency τ_N , amplitude U_N and width σ_N of negative peak of UR versus CF. The data are plotted for URs with τ_N between -0.6 and 0.1 ms, U_N below $0.6 \mu\text{V}$ and σ_N below 1 ms. The symbols represent different SRs: circles represent high-SR fibres (SR above 30 sp/s), triangles medium-SR fibres and asterisks low-SR (SR below 5 sp/s) fibres. (A) Scatter plots of τ_N . (B) Scatter plots of U_N . (C) Scatter plots of σ_N . Top row of (A), (B) and (C): fibres of normal-hearing guinea pigs (group I); middle row: low-threshold fibres of hearing-impaired guinea pigs (group II); bottom row: high-threshold fibres of hearing-impaired animals (group III).

thresholds, but large URs were also found for low- or medium-SR fibres with normal threshold.

Fig. 3 shows examples of URs of two high-threshold fibres (group III) from acoustically traumatized animals. The tips of the associated frequency threshold curves (FTC) were elevated by 40–60 dB relative to the normal fibre's thresholds (15 ± 11 dB SPL, Versnel et al., 1990). The UR plotted in the left panel (Fig. 3A) resembled normal URs of normal guinea pigs (as, for example, in Fig. 2A): it had similar delay, amplitude and (diphasic) waveform. The UR shown in the right panel (Fig. 3B) had a normal negative component, but its peak-to-peak ratio was larger than normal: U_p/U_N was 1.3 where it is normally smaller than 1. In addition, its waveform had a triphasic character.

In the following sections we first describe the URs from the normal-threshold fibres (groups I and II), i.e. fibres from normal hearing animals (group I) and fibres with normal threshold in animals with noise trauma (group II). Subsequently, the URs for the high-threshold fibres from the noise-damaged cochleas are presented (group III). Due to the frequencies of the damaging sound (in most experiments 6 kHz), in group III high CFs were better represented than low CFs.

UR in normal-threshold fibres: relationship with CF

In Fig. 4 the distributions of latency (τ_N), amplitude (U_N) and width (σ_N) of the negative phase of UR are shown in relation to CF. For the normal fibres (I and II) these parameters did not vary significantly with CF. From the corresponding positive-peak parameters (τ_p , U_p and σ_p) only the amplitude showed a significant variation with CF (Fig. 5, groups I and II): U_p decreased slightly but significantly with CF.

UR in normal-threshold fibres: relationship with SR

We could collect only few data for low- and medium-SR fibres, so these data have to be interpreted with caution. Clear UR responses could be obtained with a small number of spike-triggered averages, typically $K < 1,000$. We verified that for a high-SR fibre which had a representative UR when K was large, the average using a small K did not yield a discernable UR.

Medium- and low-SR fibres (denoted with triangles and asterisks, respectively in Figs. 4 and 5) had very large amplitudes more frequently than high-SR fibres: while very large URs ($U_N > 0.3 \mu\text{V}$) were found in 3 out of 53 high-SR fibres, 2 out of 7 medium and 7 out

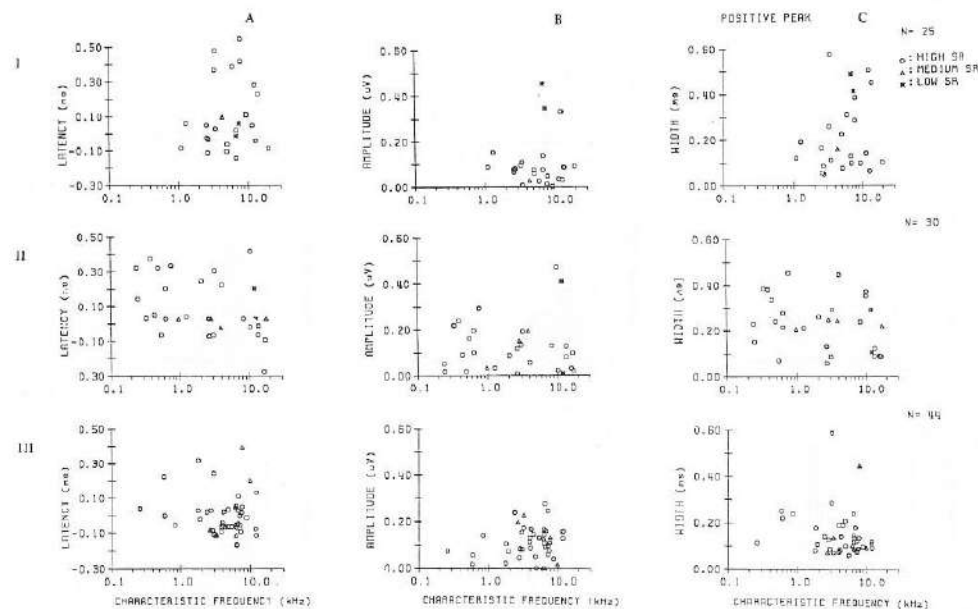


Fig. 5. Parameters of the positive peak τ_p , U_p and σ_p versus CF. Symbols and arrangement as in Fig. 4. The data correspond to the same URs as presented in Fig. 4, apart from URs of which σ_p could not be determined by curve fitting. (A) τ_p . (B) U_p and (C) σ_p . Top row: group I; middle row: group II; bottom row: group III.

of 8 low-SR fibres gave large URs. Moreover, in high-SR fibres these large URs were only found when their threshold was very low (below 10 dB SPL). Extremely large URs, with U_N above 1.0 μV , were found for four low-SR fibres. On the average the widths σ_N and σ_p and the latency τ_N were larger when the amplitude was larger. We checked that the large waveforms were present in all sections of the recordings and were detectable with a K value of about 100.

UR in normal-threshold fibres: overview of normal parameter values

For most fibres τ_N was -0.25 to -0.15 ms, the amplitude U_N was in the range of 0.1 to 0.2 μV , and the width σ_N was between 0.05 and 0.15 ms. The positive peak had a latency between -0.1 and 0.1 ms for the majority of the fibres. The amplitude U_p was of the order of 0.1 μV , as was U_N . The positive UR peak was broader than the negative one; σ_p varied from 0.05 to 0.3 ms.

Distribution histograms of the parameters were constructed (Figs. 6 and 7) for the high-SR fibres, arranged according to the three different fibre groups. Peaks with extreme values ($U_N > 0.6 \mu\text{V}$; $\tau_N < -0.6$ ms; $\sigma_N > 1$ ms) were excluded for the sake of clarity.

UR in normal-threshold fibres: elemental UR waveform for CAP simulation

We used the function $G(t)$ to describe an elemental UR-waveform for normal guinea-pig fibres. Its parameters were chosen on the basis of average values as presented in Tables I and II. The data used here are restricted to peaks with $U_N < 0.3 \mu\text{V}$ for high-SR fibres and $U_N < 0.5 \mu\text{V}$ for low- and medium-SR fibres in order to exclude extreme values. The width parameters were slightly corrected to account for $\tau_p - \tau_N$; $t_0 = -0.06$ ms, $U_N = 0.12 \mu\text{V}$, $\sigma_N = 0.12$ ms, $U_p = 0.09 \mu\text{V}$ and $\sigma_p = 0.16$ ms. The resulting model UR is presented in Fig. 8.

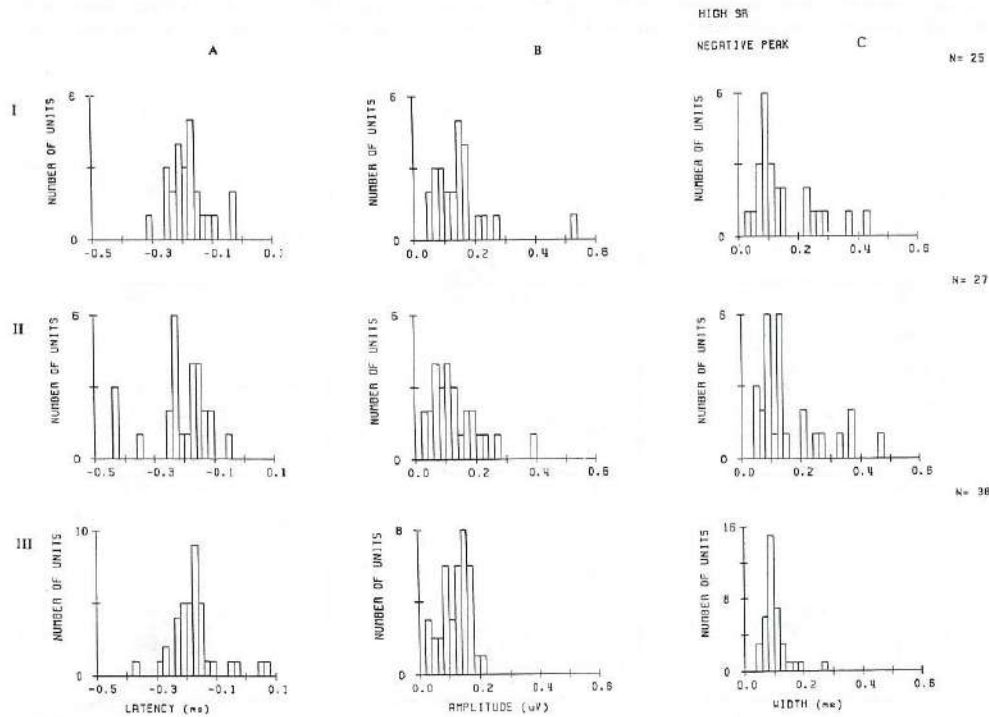


Fig. 6. Distribution histograms of τ_N , U_N and σ_N of high-SR fibres. Data as in Fig. 4. (A) Histograms of τ_N , bin width is 20 μs ; (B) histograms of U_N , bin width is 20 nV; (C) histograms of σ_N , bin width is 20 μs . Top row: group I; middle row: group II; bottom row: group III.

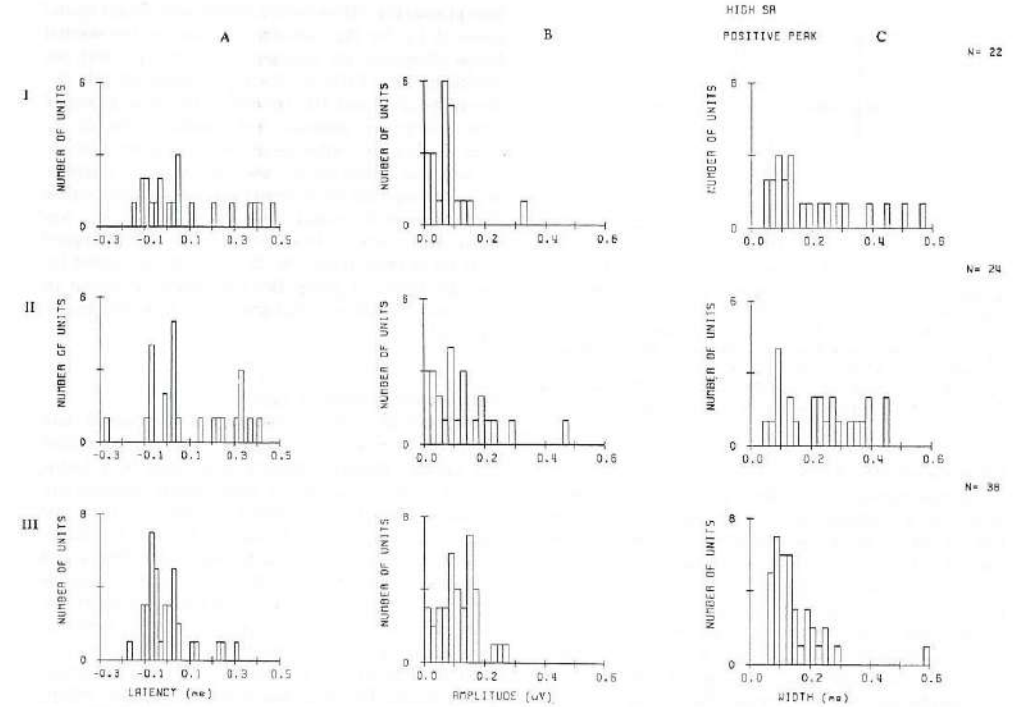


Fig. 7. Distribution histograms of τ_p , U_p and σ_p of high-SR fibres. Data as in Fig. 5, arrangement as in Fig. 6. (A) Histograms of τ_p , (B) histograms of U_p , (C) histograms of σ_p . Top row: group I; middle row: group II; bottom row: group III.

TABLE I
LATENCY, AMPLITUDE AND WIDTH OF NEGATIVE COMPONENT OF UNIT RESPONSE

SR	τ_N	S.D.	U_N	S.D.	σ_N	S.D.	N
Group I							
≥ 30 sp/s	-0.18	0.06	0.13	0.06	0.15	0.10	24
5-30 sp/s	-0.18	0.02	0.12	0.01	0.21	0.13	2
< 5 sp/s	-0.46	0.08	0.39	0.10	0.34	0.04	2
Group II							
≥ 30 sp/s	-0.21	0.09	0.12	0.06	0.15	0.11	26
5-30 sp/s	-0.34	0.12	0.14	0.02	0.17	0.07	3
< 5 sp/s	-0.27	0.07	0.32	0.01	0.18	0.03	2
Group III							
≥ 30 sp/s	-0.17	0.08	0.12	0.05	0.10	0.04	38
5-30 sp/s	-0.18	0.08	0.23	0.10	0.12	0.03	6
< 5 sp/s	-	-	-	-	-	-	-

Parameters of the negative UR component for fibres in normal-hearing guinea pigs (group I), and for fibres with normal thresholds (group II) and with abnormal thresholds (group III) in hearing-impaired guinea pigs. Only URs with τ_N between -0.6 and 0.1 ms and with U_N below 0.3 μV (or 0.5 μV for low/medium-SR fibres) are considered. Latency τ_N and measure of width σ_N are given in ms. Amplitude U_N is given in μV . S.D.: standard deviation; N: number of fibres.

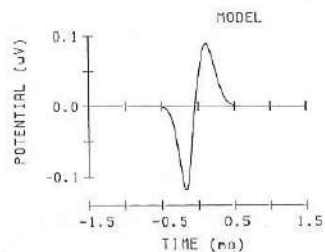


Fig. 8. Model unit response according to the function $G(t) = c(t - t_0)\exp[-(t - t_0)^2 / 2\sigma^2]$ with $c = c_N$ and $\sigma = \sigma_N$ for $t < t_0$ and $c = c_P$ and $\sigma = \sigma_P$ for $t \geq t_0$ (Eqn. (1)). Parameters $c_{N(P)}$ are related to $U_{N(P)}$, as follows: $c_{N(P)} = \sqrt{c} U_{N(P)} / \sigma_{N(P)}$; t_0 is related to τ_N according to: $t_0 = \tau_N + \sigma_N$. Parameters were chosen on the basis of the experimental data (Tables I and II): $\tau_N = -0.18$ ms, $U_N = 0.12$ μ V, $\sigma_N = 0.12$ ms, $U_P = 0.09$ μ V, $\sigma_P = 0.16$ ms. Note that the integral of the UR equals zero because $U_N\sigma_N = U_P\sigma_P$.

UR in high-threshold fibres

For the high-threshold fibres none of the six parameters varied significantly with CF (Figs. 4 and 5). The UR of those fibres showed minor deviations from normal. After a more close inspection the following details are to be mentioned. The distributions of τ_N , U_N and σ_N had similar modal values for normal and pathological fibres. On the average the negative UR peak was narrower for pathological than for normal fibres, but the modal value of σ_N was not shifted. The σ_N distributions of the normal fibres had a larger spread toward higher values.

For pathological fibres τ_P was significantly shorter (by 0.1 ms) than for normal fibres (Fig. 7). The τ_P distributions of the normal fibres showed more spread than those of the pathological ones. The distribution

histograms (Fig. 7B) showed a significantly larger modal value of U_P for the pathological than for the normal fibres. However, the difference was smaller and not significant ($P > 0.05$), if U_P s were compared only between group II and III, i.e. within the same group of hearing-impaired animals. The modal values of σ_P were smaller for pathological than for normal fibres. As was also found for σ_N , the spread of the distribution was larger for the normal than for the pathological fibres. The peak-to-peak time, $\tau_P - \tau_N$ or $\sigma_N + \sigma_P$, was significantly shorter (about 0.1 ms) for pathological than for normal fibres. As far as could be tested (in high-SR fibres of group III) the minor deviations of UR from normal were not correlated with the threshold level.

Inter-animal variation of UR

The spread of the distributions of the pooled data (Figs. 4 - 7) was larger than that of data from within one animal. Standard deviations differed by a factor 1.2-1.7. Other examples of inter-animal variation are shown in Fig. 9 where grand averages of URs, for normal-hearing animals (panels A-C) and for noise-treated animals are plotted (panels D-F). The grand averages of the animals GP110 and GP131 (panels D-F) were similar for group II (normal threshold) and group III (high-threshold) fibres. It can be seen that the negative peaks of all grand averages were similar, while their positive peaks differed. Each grand average is accompanied by two click-evoked CAPs, one before exposure of the eighth nerve and one during single-fibre measurements (Fig. 9), in order to indicate whether the condition of the nerve had changed. According to our observations, a little stretching of the nerve that may occur accidentally during exposure of the nerve causes

TABLE II
LATENCY, AMPLITUDE AND WIDTH OF POSITIVE COMPONENT OF UNIT RESPONSE

SR	τ_N	S.D.	U_P	S.D.	σ_P	S.D.	N
Group I							
≥ 30 sp/s	0.10	0.21	0.07*	0.04	0.19	0.14	21
5-30 sp/s	0.10		0.03		0.16		1
< 5 sp/s	0.03	0.03	0.41	0.05	0.45	0.04	2
Group II							
≥ 30 sp/s	0.11	0.18	0.11*	0.08	0.23	0.12	23
5-30 sp/s	0.03	0.00	0.07	0.06	0.23	0.02	3
< 5 sp/s	0.12	0.08	0.20	0.09	0.21	0.09	2
Group III							
≥ 30 sp/s	-0.00	0.10	0.11	0.07	0.15	0.09	38
5-30 sp/s	-0.01	0.12	0.11	0.09	0.10	0.02	5
< 5 sp/s	-	-	-	-	-	-	-

Parameters for the positive component corresponding to the same URs as represented in Table I, apart from URs of which σ_P could not be determined by curve fitting. Latency τ_P and measure of width σ_P are given in ms. Amplitude U_P is given in μ V. S.D.: standard deviation; N: number of fibres. * Significant correlation ($P < 0.05$) of U_P with CF for normal fibres ($r = -0.35$; $N = 44$).

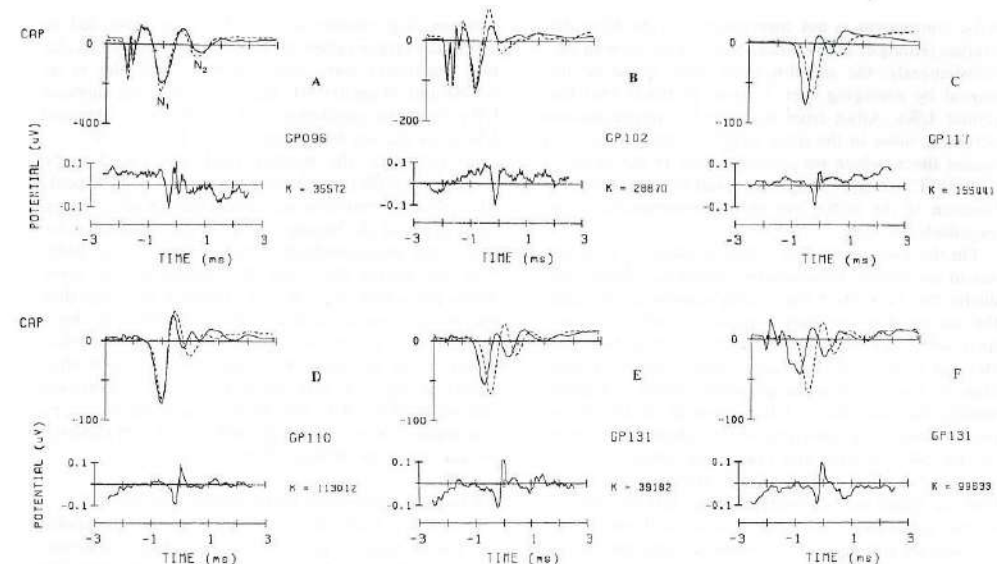


Fig. 9. The grand averages of URs in one animal (bottom part) and condensation-click CAPs in the same animal (upper part). The dashed and solid lines refer to pre- and post-nerve-exposure CAPs respectively. Click intensities pre- and post-exposure were, respectively (A), (B) 51 dB nSL both, (C) 5 and 15 dB nSL, (D), (E) 15 and 31 dB nSL, (F) 15 and 51 dB nSL. K is the number of spikes used for the averaging. The time scale is referred to the spike-trigger. (A-C) URs of fibres of normal-hearing animals (group I), grand averages of 2, 3 and 7 single fibre's URs respectively. (D-F) URs of high-threshold fibres of hearing-impaired guinea pigs (group III), averaged for 5, 4 and 7 fibres respectively. In panels E and F grand averages of the same animal (GP131) are given; (E) corresponds to the cochlear condition in the beginning of the single-fibre measurements; (F) corresponds to the final condition, which is altered in comparison to the initial condition; note that the click intensity was increased by 20 dB to reach a similar CAP amplitude.

a reduction of the N_2 component of the CAP, while the N_1 component remains intact. Therefore, we apply the N_2/N_1 ratio, which does not vary notably with intensity, as an indicator of the nerve condition. Considering the normal-hearing animals, one finds that a CAP with a reduced N_2 component is accompanied by a UR without or with only a small positive peak (Fig. 9B).

During the experiment on animal GP131 the cochlear condition suddenly declined considerably (due to respiratory depression), which was indicated by a threshold shift of 15 - 25 dB over the entire frequency range. The UR grand averages, before and after the cochlear alteration, were very similar (see Figs. 9E, F).

Discussion

The experiments demonstrated that for most high-SR fibres in the guinea pig the assumption of independence of the firings of the individual fibres is not violated. For those fibres the spike-triggered aver-

aging method yields good estimates of unit responses (URs) at the round window (Kiang et al., 1976; Wang, 1979; Prijs, 1986). In addition, we have demonstrated that spikes that occur in periods between successive acoustic-stimulus presentations can be used to determine a UR signal, if the spikes that directly follow the stimulus are excluded from the averaging procedure (see Fig. 1). Apparently, the fibres do not respond synchronously with other fibres 10 - 30 ms after a click stimulus, although there is an indirect influence of the stimulus via adaptation (cf. Prijs and Eggermont, 1980). The possibility of using silent periods between stimuli offers the opportunity to determine a UR, from spikes recorded for another purpose, without spending extra recording time. The mathematical function $G(t)$ of Eqn. (1) appears to be appropriate to describe a UR and it could be applied to determine measures for the width of the UR components, namely σ_N and σ_P (see Eqn. (1)).

The signal-to-noise ratio was mostly larger for those URs that were determined with a large number of spike triggers. This supports the assumption that the

noise component is not correlated with the fibre discharges (Kiang et al., 1976) and thus decreases with \sqrt{K} . Consequently, the signal-to-noise ratio could be improved by averaging over a group of fibres that had similar URs. Apart from noise in the round-window potential, noise in the spike signal will lead to jitter in trigger times, which we estimate to be in the order of 0.05 ms. This trigger noise may result in a slight overestimation of the width and an underestimation of the amplitudes of UR.

On the assumption that a fibre is infinitely long and lies in an infinite homogeneous medium, volume conductor theory predicts that a fibre's discharge causes in the surrounding medium a triphasic potential waveform with integral equal to zero (Lorente de N6, 1947; Heringa et al., 1989). If such a waveform is recorded close to the site of spike initiation, which is approximately the case for a UR recording at the round window, then, the waveform will be diphasic (Lorente de N6, 1947; Gydikov and Trayanova, 1986) and this is what we found for most URs. For normal nerve conditions we found that the integral of the UR was approximately equal to zero (cf. Fig. 8), which is, however, not a necessary condition for a bounded complex volume conductor (Heringa et al., 1989; Schoonhoven and Stegeman, 1991).

UR in normal-threshold fibres: relationship with CF

Inter-animal differences were larger than intra-animal differences, which was also found in other studies (Wang, 1979; Prijs, 1986). Despite this we decided to pool the data for the analysis of CF- and SR-variations of the UR parameters.

The parameters of the negative UR component did not vary with CF, which confirms earlier results of Prijs (1986), who reported values of τ_N and U_N . For an extensive data set Wang (1979) found similar results in cats, except for a strong increase of the latency ($|\tau_N|$) with CF for CFs above 12 kHz. Our results, together with those of Prijs (1986), which cover largely the range above 10 kHz, unambiguously contradict such a CF variation in the guinea pig. Although one is tempted to look for morphological causes of this species difference, the morphometry data available (Liberman and Oliver, 1984; Brown, 1987) do not provide a simple explanation.

The values we found for U_N agree with the value of $0.10 \pm 0.05 \mu\text{V}$ reported by Prijs (1986). The URs in guinea pigs appeared to have a similar size as in cats: the peak-to-peak amplitude $U_N + U_P$ ($0.21 \mu\text{V}$) is similar to the average value of $0.24 \mu\text{V}$ reported for cats (Wang, 1979). While for low-threshold fibres U_N was CF invariant, we found that U_P slightly decreased with CF. Possibly the relatively low signal-to-noise ratio that we observed in some low-CF fibres due to oscillatory

patterns (e.g. shown in Fig. 2A) may have led to artificially larger values of U_P for those fibres. Oscillatory waveforms were also reported by Kiang et al. (1976) and Wang (1979). They separated the diphasic URs from the oscillation and for the thus obtained URs they did not find a variation of U_P with CF.

In our data, the positive peak was found to be somewhat smaller and broader than the negative peak, which was also found in other experimental data (Wang, 1979; Charlet de Sauvage et al., 1983). The peak-to-peak time as determined visually, $\tau_P - \tau_N$, was 0.06–0.10 ms shorter than that determined by the curve fitting procedure, $\sigma_N + \sigma_P$ (see Tables I, II), while they had to be equal according to Eqn. (1). Probably, for a number of URs σ_P was over-estimated by imperfect fitting to the positive UR component, such as is illustrated in Fig. 1A and indicated in the distribution histogram (Fig. 7C). The peak-to-peak time $\tau_P - \tau_N$ was about 0.30 ms, which is similar with that reported for cats (0.26 ms; Wang, 1979).

UR in normal-threshold fibres: relationship with SR

For a few high-SR fibres with very low thresholds we found large ($U_N > 0.3 \mu\text{V}$) and broad UR-estimates, as shown in Fig. 2B. Such large URs have also been reported occasionally for very sensitive cat fibres (Kiang et al., 1976; Wang, 1979; Evans, 1987). Evans (1987) suggested that these large URs are caused by synchronized discharges of 10–100 fibres with similar CFs responding to animal-generated or external noise. Hence, in those cases the independence of unit firings is violated. Another reason for these abnormal UR waveforms could be stretching of the nerve (Prijs, 1986), during the exposure of the nerve. Because the CAP waveform, which corresponds to the large URs in Fig. 2B, was not notably changed (Fig. 9C), we assume that nerve stretching was not involved. Our finding that large URs of high-SR fibres only occurred with very low thresholds (below 10 dB SPL) seems to support Evans' suggestion.

While large URs were exceptionally found in high-SR fibres they were found in most of the low- and medium-SR fibres. The origin of the large URs of the lower-SR fibres might be different from that for high-SR fibres, since the waveforms were sharper (but still broader than normal) and since they were found both for low- and high-threshold fibres. On the basis of unchanged CAP waveforms (Fig. 9) we again exclude nerve stretching as the cause of these enlarged URs (Prijs, 1986). The large URs cannot be ascribed to differences in fibre diameters either since, instead, the relatively small diameters of low-SR fibres (Liberman and Oliver, 1984) should theoretically result in small URs (Schoonhoven et al., 1986; Schoonhoven and Stegeman, 1991). Possibly, as for the large URs in high-SR fibres, the independence of fibre discharges is

violated, and the measured URs are the result of synchronized discharges of several fibres. A support for this hypothesis is the change of large URs to normal UR in cat after (high-CF tone) stimulation (Kiang et al., 1976; Evans, 1987) and the absence of large URs for stimulated low- and medium-SR fibres in cat (Wang, 1979). A definite explanation for the inter-fibre discharge dependence among this group of fibres is not obvious. Some possibilities can be mentioned: crosstalk between auditory-nerve fibres or hair cells, or a synchrony between firings of low-, medium- and high-SR fibres innervating one inner hair cell (IHC); these may discharge synchronously upon extrema in the IHC membrane noise. Presuming that most spontaneous discharges of a low-SR fibre will be triggered by this type of event, a large UR will be measured. In high-SR fibres the UR is based on spontaneous discharges that are driven in the main by the IHC resting current (Liberman and Dodds, 1984) and that are hardly driven by noise-fluctuation extrema; therefore, the effect of spontaneous synchrony will be smaller for high-SR fibres.

In conclusion, we will assume that the actual single-fibre's URs, in contrast to our experimental estimates, do not vary significantly with SR nor are they larger for very sensitive fibres.

UR in normal-threshold fibres: elemental UR and CAP

The interest in the UR is mainly in connection with the CAP. From our experiments and considerations we assume the potential change at the round window resulting from an auditory-nerve fibre's discharge to be fibre-independent i.e. invariant for CF or SR. Hence, in the normal hearing guinea pig an elemental UR can be used for convolution computations, e.g. to simulate CAPs (cf. Charlet de Sauvage et al., 1987). The elemental UR, here proposed, (Fig. 8) is used in the convolutions in the accompanying paper (Versnel et al., 1992). The function $G(t)$ is used as a description of the elemental UR. It has a discontinuity of the slope at $t = t_0$ if $\sigma_N \neq \sigma_P$, but the introduced imperfection will be limited since σ_N is about equal to σ_P . Elemental URs as used by Dolan et al. (1983) and Charlet de Sauvage et al. (1987) contained larger discontinuities.

UR in high-threshold fibres: parameters in relation to CF and SR

The hearing impairment was mainly induced by acoustic overstimulation, and occasionally by hypoxia during the experiment as in animal GP131 (see Fig. 9F). In the case of GP131 hypoxia did not affect the UR, as shown in the panels E and F in Fig. 9. Generally, we found that changes in UR could occur for a high-threshold fibre: sharpening of the waveform and occasionally an increase of U_P . This general finding cannot be accounted for by inter-animal variations

since such differences were also present between normal (group II) and pathological fibres (group III) within the same guinea pigs.

The chronic effect of noise exposure in mammals is the disruption of stereocilia of the outer hair cells in the first row and of the IHCs (e.g. Cody and Robertson, 1983; Liberman, 1987) or the damage of the cuticular plate, the entire hair cells, supporting cells and the afferent IHC terminals (Cody and Robertson, 1983; Robertson, 1983; Carlon et al., 1987). Of the different degrees of damage that have been reported only swelling of the afferent IHC dendrite might be related to a change of UR because it is close to the spike-generation site (Siegel and Dallos, 1986). Effects on the neuron itself which could give rise to a UR change only occur for severe damage to the cochlea that is not associated with pure noise trauma (Suzuka and Schuknecht, 1988). In most experiments on chronic noise-induced hearing loss the swelling of dendrites was absent (Cody and Robertson, 1983; Liberman, 1987). The possibility cannot be excluded, however, that some deviant URs were associated with dendritic swelling (Carlon et al., 1987).

UR in high-threshold fibres: consequences of UR changes for CAP

Changes of the UR, even when they are small, can be responsible for substantial changes of the CAP (Hoke et al., 1979; Schoonhoven et al., 1989). Exam-

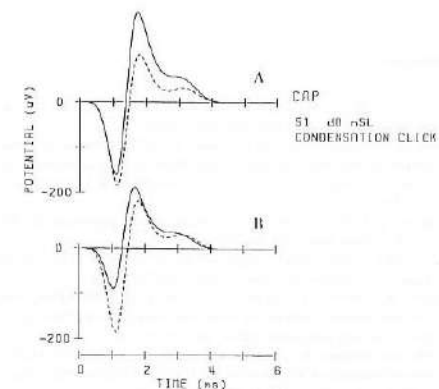


Fig. 10. Click-evoked CAPs synthesized with use of a modelled sum of normal fibre's discharge probabilities for various UR models. The sum of discharge probabilities is taken from Versnel et al. (1992) for a condensation click at 51 dB nSL. The dashed lines represent the CAP with the normal model UR as shown in Fig. 8, solid lines represent CAPs for modified URs. Modifications compared to the normal UR are: (A) $U_P = 0.12 \mu\text{V}$ (normal: $0.09 \mu\text{V}$), (B) $U_P = 0.12 \mu\text{V}$ (normal: $0.09 \mu\text{V}$), $\sigma_N = 0.09 \text{ ms}$ (normal: 0.12 ms), $\sigma_P = 0.12 \text{ ms}$ (normal: 0.16 ms).

ples of such changes in the CAP are shown in Fig. 10. We synthesized click-evoked CAPs by convolution of a modelled sum of normal discharge probabilities (for details see Versnel et al., 1992) both with the elemental UR for normal-threshold fibres (dashed lines) and with a model UR for high-threshold fibres (solid lines). To that end, the parameters of $G(t)$ that could change with noise trauma, U_p , σ_N and σ_p , were modified. The synthesized CAPs give an indication of deviations of CAPs that may occur as a consequence of UR changes. An increase of U_p by 33% causes an increase of the positive CAP peak by about 100% (Fig. 10A) and a decrease of the width by 25% causes a decrease of the N_1 amplitude by about 50% (Fig. 10B). These examples stress the importance of a proper UR choice for CAP modelling and the consequences that a change of UR can have for the CAP.

Acknowledgements

This study was supported by the Netherlands organization for scientific research (NWO) and by the Heinsius Houbolt Fund. The authors thank E. de Boer (ENT Dept., University of Amsterdam) for his valuable comments and A.R. Palmer (Nottingham, U.K.) for carefully reading this manuscript. The computer-technical support, in particular concerning the off-line determinations of the unit responses, was given by A. van Wijngaarden.

References

- Bevington, P.R. (1969) Data reduction and error analysis for the physical sciences. McGraw-Hill, New York.
- Biondi, E., Daquino, G., and Grandori, F. (1975) Compound action potential and single acoustic nerve fibres activity generation: an equivalent neuron approach. *Int. J. Bio-Medical Computing* 6, 157-166.
- de Boer, E. (1975) Synthetic whole-nerve action potentials for the cat. *J. Acoust. Soc. Am.* 58, 1030-1045.
- Brown, M.C. (1987) Morphology of labeled afferent fibers in the guinea pig cochlea. *J. Comp. Neurol.* 260, 591-604.
- Canlon, B., Miller, J.F., Flock, A. and Borg, E. (1987) Pure tone oversimulation changes the micromechanical properties of the inner hair cell stereocilia. *Hear. Res.* 30, 65-72.
- Charlet de Sauvage, R., Aran, J.-M. and Erre, J.-P. (1987) Mathematical analysis of VIIIth nerve CAP with a linearly-fitted experimental unit response. *Hear. Res.* 29, 105-115.
- Charlet de Sauvage, R., Cazals, Y., Erre, J.-P. and Aran, J.-M. (1983) Acoustically derived auditory nerve action potential evoked by electrical stimulation: An estimation of the waveform of single unit contribution. *J. Acoust. Soc. Am.* 73, 616-627.
- Cody, A.R. and Robertson, D. (1983) Variability of noise-induced damage in the guinea pig cochlea: Electrophysiological and morphological correlates after strictly controlled exposures. *Hear. Res.* 9, 55-70.
- Dolan, D.F., Teas, D.C. and Walton, J.P. (1983) Relation between discharges in auditory nerve fibres and the whole-nerve response shown by forward masking: an empirical model for the AP. *J. Acoust. Soc. Am.* 73, 580-591.
- Evans, E.F. (1979) Single-unit studies of mammalian cochlear nerve. In: H.A. Beagley (Ed.), *Auditory investigation: the technological and scientific basis*, Clarendon Press, Oxford, pp. 324-267.
- Evans, E.F. (1987) On the nature of the round window recorded "unit response": the contribution of single unit responses to the gross cochlea action potential. *Br. J. Audiol.* 21, 103-104.
- Goldstein, M.H. and Kiang, N.Y.S. (1958) Synchrony of neural activity in electric responses evoked by transient acoustic stimuli. *J. Acoust. Soc. Am.* 30, 107-114.
- Gydikov, A.A. and Trayanova, N.A. (1986) Extracellular potentials of single active muscle fibres: effects of finite fibre length. *Biol. Cybern.* 53, 363-372.
- Heringa, A., Stegeman, D.F. and de Weerd, J.P.C. (1989) Calculated potential and electric field distributions around an active nerve fiber. *J. Appl. Phys.* 66, 2724-2731.
- Hoke, M., Elberling, C., Hieke, D. and Bappert, E. (1979) Deconvolution of compound PST histograms. *Scand. Audiol. Suppl.* 9, 141-154.
- Kiang, N.Y.S., Moxon, E.C. and Kahn, A.R. (1976) The relationship of gross potentials recorded from the cochlea to single unit activity in the auditory nerve. In: R.J. Ruben, C. Elberling and G. Salomon (Eds.), *Electrocochleography*, University Park Press, Baltimore, pp. 95-115.
- Liberman, M.C. (1987) Chronic ultrastructural changes in acoustic trauma: Serial-section reconstruction of stereocilia and cuticular plates. *Hear. Res.* 26, 65-88.
- Liberman, M.C. and Dodds, L.W. (1984) Single-neuron labeling and chronic cochlear pathology. II. Stereocilia damage and alterations of spontaneous discharge rates. *Hear. Res.* 16, 43-53.
- Liberman, M.C. and Oliver, M.E. (1984) Morphometry of intracellularly labeled neurons of the auditory nerve: correlations with functional properties. *J. Comp. Neurol.* 223, 163-176.
- Lorente de N6, R. (1947) Analysis of the distribution of action currents of nerve in volume conductors. *Studies of the Rockefeller Institute of medical Research* 132, 384-482.
- Prijs, V.F. (1986) Single-unit response at the round window of the guinea pig. *Hear. Res.* 21, 127-133.
- Prijs, V.F. and Eggermont, J.J. (1980) On peripheral auditory adaptation I. Dependence on the recording site. *Acustica* 44, 283-300.
- Prijs, V.F. and Eggermont, J.J. (1981) Narrow-band analysis of compound action potentials for several stimulus conditions in the guinea pig. *Hear. Res.* 4, 23-41.
- Robertson, D. (1983) Functional significance of dendritic swelling after loud sounds in the guinea pig cochlea. *Hear. Res.* 9, 263-278.
- Schoonhoven, R., Stegeman, D.F. and de Weerd, J.P.C. (1986) The forward problem in electroneurography I: A generalized volume conductor model. *IEEE Trans. Biomed. Eng.* 33, 327-334.
- Schoonhoven, R., Versnel, H., Prijs, V.F. and Keijzer, J. (1989) The unit response and the relation between single fibre discharge patterns and the compound action potential. In: G. Cianfrone, F. Grandori and D.T. Kemp (Eds.), *2nd International Symposium on Cochlear Mechanics and Otoacoustic Emissions, 1989, Rome. II Valsalva* 54, Suppl.1, pp. 48-53.
- Schoonhoven, R. and Stegeman, D.F. (1991) Models and analysis of compound nerve action potentials. *Crit. Rev. Biomed. Eng.* 19, 47-111.
- Siegel, J.H. and Dallos, P. (1986) Spike activity recorded from the organ of Corti. *Hear. Res.* 22, 245-248.
- Suzuka, Y. and Schuknecht, H.F. (1988) Retrograde cochlear neuronal degeneration in human subjects. *Acta Otolaryngol. Suppl.* 450, 1-20.
- Versnel, H., Prijs, V.F. and Schoonhoven, R. (1990) Single-fibre responses to clicks in relationship to the compound action potential in the guinea pig. *Hear. Res.* 46, 147-160.
- Versnel, H., Schoonhoven, R. and Prijs, V.F. (1992) Single-fibre and whole-nerve responses to clicks as a function of sound intensity in the guinea pig. *Hear. Res.* 59, 138-156.
- Wang, B. (1979) The relation between the compound action potential and unit discharges of the auditory nerve. Doctoral dissertation, Dept. of Electrical Engineering and Computer Science, M.I.T., Cambridge, MA.

Chapter V

Click responses in noise-damaged guinea-pig cochleas. I. Abnormal single-fibre responses

Huib Versnel, Vera F. Prijs and Ruurd Schoonhoven

Summary

We simultaneously measured single-fibre responses and compound action potentials (CAPs) to clicks in noise-damaged cochleas in order to analyse deviations of the CAP from the single-fibre level. In the companion paper (Versnel et al., *) we discuss the CAPs, in this paper we present the single-fibre data. We distinguish five types of abnormal frequency threshold curves (FTCs). These types are comparable to types of tuning curves reported by Liberman and Dodds (1984b). The click responses were recorded as poststimulus time histograms (PSTHs) for various intensities (typical range 30-40 dB) and for the two click polarities. As a basis for an empirical CAP model presented in the companion paper, we describe for each FTC type parameters of the dominant PSTH peak: latency, amplitude, and synchronization (cf. Versnel et al., 1990a). The PSTHs showed various deviations from normal, which corresponded to the classification of the FTCs. Remarkable changes were found in the response patterns of fibres that had a relatively low threshold of the FTC tail. Fourier analysis on the PSTHs of these fibres showed a correspondence between the FTC tail and the power spectrum of the click response.

Key words: Noise trauma; Single fibre; Frequency threshold curve; Hypersensitivity; Click responses; Guinea pig.

This chapter has been submitted for publication to *Hearing Research*. Preliminary results were presented at the XXVIth Workshop on Inner Ear Biology, Paris, 1989; at the Symposium on Mechanics and Biophysics of Hearing, Madison, 1990; at the 9th International Symposium on Hearing, Auditory Physiology and Perception, Carcans, 1991.

Introduction

Over the last few decades several experiments have been performed to examine the changes in physiological functioning of the cochlea as a result of damage. Those experiments involved recordings of compound action potentials (CAPs) or single-fibre responses. A primary phenomenon in damaged cochleas is elevation of the response threshold. Furthermore, amplitude-versus-intensity curves for CAPs are typically steeper than normal (see overview for humans in Eggermont, 1976), single-fibre discharge rate-versus-intensity functions can be similar to normal but are mostly steeper than normal and saturation discharge rates can be either normal, increased, or decreased (Evans, 1975; Harrison, 1981; Salvi et al., 1983; Liberman and Kiang, 1984). Studies of CAP tuning curves (Eggermont, 1977; van Heusden and Smoorenburg, 1981; Rutten, 1986; Dolan and Mills, 1989) and frequency threshold curves (FTCs) or reverse-correlation functions in single fibres (Evans, 1975; Harrison and Evans, 1982; Salvi et al., 1983) show that in most hearing-loss cases the tuning broadens. Generally, in similar experiments a large variety of morphological damage and corresponding frequency characteristics is found (Hunter-Duvar et al., 1982; Robertson, 1982; Cody and Robertson, 1983; Salvi et al., 1983; Harrison and Prijs, 1984; Liberman and Dodds, 1984b).

In contrast to the spectral response properties only few data are available on the temporal patterns of single-fibre responses in damaged cochleas. Dallos and Harris (1978) and Salvi et al. (1979) found in abnormal cochlear fibres over a wide range of characteristic frequencies (CFs) that click latencies as well as temporal patterns of tone responses were unchanged. On the other hand, Salvi et al. (1979) reported that the number of peaks in click responses of low-CF fibres decreased. Extensive knowledge of the temporal aspects of fibre responses in pathology is required, firstly, for interpretation of CAPs, and secondly, for understanding of the consequences for the temporal coding of complex sounds such as speech.

Our goal is to find the single-fibre discharge patterns underlying abnormal CAPs in pathological cochleas. This knowledge is useful in clinical diagnosis of human hearing by electrocochleography. Moreover, it may support interpretation of click-evoked CAPs as is often applied in animal auditory research. In order to reach our goal, we recorded simultaneously single-fibre responses and CAPs to clicks in acoustically traumatized guinea pigs. In this paper we describe the single-fibre click responses in relation to the tuning curves or frequency threshold curves (FTCs). In the companion paper (Versnel et al., *) the CAPs are discussed in relation to the single-fibre responses with the use of an empirical CAP model.

With respect to the large variety of FTCs observed in noise-damaged cochleas (Liberman and Kiang, 1978; Robertson, 1982; Salvi et al., 1983) this paper will distinguish between different types of FTCs. An elegant scheme of FTC types in pathology is given by Liberman and Dodds (1984b). Globally, our question is as follows: what are the click responses for each damage-associated type of FTC? The click responses presented as poststimulus time histograms (PSTHs) and FTCs will be

compared to normal data in guinea pigs that we published in previous reports (Versnel et al., 1990a, 1992a). In this comparison latency, amplitude, and synchronization of the dominant peak are the relevant PSTH parameters because they are to be applied in the empirical CAP model (Versnel et al., *). More specifically we pose the question: do alterations in PSTHs uniquely relate to alterations in FTCs? To answer this, Fourier analysis on PSTHs that show any form of periodicity may be helpful (Versnel et al., 1992a).

A part of the data we present here has been published in two symposium reports that present a model study of the single-fibre data (Prijs et al., 1990; Versnel et al., 1992c). A more elaborate model study also related to data in this paper is presented elsewhere (Schoonhoven et al., --). We note, finally, that our interest concerns functional changes irrespective of the inducement of damage (acoustic overstimulation as applied in this study, ototoxic drugs, respiratory depression). We might assume that cochlear dysfunction relates to histological damage independent of the kind of inducement.

FTCs and PSTHs in normal cochleas (in summary)

As data in hearing-impaired cochleas will be described with respect to normal data, we summarize here the relevant normal response properties as described in Versnel et al. (1990a; on FTCs) and in Versnel et al. (1992a; on click PSTHs). The Q_{10dB} (ratio of CF and bandwidth at 10 dB above the threshold at CF) could be described as $Q_{10dB} = 2.70f_c^{0.28}$, with symbol f_c for CF (in kHz). With respect to their spontaneous discharge rate (SR) we divide the fibres in three groups with boundaries of 5 and 30 spikes/s; the distribution of fibres over the low-, medium-, and high-SR ranges was 15-23-62 %, respectively. Low-SR fibres have significantly higher thresholds than high-SR fibres and medium-SR fibres have intermediate thresholds.

On the basis of two distinct click-response patterns we distinguished low- and high-CF fibres with a frequency boundary of 3 kHz. Figure 1 shows representative examples of click PSTHs for a high-CF (panel A) and a low-CF (panel B) fibre. The PSTHs are presented in compound mode (cf. Pfeiffer and Kim, 1972) with PSTHs to condensation clicks plotted upwards and to rarefaction clicks downwards. The PSTHs of the high-CF fibre are similar for condensation and rarefaction clicks. The PSTHs show one or two peaks, and have a short latency. The low-CF fibre shows a polarity dependent click response. The PSTHs have several peaks which alternate with polarity, and interpeak intervals are about $1/f_c$; the multiple-peak pattern is generally associated with phase following, i.e. the neural firings follow the oscillatory mechanical responses to the click. Compared to the high-CF fibres the PSTH latency is longer for low-CF fibres and the peak amplitude is larger.

Methods

Physiological Experiments

The data are based on acute experiments on 13 female, albino guinea pigs

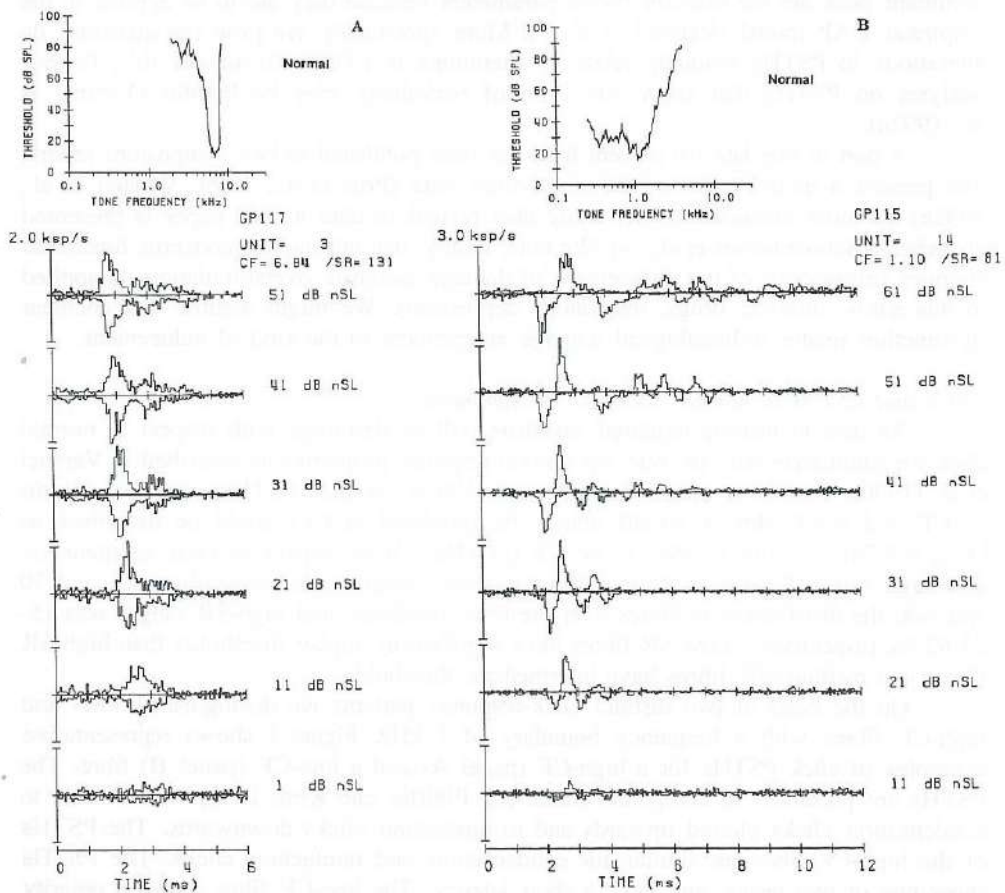


Fig. 1. Frequency threshold curve (FTC) and compound poststimulus time histograms (PSTHs) in normal cochleas. The condensation-click PSTHs are plotted upwards, the rarefaction-click PSTHs downwards; the compound PSTHs are arranged in order of decreasing click intensity. Bin width of the PSTH is 60 μ s. The ordinate represents the ratio of average number of spikes per bin and the bin width. (A) Responses of a fibre with a high CF (6.8 kHz); the PSTHs are similar for the two click polarities. (B) Responses of a fibre with a low CF (1.1 kHz); the PSTH-peak latencies are different for the two click polarities. Note the differences in ordinate scales between panels A and B.

weighing 200–800 g. They were exposed under anaesthesia during 2 hours to a loud tone in a closed sound box with speaker (Fane type Classic 10-125T), eight animals to a tone of 6.0 kHz and 121–123 dB SPL, five others to a tone of 1.4–1.7 kHz and 112–122 dB SPL. By recordings of auditory brainstem responses (ABR), thresholds to clicks and to short tone bursts over a range from 1 or 4 to 11 kHz were measured before and directly after the acoustic overstimulation. A needle placed closely behind the pinna served as active ABR electrode, a needle on the vertex was reference electrode. The acute experiments were performed after a survival time of 14–123 days.

For animal preparation, sound stimulation, and signal recording and processing, we used essentially the same methods and equipment as in the experiments on normal hearing animals (Versnel et al., 1990a, 1992a). Briefly, both for noise exposure and acute experiments, anaesthesia was obtained with Nembutal® (27 mg/kg). A tone threshold audiogram, determined by CAP recordings from the round window, served as a criterion for (ab)normal hearing (Versnel et al., 1990a). ABR was recorded before the actual experiment in order to verify the correspondence to CAP recordings. The single-fibre activity was recorded with glass micropipettes. Sound stimuli were presented in a closed field by a dynamic earphone of Standard Telephones and Cables. The clicks had a width of 100 μ s and a spectrum that was flat within 10 dB up to about 8–9 kHz where it fell off rapidly (see Versnel et al., 1992a). After an FTC of a fibre was determined by threshold tracking (Evans, 1979), PSTHs to condensation and rarefaction clicks were recorded using 256 sweeps and a bin width of 60 μ s.

Data analysis

Fibres with a threshold at CF raised by more than 2 S.D. (≈ 20 dB) from the mean values in an extensive sample of normal-hearing guinea pigs (see Fig. 1 in Versnel et al., 1990a) were considered abnormal. We distinguish three groups of responses (cf. Versnel et al., 1992b): from normal fibres in normal cochleas (group NF/NC), from normal fibres in abnormal cochleas (group NF/AC) and from abnormal fibres in abnormal cochleas (group AF/AC). The responses of group NF/AC and AF/AC will be compared to those of group NF/NC.

The PSTHs were slightly smoothed using a three-point (1/4, 1/2, 1/4) window, and were normalized to a firing probability density by dividing the number of spikes by the number of sweeps and the bin width. We determine P-parameters which were introduced in Versnel et al. (1990a) and applied in the empirical CAP model in the companion paper (Versnel et al., *): latency t_p , amplitude A_p , and synchronization S_p of the dominant PSTH peak. The latency, defined at the peak's maximum, is referred to the start of the cochlear microphonics in order to eliminate the acoustic and middle-ear delays. The amplitude A_p is the normalized spike rate at time t_p , note the amplitude's dimension of spikes/s. The synchronization S_p is defined as the ratio of A_p and area p_p of the PSTH peak (cf. Versnel et al., 1990a, 1992a): $S_p = A_p/p_p$, with a dimension of s^{-1} ; p_p represents the discharge probability in a peak.

We present PSTHs in compound graphs as shown in Fig. 1. If we found compound PSTHs with an oscillatory pattern (which normally is the case for low-CF

fibres) we performed Fourier analysis on difference PSTHs. These mathematical correlates of the compound PSTH are obtained by subtracting PSTHs to rarefaction clicks from PSTHs to condensation clicks (Versnel et al., 1992a). We will indicate the frequency where the power spectrum of the difference PSTH has its maximum as the best frequency (BF) according to Eggermont et al. (1983). Finally, the term tail frequency will be used as the frequency where the FTC tail has its minimum.

Results

Data were sampled in 13 guinea pigs that suffered a hearing impairment after exposure to a loud tone. Recordings in the same ears showed that ABR thresholds were within 10 dB from the CAP thresholds. This allowed the conclusion from ABR recordings that in four animals a hearing loss had been present already before the loud-tone exposure. Pre-exposure lesions would explain hearing losses in regions below 1 kHz. CAP audiograms measured before the single-fibre recordings showed that 8 animals had a moderate hearing loss (20-40 dB at the frequency where the threshold shift was maximum); 5 animals, of which 3 had a pre-exposure impairment, had a severe loss (40-60 dB). One animal exhibited an additional loss of 20 dB during the acute recordings. In 166 fibres we determined an FTC and at least one click PSTH: 77 of these fibres had normal thresholds at CF (group NF/AC), 89 had abnormal thresholds (group AF/AC). Most single-fibre thresholds at CF agreed with the CAP thresholds within 20 dB. Some of the abnormal single-fibre thresholds (AF/AC) were higher than the CAP threshold by more than 20 dB.

TABLE I
CRITERIA FOR FTC CHARACTERIZATION

FTC type	Distinct tip	Tail threshold (dB SPL)	Tail-notch level difference (dB)	Global shape
I	yes	$\Theta_{tl} > 80$	and $\Theta_{nch} - \Theta_{tl} < 20$	entirely elevated
II	yes	$80 \geq \Theta_{tl} > 65$	and $\Theta_{nch} - \Theta_{tl} < 20$	tip elevated
III	yes	$\Theta_{tl} \leq 65$	or $\Theta_{nch} - \Theta_{tl} \geq 20$	tip elevated/ tail low
IV	no	$\Theta_{tl} > 65$	and $\Theta_{nch} - \Theta_{tl} < 20$	flat
V	no	$\Theta_{tl} \leq 65$	or $\Theta_{nch} - \Theta_{tl} \geq 20$	flat/ tail low

Symbols: Θ_{cf} : threshold at CF; Θ_{tl} : level of tail region; Θ_{nch} : level at notch between tip and tail; S_{hf} : high-frequency slope of FTC. Tip definition: $\Theta_{cf} < \Theta_{nch} - 10$ and $S_{hf} > 30$ dB/oct over $\frac{1}{3}$ octave. The tail is assumed to be at least one octave below the tip. The notch of the FTC is the high-threshold part of FTC between tip and tail (in case of type IV and V: maximum threshold in responsive frequency range).

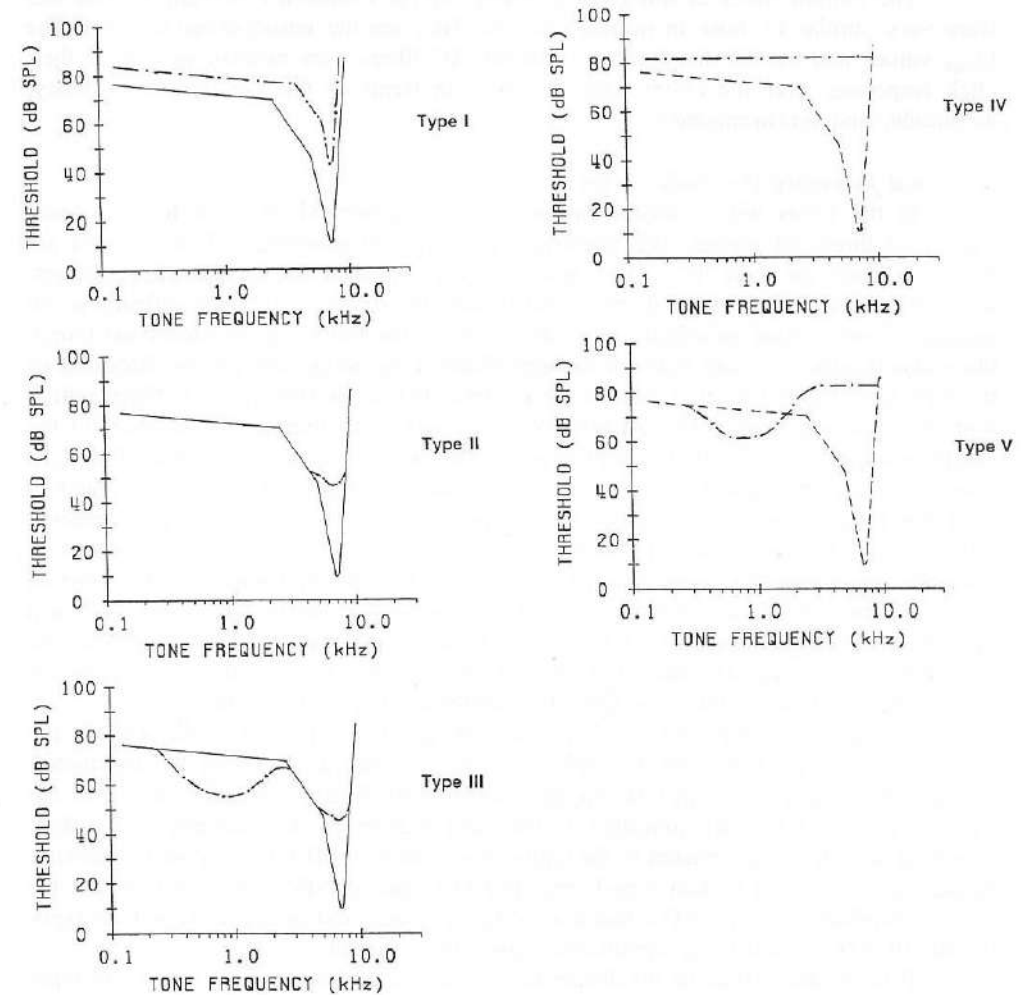


Fig. 2. Five types of FTCs found in fibres with a raised threshold. They are schematized for high-CF fibres. The solid line represents the normal FTC. The dash-dotted lines represent the segments of the curve that deviate from normal. For types IV and V the normal FTC is represented by a dashed line indicating the uncertainty of the original FTC that is associated to the abnormal curve.

FTCs and PSTHs of normal-threshold fibres in pathological cochleas

The normal fibres in abnormal cochleas (NF/AC) showed FTCs and PSTHs that were very similar to those in normal ears (NF/NC; see the introduction section). The Q_{10dB} values and the SR distribution of the NF/AC fibres were normal, as well as their click responses over the entire intensity range in terms of the P-parameters latency, amplitude, and synchronization.

Abnormal frequency threshold curves

In the fibres with a raised threshold at CF (group AF/AC) we found a great variety of threshold curves. We classified five types of abnormal FTCs. We did not follow schemes (as with "U"-, "V"-, and "W"-type) of other investigators (e.g. Robertson, 1982; Salvi et al., 1983; Liberman and Dodds, 1984b) since those classifications are qualitative rather than quantitative and do not cover the full range of curves we found. Our classification is based both on the identification of the tip and on the threshold of the FTC tail. The tail level is compared to normal tail levels (for high-CF fibres with a high SR in normal ears: 74 ± 7 dB SPL, $N = 19$), and it is compared to the level of the notch between tip and tail. For FTCs where the tail is sloping rather than flat (CFs below 1-2 kHz) it is qualitatively compared to tails of normal FTCs with a similar CF. In Table I the quantitative criteria for classification are listed, and Fig. 2 presents schematically the five types of abnormal FTCs. Types I, II, and III have distinct tips with elevated thresholds; type I shows elevation of the tail threshold, type II a normal tail level, and type III an abnormally low tail threshold. Types IV and V are lacking a tip that can be associated with a CF, which implies an extreme broadening or total loss of tuning at CF. Type IV has a tail segment at a similar level as the high-frequency thresholds, and type V shows, as type III, a distinct tail with a low threshold.

In Fig. 3 the threshold at CF (A) and Q_{10dB} (B) are plotted versus CF for the various FTC types. For types IV and V, where CF and Q_{10dB} cannot be determined because of the absence of an FTC tip, thresholds of the higher-frequency region of the type-IV and -V FTCs are indicated in the right margin of the scatterplot (A). Both threshold and Q_{10dB} were related to the typification. The type-III FTCs showed somewhat higher thresholds at CF than type-I and -II FTCs, the type-IV and -V FTCs had the highest thresholds. Type-I FTCs had normal Q_{10dB} values, and on the average both type-II and -III FTCs had a Q_{10dB} significantly lower than normal.

Table II shows that the SR distribution is normal for fibres with a type-I and type-II FTC. For fibres with a type-III FTC the SR distribution is shifted towards high, for types IV and V it is shifted towards low. As shown in Fig. 3 and Table II most abnormal FTCs were found in the high-CF range. Each FTC type could be found at any place in a hearing-loss region of the CAP audiogram (see examples in Versnel et al., *), except for regions below 1 kHz where only FTCs of type I were classified. Each type occurred in both moderate (20-40 dB) and severe hearing losses (40-60 dB), except for type V which was only found for severe losses.

Except for one, all FTCs classified as type IV or V represented fibre responses

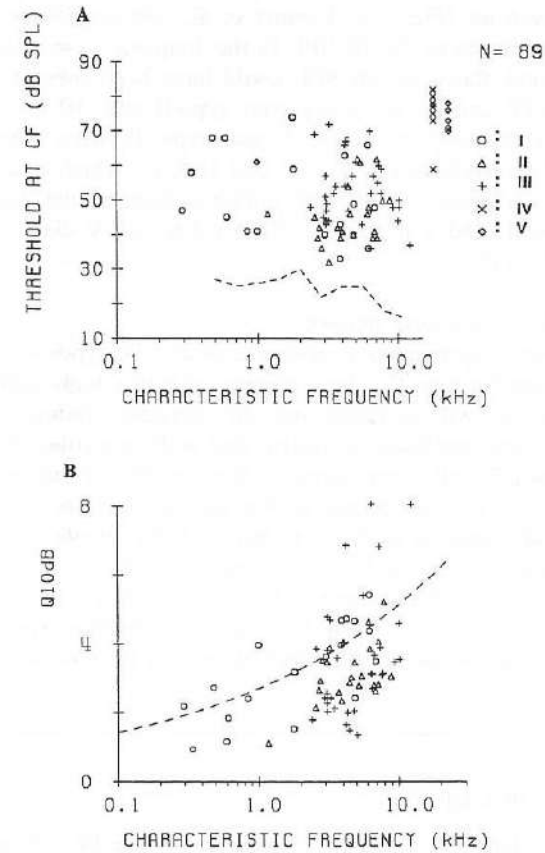


Fig. 3. (A) The threshold at CF versus CF for fibres with a raised threshold. The types of abnormal FTCs are represented by different symbols. The dashed line represents normal compound-action-potential thresholds. A CF cannot be ascribed to types IV and V, hence their thresholds are plotted at the right side. A CF is ascribed only to the fibre with a type-V FTC which probably had a low CF (see in Fig. 4I). Average thresholds at CF (dB SPL) for high-CF fibres: I: 46 ± 10 ($N=9$), II: 46 ± 8 ($N=18$), III: 52 ± 9 ($N=30$); average minimum thresholds: IV: 75 ± 7 ($N=9$), V: 74 ± 4 ($N=5$); thresholds of normal high-SR fibres: 15 ± 11 dB SPL ($N=42$). (B) The Q_{10dB} versus CF for the abnormal fibres. The dashed line represents normal values: $Q_{10dB}(f_c) = 2.70 f_c^{0.28}$. Average Q_{10dB} values for the CF range between 3 and 6 kHz: I: 4.0 ± 0.8 ($N=6$), II: 3.2 ± 0.5 ($N=10$), III: 3.1 ± 1.6 ($N=16$), normal: 4.7 ± 1.5 ($N=16$); average Q_{10dB} for the CF range between 6 and 12 kHz: I: 4.4 ± 0.8 ($N=3$), II: 3.6 ± 0.9 ($N=8$), III: 3.8 ± 1.9 ($N=13$), normal value: 5.0 ± 1.7 ($N=37$). The normal values in (A) and (B) are from (Versnel et al., 1990).

to high-frequency tones thus indicating a high original CF. Since the high-frequency fall-off in the earphone spectrum (Fig. 1 in Versnel et al., 1992a) does not allow proper measurement of thresholds above 50 dB SPL in the frequency range above 12 kHz, a CF tip above 12 kHz and above 50 dB SPL could have been present in FTCs which were classified as type-IV and -V but really were type-II and -III FTCs, respectively. Yet, this artifact is not very likely. In 7 out of 9 cases types IV were found for CAP tone audiograms with small threshold shifts at 11.3 and 16 kHz, which makes the presence of a tip above 12 kHz and above 50 dB SPL unlikely. Further, the distinctly different SR distributions of type III and V (Table II) suggest that type-V classified FTCs really differ from the type-III FTC.

PSTHs of abnormal fibres: response patterns

Figure 4(A-I) shows representative examples of all FTC types with corresponding compound PSTHs. Except for type IV, the responses of both a high- and a low-CF fibre are presented. Aspects we will consider are: the response duration, occurrence of multiple peaks, latency and amplitude of peaks, and with particular attention, polarity and intensity dependence of all these aspects. We describe deviations from normal response behaviour which is summarized in the introduction section and in Fig. 1. A common feature in all examples in Fig. 4 is that click thresholds are elevated, which in most cases corresponds well to the CF-tone-threshold shift.

Figures 4A, B show the PSTHs for two fibres with a type-I FTC, one with a high CF (A), and the other with a low CF (B). In both cases the PSTHs have normal patterns. One deviation occurs in case of the low-CF fibre, where the peak amplitudes are smaller

TABLE II
DISTRIBUTION OF TYPES OF FTC

CF	SR	type I	type II	type III	type IV	type V
low	low	1	0	0	0	1
	medium	1	2	1	0	0
	high	7	3	2	0	0
high	low	1	1	0	0	1
	medium	3	5	5	4	3
	high	5	12	25	5	1
all	all	18	23	33	9	6
		20 %	26 %	37 %	10 %	7 %

In 89 fibres with abnormally high thresholds at CF the FTC was typified. Figures of types IV and V are given under high CF, unless the high-frequency slope was observed below 3 kHz. High CF: CF above 3 kHz; low CF: CF below 3 kHz. High SR: SR above 30 spikes/s; medium SR: between 5 and 30 spikes/s; low SR: SR below 5 spikes/s.

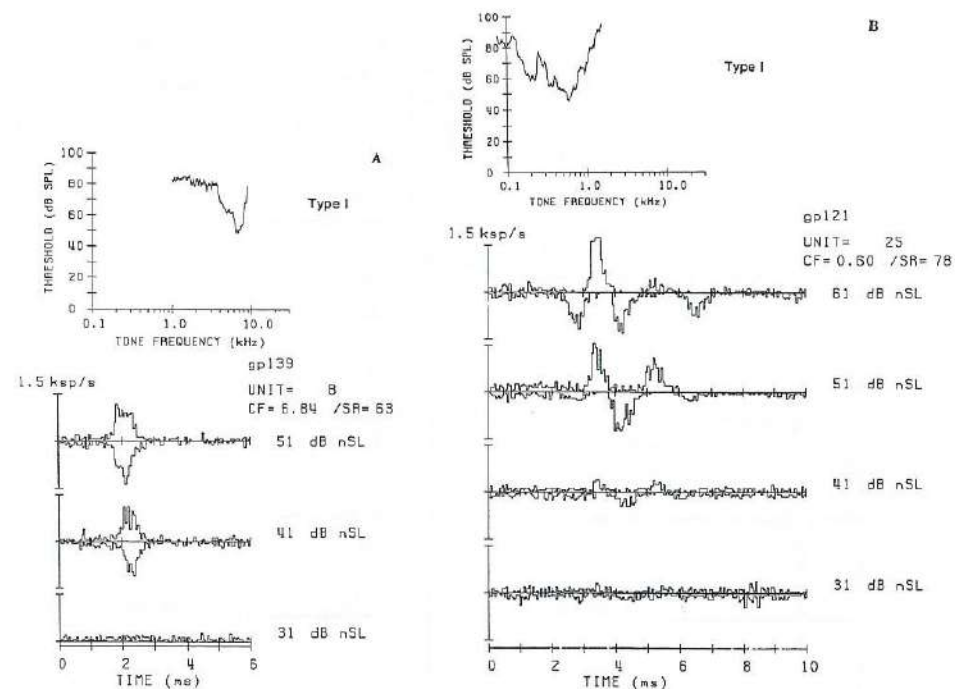


Fig. 4. Different types of FTCs with compound click PSTHs. The condensation-click PSTHs are plotted upwards, the rarefaction-click PSTHs downwards. Bin width of PSTH is 60 μ s. The ordinate represents the ratio of average number of spikes per bin and the bin width. Note the differences in ordinate scales between different panels. Compound PSTHs are arranged in order of decreasing click intensity. (A) Type-I responses; CF of 6.9 kHz and SR of 63 spikes/s. (B) Type-I responses; CF of 0.60 kHz and an SR of 78 spikes/s.

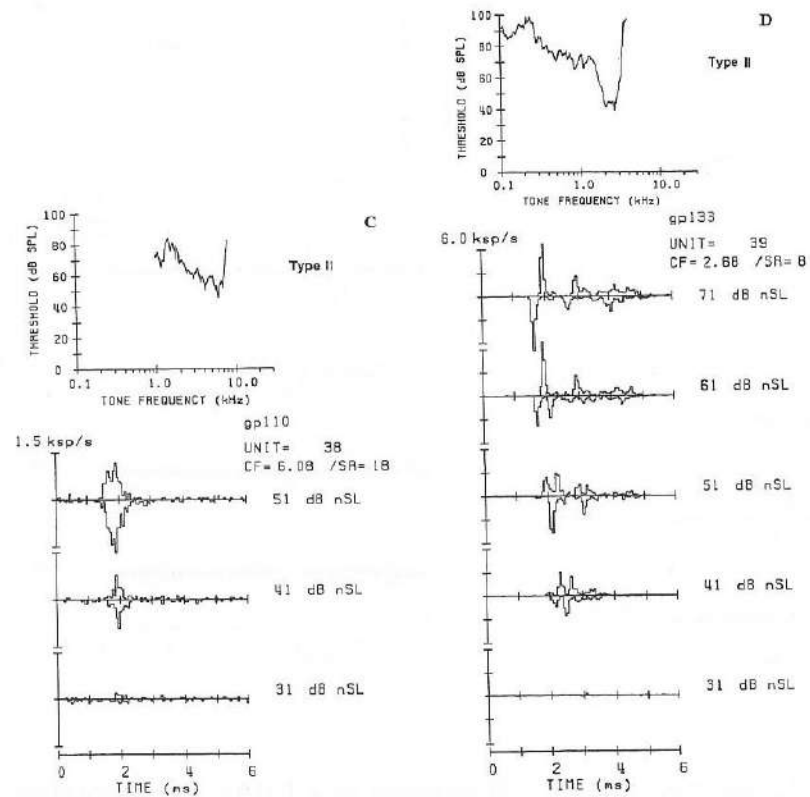


Fig. 4. (continued). (C) Type-II responses; CF of 6.1 kHz and an SR of 18 spikes/s. (D) Type-II FTC and compound PSTH for a CF of 2.7 kHz and an SR of 8 spikes/s.

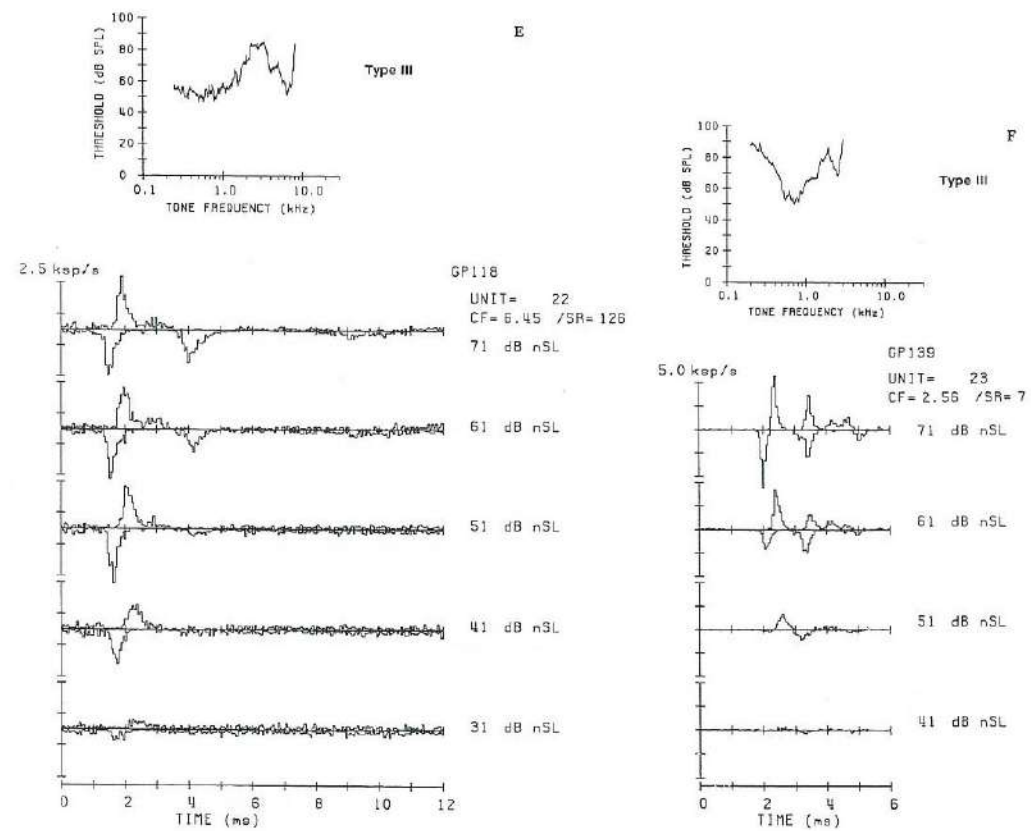


Fig. 4. (continued). (E) Type-III responses for a CF of 6.5 kHz and an SR of 126 spikes/s. (F) Type-III responses; CF of 2.6 kHz and SR of 7 spikes/s.

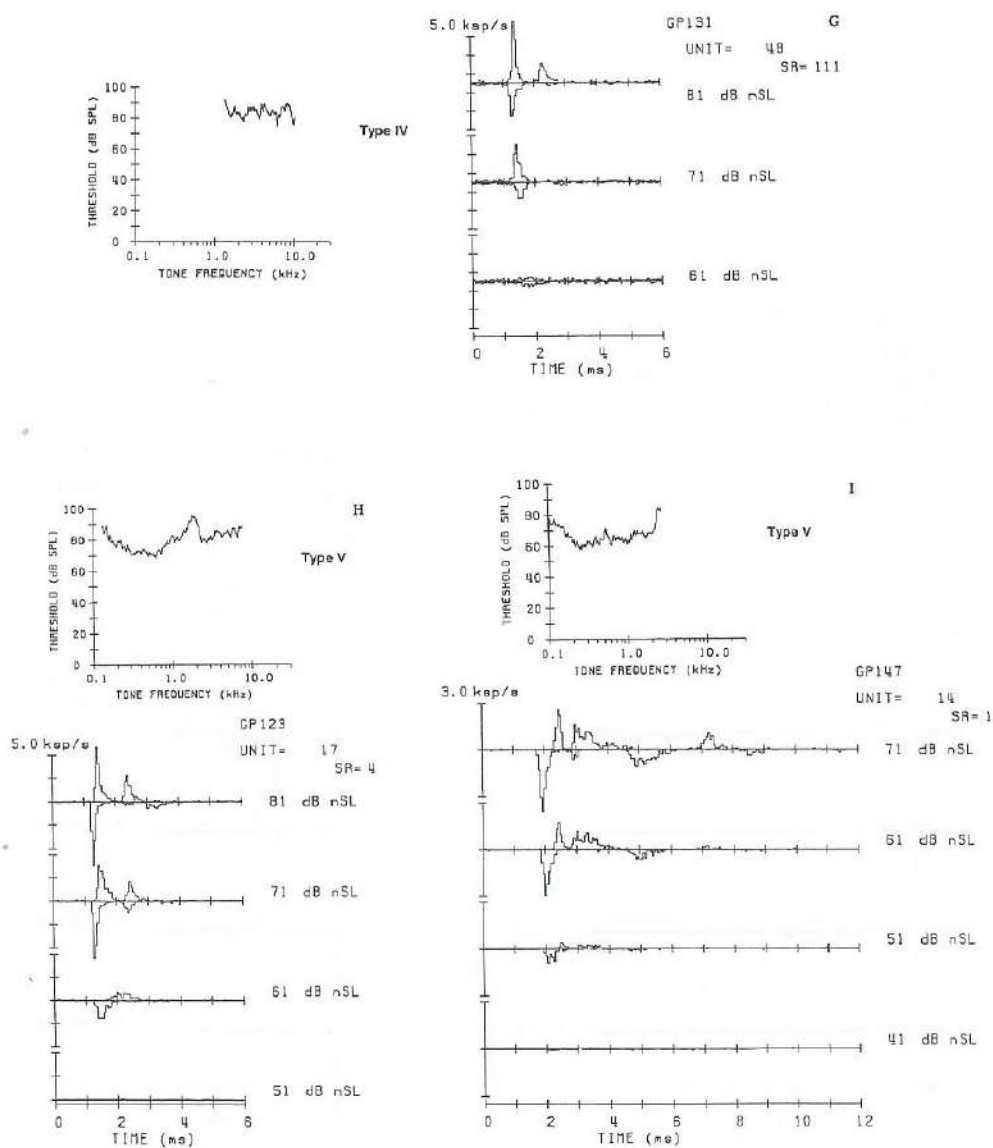


Fig. 4. (continued). (G) Type-IV responses; CF is unknown, SR of 111 spikes/s. (H) Type-V responses; CF unknown (presumably high), minimum threshold at 0.63 kHz (tail), SR of 4 spikes/s. (I) Type-V responses; CF unknown (presumably between 1 and 3 kHz), minimum threshold at 0.25 kHz (tail), and SR of 1 spike/s.

than normal even at high levels.

Figure 4C shows an example of type-II responses of a high-CF fibre. The PSTHs have changed in some respects. The response duration is shorter than normal over all intensities. The peak amplitude shows a large increase with intensity, such that it reaches a normal level already at 20-30 dB above the threshold. The click PSTHs of a low-CF fibre with a type-II FTC (Fig. 4D) show similar deviations: a short duration of the responses (e.g. at 51 dB nSL the response dies after 3 ms whereas normally it continues after 4 ms), and a rapid amplitude increase to normal values.

Large deviations in click responses were found in fibres which were tuned to two distinct frequencies, i.e. to the tip and tail frequencies. A prominent example of such tuning - type III - is presented in Fig. 4E. The main anomaly in the PSTHs is the dissimilarity of the responses to condensation and rarefaction clicks. The latency of the dominant rarefaction peak is shorter than that of the condensation peak, and with a reversal of click polarity a response peak changes to a response dip below the spontaneous level. Furthermore, with increasing intensity the rarefaction-click PSTH shows a late second and a third peak, whereas in normal high-CF fibres second peaks occur early and more than two peaks appear only at very high levels (above 60-70 dB nSL). Abnormal behaviour as a function of intensity occurs in a smaller latency decrease and a larger increase of peak amplitude. All these aspects are typical for low-CF fibres rather than for high-CF fibres (cf. Fig. 1B). Figure 4F shows type-III responses for a low-CF fibre. The tail has a threshold (50 dB SPL) that is even lower than the CF threshold (70 dB SPL). Here the click threshold (40 dB nSL) does not correspond to the tip threshold but to the tail threshold as indicated by a typical difference of 10 dB between tone and click thresholds (Versnel et al., 1992a). Just above the threshold the compound click PSTHs show an oscillatory pattern corresponding to the tail frequency (0.7 kHz). For higher intensities the first and third peaks shift with click polarity and the second peaks overlap such that the interpeak intervals for rarefaction are longer than for condensation clicks.

Figure 4G illustrates click responses of a fibre with a type-IV FTC, i.e., where tuning is lost. The PSTHs were normal for high-CF fibres in view of a very short and polarity independent latency and a second peak at an interpeak time of about 1.0 ms. However, in comparison to high-CF fibres, the amplitude was larger than normal already 10-20 dB above the fibre's click threshold for both polarities. In turn, the PSTH peak to condensation clicks was significantly larger than to rarefaction clicks. The dominant peaks were only half as narrow as normal.

Type-V FTCs show loss of tuning to high-frequency tones as in type IV, and relatively high sensitivity to low frequencies as in type III. Analogously to the FTC, the click PSTHs (compared with responses of normal high-CF fibres) showed abnormal properties reflecting both aspects of type-III and type-IV response behaviour (Fig. 4H). Similarly to type III, the PSTHs largely varied with polarity. On the other hand, the large amplitude and the narrow width of the dominant peaks observed from 20 dB above threshold were characteristic for type IV. We found one fibre with a type-V FTC which did not respond to high frequencies, implying a low original CF (i.e. below 3 kHz).

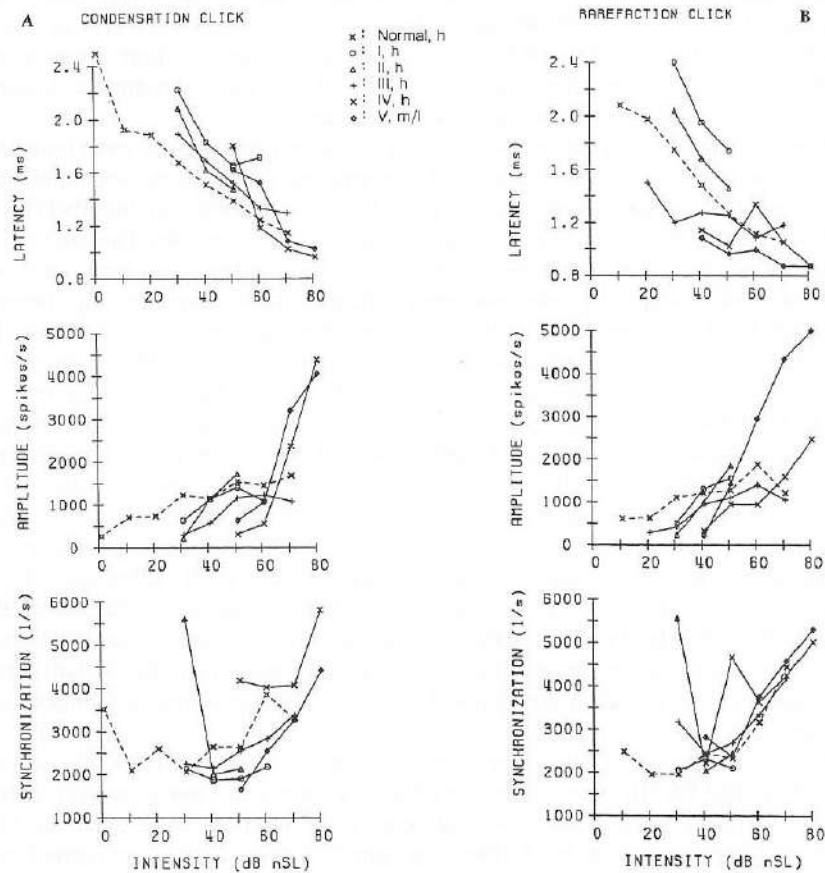


Fig. 5. Parameters of dominant PSTH peak versus click intensity averaged over subgroups of fibres. From top to bottom plots of latency, amplitude and synchronization are given. The dashed lines represent normal curves. The solid lines represent curves for abnormal fibres. The different abnormal types of fibres are represented by symbols. (A) Mean values of fibres with a CF between 6 and 12 kHz, for condensation clicks. All fibres are of a high SR except for type-V fibres which are of low or medium SR. Numbers of fibres involved: normal: 19; type I: 2; type II: 5; type III: 11; type IV: 5; type V: 4. (B) As Fig. 5A, but for rarefaction clicks.

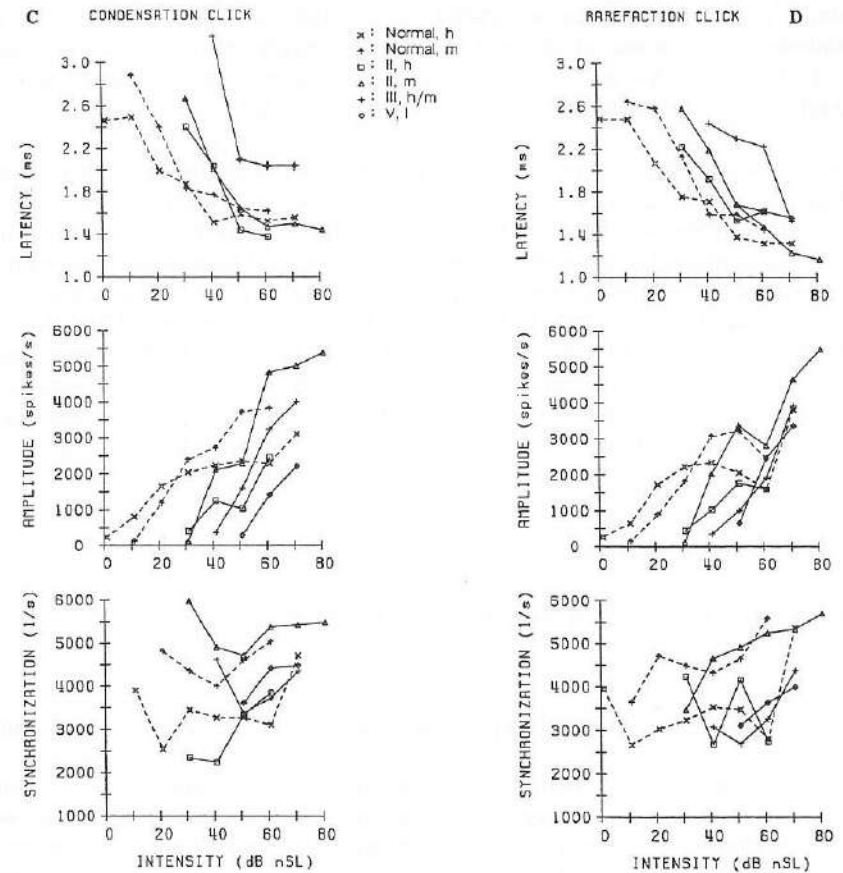


Fig. 5. (continued). (C) P-parameters for fibres with CF between 2 and 3 kHz for condensation clicks. The normal and type-II responses are given for high SR (crosses and squares, respectively) and medium SR (arrows and triangles); the type-III responses are for medium or high SR (values were similar), the type-V response is derived from the fibre with presumably a CF between 1 and 3 kHz (Fig. 4I). Data on other types were not available. Numbers of fibres involved: normal/h: 4; normal/m: 5; type II/h: 2; type II/m: 2; type III: 2; type V: 1. (D) As Fig. 5C, but for rarefaction clicks.

Figure 4I shows the responses of this fibre. The high-frequency slope of the FTC test at 2-3 kHz indicates that the CF tip might have been originally between 1 and 2 kHz, and the PSTH latencies agree with this. The PSTHs were abnormal in that they had two distinct interpeak intervals: one in the rarefaction-click PSTHs of about 3 ms which corresponds to the frequencies associated to the tail, and the other in the early condensation-click response of about 0.5 ms which might reflect the high-frequency region of the FTC. As in the other type-V responses, the dominant peak was considerably larger for rarefaction than for condensation clicks.

PSTHs of abnormal fibres: latency, amplitude, and synchronization of dominant peaks

Figure 5 shows average values of the P-parameters - latency, amplitude, and synchronization of the dominant PSTH peak - for the various types of abnormalities (solid lines) in comparison to normal values (dashed lines). These results are applied to simulate deviating click CAPs (Versnel et al., *). In Fig. 5 the CF ranges are covered for which we collected most data. In Figs. 5A, B the P-parameters are plotted for fibres with CFs between 6 and 12 kHz for all types I-V; in Figs. 5C, D the parameters are presented for CFs between 2 and 3 kHz for types II, III and V. If possible, the comparison is made between fibres of similar SR. Basically, abnormal features do not differ with SR. It should be noted that parameters found in other CF regions than presented here did not reveal different features. A brief survey of the PSTH pattern and

TABLE III
GLOBAL FEATURES IN CLICK PSTHS CORRESPONDING TO THE DIFFERENT FTC TYPES

FTC type	t_p	A_p (slope)	A_p (max)	S_p	pattern
I	long	norm ²⁾	norm	norm	norm
II	norm	steep	norm	norm	narrow/norm
III	norm&pol ¹⁾	steep/norm	norm	norm&pol	multi-peaks
IV	short/norm	steep	large&pol	large	narrow
V	norm&pol	steep	large	large/norm&pol	multi-peaks

The results of PSTH parameters t_p (latency), A_p (amplitude) and S_p (synchronization) and PSTH patterns, as shown in Figs. 4 and 5, are summarized in this Table. Most features do not vary significantly with CF. The Table refers to the results for high-CF fibres, and apply to those for low-CF fibres, except for 1): long & pol, and 2): small. All qualifications but 'norm' refer to deviations from normal which are significant for most click intensities/polarities. Pol: dependent on click polarity. Norm & pol: per polarity normal, but significant polarity dependence; other qualifications with '/norm' point to tendencies, i.e. deviations are not significant for most intensities, polarities or for all CF groups.

P-parameters is presented in Table III.

For fibres with a type-I FTC the input/output curves of the P-parameters are normal but shifted with level according to a threshold shift of 20-30 dB, i.e., the P-parameters are normal relative to threshold. This implies, e.g., that the latency is longer than normal compared at absolute click level. On the other hand, P-parameters of fibres with a type-II FTC do not differ significantly from normal in terms of absolute levels when measured at 20 dB above threshold, which is found both for high-CF (Fig. 5A,B) and low-CF fibres (Figs. 5C,D). In this case the input/output curves of the amplitude are steeper than normal.

The type-III abnormality in P-parameters of click responses of high-CF fibres (Figs. 5A, B) is reflected by polarity dependence rather than by great deviations for one polarity. The rarefaction-click latency is considerably shorter than the condensation-click latency, the difference is largest for low intensities, and is normal only at a very high level (71 dB nSL). The peak synchronization is significantly larger for rarefaction than for condensation clicks over the entire intensity range. The 2-3 kHz fibres with type-III responses (Figs. 5C, D) have latencies that are considerably longer than normal over the entire intensity range. The slope of the amplitude curve is steeper than in normal 2-3 kHz fibres.

We compare type-IV responses in the plot for the CF range between 6 and 12 kHz (Figs. 5A, B). Typical deviations concern the amplitude: maximum value, increase with intensity, and polarity dependence are all extremely large. For instance, the rate of increase for the condensation polarity is larger than normal by a factor of 5. The peak synchronization is also significantly larger than normal.

The peak parameters of type V reveal a large polarity dependence (Figs. 5A-D). The rarefaction-click latency is shorter than the condensation-click latency, and this polarity difference decreases with intensity in a similar fashion as shown by type-III responses. Both the peak amplitude and synchronization are larger for rarefaction than for condensation clicks. The slope of the amplitude curve is very steep and the amplitude is larger than normal at 20 dB above fibre's threshold.

Fourier analysis of difference PSTHs

We performed Fourier analysis on difference PSTHs with an oscillatory pattern, i.e. for fibres with a low CF (normal, types I or II) or relatively low tail threshold (types III or V). Figure 6A shows an example of the intensity dependence of the power spectra of a fibre in a normal cochlea (group NF/NC). Similar results were found in fibres of group NF/AC: near click threshold the best frequency (BF) was similar to the CF, and in most fibres with a CF above 0.5 kHz the BF decreased and the spectrum peak broadened with intensity. Significant BF decreases were not found in fibres with a CF below 0.5 kHz ($N = 11$). Figure 6B presents a series of power spectra of difference PSTHs of a fibre with a type-II FTC. The BF and width of the spectrum peak showed the normal behaviour with intensity, which was representative both for fibres with a type-I and with a type-II FTC.

Fourier analysis illustrates the relation between the oscillatory PSTH pattern and

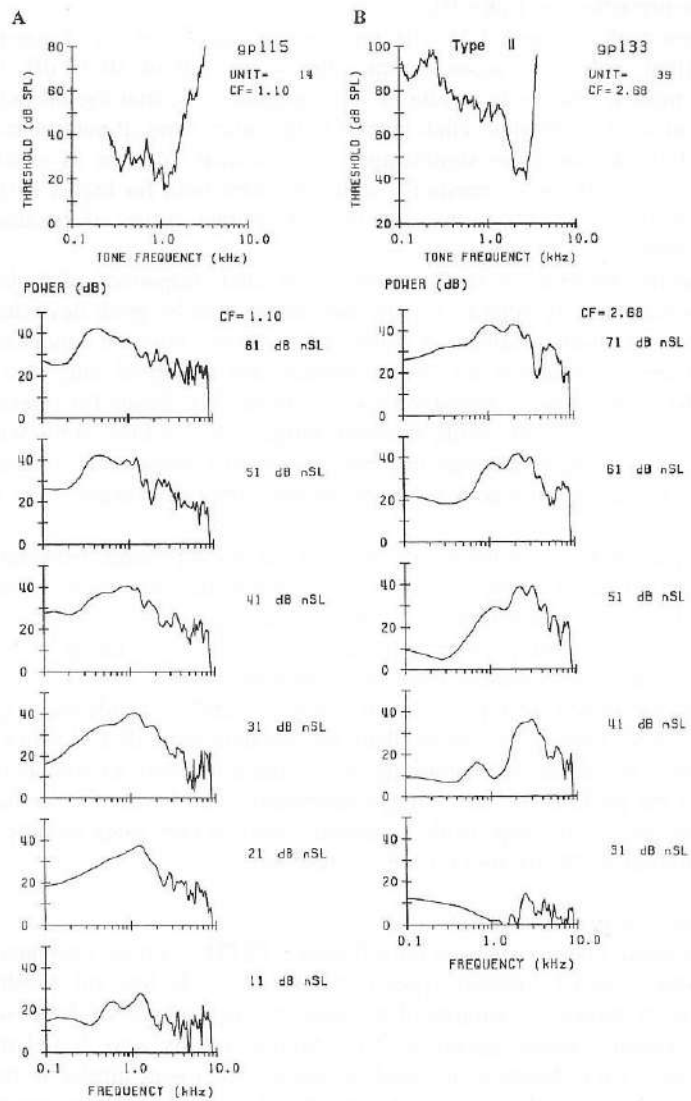


Fig. 6. Power spectra of difference PSTHs as a function of click intensity with the FTC in the top panel. (A) Spectra for a normal fibre with a CF of 1.1 kHz (see corresponding PSTHs in Fig. 1B). (B) Spectra of a type-II fibre with a CF of 2.7 kHz (see corresponding PSTHs in Fig. 4D).

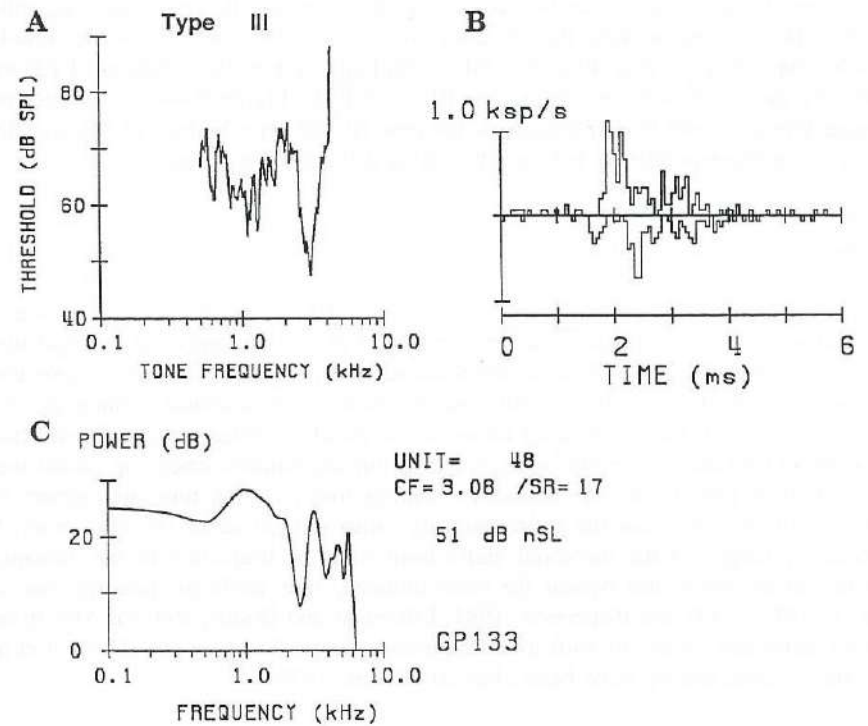


Fig. 7. Type-III FTC with compound click response and Fourier power spectrum. (A) FTC with a CF of 3.1 kHz and a tail with a minimum at 1.1 kHz. (B) Compound PSTH to click intensity of 51 dB nSL, about 15 dB above fibre's click threshold. (C) Power spectrum of difference PSTH corresponding to compound PSTH of (B), BF is 1.0 kHz, frequency of second local maximum is 3.1 kHz.

the FTC in simple cases shown above. Also in cases of type III or V where the oscillatory response patterns are more complex (cf. Figs. 4E, F, H, and I) Fourier analysis may be useful in that it reveals the extent that the response patterns reflect the tail frequency. Figure 7 shows an example of a type-III FTC (A), its corresponding temporal response (B), and the power spectrum of the difference PSTH (C). The power spectrum shows two peaks that correspond to the CF tip (around 3.1 kHz) and the tail (around 1 kHz) of the FTC. Hence, in this case the abnormal response pattern might be caused by superposition of the residual sensitivity to CF and hypersensitivity of the tail. Figure 8 shows the power spectra for two fibres with a type-III (A, B) and one with a type-V (C) FTC. In all three cases the power spectrum at intensities near threshold reflects the FTC tail. The spectra broaden with increasing intensity, either directed towards lower frequencies (A) or towards higher frequencies (B, C). Note that, unlike in Fig. 7, a (local) peak around the CF does not occur in the spectrum of the low-CF fibre with a type-III FTC (Fig. 8B). We did not find any systematic variation of BF with intensity in a group of 24 fibres with a type-III or -V FTC. Figure 9 shows a scatter plot of BF near threshold versus tail frequency for type III and type V. For all but one fibre there is a close correspondence between the BF and the tail frequency.

Discussion

This paper presents single-fibre responses to clicks in relation to tuning curves in impaired ears; in the companion paper (Versnel et al., *) we apply these single-fibre results to construct a model to simulate simultaneously recorded CAPs. For interpretation of single-fibre and electrocochleographic results in terms of cochlear pathology, it is important to ascertain that the hearing losses are of purely cochlear origin. Dysfunction of the outer and middle ear could be excluded in our experiment since ear canals were clean and typical phenomena in conductive hearing loss as a flat tone audiogram and elongated CAP latencies over the entire intensity range did not occur (Versnel et al., *). The frequency ranges of the threshold shifts from near the frequency of the damaging tone to an octave above are typical for noise-induced, thus cochlear, hearing loss (cf. Salvi et al., 1982; Cody and Robertson, 1983; Liberman and Dodds, 1984b). Also in one case of an additional threshold shift after respiratory depression (see also Versnel et al., 1992b), the cochlea should have been affected (Evans, 1975).

Responses of normal fibres in pathological cochleas

Pure-tone responses from cochlear regions that are morphologically intact but located near damaged regions can be affected (Robertson, 1982; Liberman and Dodds, 1984b). We found that fibres which had normal pure-tone thresholds (NF/AC) had normal click responses over the entire intensity range. This means that a possibly existing non-local effect of damage (which causes threshold shifts up to 60 dB) is not expressed earlier in click than in tone responses.

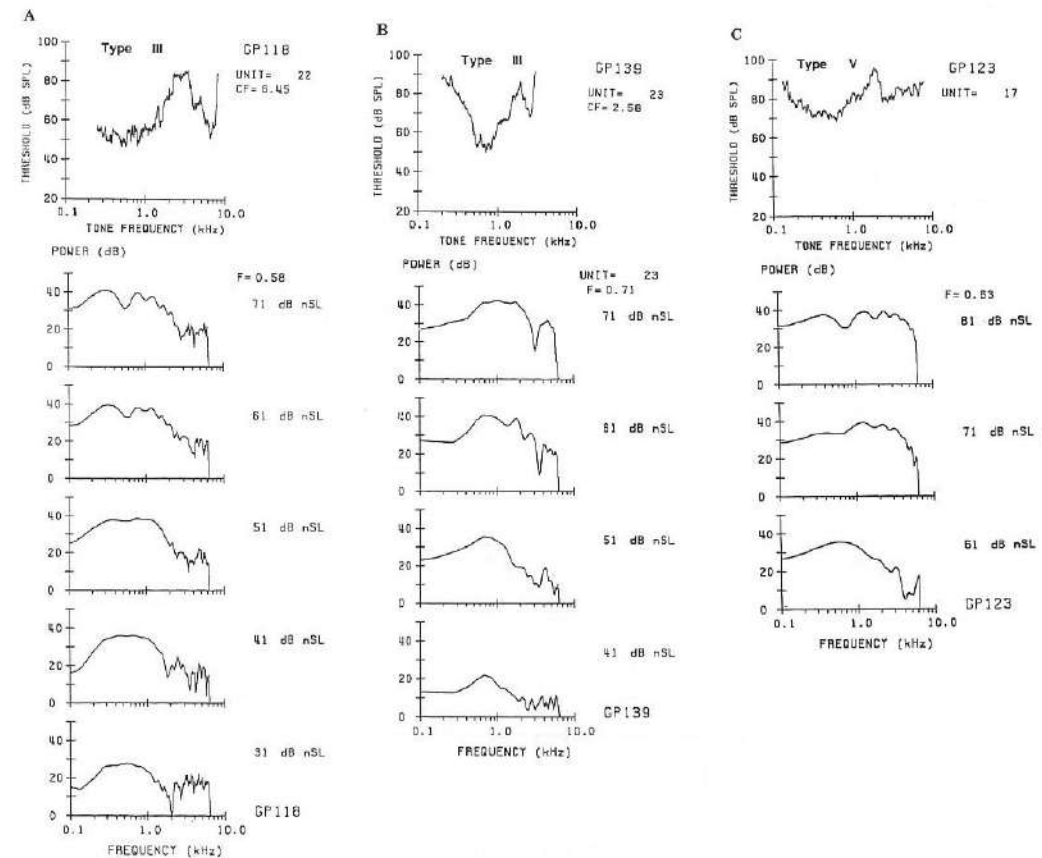


Fig. 8. Power spectra of difference PSTHs at various intensities for abnormal fibres. Their FTC is plotted at the top. F indicates the tail frequency with which the BF of the spectrum is compared. (A) Plots for the fibre with a type-III FTC, a CF of 6.5 kHz and a tail frequency of 0.58 kHz (original PSTHs in Fig. 4E). (B) Plots for the fibre with a type-III FTC, CF of 2.6 kHz and tail around 0.71 kHz (original PSTHs in Fig. 4F). (C) Plots for the fibre with a type-V FTC, tail around 0.63 kHz (corresponding PSTHs in Fig. 4H).

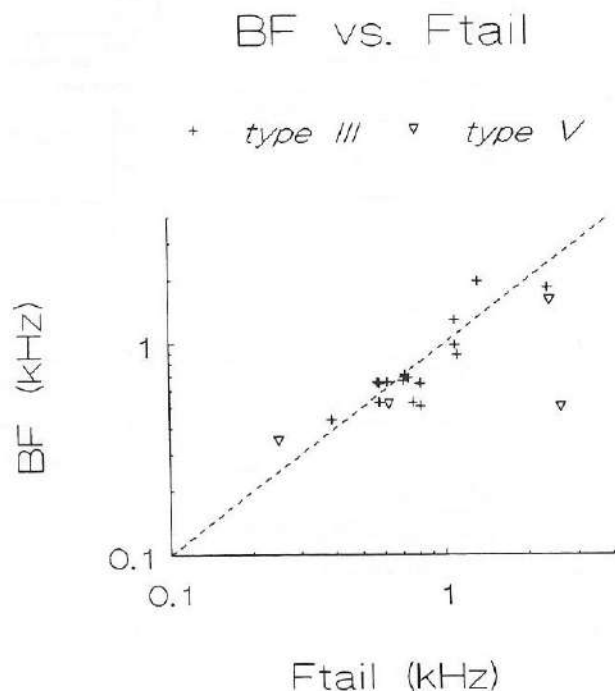


Fig. 9. Best frequency (BF) of Fourier power spectra of difference PSTHs versus frequency of FTC tail for 20 fibres. The PSTHs are considered at low click levels, usually 5-20 dB above threshold. FTCs are of type III and V, types with a relatively sensitive tail. Dashed line represents BF equal to tail frequency. Some of the fibres in which series of PSTHs were measured are not represented in the plot since the tail was not sufficiently measured to estimate properly a tail frequency.

Abnormal frequency threshold curves

The criteria for typification of abnormal threshold curves were based on changes of sensitivities in both tip and tail (Table I). The distinction of tip and tail is well known in pathology (Lieberman and Kiang, 1978; Schmiedt et al., 1980; Salvi et al., 1983; Liberman and Dodds, 1984b), and in normal cochleas a notch that separates the tip and tail regions is observable (cf. Liberman and Kiang, 1978; Schmiedt, 1982; Versnel et al., 1992a). Our scheme of FTC types for the most part agrees to that described by other authors. The "V" type of Liberman and Kiang (1978) and Salvi et al. (1983) corresponds to type I, their "W" type corresponds to type III, and Salvi et al. (1983) reasoned that their "U" type probably represented a sensitive tail, which we classify type V. The types 2, 3 and 4 used by Robertson (1982) largely correspond to the "U"-, "W"-, and "V"-types, respectively. Three of the four schematic tuning curves given in Fig. 14 in the paper of Liberman and Dodds (1984b) correspond closely to our types I, III, V, respectively, and their fourth curve is reflected by II or IV.

Generally, across all FTC types, we find that tuning broadens with increase of the threshold shift (Figs. 3A, B), which is consistent with the general line in experimental findings in cochlear damage (Harrison and Evans, 1982; Salvi et al., 1983).

Abnormal click responses

The click responses in abnormal fibres showed several distinct deviations apart from threshold shifts. Table III demonstrates the unique relation between FTC type and abnormal click PSTH. Each FTC type corresponds to a different set of deviations in PSTHs. Here we consider the question whether altered PSTHs can be explained from altered FTCs. As a first thought, we consider the cochlea as a unidirectional sequence of transduction stages representing the following mechanisms: i) cochlear mechanics, ii) IHC transduction, iii) the synaptic process, and iv) spike generating mechanism. Since the FTC reflects the filter characteristics of the basilar membrane (e.g. Sellick et al., 1982), a click PSTH can be predicted from the FTC (Versnel et al., 1992a; Schoonhoven et al., --). This concept applies to normal cochleas. In this study of abnormal cochleas mainly the first two stages are subject to change, since noise causes damage to OHCs (affecting stage i) and damage to IHCs (affecting stage ii). For an alteration in the first stage the PSTH and FTC will be related to each other analogously to the normal case. A change in the second stage might only involve simple threshold shifts. We may thus expect that in most occasions changes in a click response can indeed be predicted from the altered FTC. We discuss the deviations in click PSTHs related to the FTC type in more detail in the following subsections.

Click responses for type I

The FTCs and click PSTHs of type I are simply related by a threshold elevation with respect to normal. The equal threshold shift for tones of all frequencies and clicks indicates damage in IHCs (Lieberman and Dodds, 1984b; Patuzzi et al., 1989). Type-I responses appear to be comparable to normal responses of low-SR fibres. The type-I FTC of a high-CF fibre of high SR (Fig. 4A) resembles an FTC of a normal fibre of

low SR; and the I/O curves of the P-parameters of type I run, as those of low-SR fibres do (Versnel et al., 1992a), parallel to normal high-SR curves (Figs. 5A, B). Both in the case of low-SR responses where the synapse is different (Lieberman, 1982), and in a type-I abnormality where presumably the IHC depolarization is smaller due to damage to the IHC cilia (Lieberman and Dodds, 1984a), the postsynaptic generator potential becomes smaller (cf. Versnel et al., 1990b). Since the SR distribution for type I was normal (Table II) it is likely that only the depolarization process was affected and not the resting current which controls the spontaneous neural activity (Lieberman and Dodds, 1984a). This points to a mild damage to the IHC cilia.

Click responses for types II and IV

According to Liberman and Dodds (1984b) and Patuzzi et al. (1989) the mechanical response corresponding to the type-II FTC is deteriorated by OHC damage. Considering the absence of the tip and the increase of the tail threshold, one can assume that the type-IV response is due to severe damage to both IHCs and OHCs (cf. Robertson, 1983; Liberman and Dodds, 1984b; Patuzzi et al., 1989). With respect to the degradation of tuning as well as the synchronization and amplitude of the click response, the type-IV responses can be considered as extreme forms of type-II responses. Three aspects of the click responses are discussed here.

A broader filter corresponds to a shorter duration of the impulse response (both can be thought of as a result of larger damping). It shows in basilar-membrane click responses in deteriorated preparations (Robles et al., 1976; Ruggero et al., 1992), and it is expressed by the neural responses in our experiments (Figs. 4C, D, G). Our results agree with those of Salvi et al. (1979) who found in noise-exposed chinchillas low Q_{10dB} s of FTCs and a decrease in number of PSTH peaks of low-CF fibres.

The large increase of PSTH amplitude with intensity agrees with steep rate-intensity curves to CF tones found in fibres with elevated thresholds (Evans, 1975; Harrison, 1981; Liberman and Kiang, 1984), and is probably caused by a decrease of compressive nonlinearity of the cochlear mechanics (cf. Ruggero et al., 1992). In the type-IV case a large synchronization of discharges contributes to the large value of the maximum amplitude. Here a preference for the condensation polarity might be due to such a strong damping in the basilar membrane response that the largest displacement is reached in the second half-cycle (Ruggero et al., 1992) which is excitatory for the condensation polarity.

In agreement with click data of Salvi et al. (1979) and van Heusden and Smoorenburg (1983), the latency of type-II responses did not change significantly from normal at the same absolute level. This finding fits in with considerations of Eggermont (1979) who pointed out that the time shift of the maximum of the basilar-membrane response related to a decrease of Q_{10dB} is very small if the high-frequency slope of the tuning curve is not changed (Goldstein et al., 1971), which is approximately the case for type-II FTCs. Accordingly, shorter latencies of type-IV click responses result from a flat tuning curve with a shallow high-frequency slope.

Click responses for types III and V, consequences of hypersensitivity

Tuning curves of type III or V, i.e. W-shaped and/or having a hypersensitive tail, are found in cochleas damaged by noise (Lieberman and Kiang, 1978; Robertson, 1982; van Heusden and Smoorenburg, 1983; Salvi et al., 1983; Liberman and Dodds, 1984b), ototoxic drugs (Schmiedt et al., 1980) or endolymphatic hydrops (Harrison and Prijs, 1984). In agreement with reports of Liberman and colleagues we found that type-III FTCs were far from exceptional and tended to have a higher SR (Table II).

It has been suggested that hypersensitivity is caused by selective severe damage to OHCs with IHCs functionally intact (Lieberman and Kiang, 1978; Liberman and Dodds, 1984b; Schmiedt et al., 1980; Smith et al., 1988). The type-V FTC is thought to be caused by total dysfunctioning of OHCs (Lieberman and Dodds, 1984b). Different cochlear models support these suggestions. Zwislocki (1984) explained tail hypersensitivity as an increase of shear force between reticular lamina and tectorial membrane which can occur if OHCs are damaged; mechanical coupling between OHCs and IHCs via the tectorial membrane was assumed. Geisler (1991) could simulate the type-III tuning curve by varying motile feedback forces from OHCs, and Neely (1992) simulated the type-V curve by eliminating OHC motility. Geisler suggests that OHC damage basal from the CF location would lead to hypersensitivity. This demonstration of non-local effect is consistent with experiments in a normal cochlea where a suppressor tone presented above CF resulted in tail hypersensitivity (Schmiedt, 1982). These data are not, however, supported by findings in damaged cochleas: type-III FTCs are found at the high-frequency border of damage (Lieberman and Kiang, 1978; Robertson, 1982), as well as at other locations relative to the damaged area (Lieberman and Dodds, 1984b; this report and Versnel et al., *). Considering the variations in experiments and models, we could state that in general type-III FTCs occur in regions with moderate hearing loss where the necessary specific conditions for OHC damage can occur. As a consequence of our criteria some of the fibres with a type-III or -V FTC involve tail hypersensitivity (e.g. Figs. 4E, F, I) and some do not (e.g. Fig. 4H). We hypothesize that in all these cases the basilar membrane is hypersensitive to low frequencies caused by OHC lesions, and that in those type-III and -V cases with a normal tail level the mechanical hypersensitivity is neutralized by additional damage to the IHC or afferent synapse.

In spite of this intriguing phenomenon of double tuning and hypersensitivity (*a paradox*, Zwislocki, 1984), only little attention has been given to corresponding temporal response features. The temporal responses we found can be understood on the basis of the FTCs. The high-CF fibres showed click PSTHs with normal short latencies but with low-CF like patterns (cf. Fig. 4E). The suggestion that these patterns are caused by the low-frequency hypersensitivity is supported by the close correspondence between Fourier power spectrum of the difference PSTHs and the FTC tail (Fig. 8; Fig. 9). The click response patterns are fairly predictable from the FTC over all levels. At low click levels the PSTHs to both click polarities do not overlap indicating a dominant response to tail frequencies, and with increase of intensity an overlap of response peaks grows which indicates an additional contribution of resonance at the tip frequency (see Fig. 4E). A comparable but reverse pattern is found in normal high-CF fibres where at high levels

oscillations with the tail frequency seem to show up in click PSTHs (Antoli-Candela and Kiang, 1978; Versnel et al., 1992a). A type-III response of a low-CF fibre is of interest because the fibre is tuned to two low frequencies and, consequently, is expected to have an oscillatory click-response pattern consisting of a superposition of oscillations with CF and the tail frequency. This pattern is nicely demonstrated in Fig. 7 for a fibre with a CF of 3.1 kHz and tail around 1 kHz; also, it is reflected by the short and long interpeak intervals in the PSTHs of the low-CF fibre with a type-V FTC (Fig. 4I). On the other hand, in one fibre we did not find an oscillation with CF (2.6 kHz) in the click responses at levels (61 and 71 dB nSL, Figs. 4F, 8B) while it was expected in view of the threshold at CF (Versnel et al., 1992a). This discrepancy is not well understood.

As type-V FTCs are considered as a combination of type III (represented by the low tail threshold) and type IV (represented by an absence of the tip), so do click PSTHs of type V reflect this combination which is another indication that deviating PSTHs are predictable from the corresponding abnormal FTC.

Finally, we have demonstrated that given a type-III FTC one can compute PSTHs which well resemble our experimental PSTHs (Versnel et al., 1992c; Schoonhoven et al., --). Briefly, the mechanical output in this model is reproduced by application of two parallel linear filters representing the tip and tail regions of the FTC, and parameters are set to fit the FTCs. In combination with cascaded transduction sections (IHC, synaps, spike generator) neural click responses are simulated. The model results support above discussed suggestions that the tail hypersensitivity causes the greatly deviating click responses.

Deviations in click responses not related to FTC

In previous subsections we showed that for each FTC type the associated click PSTH can be predicted. However, occasionally we found cases where the compound PSTH showed deviations which cannot be explained on the basis of the FTC. We mention here two cases. (a) For the low-CF fibre with a type-III FTC (Fig. 4F) the second peak of the condensation-click PSTH disturbs the regular pattern in the compound PSTH that is oscillatory with the tail frequency. (b) In case of type-IV responses, the PSTH to rarefaction clicks is single-peaked and narrow, this seems to correspond well to the flat tuning (see subsection on type II/IV), but the PSTH to condensation clicks has in addition a second peak (Fig. 4G). This second peak is puzzling. It is noteworthy that both cases (a) and (b) occur at high click levels and that they involve a second peak at about 1 ms after a full first peak ($p_r \approx 1$). In the literature unexpected secondary discharges are reported to occur to a small extent in click responses in normal cochleas (Lütkenhöner et al., 1980). According to these authors' analysis mechanical behaviour appeared to be normal. This leads us to speculate that unexpected discharges are due to some synaptic mechanism that is active at high intensities, and more apparent in abnormal than in normal conditions (Prijs et al., --).

Consequences for CAPs and speech processing

We can adequately model CAPs to clicks on the basis of the P-parameters for

normal cochleas (Versnel et al., 1992a). Since P-parameters reflect the various types of abnormal responses (see Table III), we should be able to simulate deviations of CAPs in pathological cochleas too. This issue is extensively addressed in the companion paper (Versnel et al., *), but here we give qualitative predictions of CAP features. Deviations of type III might result in increased polarity difference in CAPs. In spite of severe hearing loss CAP amplitudes can be larger than normal as a consequence of abnormally large responses of types IV and V. Abnormally short latencies even in cochleas with high-frequency loss might occur if there is a significant number of fibres with response types III, IV or V. Vice versa, from specific deviations in click CAPs as just mentioned one might try to assess the underlying single-fibre response patterns. Subsequently, from that one would like to derive the local frequency tuning. This should be possible given the unique relationship between FTC types and compound click PSTHs.

Various types of abnormal tuning properties are reflected by changes in responses to clicks, especially in the temporal pattern. Single-neuron responses to complex sounds such as speech may change accordingly. Since temporal cues presumably play a significant role in peripheral speech processing (Young and Sachs, 1979; Shamma, 1985), this processing will be disturbed in subjects with cochlear pathologies. The reduced tip-to-tail ratio which occurs for most abnormal FTCs will cause a significant temporal influence of the tail at the expense of the role played by the tip, thus dramatically changing the information carried by the fibre. Disorders in information processing will be preserved up to central auditory levels; in this context it is relevant that type-III characteristics as a result of cochlear damage could be found in the central nervous system (Smith et al., 1988; Harrison et al., 1991). In conclusion, phenomena at the auditory-nerve level as described in this paper may contribute to our understanding of the nature of impaired sound perception.

Acknowledgements

This study was supported by the Netherlands organization for scientific research (NWO) and by the Heinsius Houbolt Fund. The authors are grateful to V. Gerritsma, A. van Wijngaarden, and P. Schotel for technical assistance. We sincerely thank E. de Boer (ENT dept., University of Amsterdam) for many valuable comments, and G. Hunt for careful proofreading of original versions of the manuscript.

References

- Antoli-Candela, F.Jr. and Kiang, N.Y.S. (1978) Unit activity underlying the NI potential. In: R.F. Naunton, and C. Fernandez (Eds.), *Evoked electrical activity in the auditory nervous system*, Academic Press, New York, pp. 165-189.
- Cody, A.R. and Robertson, D. (1983) Variability of noise-induced damage in the guinea pig cochlea: Electrophysiological and morphological correlates after strictly controlled exposures. *Hear. Res.* 9, 55-70.

- Dallos, P. and Harris, D. (1978) Properties of auditory nerve responses in absence of outer hair cells. *J. Neurophysiol.* 41, 365-383.
- Dolan, T.G. and Mills, J.H. (1989) Recoveries of whole-nerve AP thresholds, amplitudes and tuning curves in gerbils following noise exposure. *Hear. Res.* 37, 193-202.
- Eggermont, J.J. (1976) Electrocochleography. In: W.D. Keidel and W.D. Neff (Eds.), *Handbook of sensory physiology*, Springer Verlag, Berlin, Heidelberg, New York, Vol. V, pp. 626-705.
- Eggermont, J.J. (1977) Compound actionpotential tuning curves in normal and pathological human ears. *J. Acoust. Soc. Am.* 62, 1247-1251.
- Eggermont, J.J. (1979) Narrow-band AP latencies in normal and recruiting human ears. *J. Acoust. Soc. Am.* 65, 463-470.
- Eggermont, J.J., Johannesma, P.I.M. and Aertsen, A.M.H.J. (1983) Reverse-correlation techniques in auditory research. *Quart. Rev. Biophys.* 16, 341-414.
- Evans, E.F. (1975) The sharpening of cochlear frequency selectivity in the normal and abnormal cochlea. *Audiology* 14, 419-442.
- Evans, E.F. (1979) Single-unit studies of mammalian cochlear nerve. In: H.A. Beagley (Ed.), *Auditory investigation: the technological and scientific basis*, Clarendon Press, Oxford, pp. 324-367.
- Geisler, C.D. (1991) A cochlear model using feedback from motile outer hair cells. *Hear. Res.* 54, 105-117.
- Goldstein, J.L., Baer, T., Kiang, N.Y.S. (1971) A theoretical treatment of latency, group delay, and tuning characteristics for auditory nerve responses to clicks and tones. In: M.B. Sachs (Ed.), *Physiology of the auditory system*. National educational consultants, Baltimore, 133-141.
- Harrison, R.V. (1981) Rate-versus-intensity functions and related AP responses in normal and pathological guinea pig and human cochleas. *J. Acoust. Soc. Am.* 70, 1036-1044.
- Harrison, R.V. and Evans, E.F. (1982) Reverse correlation study of cochlear filtering in normal and pathological guinea pig ears. *Hear. Res.* 6, 303-314.
- Harrison, R.V. and Prijs, V.F. (1984) Single cochlear fibre responses in guinea pigs with long-term endolymphatic hydrops. *Hear. Res.* 14, 79-84.
- Harrison, R.V., Nagasawa, A., Smith, D.W., Stanton, S. and Mount, R.J. (1991) Reorganization of auditory cortex after neonatal high frequency cochlear hearing loss. *Hear. Res.* 54, 11-19.
- van Heusden, E. and Smoorenburg, G. F. (1981) Eighth-nerve action-potential tuning curves in cats before and after inducement of an acute noise trauma. *Hear. Res.* 5, 25-48.
- van Heusden, E. and Smoorenburg, G.F. (1983) Responses from AVCN units in the cat before and after inducement of an acute noise trauma. *Hear. Res.* 11, 295-326.
- Hunter-Duvar, I.M., Suzuki, M. and Mount, R.J. (1982) Anatomical changes in the organ of Corti after acoustic stimulation. In: R.P. Hamernik, D. Henderson and R. Salvi (Eds.), *New perspectives on noise-induced hearing loss*, Raven Press, New York, pp. 3-22.
- Liberman, M. C. (1982) Single-neuron labelling in the cat auditory nerve. *Science* 216, 1239-1241.
- Liberman, M.C. and Dodds, L.W. (1984a) Single-neuron labeling and chronic cochlear pathology. II. Stereocilia damage and alterations of spontaneous discharge rates. *Hear. Res.* 16, 43-53.
- Liberman, M.C. and Dodds, L.W. (1984b) Single-neuron labeling and chronic cochlear pathology. III. Stereocilia damage and alterations of threshold tuning curves. *Hear. Res.* 16, 55-74.
- Liberman, M.C. and Kiang, N.Y.S. (1978) Acoustic trauma in cats. *Acta Otolaryngol. Suppl.* 358, 1-63.
- Liberman, M.C. and Kiang, N.Y.S. (1984) Single-neuron labeling and chronic cochlear pathology. IV. Stereocilia damage and alterations in rate- and phase-level functions. *Hear. Res.* 16, 75-90.
- Lütkenhöner, B., Hoke, M. and Bappert, E. (1980) Effect of recovery properties on the discharge pattern of auditory nerve fibres. In: M. Hoke, G. Kauffmann and E. Bappert (Eds.), *Scand. Audiol. Suppl.* 11, 25-43.
- Neely, S.T. (1992) The role of outer hair cell motility in cochlear mechanics. A.R.O. midwinter meeting, St Petersburg Beach, Florida, poster 297.
- Patuzzi, R.B., Yates, G.K. and Johnstone, B.M. (1989) Outer hair cell receptor current and sensorineural hearing loss. *Hear. Res.* 42, 47-72.
- Pfeiffer, R.R. and Kim, D.O. (1972) Response patterns of single cochlear nerve fibers to click stimuli: descriptions for cat. *J. Acoust. Soc. Am.* 52, 1669-1677.
- Prijs, V.F., Keijzer, J., Schoonhoven, R. and Versnel, H. (1990) The sting is in the tail. In: P. Dallos, C.D. Geisler, J.W. Matthews, M.A. Ruggero and C.R. Steele (Eds.), *The Mechanics and Biophysics of Hearing*, 1990, Madison. Springer-Verlag, Berlin Heidelberg, pp. 154-161.
- Prijs, V.F., Keijzer, J., Versnel, H. and Schoonhoven, R. (--) Recovery characteristics of auditory nerve fibres in the normal and noise-damaged cochlea. *Hear. Res.*, in press.
- Robertson, D. (1982) Effects of acoustic trauma on stereocilia structure and spiral ganglion cell tuning properties in the guinea pig cochlea. *Hear. Res.* 7, 55-74.
- Robertson, D. (1983) Functional significance of dendritic swelling after loud sounds in the guinea pig cochlea. *Hear. Res.* 9, 263-278.
- Robles, L., Rhode, W. S. and Geisler, C. D. (1976) Transient response of the basilar membrane measured in squirrel monkeys using the Mössbauer effect. *J. Acoust. Soc. Am.* 59, 926-939.
- Ruggero, M.A., Rich, N.C. and Recio, A. (1992) Basilar membrane responses to clicks. In: Y. Cazals, L. Demany and K.C. Horner (Eds.), *Auditory Physiology and Perception, Advances in the Biosciences*, Pergamon Press, Oxford, Vol. 83, pp. 85-92.
- Rutten, W.L.C. (1986) The influence of cochlear hearing loss and probe tone level on compound action potential tuning curves in humans. *Hear. Res.* 21, 195-204.
- Salvi, R.J., Hamernik, R.P. and Henderson, D. (1983) Response patterns of auditory nerve fibers during temporary threshold shift. *Hear. Res.* 10, 37-67.
- Salvi, R.J., Henderson, D. and Hamernik, R.P. (1979) Single auditory nerve fiber and action potential latencies in normal and noise-treated chinchillas. *Hear. Res.* 1, 237-251.
- Salvi, R.J., Perry, J., Hamernik, R.P. and Henderson, D. (1982) Relationships between cochlear pathologies and auditory nerve and behavioral responses following acoustic trauma. In: R.P. Hamernik, D. Henderson and R. Salvi (Eds.), *New perspectives on noise-induced hearing loss*, Raven Press, New York, pp. 165-188.
- Schmiedt, R.A. (1982) Boundaries of two-tone rate suppression of cochlear-nerve activity. *Hear. Res.* 7, 335-351.
- Schmiedt, R.A., Zwislocki, J.J. and Hamernik, R.P. (1980) Effects of hair cell lesions on responses of cochlear nerve fibers. I. Lesions, tuning curves, two-tone inhibition, and responses to trapezoidal-wave patterns. *J. Neurophysiol.* 43, 1367-1389.
- Schoonhoven, R., Keijzer, J., Versnel H. and Prijs, V.F. (--) A dual resonance model describing single-fiber responses to clicks in the noise-damaged cochlea. Submitted to *J. Acoust. Soc. Am.*
- Sellick, P.M., Patuzzi, R.B. and Johnstone, B.M. (1982) Measurement of basilar membrane motion in the guinea pig using the Mössbauer technique. *J. Acoust. Soc. Am.* 72, 131-141.
- Shamma, S.A. (1985) Speech processing in the auditory system II: Lateral inhibition and the central processing of speech evoked activity in the auditory nerve. *J. Acoust. Soc. Am.* 78, 1622-1632.
- Smith, D.W., Moody, D.B. and Stebbins, W.C. (1988) Effects of selective outer hair cell lesions on the frequency selectivity of the auditory system. In: H. Duifhuis, J. W. Horst and H. P. Wit (Eds.), *Basic issues in hearing*, Academic Press, London, pp. 448-456.
- Versnel, H., Prijs, V.F. and Schoonhoven, R. (1990a) Single-fibre responses to clicks in relationship to the compound action potential in the guinea pig. *Hear. Res.* 46, 147-160.
- Versnel, H., Schoonhoven, R. and Prijs, V.F. (1990b) Latencies of eighth nerve fibre responses with respect to their relative contribution to the compound action potential in the guinea pig. *Eur. Arch. Otorhinolaryngol.* 247, 33-36.
- Versnel, H., Schoonhoven, R. and Prijs, V.F. (1992a) Single-fibre and whole-nerve responses to clicks as a function of sound intensity in the guinea pig. *Hear. Res.* 59, 138-156.
- Versnel, H., Prijs, V.F. and Schoonhoven, R. (1992b) Round-window recorded potential of single-fibre discharge (unit response) in normal and noise-damaged cochleas. *Hear. Res.* 59, 157-170.
- Versnel, H., Schoonhoven, R. and Prijs, V.F. (1992c) Aberrant temporal discharge patterns in noise-damaged guinea-pig cochleas. In: Y. Cazals, L. Demany and K.C. Horner (Eds.), *Auditory Physiology and Perception, Advances in the Biosciences*, Pergamon Press, Oxford, Vol. 83, pp. 607-615.
- Versnel, H., Prijs, V.F. and Schoonhoven, R. (*) Click responses in noise-damaged guinea-pig cochleas. II. Sensorineural causes of deviations in the compound action potential. *Hear. Res.*--

- Young, E.D. and Sachs, M.B. (1979) Representation of steady-state vowels in the temporal aspects of the discharge patterns of populations of auditory-nerve fibers. *J. Acoust. Soc. Am.* 66, 1381-1403.
- Zwislocki, J.J. (1984) How OHC lesions can lead to neural cochlear hypersensitivity. *Acta Otolaryngol.* 97, 529-534.

Chapter VI

Aberrant temporal discharge patterns in noise-damaged guinea-pig cochleas

Huib Versnel, Ruurd Schoonhoven and V.F. Prijs

Summary

Single-fibre responses to clicks were studied in hearing-impaired guinea pigs. The click PSTHs showed various patterns that were related to different types of frequency threshold curves (FTCs). Aberrant PSTHs were found for those types of FTCs where the tail threshold was similar to or lower than the tip threshold. Fourier analysis of compound PSTHs showed a close correspondence between the frequency content of the PSTH and the tail frequency. With a simple cochlear model we demonstrate that basilar-membrane frequency characteristics that correspond to the abnormal FTCs cause aberrant neural responses that resemble in main aspects the experimental observations.

This chapter is presented at the 9th International Symposium on Hearing, Auditory Physiology and Perception, Carcans, France, June 1991. It has been published in the proceedings of the symposium (editors: Y. Cazals, L. Demany and K.C. Horner), *Advances in the Biosciences*, Pergamon Press, Oxford, Vol. 83: 607-615 (1992).

Aberrant Temporal Discharge Patterns in Noise Damaged Guinea-pig Cochleas

H. Versnel, R. Schoonhoven and V.F. Prijs

Ear, Nose and Throat Department, University Hospital,
P.O. Box 9600, 2300 RC Leiden, The Netherlands

ABSTRACT

Single-fibre responses to clicks were studied in hearing-impaired guinea pigs. The click PSTHs showed various patterns that were related to different types of frequency threshold curves (FTCs). Aberrant PSTHs were found for those types of FTCs where the tail threshold was similar to or lower than the tip threshold. Fourier analysis of compound PSTHs showed a close correspondence between the frequency content of the PSTH and the tail frequency. With a simple cochlear model we demonstrate that basilar-membrane frequency characteristics that correspond to the abnormal FTCs cause aberrant neural responses that resemble in main aspects the experimental observations.

KEYWORDS

Single fibre; Noise trauma; Click response; Frequency selectivity; Guinea pig; Model.

INTRODUCTION

Manifestations of sensorineural hearing loss are an elevation of response threshold and a decrease of frequency selectivity. These manifestations are characterized by frequency threshold curves (FTCs) that can be determined from single-fibre responses. Various types of FTCs are found (Robertson, 1982; Salvi *et al.*, 1983; Liberman and Dodds, 1984). Temporal coding of responses to complex sounds which is of importance for neural speech processing will change if the frequency selectivity changes. Distinct changes are expected in a click response, because this reflects the (rectified, low-pass filtered) impulse response of the cochlear filter the Fourier transform of which corresponds to the tuning curve. Click experiments of Salvi *et al.* (1979) also point to that suggestion.

In this paper we present click responses of fibres with various abnormal FTCs in noise-damaged guinea pigs. We are interested in the extent to which temporal discharge patterns, reflected by poststimulus time histograms (PSTHs), differ from normal (Versnel *et al.*, 1990; Versnel *et al.*, —). Using a simple cochlear model (Prijs *et al.*, 1990) we examine how the abnormal

temporal patterns are related to the abnormal tuning curves. The basilar-membrane tuning is modelled by two parallel filters that reflect the tip- and tail-segment of the FTC. Parameters of the filters are estimated on the basis of both FTCs and click PSTHs.

METHODS

Physiological Experiments

Terminal experiments were performed in 11 female albino guinea pigs weighing 200–800 g. These had been exposed under anaesthesia to a loud tone (6 kHz, 121–123 dB SPL, 2 hours or 1.0–1.7 kHz, 112–122 dB SPL, 2 hours) in a closed sound box with speaker (Fane type Classic 10-125T). After a survival time of 14–123 days single-fibre experiments were performed.

Premedication was given by atropine sulphate (25 µg/kg) and Thalamonal (1.6 cc/kg) and anaesthesia was obtained with Nembutal® (27 mg/kg). Single-fibre responses were recorded using micropipettes filled with 0.5 M KCl/0.1M TRIS buffer. For each fibre a frequency threshold curve (FTC) according to a threshold tracking algorithm was determined. We presented 100-µs clicks with a spectrum that was flat within 10 dB up to 10 kHz where it fell off rapidly. Both polarity and intensity of the click were varied using 256 sweeps for each click and an interstimulus interval of 128 ms. We present compound PSTHs with PSTHs to condensation clicks (CC) plotted upwards and PSTHs to rarefaction clicks (RC) plotted downwards (cf. Pfeiffer and Kim, 1972). Further details of animal preparation and equipment for sound stimulation and signal recording have been described in Versnel *et al.* (1990).

Data analysis

We assume that the impulse response $h(t)$ of the cochlear filter can be described by two parallel filter components (Prijs *et al.*, 1990):

$$h(t) = h_1(t) + h_2(t) \quad (1)$$

The components $h_1(t)$ and $h_2(t)$ correspond to the CF section and the tail section respectively. For a normal fibre $h(t) \approx h_1(t)$. A single component of the impulse response, $h_i(t)$, is described as follows (de Boer, 1975):

$$h_i(t) = g_i(t) \cos(2\pi f_{0i}t + \phi_{0i}) \quad \text{with } i=1,2 \quad (2)$$

where f_{0i} is the resonance frequency and ϕ_{0i} is the phase angle, and where

$$g_i(t) = \begin{cases} c_i \{ (t - \alpha_i) / \beta_i \}^{\gamma_i} \exp\{ -(t - \alpha_i) / \beta_i \} & \text{for } t \geq \alpha_i \\ 0 & \text{for } t < \alpha_i \end{cases} \quad (3)$$

The parameter c_i controls the sensitivity of the filter. The parameters α_i may be assumed to reflect the travelling-wave delay; β_i and γ_i determine the shape of the filter; β_i reflects a damping factor. The time delay parameters, ϕ_i and α_i , are corrected for an acoustic and a synapto-neural delay. For some abnormal low-CF fibres (CFs below 3 kHz) with a dominant tuning frequency fits of $g(t)$ to the PSTH envelopes were performed. The fit procedures yielded estimates of α_i , β_i and γ_i . The fitting procedure and results for normal fibres are described in Versnel *et al.* (—).

We performed Fourier analysis on difference PSTHs, which are obtained by subtracting PSTHs to RC from PSTHs to CC. From these we derived a best frequency (BF) and a phase-frequency curve, $\phi = \phi(f)$. The parameters ϕ_{0i} are estimated as follows: $\phi_{01} = \phi(f=f_b)$ if $f_b \approx f_c$ and $\phi_{02} = \phi(f=f_b)$ if $f_b \approx f_{\text{tail}}$ (with f_c : CF, f_{tail} : tail frequency, f_b : BF).

Computational Model

The model is built up of a unidirectional sequence of sections that reflect different cochlear transduction processes. The first step of the model reflects the basilar-membrane mechanics. The basilar-membrane impulse response $h(t)$ is described according to Eqns. (1)-(3). The parameter α_1 is estimated by the minimum values which are found for high intensities. Subsequently, α_1 and ϕ_{01} are chosen under the condition that the starting phase at $t = \alpha_1$ was equal for all CFs:

$$2\pi\alpha_1(f_c)t_c + \phi_{01}(f_c) = \text{const.} \quad (4)$$

Assuming that all frequencies travel with equal velocity along the basilar membrane, both in normal and damaged cochleas, we chose $\alpha_2(f_c) = \alpha_1(f_c)$. We estimated γ_1 from the fit of $g(t)$ to the PSTH envelope for low intensities, where the click PSTH fairly approximates the (rectified) impulse response. From Eqns. (2)-(3) follows the Q_{10dB} of the power spectrum, denoted as Q_γ :

$$Q_\gamma = \pi\beta_1 f_{01} k(\gamma_1) \quad \text{with } k(\gamma) = (10^{1/\gamma} - 1)^{-1/2} \quad (5)$$

The parameter β_1 is taken such that Q_γ equals the Q_{10dB} of the FTC-tip (β_1) or -tail (β_2).

The second stage of the model consists of an inner-hair-cell transduction section modelled (including parameters) according to Shamma *et al.* (1986). Third, a first-order low-pass filter with cut-off frequency of 2 kHz is added to achieve realistic neural phase-locking properties, and a synapto-neural delay is modelled by a time shift. The fourth step reflects the spike generation. The model discharge probability depends linearly on the synaptic output with a conversion factor controlling the recovered discharge rate. The refractory mechanism is modelled according to Lütkenhöner *et al.* (1980), with recovery parameters obtained from spontaneous-activity data recorded in our laboratory.

RESULTS

Abnormal Frequency Threshold Curves

The fibres were divided into low-threshold (normal) and high-threshold (abnormal) fibres. Fibres with a threshold at CF raised by more than 2 S.D. from mean values in a sample of normal-hearing guinea pigs (see Fig. 1 in Versnel *et al.*, 1990) were considered abnormal. For 70 abnormal fibres we distinguish 5 types of FTC on the basis of tip and tail thresholds. In this paper two types are discussed: type II (27%): tip threshold is raised and broadened, tail threshold is normal; type III (36%): tip as type II, but tail threshold is lowered.

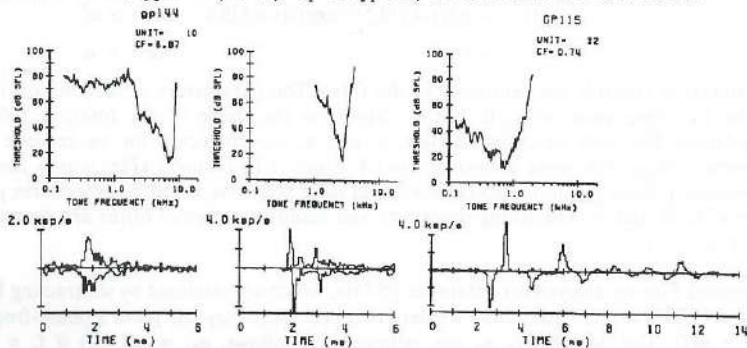


Fig. 1. FTCs (upper panels) and compound PSTHs to clicks of 51 dB nSL (bottom panels) of normal fibres.

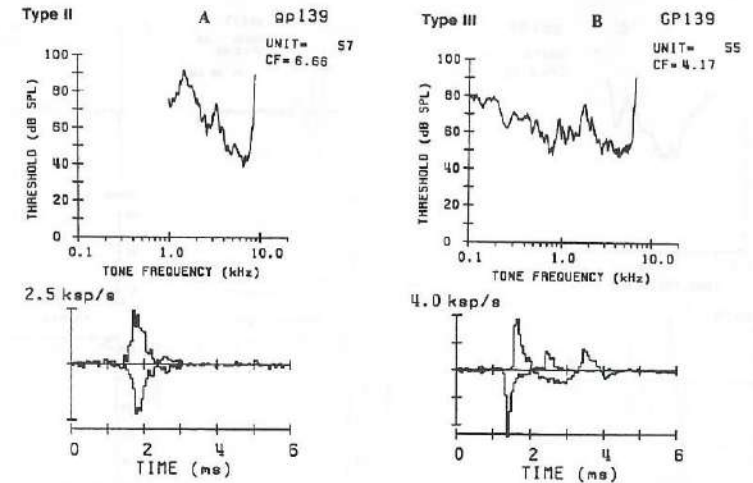


Fig. 2. FTCs and compound PSTHs of abnormal fibres. A: type II, $Q_{10dB} = 2.8$; click intensity: 51 dB nSL; B: type III, $Q_{10dB} = 1.5$, $f_{tail} = 0.74$ kHz, $Q_{tail} = 1.4$, click intensity: 71 dB nSL.

Normal PSTHs

Examples of compound PSTHs and corresponding FTCs of normal fibres are shown in Fig. 1 for three fibres of different CFs. For the fibre of 6.9 kHz the PSTHs to the opposite polarity are almost identical with similar short latencies. This pattern is typical for fibres with high CF (above 3 kHz). The PSTHs of low-CF fibres show multiple peaks arranged in an oscillatory pattern with an oscillation frequency of approximately CF, thereby reflecting the phase-lock phenomenon. The response peaks to the opposite polarity occur in opposite phase.

Changes in Click PSTHs

For type-II fibres of high CF the PSTHs to CC and RC were identical, as normal. Figure 2A shows an example of type-II response behaviour. The peak amplitude reaches a normal level at 20-30 dB above the threshold. The response duration is shorter than normal. The PSTHs of low-CF type-II fibres showed less peaks than normal.

Remarkable changes of click responses were found for type-III fibres. Figure 2B shows a representative example of the responses of a high-CF type-III fibre. The PSTHs showed multiple peaks occurring at long latencies and they showed large differences between CC- and RC-responses in contrast to normal responses. For RC the dominant-peak latency was shorter than for CC. The dominant-peak amplitude of the RC PSTH was larger than that of the CC PSTH. The amplitudes were larger than for normal high-CF fibres, but similar to that for normal low-CF fibres. In Fig. 2C an other example is shown of a type-III click PSTH, now for a low-CF fibre which normally has a multiple-peaked pattern. One would expect that the compound PSTH showed an oscillatory pattern consisting of a superposition of oscillations with CF and the tail frequency. We found, however, that a part of the responses (especially the second peaks) to CC and RC overlapped considerably. This pattern is comparable with that shown in Fig. 2B. We see in both compound PSTHs that the interpeak intervals for RC responses were longer than those for CC.

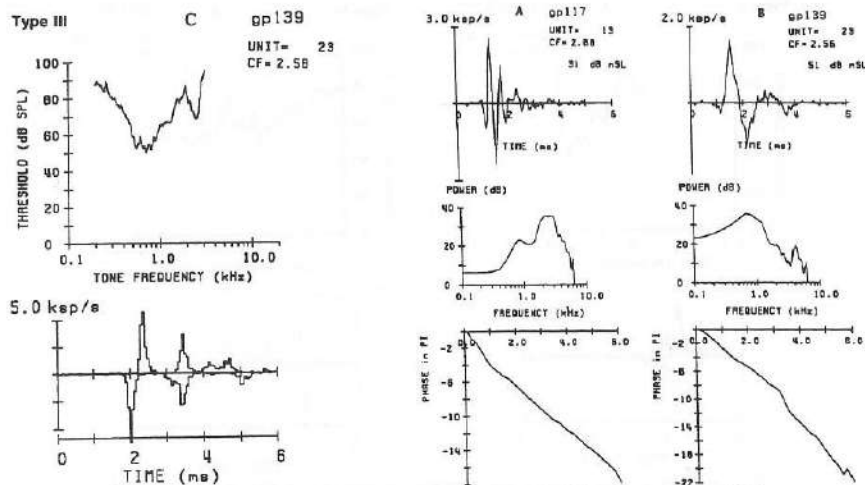


Fig. 2. C (left): type III, $Q_{10dB} = 3.9$, $f_{tail} = 0.71$ kHz, $Q_{tail} = 1.5$, click intensity: 71 dB nSL.

Fig. 3. Difference PSTHs (upper panels) and corresponding Fourier power spectra (medium panels) and phase characteristics (bottom panels). A: normal fibre (CF: 2.7 kHz), click: 31 dB nSL; B: abnormal fibre (CF: 2.6 kHz), click: 51 dB nSL.

Parameters of Double Filter

Examples of the difference PSTHs, Fourier power spectra and phase spectra are shown in Figs. 3A (normal) and 3B (abnormal, type III). For low intensities the PSTH power spectrum of the normal fibre resembles its FTC (see Fig. 1B), albeit less sharp. The main part of the power spectrum of the type-III fibre resembles the tail segment of the FTC (see Fig. 2C). An agreement of the BF of the power spectrum with the tail frequency was found for most fibres with relatively sensitive tails. The absolute values of ϕ_{01} ($= \phi(f=f_c)$) and ϕ_{02} ($= \phi(f=f_{tail})$) are plotted in Fig. 4. For both normal and abnormal fibres values of ϕ_{01} are plotted since they

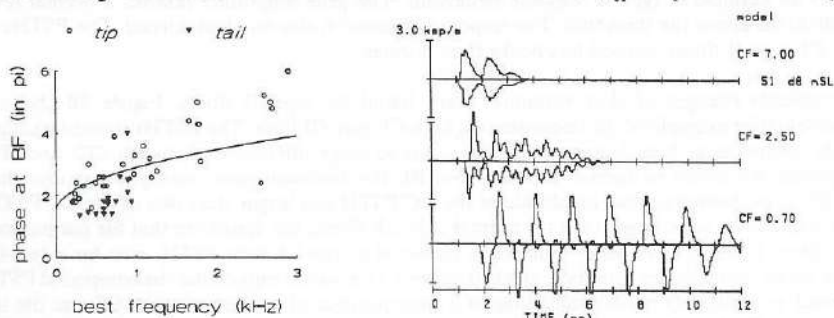


Fig. 4. (Left) Absolute value of phase $-\phi_{01}$ vs. BF or f_{01} . Circles: $i=1$ (tip); Triangles: $i=2$ (tail). The solid line represents the phase used in the model: $-\phi_{01}(f_c) = 1.4\pi f_c^{0.5} + 1.5\pi$

Fig. 5. Modelled PSTHs for CFs as shown in Fig. 1.

Table 1. Parameters of model impulse response of basilar-membrane filter $h(t) = h_1(t) + h_2(t)$

Parameters of $h_1(t)$		Parameters of $h_2(t)$	
f_{01}	$= f_c$	f_{02}	$= f_{tail}$
$\phi_{01}(f_c)$	$= -1.4\pi f_c^{0.5} - 1.5\pi$	$\phi_{02}(f_{tail})$	$= -2.0\pi f_{tail}^{0.41}$
$\alpha_1(f_c)$	$= 0.7f_c^{-0.5}$	$\alpha_2(f_{tail})$	$= \alpha_1(f_{tail})$
$\beta_1(f_c)$	$= Q_{10dB}(f_c)/2.92f_c$	$\beta_2(f_{tail})$	$= Q_{tail}/2.92f_{tail}$
γ_1	$= 3$	γ_2	$= 3$

were similar. The parameter $|\phi_{01}|$ increased with CF; $|\phi_{02}|$ was lower than $|\phi_{01}|$ and it tended to increase with CF too.

The parameter α_1 decreased with CF, this decrease is larger for lower CFs. Without taking into account the phase condition of Eqn. (4) we found for a high intensity in normal guinea pigs $\alpha_1(f_c) = 0.67f_c^{-0.85}$. Comparing at one click level we found that α_1 for abnormal fibres did not differ significantly from normal. For fibres with broad tuning β_1 was smaller than normal and γ_1 was similar to the normal value (about 3). In a fibre for which a FTC tip could not be distinguished but for which a tail was present we found that γ_2 was similar to γ_1 . For most fibres where we determined a tail (CFs of 2.5-10 kHz) f_{tail} was between 0.5 and 1 kHz; Q_{tail} , the Q_{10dB} of the FTC tail, varied from 0.5 to 2.

Model Simulations

Our choices of the parameters are listed in Table 1. For normal fibres we applied the relation $Q_{10dB}(f_c) = 2.70f_c^{0.28}$ (Versnel *et al.*, 1990). In Fig. 5 the neural outputs of the model are shown for three different CFs that correspond to the normal fibres shown in Fig. 1. The input level is chosen in order to simulate a level above click threshold that correspond to the intensity used in Fig. 1. Latencies and amplitudes of the early peaks are well reproduced; the late responses of the model are larger than in the animal's responses.

In Fig. 6 model responses are shown for a type-II (A) and type-III (B) fibre: the inverted power spectrum of the basilar-membrane impulse response reflecting the FTC, the basilar-membrane click response and the neural output. The modelled type-II PSTH fairly resembles the experimental PSTH: amplitude, latency and duration of response. The type-II model PSTH is narrower than the normal model PSTH while the peak amplitudes are similar. The more complex response pattern of the type-III fibre is in several aspects reproduced: the RC first-peak latency is shorter than that for CC; the RC first-peak amplitude is larger than that for CC; the interpeak distance for RC is longer than for CC. As for the modelled normal PSTHs, the amplitudes of the late responses are not well simulated.

DISCUSSION

We found that abnormal frequency characteristics in a pathological cochlea resulted in changed patterns of click responses. As one should expect, broadening of the tuning at CF resulted in narrower click responses (type II, Fig. 2A). Comparable short-duration responses were also found by Salvi *et al.* (1979). If the low-frequency sensitivity increases in comparison to the high-frequency (CF) sensitivity, the click response patterns were unusual, they partly resemble normal low-CF click responses (type III, Fig. 2B, C). This suggests that the aberrant pattern is caused

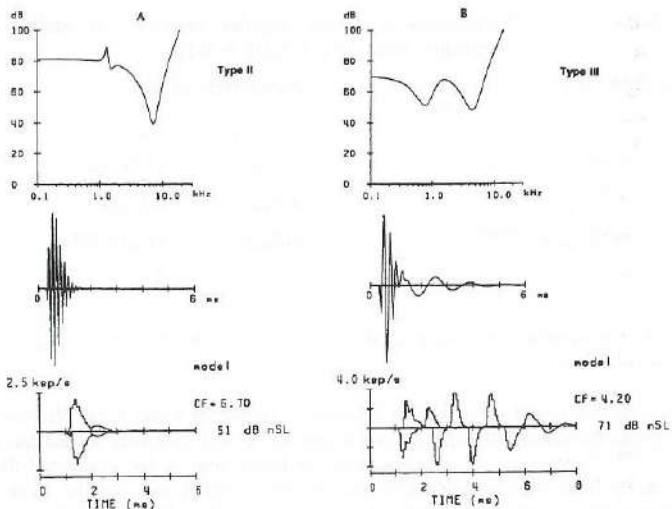


Fig. 6. Tuning curve (upper panels), basilar-membrane click response (medium) and PSTH (bottom), simulated for A: the type-II fibre of Fig. 2A, and B: for the type-III fibre of Fig. 2B.

by the tail hypersensitivity, which is supported by the close correspondence between tail and Fourier spectrum of difference PSTH (Fig. 3B). Under the condition that the double tuning originates in the basilar-membrane filter the model could simulate PSTHs of type-III fibres in some important aspects. The discrepancy between animals' and model's PSTHs that concern the late responses occurring both for normal and abnormal cochleas is probably due to a model simplification, as e.g. an omission of synaptic mechanisms (adaptation, spontaneous activities). Hence, it is likely that the aberrant transient single-fibre responses are mainly caused by abnormal double tuning of the basilar membrane.

ACKNOWLEDGEMENTS

This study was supported by the Netherlands organization for scientific research (NWO) and by the Heinsius Houbolt Fund. The authors thank J. Keijzer for assistance in model work.

REFERENCES

- de Boer, E. (1975). Synthetic whole-nerve action potentials for the cat. *J. Acoust. Soc. Am.*, **58**, 1030-1045.
- Liberman, M. C. and L.W. Dodds (1984). Single-neuron labeling and chronic cochlear pathology. III. Stereocilia damage and alterations of threshold tuning curves. *Hear. Res.*, **16**, 55-74.
- Lütkenhöner, B., M. Hoke and E. Bappert (1980). Effect of recovery properties on the discharge pattern of auditory nerve fibres. In: Cochlear and Brainstem Evoked Response Audiometry and Electrical Stimulation of the VIIIth Nerve (M. Hoke, G. Kauffmann and E. Bappert, eds.), *Scand. Audiol., Suppl.* **11**, 25-43.

- Pfeiffer, R. R. and D. O. Kim (1972). Response patterns of single cochlear nerve fibers to click stimuli: descriptions for cat. *J. Acoust. Soc. Am.*, **52**, 1669-1677.
- Prijs, V. F., J. Keijzer, R. Schoonhoven and H. Versnel (1990). The sting is in the tail. In: *The Mechanics and Biophysics of Hearing* (P. Dallos, C. D. Geisler, J. W. Matthews, M. A. Ruggero and C. R. Steele, eds.), pp. 154-161. Springer-Verlag, Berlin Heidelberg.
- Robertson, D. (1982). Effects of acoustic trauma on stereocilia structure and spiral ganglion cell tuning properties in the guinea pig cochlea. *Hear. Res.*, **7**, 55-74.
- Salvi, R. J., R. P. Hamernik and D. Henderson (1983). Response patterns of auditory nerve fibers during temporary threshold shift. *Hear. Res.*, **10**, 37-67.
- Salvi, R. J., D. Henderson and R. P. Hamernik, R. P. (1979). Single auditory nerve fiber and action potential latencies in normal and noise-treated chinchillas. *Hear. Res.*, **1**, 237-251.
- Shamma, S. A., R. S. Chadwick, W. J. Wilbur, K. A. Morrish and J. Rinzel (1986). A biophysical model of cochlear processing: intensity dependence of pure tone responses. *J. Acoust. Soc. Am.*, **80**, 133-145.
- Versnel, H., V. F. Prijs and R. Schoonhoven (1990). Single-fibre responses to clicks in relationship to the compound action potential in the guinea pig. *Hear. Res.*, **46**, 147-160.
- Versnel, H., R. Schoonhoven and V. F. Prijs (—). Single-fibre and whole-nerve responses to clicks as function of sound intensity in guinea pigs. Submitted to *Hear. Res.*

Commentaries

EVANS

How can you be sure that the pathological changes you describe are a result of acoustic trauma, and not a result of well-known problems in the guinea pig preparation producing spurious pathological features. What controls did you carry out (blood pressure etc.) to minimize the latter?

VERSNEL

By means of auditory brainstem responses measurement of the tone audiogram the pre-noise exposure condition of the cochlea was controlled. During the single-fiber experiment the condition was controlled by measurement of round window recorded compound action potential to clicks. The click CAPs are very sensitive to changes in cochlear condition. Moreover the CAP tone audiogram has been determined before and after the single fiber recordings. On the basis of brainstem and CAP measures we conclude that the examples we show in the paper concern pure noise-induced losses.

HARRISON

The authors report that for the most part, there is a good correlation between the FFT of the click-evoked compound PSTH and the threshold tuning curve. This is consistent with previous reports that FFTs of (broad band noise derived) "revcor" functions and FTCs of pathological cochlear fibres are almost identical (Harrison and Evans, 1982).

There are, as the authors note, some discrepancies between the real PSTMs and their model-derived PSTMs, especially for "type III" abnormal FTCs (W-shaped tuning curves). The authors conclude that these aberrant PSTMs are possibly caused by abnormal double tuning of the basilar membrane. Alternatively, one could suggest that the double tuning relates to one low-frequency (passive) basilar membrane filter, and one high-frequency (active) filter tuned to CF, perhaps having an increased separation of centre frequency. In any case, the authors should take into account in their model (and/or in their data interpretation) the fact that input/output characteristic of the "tip" and "tail" components of the FTC differ. The former is much less steep than the latter (Harrison, 1981) and perhaps non-linear.

References

Harrison, RV (1981). Rate versus intensity functions and related AP responses in normal and pathological guinea pig and human cochleas. *J. Acoust. Soc. Am.* 70, 1036-1044.

Harrison, RV and Evans, EF (1982). Cochlear filtering by reverse correlation in normal and pathological guinea pig cochleas. *Hearing Research* 6, 303-314.

VERSNEL

First, we stress that the main discrepancy between the model and the experimental results which applies to the click responses of normal and type II fibers concerns the late response peak. Probably this cannot be accounted for by simplifications in the basilar membrane model; the omission of synaptic adaptation in the model is likely the origin. The basilar membrane section of the model consists of two (parallelly set) linear and passive filters. This simple model is able to demonstrate that the real PSTHs of the fibers with a type III tuning curve can be explained by a double (tip and tail) tuning of the basilar membrane. Different I/O characteristics for tip and tail segments that are found in normal cochleas indeed should be incorporated in a more realistic model. However, in abnormal cochleas the differences in I/O behavior might be less or even absent (cf Harrison 1981). Unfortunately there are no data on I/O curves for type III abnormalities. At this point it seems wise to start from invariance of I/O characteristics.

PUJOL

The type III aberrant discharge you described, with an enhanced and repetitive firing, is reminiscent of an activity driven by NMDA receptors. As these receptors are probably activated at high intensities (see Puel's paper), you could also think about a synaptic explanation for this pathology.

VERSNEL

We did not think yet about that interesting point. However, seeing the close correspondence between the click responses and the tone threshold curve for type III (with repetitive firings) as well as for other pathologies (without repetitive firings, see type II in the paper) we still strongly suggest that the multiple-peak pattern in type II PSTHs is caused by hypersensitivity to low (tail) frequencies.

Chapter VII

Click responses in noise-damaged guinea-pig cochleas. II. Sensorineural causes of deviations in the compound action potential

Huib Versnel, Vera F. Prijs and Ruurd Schoonhoven

Summary

We measured simultaneously compound action potentials (CAP) and single-fibre responses to clicks in acoustically traumatized guinea pigs in order to study the single-fibre origins of deviations of the CAP in cochlear pathology. The companion paper (Versnel et al., *) presents the single-fibre data, in this paper we analyse the CAPs. Whole-nerve responses to both condensation and rarefaction clicks were recorded for various intensities. We describe the waveforms and input-output curves of the N_1 latency and amplitude for four different types of audiograms. Usually, at low intensities N_1 latencies and amplitudes were longer and smaller, respectively, but near normal at high intensities. A notable deviation in the CAP observed in cases of high-frequency loss was an increase of the polarity dependence that occurred either in the N_1 or in late oscillatory waveforms. We apply an empirical CAP model, which has been shown to reproduce normal CAPs (Versnel et al., 1992a), in order to synthesize CAPs for each of the four abnormal audiograms. If we do not account for other changes than threshold shifts then only a few typical CAP deviations can be simulated, in particular those at low intensities. Adjustment of the model with parameter values that reflect abnormal single-fibre responses (Versnel et al., *) results in notably better simulations of the CAPs at high intensities. The model results demonstrate that aberrant single-fibre responses play a major role in determining high-intensity click CAPs in pathological ears, and thus, recording of click CAPs might be useful in assessing deviations at the single-fibre level.

Key words: Noise trauma; Click polarity; Compound action potential; Guinea pig; Empirical model.

This chapter has been submitted for publication to *Hearing Research*. Preliminary results were presented at the A.R.O. midwinter meeting, St Petersburg Beach, 1993.

Introduction

Electrocochleography, the recording of the compound action potential (CAP) from a site close to the cochlea or auditory nerve, provides the opportunity to assess objectively the condition of the cochlea. Analysis of deviations in the input/output functions of the CAP and in its waveform can contribute to diagnosis of a hearing disorder (cf. Eggermont, 1976). The interpretation of the CAP is based on large sets of phenomenological CAP data in man (e.g. Eggermont, 1976; Elberling and Salomon, 1976), and on CAP and single-fibre studies in animals often in combination with histological data (e.g. Wang and Dallos, 1972; Liberman and Kiang, 1978; Aran and Cazals, 1978; Salvi et al., 1979; van Heusden and Smoorenburg, 1981; Pettigrew et al., 1984). These studies show the following CAP features in relation to pathology. The N_1 latency does not change considerably with hair-cell loss in most instances (Wang and Dallos, 1972; Eggermont, 1976; Salvi et al., 1979; Pettigrew et al., 1984). However, in high-frequency loss elongation of the click latency occurs at low intensities, and shortening can occur in patients with Menière's disease and in specific cases of hair cell loss (Elberling and Salomon, 1976; Aran and Cazals, 1978; Eggermont, 1976, 1979; Pettigrew et al., 1984). Extreme latency increases are found for an acoustic neuroma (Eggermont, 1976), and for reduction of body temperature (Prijs and Eggermont, 1981). Apart from the common reduction of the N_1 amplitude (Eggermont, 1976; van Heusden and Smoorenburg, 1981; Salvi et al., 1983; Pettigrew et al., 1984; Popelář et al., 1987; Dolan and Mills, 1989), amplitude-versus-intensity curves can be steeper than normal such that amplitudes at high intensities are normal (Eggermont, 1976; Elberling and Salomon, 1976; Salvi et al., 1983). Only in rare conditions is the CAP enhanced (Shivapuja and Gu, 1992). Further, changes in waveform are reported such as in cases of high-frequency loss where click responses show multiple peaks which strongly depend on click polarity (Coats and Martin, 1977; Pettigrew et al., 1984; Schoonhoven, 1990; Møller and Jho, 1991).

In order to refine analysis of the CAP various model studies have been done (de Boer, 1975; Elberling and Salomon, 1976; Wang, 1979; Bappert et al., 1980; Dolan et al., 1983; Versnel et al., 1992a). All of these studies apply the theorem of Goldstein and Kiang (1958) which assumes the CAP to be the convolution of the sum of discharge probability densities of single auditory-nerve fibres with a unit response (UR). The UR is the potential at the CAP-recording site induced by a single fibre discharge, and it is considered to be invariant across fibres. Discharge probabilities are usually estimated from poststimulus time histograms (PSTHs). Remarkably enough, model work on pathological cochleas is only known from Elberling and Salomon (1976) who modelled CAPs to rarefaction clicks in humans. In their model the PSTH patterns were derived from cat data (Kiang et al., 1965); latencies and excitation patterns (corresponding to PSTH amplitudes) were computed from narrow-band derived click CAPs in humans (see Elberling, 1976). Elberling and Salomon simulated CAPs for various abnormal audiograms by eliminating contributions from affected regions for levels below threshold, whereas contributions above threshold were kept normal (compared at the

same sound level) both in latency and amplitude, this model thus ignores variability of abnormal local responses. For a majority of ears the general trends in the CAP input/output functions of latency and amplitude were well reproduced.

Our goal is to explain CAPs in pathological cochleas on the basis of changes in single-fibre responses. For that purpose we simultaneously recorded single-fibre responses and round-window CAPs to clicks in normal (Versnel et al., 1990, 1992a) as well as in acoustically traumatized guinea pigs (Versnel et al., *). Also, the unit response was experimentally determined in these animals (Versnel et al., 1992b). Subsequently, we developed a phenomenological CAP model that was based on the PSTH and UR data (Versnel et al., 1992a). In this paper we focus on the actual abnormal CAPs and we discuss these for four different types of audiogram. The CAPs are compared to normal with respect to wave patterns (N_2 and multiple peaks), and input/output characteristics of the latency and amplitude of the N_1 peak. Two factors can play a role in deviations in the click CAP: the threshold audiogram, and the specific responses of fibres with elevated thresholds. It can be assumed that CAPs fully depend on the audiogram for intensities below elevated single-fibre thresholds since fibre responses from cochlear regions with normal CAP thresholds are not changed (Versnel et al., *). In most fibres with elevated thresholds the click responses deviate from normal to an extent depending on the type of abnormal tuning curve (Versnel et al., *). These changed responses can influence the CAPs at high intensities. The deviations in CAPs are analysed with an empirical model described in preliminary form in Versnel et al. (1992a). It is assumed that the UR is unaffected (Versnel et al., 1992b), and two types of adjustments are introduced in the PSTH section of the model. First, we make pure audiogram-based adjustments to the model. The single-fibre responses from hearing loss areas are computed as virtually normal by reducing the effective click intensity according to the audiogram. This adjusted model is denoted M1. Second, we adapt the model (denoted M2) by implementation of parameter values as found for the abnormal PSTHs (Versnel et al., *). A comparison of the M1 and M2 simulation results will reveal the effects of deviations in single-fibre responses on CAPs.

Methods

The physiological CAP data were obtained during experiments described in the companion paper (Versnel et al., *) in which we used 13 albino guinea pigs weighing 200-800 g. The guinea pigs placed in a sound box with speaker (Fane type Classic 10-125T) were exposed under anaesthesia to a loud tone for 2 hours, eight animals to a tone of 6 kHz and 121-123 dB SPL, and five animals to 1.4-1.7 kHz and 112-122 dB SPL. By means of recordings of auditory brainstem responses (ABR), thresholds to clicks and tone bursts were measured before and directly after the traumatizing sound exposure. The CAPs and single-fibre responses were measured in an acute experiment after a survival time of 14-123 days.

Premedication consisted of atropine sulphate (25 µg/kg) and Thalamonal

(1.6 cc/kg) and the animals were anaesthetized with Nembutal® (27 mg/kg). A silver ball electrode was used to derive the cochlear potentials, and the round window was chosen as the recording site. The sound stimuli were presented to the animal by a dynamic earphone in a closed field. An audiogram was determined by CAP recordings to tone bursts of 4 ms plateau and 2 cycles rise/fall time, the threshold criterion being 1 μ V. Condensation and rarefaction clicks of a fixed width of 100 μ s were presented at intensities varied in 10 dB steps. Simultaneously with the recording of the single-fibre responses (Versnel et al., *), the round-window signals were amplified (2,500x -25,000x) and stored on magnetic tape with the use of a TEAC datarecorder (XR-510WB) with a recording bandwidth of 0-6.25 kHz. The CAPs were determined off-line over typically 64 or 128 sweeps. The timing of the CAP was referred to the start of cochlear microphonics in order to eliminate non-cochlear delays. For further details on the methods see the companion paper or Versnel et al. (1990).

Empirical model of CAP

A general outline of the model is given in this section, and a detailed description is presented in the Appendix. We elaborated on a preliminary version of a model for normal cochleas that has been discussed in a previous paper (Versnel et al., 1992a). The model CAP is computed by convolution of a compound discharge latency distribution with a unit response (cf. Goldstein and Kiang, 1958). The latency distribution is synthesized by summation of model PSTHs which reflect single-fibre discharge probabilities. The model PSTHs are computed on the basis of experimentally derived P-parameters (Versnel et al., 1992a, *), i.e. the latency t_p , the amplitude A_p , and the synchronization S_p of the dominant PSTH peak; t_p is defined by the time instant with the maximum spike rate, A_p is the normalized spike rate at t_p , S_p is defined as the ratio of A_p and area p_p of the PSTH peak (cf. Versnel et al., 1990): $S_p = A_p/p_p$. These parameters are described as functions of the fibre variables characteristic frequency (CF) and spontaneous rate (SR), and the stimulus variables intensity (L_0) and click polarity (m). The PSTHs are simulated for a hypothetical population of fibres each represented by a CF and an SR, and then summed to a latency distribution. A model unit response is chosen on the basis of potential waveforms at the CAP recording site (round window) that have been derived by a spike-triggered averaging method (Versnel et al., 1992b). The synthesized CAPs for normal cochleas presented in Versnel et al. (1992a) agree with the experimental CAPs with respect to the latency of the N_1 component, the N_1 amplitude at low and moderate intensities (below 60 dB nSL), and the global waveform of the N_1 . The second negative peak (N_2), the increase of N_1 amplitude at high intensities, and the onset of the CAP were insufficiently simulated.

Before we describe the model for CAPs in pathological cochleas we mention the main refinements made in order to eliminate discrepancies between the model and the data for a normal cochlea. Several of these modifications have been suggested in Versnel et al. (1992a). In the preliminary model the PSTHs consisted of one single peak

representing the dominant peak, which was sufficient to simulate the N_1 . Now, a secondary peak with P-parameters t_{ps} , A_{ps} and S_{ps} is added in order to obtain a more realistic simulation of the late components of the CAP, such as the N_2 , which can be important in pathological cochleas (Pettigrew et al., 1984). For the description of the shape of PSTH peaks of high-CF fibres we use now a function that is associated with a gamma distribution (Grashuis, 1974). This function is comparable to the originally applied Gaussian function but has a finite starting point, which results in a more realistic

TABLE IA
PARAMETERS FOR MODEL PSTHS OF NORMAL AND ABNORMAL FIBRES

Parameter	Normal/I	II	III	IV	V	Unit
$c_1(L \leq 41)$	1.13	1.13	1.61	#	#	ms
$c_1(L > 41)$	1.24	1.24	1.45	0.94	1.83	ms
$c_1(L > 61)$	1.24	1.24	1.45	0.94	1.02	ms
c_2	0.90	0.90	0.90	0.90	0.90	1
c_3	0.0143	0.0143	0.0143	0.0143	0.0143	dB ⁻¹
$c_1(L \leq 41)$	0	0	-0.44	#	#	ms
$c_1(L > 41)$	-0.11	-0.11	-0.27	0	-0.60	ms
$c_1(L > 61)$	-0.11	-0.11	-0.27	0	-0.18	ms
$t_2(0)$	1.99	1.99	1.99	1.99	1.99	ms
$a(f_c \leq 3)$	100	100	100	#	100	sp/s/dB
$a(f_c > 3)$	40	80	50	150+50m	150	sp/s/dB
$L_s(f_c \leq 3)$	30	30	30	#	30	dB
$L_s(f_c > 3)$	40	20	30	20	30	dB
b	2.5	2.5	3.0-0.5m	4.5	4.5-0.5m	ms ⁻¹
d_h	50	50	50	50	50	dB/oct
d_1	10	10	10	10	10	dB/oct
σ_1	0.15	0.15	0.15	0.15	0.15	ms
$\delta L(r_s \leq 5)$	26	26	26	26	26	dB
$\delta L(5 < r_s \leq 30)$	10	10	10	10	10	dB
$\delta L(r_s > 30)$	0	0	0	0	0	dB
c_4	1.0	1.0	1.75-0.75m	1.0	1.25-0.25m	ms
L_T	60	60	40	60	40	dB
$r(f_c \leq 3)$	0.4	0.4	0.4	0.4	0.4	1
$r(f_c > 3)$	0.3	0.2	0.3	0.2	0.3	1

$m = 1$ for condensation clicks; $m = -1$ for rarefaction clicks; L in dB nSL; f_c in kHz; r_s in spikes/s; #: value not applicable. Parameters not shown: $j(f_c, L) = -1$ for $f_c \leq 0.5$ and $L > 11$, $f_c \leq 1.0$ and $L > 21$, $f_c \leq 2.0$ and $L > 31$, $f_c \leq 3.0$ and $L > 41$; $j(f_c, L) = 1$ for the other conditions. t_{ps} as given in step v), except for type III with $f_c \leq 3$ kHz: $t_{ps} = 1.0$ ms (independent of CF).

TABLE IB
MAIN CHARACTERISTICS IN ABNORMAL CLICK PSTHS

type I ¹⁾ :	input/output curves of latency and amplitude shifted with threshold shift along intensity axis
type II:	normal latencies, and relatively steep amplitude-versus-intensity curves
type III:	shorter latency for rarefaction clicks than for condensation clicks
type IV:	very high thresholds, and very steep amplitude-versus-intensity curves (an extreme case of type II)
type V:	abnormal polarity dependence as type III, steep amplitude-versus-intensity curves.

*) PSTHS in the M1 model have type-I parameters.

PSTH onset. Some modifications were made with respect to the increase of click threshold with CF for CFs above 12 kHz which results from the high-frequency cut-off in the click spectrum (Versnel et al., 1992a). These modifications will have an effect on the high-intensity CAP behaviour. On the basis of a few available single-fibre data, we assigned a larger increase of amplitude with intensity to fibres which have high click thresholds because of a very high CF (above 18 kHz). An upper click-threshold limit (60 dB) was introduced, which accounts for the fibre's sensitivity to the low-frequency components of the click stimulus (Versnel et al., 1992a). As a consequence, a large number of fibres will have the same high threshold. Furthermore, the group of high-CF fibres was extended by half an octave from 24 up to 34 kHz.

Figure 1 presents results of simulations of normal discharge latency distributions in high-CF (A) and low-CF (B) ranges. The distributions are PSTHS summed over a small group of fibres with a similar CF, a distribution of high, medium and low SR, and a Gaussian shaped statistical latency spread that is independent of CF and SR. The histograms are very similar to single PSTHS. Note the typical difference between high- and low-CF responses: overlapping of response peaks to clicks of opposite polarity for high-CF fibres (A) and the interlacing of peaks for low-CF fibres (B).

Adaptations to the model for pathological cochleas

We applied two adaptations to the model in order to simulate CAPs found in guinea pigs with a hearing impairment. For both approaches the hearing loss area was represented by one or two rectangular areas of a certain threshold shift over a certain frequency range. The first adjustment (M1) is straightforward: we assume that the PSTHS in the hearing-loss area are normal relative to the fibre's click threshold, i.e., the input/output curves of the P-parameters are shifted with intensity by the amount of the threshold shift present in the audiogram. The second adaptation of the model (M2) is based on experimentally determined PSTHS of fibres with a threshold shift. We have

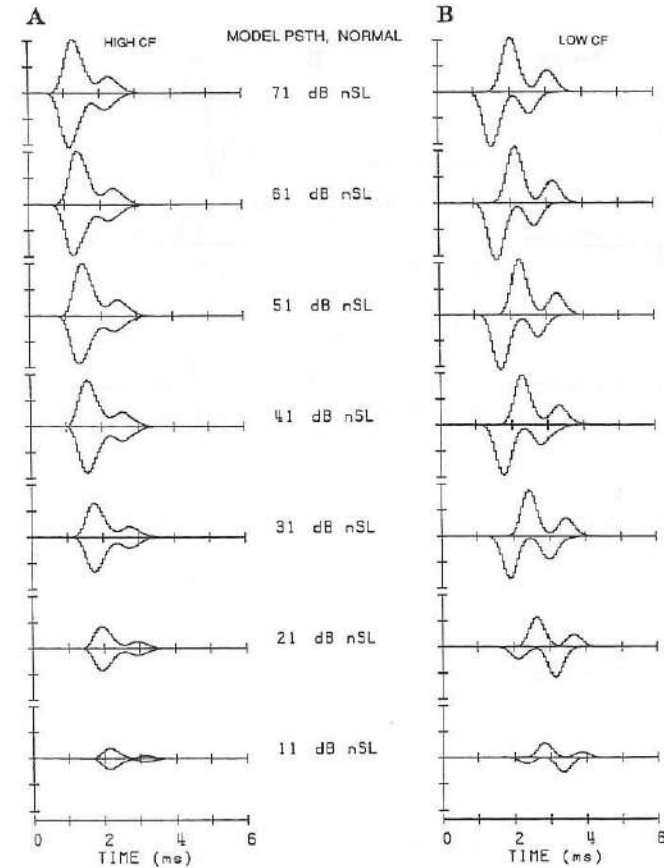


Fig. 1. Model-computed discharge latency distributions over narrow CF bands, i.e. sums of model PSTHS of single fibres of similar CF (but different SR). The histograms are representative for single-fibre PSTHS. The response to condensation clicks is plotted upwards, that to rarefaction clicks downwards. (A) Sum of model PSTHS for high CFs, in this case between 3 and 12 kHz where PSTH is independent on CF. The shape is determined by a γ -tone function, which simulates a single-fibre's response, convolved with a Gauss distribution, which simulates the latency spread across fibres of similar CF. The PSTHS show the typical early dominant peak and the small secondary peak after 1 ms. Note the amplitude increase over a range of 40 dB, and the gradual latency decrease with intensity. (B) Model PSTHS for low CFs between 950 and 990 Hz. The shape is determined by a half-cycle sinusoid reflecting the single-fibre's PSTH, and a Gaussian distributed latency spread. The dominant peak of the rarefaction-click PSTH shifts by a cycle above 21 dB. The dynamic range is about 30 dB.

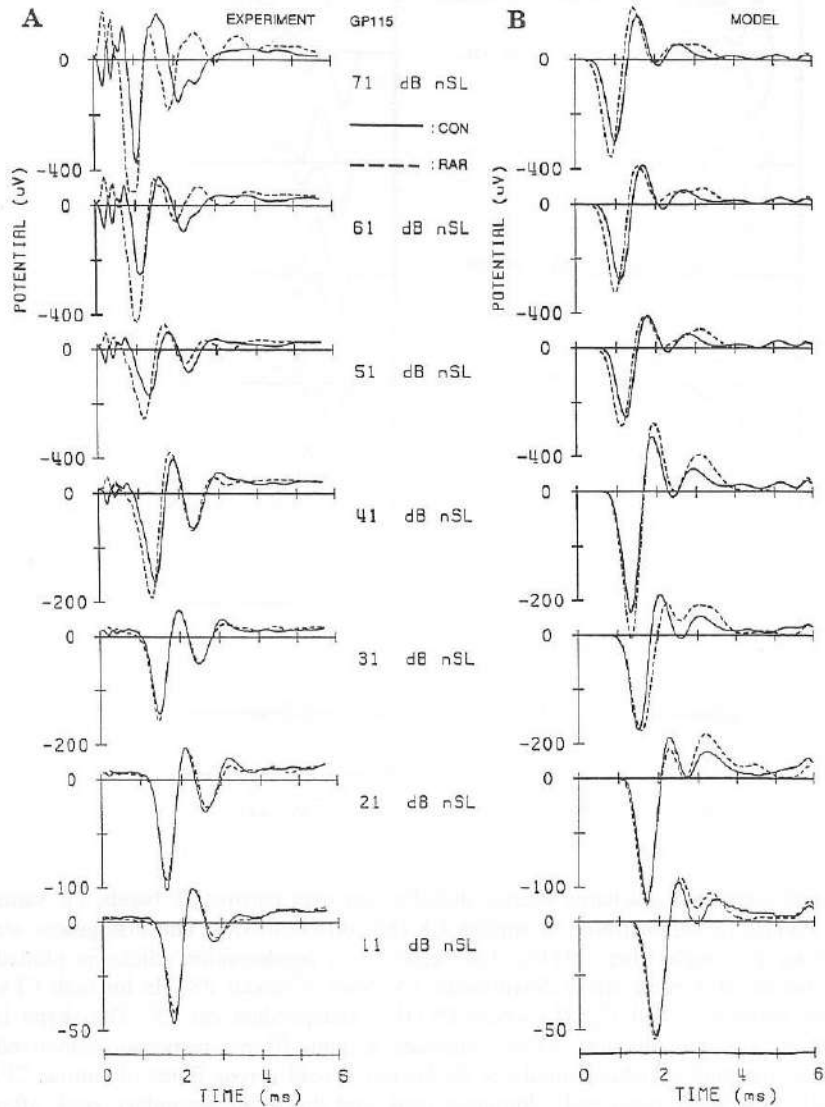


Fig. 2. Normal hearing, experiment and model: compound action potentials (CAPs) to condensation (solid lines) and to rarefaction clicks (dashed lines) for various intensities. (A) CAPs recorded from animal GP115. (B) Model simulated CAPs.

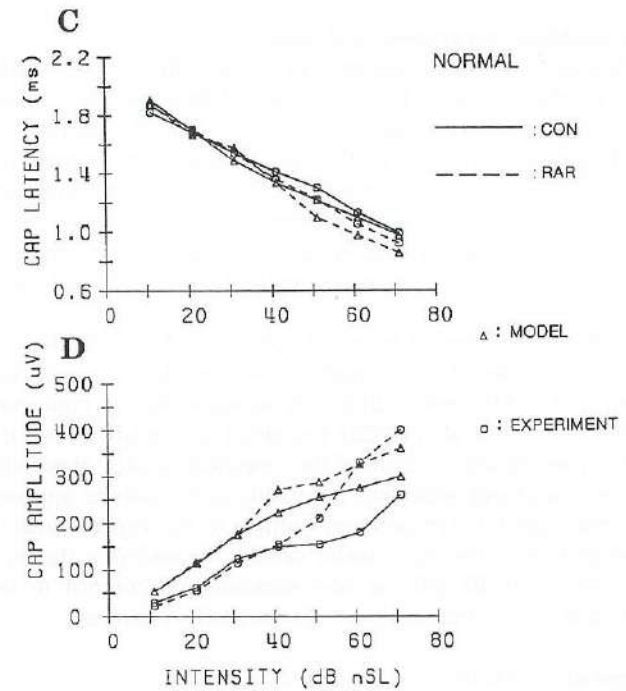


Fig. 2. (continued). (C) Latencies and (D) amplitudes of N_1 for an average of CAPs of a sample of normal guinea pigs ($N = 10$) and for the synthesized waveforms. The experimental data are represented by circles, the model data by triangles.

distinguished five types of abnormal tuning curves (or, frequency threshold curves, FTCs) to each of which specific abnormal click PSTHs are associated (Versnel et al., *). These abnormal PSTHs are synthesized. The values of the PSTH model parameters are derived from average response behaviour, as e.g. reflected in the average P-parameters (Fig. 4, Versnel et al., *). Table IA gives the parameters for the PSTHs for each FTC type (denoted by Roman numerals I to V), and Table IB gives the corresponding characteristic response features. Note that the PSTHs for type I are modelled according to M1.

The Appendix gives a detailed description of the various components of the present CAP model, including the model PSTH, the fibre population, and the model UR.

Results

CAPs in normal cochleas: experiment and model

Figure 2A presents a typical example of an intensity series of click-evoked CAPs recorded from a normal cochlea. The CAPs are plotted for both condensation (solid lines) and rarefaction (dashed lines) polarity. The N_1 latency, t_{N1} , decreases monotonically with intensity. The N_1 amplitude, A_{N1} , shows an increase over an intensity range of 30-40 dB, and as in most guinea pigs, it has a second increase above 50 dB nSL. At low intensities the CAPs are similar for the two click polarities; at high intensities, however, t_{N1} is slightly shorter and A_{N1} considerably larger for rarefaction clicks. A second negative peak, N_2 , with an amplitude of 30-50 % of A_{N1} , appears about 1.0 ms after the N_1 .

Figure 2B shows a series of normal CAPs computed with the empirical model. In Figs. 2C, D we compare the important parameters t_{N1} (C) and A_{N1} (D) between averaged experimental CAPs and synthesized waveforms, for both condensation and rarefaction clicks. Versnel et al. (1992a) presented a similar series of normal CAPs synthesized with a preliminary version of the empirical model. Basically, with respect to t_{N1} , A_{N1} , and the waveform including the width of N_1 and the appearance of the N_2 component, the synthesized CAPs are very similar to the experimental CAPs. Several aspects appear better than in the early model version, in particular the N_2 . Also a second increase of A_{N1} , above 50 dB nSL, is now simulated in contrast to the early model version, although it remains smaller than experimentally observed.

CAPs in pathological cochleas: experiment and model

In considering the audiograms of pathological ears, we define three frequency ranges: high-frequency range: above 6 kHz, mid-frequency range: 1-6 kHz, and low-frequency range: below 1 kHz. In twelve noise-exposed guinea pigs we categorized four different types of audiograms: i) high- and mid-frequency loss, ii) high-frequency loss, iii) mid-frequency loss, and iv) high- and low-frequency loss. In general, deviations in recorded click CAPs were related to the type of audiogram. We modelled CAPs according to both M1 and M2 for each of the four audiograms. The simulations of

abnormal CAPs are compared to the simulations for normal CAPs in order to judge the deviations in the CAP predicted by the model. Model results will be considered in particular at high intensities where the abnormal single-fibre responses may play a role and thus simulations with M1 and M2 may differ. Note that features in abnormal CAPs are compared to normal at the same sound level (as opposed to sensation level).

CAPs in cochleas with high- and mid-frequency loss, experiment

Two guinea pigs, which showed initial threshold shifts and in addition were exposed to traumatizing tones of 6 kHz, experienced severe hearing losses in the high- and mid- frequency range. The deviations in the click CAPs were similar in both animals. Figure 3 presents the data of GP123 which shows the abnormal features most pronouncedly. The audiogram (Fig. 3A) indicates losses of 40-50 dB for frequencies above 1 kHz. The click CAPs deviated markedly from normal. Both the early and late parts of the waveforms manifested a large dependence on click polarity (Fig. 3B). At low intensities this behaviour was expressed by multiple peaks shifting half an interpeak period with reversal of click polarity. In Figs. 3C, D the latency and amplitude of the N_1 , t_{N1} and A_{N1} , are compared to average normal values. At low intensities t_{N1} was considerably longer than normal and A_{N1} was smaller. At high intensities, however, in spite of the severe high-frequency loss, t_{N1} and A_{N1} were as short and large, respectively, as normal. Table IIA (third column) gives a summary of the results.

CAPs in cochleas with high- and mid-frequency loss, model

We simulated CAPs for an audiogram as found for GP123 (cf. Fig. 3A) by choosing a threshold shift of 30 dB for the octave range from 1.5 to 3 kHz, and 40 dB for the range above 3 kHz. Figure 4 presents the results of the simulation with model M1. An important implication of this model version is an elongated PSTH latency at each level. In this paragraph we mention the score for the simulation of a feature ('+', '0', or '-'), in order to illustrate the scoring criteria used in Table II. At low intensities the model results partially agree with the experiment: the synthesized waveforms show the trend of the experimentally observed pattern (0; Fig. 4A), t_{N1} is longer (+; Fig. 4B), and A_{N1} is smaller than normal (+; Fig. 4C). At high intensities the model is not adequate: t_{N1} is too long (-), A_{N1} is too small (-), and the polarity effect is too small or inverted (-).

Simulations with the M2 model were performed with each of the four single-fibre response types II-V separately, in order to compare the effects of each type on the CAPs. Since types IV and V are associated to high-CF fibres, these types were only applied to the high-frequency hearing loss region (above 3 kHz), and type-II and type-III responses, respectively, were substituted for the low-frequency region (1.5-3 kHz) of the audiogram. Table IIA shows the scores of the four simulations. Note that the scores are equal at low intensities since the abnormal response patterns are only effective at high intensities. Comparing then at the relevant high intensities we see that each of the four M2 models scores better than the M1 model. Simulations with types II, III or IV/II are good with respect to t_{N1} and A_{N1} but they are insufficient with respect to the polarity dependence

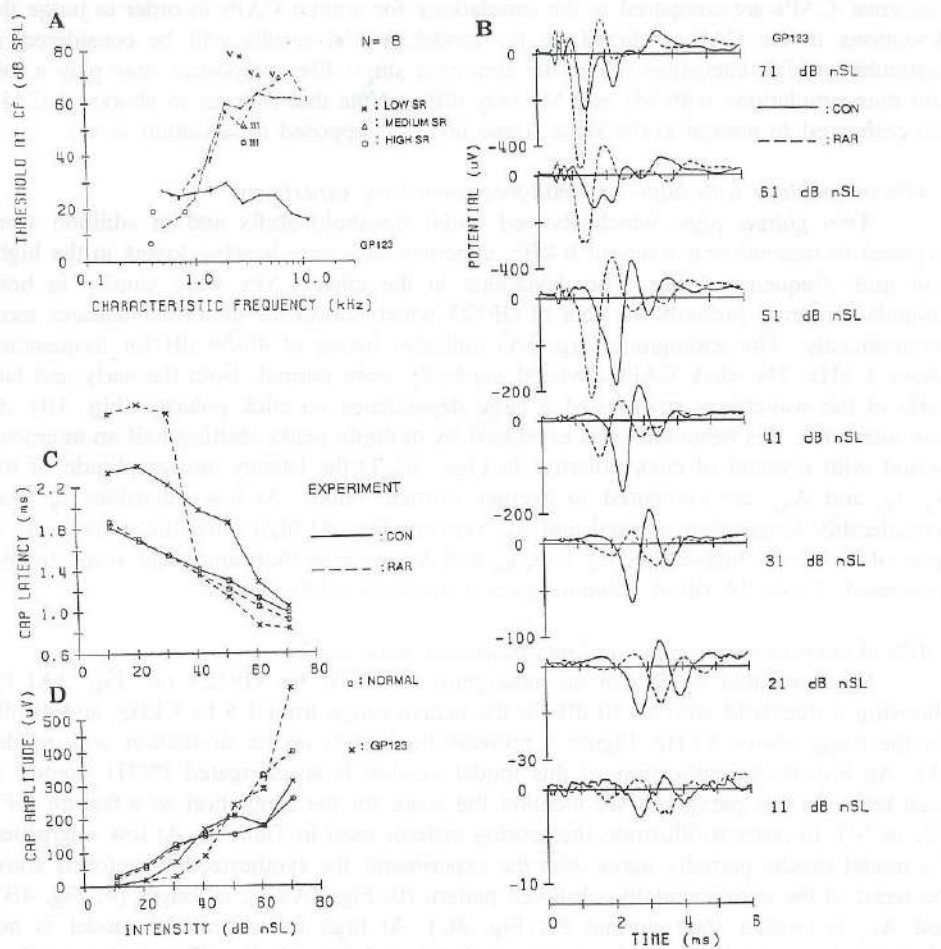


Fig. 3. High- and mid-frequency loss, experiment. (A) CAP tone audiogram of GP123, which indicates a high- and medium-frequency hearing loss (above 1.4 kHz). The CAP thresholds of GP123 are represented by dot-dashed lines (first recordings) and dashed lines (last recordings). The normal audiogram averaged over 12 normal ears (cf. Versnel et al., 1990) is given by solid lines. Asterix, triangle or circle symbols indicate thresholds at CF for single fibres. The roman digits indicate the type of FTC in an abnormal fibre (Versnel et al., *) (B) CAPs of GP123, ordered as in Fig. 2. (C) Latency of N_1 versus click intensity. As in B condensation and rarefaction polarities are represented by solid and dashed lines, respectively. Stars symbolize the responses of GP123, circles the averaged normal values as given in Fig. 2. (D) Amplitude of N_1 with symbols as in C.

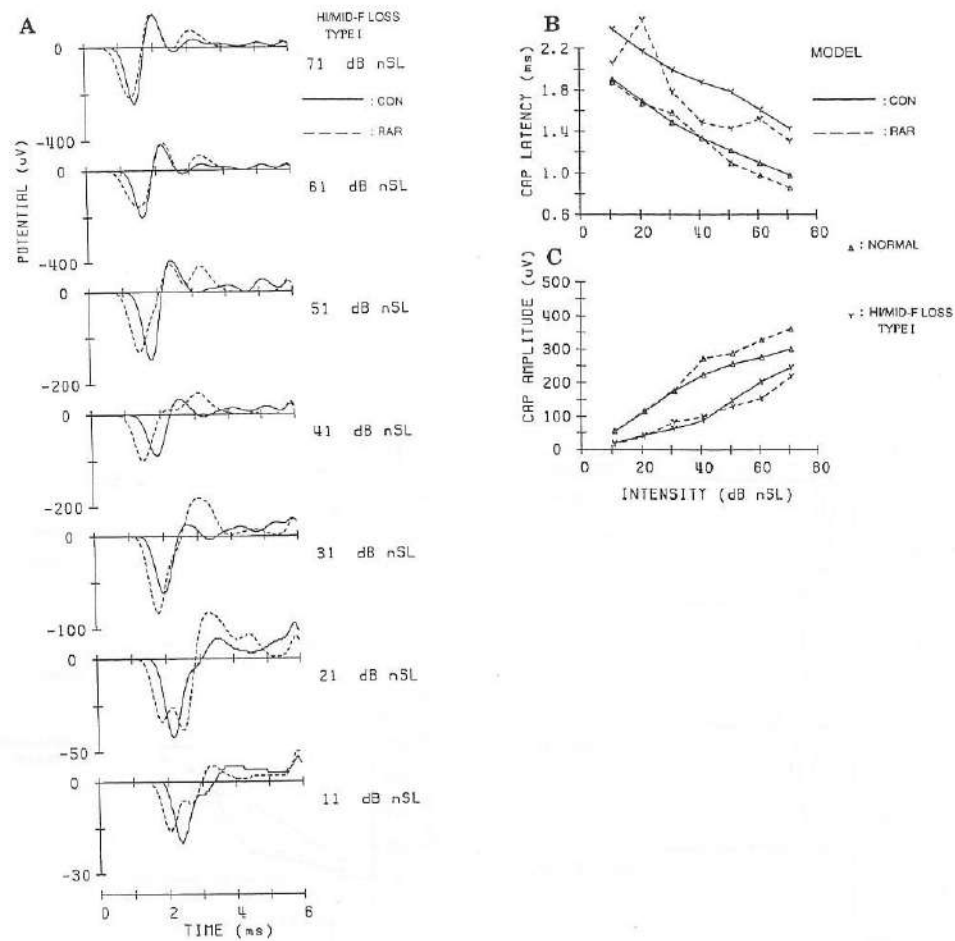


Fig. 4. High- and mid-frequency loss, simulations of click CAPs with model M1, i.e. all abnormal fibres have response type I (normal response behaviour for reduced effective intensity). Threshold shifts are 30 dB for the frequency range 1.5-3 kHz, and 40 dB for 3-34 kHz. Panels (A)-(C) as Figs. 3A-C, respectively. (A) Synthesized CAP waveforms for condensation (solid lines) and rarefaction (dashed lines), respectively. (B) Latency of N_1 , and (C) amplitude of N_1 versus click intensity for CAPs shown in panel A (Y-symbol) and for modelled normal responses as shown in Fig. 2B (triangle). Compared with experimental data at high intensities (cf. Fig. 3): model latencies are too long; model amplitudes are too small; click-polarity effect too small.

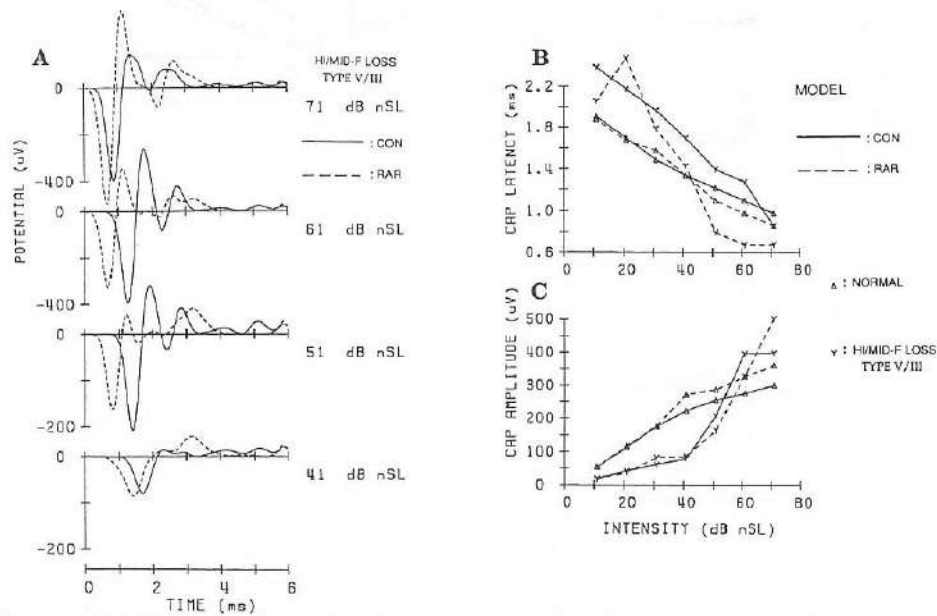


Fig. 5. High- and mid-frequency loss, simulations of click CAPs with model M2. Simulations are done with responses of type V in the frequency range 3-34 kHz (3.5 octaves) with threshold shift of 40 dB, and type III for the range of 1.5-3 kHz (1 octave), with threshold shift of 30 dB. Model agrees with experimental data at high intensities (Fig. 3): model latencies are short; model amplitudes are large (normal range); significant polarity dependence.

of the CAP. Obviously, the best model simulations are obtained with parameters of response type V (in combination with type III), which shows among others an abnormal polarity dependence (cf. Table I). This model version scores better than the M1 model for each feature, and better than or equal to the other M2 versions except for t_{NI} where the type-III version is more realistic. The results of the type-V/III version of the M2 model are shown in Fig. 5. Not only the absolute values of t_{NI} and A_{NI} but also the polarity effects are reproduced well. Furthermore, notice for both polarities the similarity of waveforms between model and experiment, in particular at 51 and 71 dB nSL (Fig. 5A). Also the simulation of the latency in its remarkable variation with intensity is good (Fig. 5B). The model result is encouraging since the single-fibre responses found in GP123 (see Fig. 3A) justifies a choice of both type III and V.

For the three other cases, which we consider in the next subsections, a simulation with the M2 model was only performed with the response type(s) found in the majority in the specific example animal.

TABLES II
GLOBAL FEATURES IN CAPS AND SUCCESS OF CORRESPONDING MODEL SIMULATIONS

For each type of audiogram the average features are described. Simulation with type-I characteristics represents the M1 model version, that with types II to V the M2 version. Qualifications of features: if not indicated as normal then abnormal, e.g. short means shorter than normal. Symbols: +: good result, feature closely approximated; 0: tendency of feature present, but not close approximation; -: bad result, often opposite to feature.

TABLE IIA
High- and mid-frequency loss (GP123, GP147)

Parameter	Level	Feature	I	II	III	IV/II	V/III
t_{NI}	low	long	+	+	+	+	+
	high	normal	-	+	+	+	0
t_{NI} , pol dep	low	large	0	0	0	0	0
	high	large	-	-	+	-	+
A_{NI}	low	small	+	+	+	+	+
	high	normal	-	+	0	+	+
A_{NI} , pol dep	low	large	-	-	-	-	-
	high	normal	-	+	-	-	+
waveform	low	multiple peaks	0	0	0	0	0
	high	multiple peaks	-	-	0	0	+

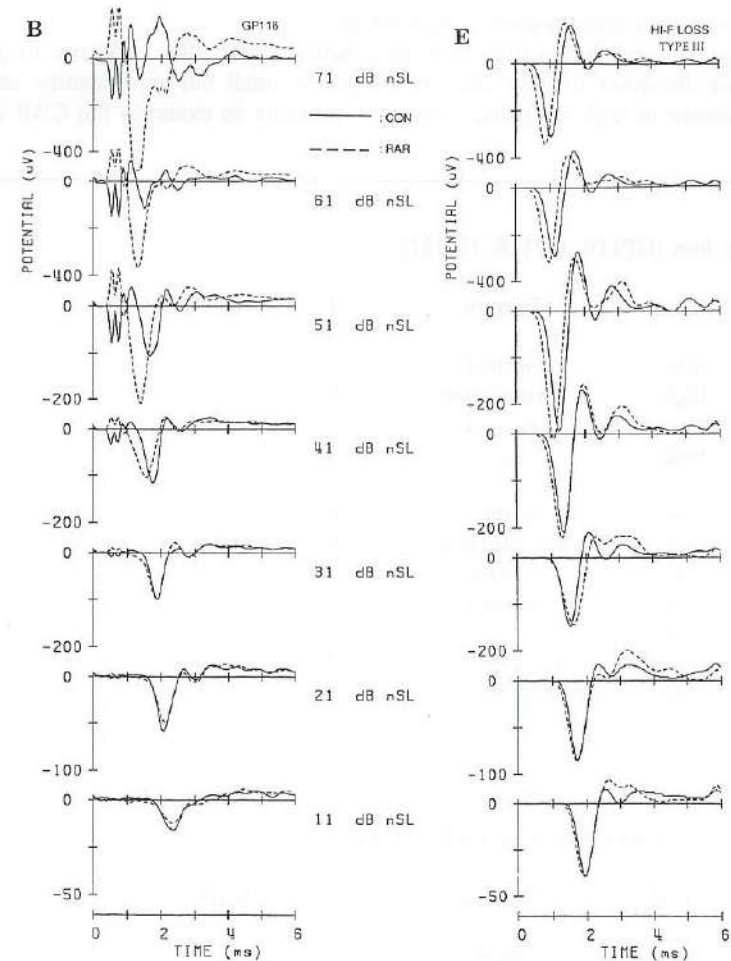
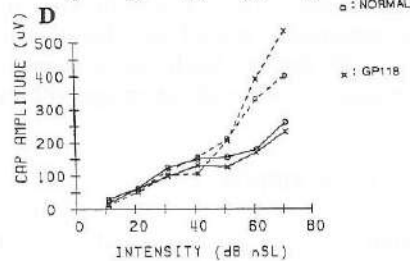
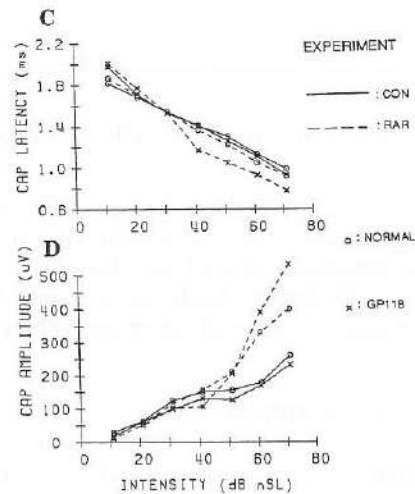
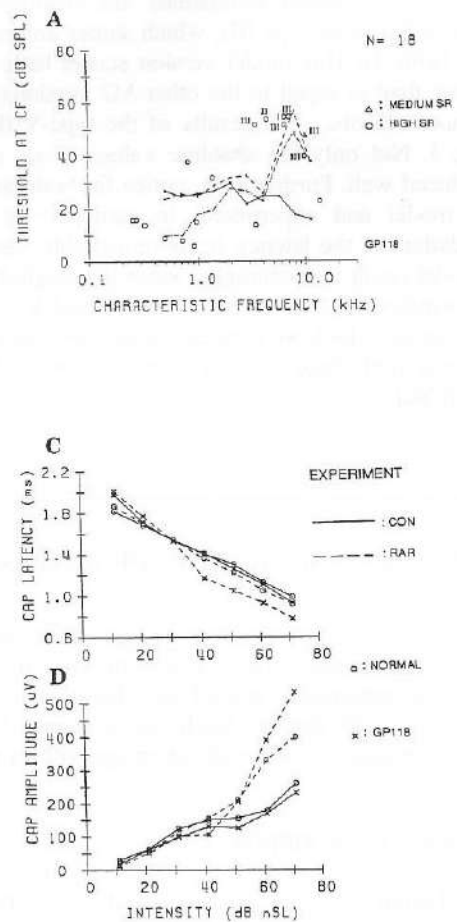


Fig. 6. High-frequency loss, experiment and model. (A) CAP tone audiogram of GP118: dot-dashed lines represent early recordings and dashed lines final recordings. The pre- and post-experiment audiograms are separately plotted symbolized by plus-signs and crosses, respectively. The averaged normal audiogram is given by a solid line. Asterix, triangle or circle symbols indicate thresholds at CF for single fibres, the roman digits indicate the FTC type of abnormal fibre. Most abnormal responses were of type III (71 %). (B) Click CAPs of GP118, see Fig. 2A for symbols. (C) N_1 latency, and (D) N_1 amplitude versus click intensity for CAPs of GP118 shown in B (stars), compared to normal experimental values (circles). (E) Model CAPs for a high-frequency hearing loss as found in GP118, computed according to M2 model with type III. The threshold shifts are 30 dB for 6-10 kHz, and 20 dB for 10-20 kHz.

Fig. 6. (continued).

CAPs in cochleas with high-frequency hearing loss

Three guinea pigs had a high-frequency hearing loss after exposure to a 6 kHz tone. The major deviation in their click CAPs was a small but significantly increased polarity dependence at high intensities. Figure 6 presents as example the CAP data for

TABLE IIB
High-frequency loss (GP110, GP118, GP131)

Parameter	Level	Feature	I	III
t_{N1}	low	normal	+	+
	high	normal/short	0	+
t_{N1} , pol dep	low	normal	+	+
	high	large	-	+
A_{N1}	low	normal	0	0
	high	normal/large	0	+
A_{N1} , pol dep	low	normal	+	+
	high	normal	+	+
waveform	low	normal/small N_2	0	0
	high	normal/small N_2	0	0

TABLE IIC
Mid-frequency loss (GP133, GP136, GP137, GP139, GP151)

Parameter	Level	Feature	I	IV/III
t_{N1}	low	short	-	-
	high	short	-	0
t_{N1} , pol dep	low	normal	-	-
	high	normal	+	+
A_{N1}	low	normal/small	+	+
	high	normal/large	-	0
A_{N1} , pol dep	low	normal	0	0
	high	normal	0	0
waveform	low	multiple peaks	0	0
	high	N_2 pol dep	-	0

TABLE IID
High- and low-frequency loss (GP121, GP130)

Parameter	Level	Feature	I
t_{N1}	low	long	-
	high	long	0
t_{N1} , pol dep	low	normal	+
	high	normal	0
A_{N1}	low	small	+
	high	normal/small	0
A_{N1} , pol dep	low	normal	+
	high	small	0
waveform	low	normal	0
	high	normal	0

GP118, which showed a moderate threshold shift in the frequency region above 6 kHz (Fig. 6A). Especially, the latencies (Fig. 6C) exhibited an increased polarity difference at high intensities because the rarefaction-click latency was significantly shorter than normal. Deviations could occur in opposite directions. For example, in two of the three guinea pigs CAPs showed a significant reduction of the N_2 - N_1 ratio (as in Fig. 6B), whereas in one the N_2 - N_1 ratio was abnormally large.

The high-frequency loss was simulated by a threshold shift of 30 dB for frequencies between 6 and 10 kHz, and 20 dB for frequencies between 10 and 20 kHz. A relatively large percentage of type-III responses, which typically vary with click polarity (cf. Table I), was found in the experiments (see Fig. 6A). Therefore, M2 simulations were performed with PSTH parameters for that type. At low intensities, where the M1 and M2 models are similar, the CAPs were simulated sufficiently (see Fig. 6E). At high intensities the M1 simulated waveforms, lacking an increase of polarity dependence and having too small amplitudes, did not agree with the experimental CAPs (Table IIB). A better simulation was achieved with the M2 model: the polarity dependence of t_{N1} was increased and A_{N1} was normal (Fig. 6E; Table IIB). Since the type-III responses have abnormal second peaks, some effect on the N_2 component could be expected in the M2 model simulations such as in the experimental CAPs. However, the simulated N_2 component had not changed.

CAPs in cochleas with mid-frequency loss

In four animals exposed to tones of 1.4 or 1.7 kHz we found a hearing loss in the frequency area between 1 and 6 kHz, and one animal exposed to 6 kHz had a moderate loss in a small area around 4 kHz. There were three major deviations in the click CAPs,

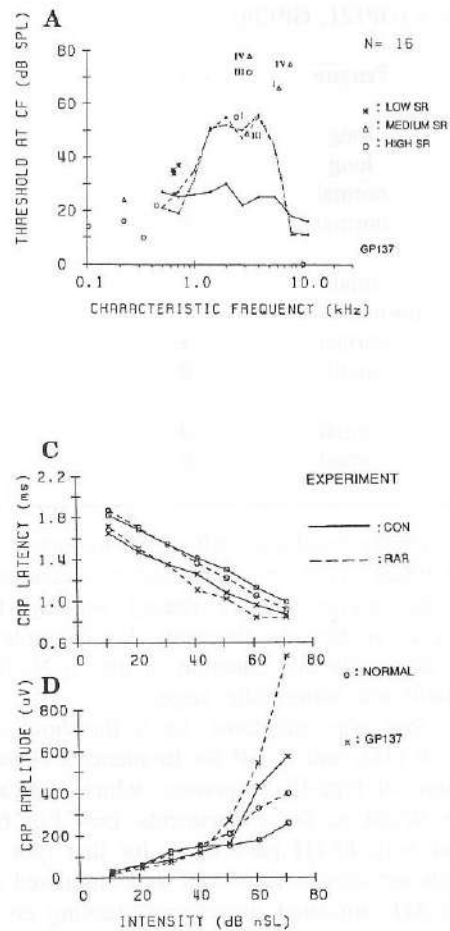


Fig. 7. Mid-frequency loss, experiment and model. Click CAPs as in Fig. 6 but for a mid-frequency loss, figures (A)-(E) are with order and symbols as in Figs. 6A-E, respectively. (A) CAP tone audiogram of GP137 (dashed lines). Abnormal FTCs in GP137 were of type I, III, or IV. (B) Click CAPs of GP137. (C) N₁ latency, and (D) N₁ amplitude versus click intensity for CAPs of GP137 shown in B (stars) compared to normal physiological values (circles). (E) CAPs computed by model M2 for a medium-frequency hearing loss. For frequencies between 1 and 3 kHz, threshold shifts are 30 dB and the abnormal responses are of type III, in the 3-6 kHz range the threshold shifts are 50 dB with the response type IV.

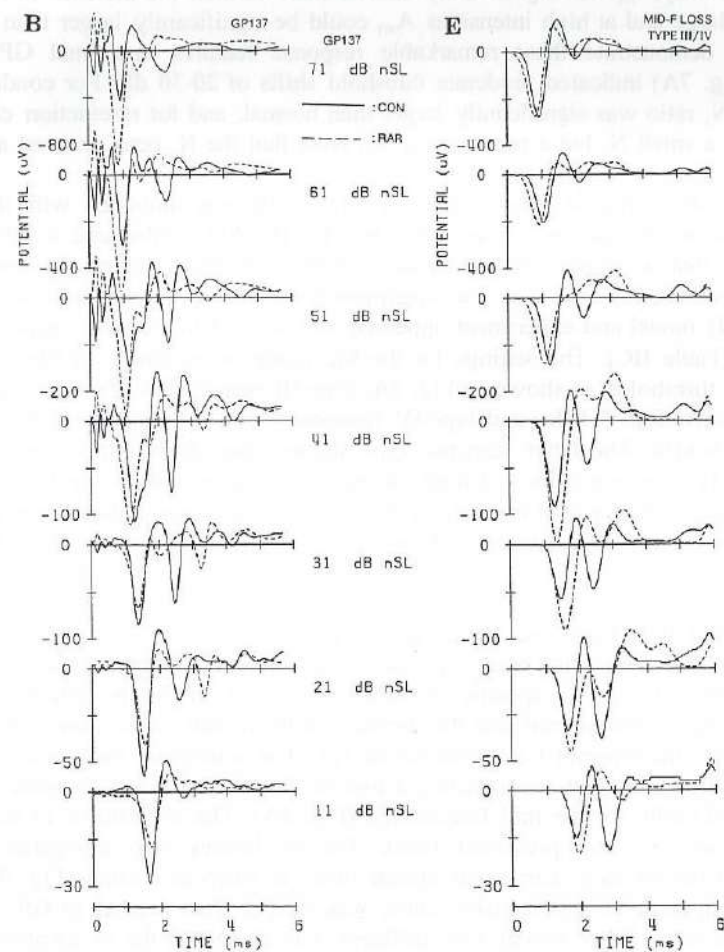


Fig. 7. (continued).

each exhibited by 4 out of the 5 animals. Late CAP components as N_2 and N_3 greatly varied with polarity; t_{N1} was significantly shorter than normal; the increase of A_{N1} with intensity was large and at high intensities A_{N1} could be significantly larger than normal. Figures 7B-D demonstrate these remarkable response features in animal GP137. Its audiogram (Fig. 7A) indicated moderate threshold shifts of 20-30 dB. For condensation clicks the N_2 - N_1 ratio was significantly larger than normal, and for rarefaction clicks we observed only a small N_2 but a pronounced N_3 . Note that the N_1 peak showed a normal polarity dependence.

The mid-frequency hearing loss in the M1 model was simulated with threshold shifts of 30 dB in a frequency range of 1 to 6 kHz. The M1-synthesized CAPs had an N_2 component that was large for condensation clicks and small for rarefaction clicks, which agreed remarkably well with the experimental waveforms. However, discrepancies between the M1 model and experiment appeared with respect to the other major features in the CAPs (Table IIC). The settings for the M2 model were based on the types and corresponding thresholds as shown in Fig. 7A: type-III responses with a threshold shift of 30 dB between 1 to 3 kHz, and type-IV responses with a threshold shift of 50 dB between 3 to 6 kHz. The latter response type shows steep amplitude-versus-intensity curves (Table I). The simulations at high intensities are improved by the M2 model in three aspects: t_{N1} is shorter than normal, the increase of A_{N1} grows above 40-50 dB nSL, and also the N_2 component at the high levels comes out better (see Table IIC and Fig. 7E).

CAPs in cochleas with high- and low-frequency loss

Two animals which had been exposed to a 6 kHz tone suffered a high- and low-frequency hearing loss. The specific deviations occurred in the N_1 latency. It was significantly longer than normal and the decrease with intensity was abnormally large. Figure 8 presents the relevant CAP data for GP121. The audiogram indicated a hearing loss of about 40 dB for high frequencies, a loss of 20-30 dB for low frequencies, and minor threshold shifts for the mid frequencies (Fig. 8A). The waveforms of the CAPs are normal (therefore, not presented here). The N_1 latency was elongated for all intensities, and the intensity curve was almost twice as steep as normal (Fig. 8B). The slope of the amplitude-versus-intensity curve was steeper than normal in GP121 (Fig. 8C). The CAPs in the other animal were different with respect to the N_1 amplitude. The slope of the intensity curve was normal such that A_{N1} remained relatively small up to high intensities.

The simulations of CAPs for low- and high-frequency loss as in GP121 are performed with a threshold shift of 45 dB in the frequency range 5 - 34 kHz, a threshold shift of 25 dB in the range below 1 kHz, and a small shift of 10 dB in the intermediate range. Only model M1 was applied to simulate the click CAPs, since most abnormal responses were classified as type I (Fig. 8A). The simulation results were partly sufficient as indicated by Table IID. The latencies were indeed longer than normal but did not show a large decrease with intensity. At low intensities A_{N1} agreed with the experiment, but the increase with intensity was shallower than normal, unlike what was

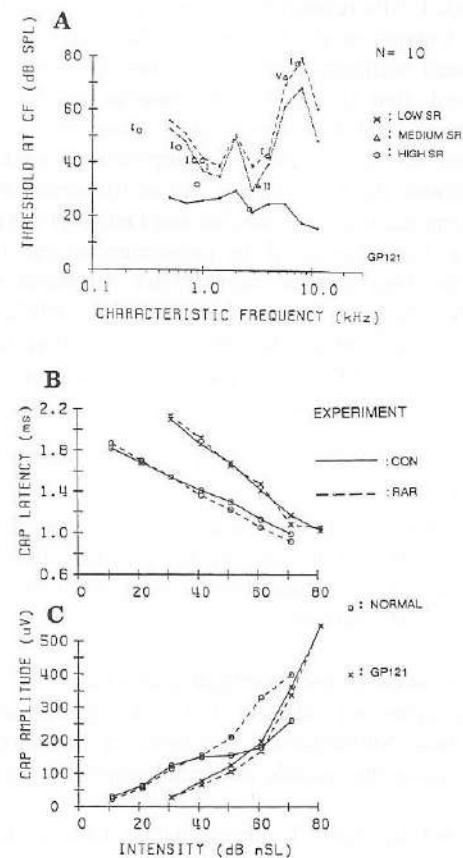


Fig. 8. High- and low-frequency loss, experiment. (A) CAP tone audiogram of GP121 (dashed lines), showing a high- and low-frequency loss. See Fig. 3A for symbol legends. Most abnormal thresholds correspond to type I. (B, C) Input/output curves for latency (B) and amplitude (C) of click N_1 from GP121. Stars symbolize the responses of GP121, circles the averaged normal values as given in Fig. 2.

experimentally found.

Discussion

Normal CAPs: experiment and model

For analysis of click CAPs recorded in guinea pigs we used an empirical model. The model introduced in Versnel et al. (1992a) has been upgraded in order to simulate CAPs for various (abnormal) audiograms, and with that, the modelling of normal CAPs is refined. The second peak that is added in the normal model PSTH causes a large contribution to the N_2 from high-CF fibres since their second peaks are, like the dominant peaks, synchronized across fibres as opposed to peaks of low-CF fibres. Hence, according to our model, the N_2 is mainly caused by second discharges of high-CF fibres, which supports interpretations of Özdamar and Dallos (1978), Dolan et al. (1983), and Versnel et al. (1992a). Adjustments of the parameters in the fibres with CFs above 12 kHz, which includes the idea that the fibres' click threshold is determined by the level of the FTC tail rather than by the tip (Versnel et al., 1992a), results in an extra increase of the amplitude at high intensities. However, the high-intensity slope is still shallower than in experimental CAPs. More data are needed on click responses of the fibres with very high CF (up to 30 kHz) to determine if they indeed are responsible for the large increase of the N_1 amplitude; for those high CFs we have now estimated parameters as amplitude increase (a), latency (t_p), and inter-fibre latency spread (σ_t) on the basis of only a few fibres.

The new model is improved with respect to the N_2 peak, the CAP onset latency, and the latency and amplitude of the N_1 peak. Normal click CAPs are properly described, and thus, the model is an adequate starting point to simulate and analyse deviations in CAPs in damaged cochleas.

Deviations in the CAPs: relation to the threshold audiogram

In the next paragraphs we discuss CAP deviations at low intensities in relationship to the audiogram. Subsequently, we consider deviations at high intensities where apart from the audiogram the specific abnormal single-fibre responses (cf. Table I) play a role.

The lack of contributing high-CF fibres, which have a short latency, explains longer N_1 latencies at low intensities for the three types of audiogram with a high-frequency loss (Figs. 3C: high/medium, 6C: high, 8B: high/low). For ears with a broad range of hearing loss (high/medium and high/low) the number of fibres contributing to the CAP at low intensities is small, and therefore, the N_1 amplitudes are markedly smaller than normal (Figs. 3D and 8C). These two phenomena and their explanations are reported by many authors (e.g. Elberling and Salomon, 1976; Aran and Cazals, 1978; Pettigrew et al., 1984). The explanations are confirmed by our model simulations (Table II).

The low-intensity CAPs in ears with a mid- or high/mid-frequency loss comprise

a multiple-peaked wave pattern that shifts with reversal of click polarity. An early component (N_1) is present in case of the mid-frequency losses (Fig. 7B), but it has disappeared in case of the high/mid-frequency losses due to the lack of contributing high-CF fibres (Fig. 3B). The occurrence of late multiple CAP peaks that shift with polarity can be ascribed to a dominant contribution of normal low-CF fibres which have polarity dependent multiple-peaked click responses (e.g. Kiang et al., 1965; Versnel et al., 1992a). In both cases the interpeak intervals in the quasi-periodic pattern of the CAPs correspond to the CF range of the most sensitive fibres (around 800 Hz). This pattern is reported for high- (and mid-) frequency losses in cats (Pettigrew et al., 1984), and in humans (Coats and Martin, 1977; Schoonhoven, 1990; Møller and Jho, 1991). The strong polarity dependence of the N_2 peak, an aspect of the multiple-peaked pattern in mid-frequency loss, is fairly well reproduced by the model (see Fig. 7E at low intensities, Table IIC). From the model latencies follows that for condensation clicks second discharges of high-CF fibres and first discharges of fibres with CFs around 800 Hz respond in phase and for rarefaction clicks out of phase. This underlines the crucial role of fibres with CFs of about 800 Hz. The quasi-periodic patterns in the CAPs of GP123 were simulated to some extent but not in its very pronounced form (Fig. 4A). The PSTH model in its simplified description of average response behaviour does not account for individual variations in amplitudes and thresholds. Therefore, the simulated contributions from remaining responding fibres with different CFs (below 1.5 kHz) are equally large, and can cancel in view of the different peak periods and latencies (cf. Møller and Jho, 1991). However, we assume that in cases as GP123 a group of fibres in a narrow CF band is dominant; this is plausible since normal PSTH amplitudes seem to be largest for a particular range of low CFs (Versnel et al., 1990).

Another relation between audiogram and click CAPs at low intensities is found in animals with a mid-frequency loss where four out of five had abnormally short N_1 latencies. This finding is not supported by the model simulations, and we do not have a satisfactory explanation for this discrepancy.

In conclusion, for low intensities there are several deviations in click CAPs that are systematically related to the type of audiogram, and according to the model results, most of these CAP features can be predicted. Also for high intensities we see common deviations in CAPs for animals with the same type of audiogram. Here the low simulation scores of model version M1 strongly indicate that it is not sufficient to know the audiogram in order to explain the abnormal CAPs (cf. Table II; Fig. 4).

Deviations in the CAPs: relation to aberrant single-fibre responses

Since simple assumptions on PSTHs (M1) are not adequate for high intensities we have to consider response characteristics of abnormal single fibres in order to explain abnormal response features of CAPs. In this analysis we assume that the UR (see Eqn. (2) in the Appendix) does not change in pathology (Versnel et al., 1992b). It must be stressed that the modelled responses can only be a global representation of actual responses, since there is a great variety of single-fibre responses in damaged cochleas (Lieberman and Kiang, 1978) and the abnormal responses are represented on the basis of

relatively few fibres. Furthermore, for some parameters we did not have sufficient data and thus took for simplicity the normal value (such a parameter is σ_t , see Appendix step ix)), a significant variable of the N_1 amplitude).

The global features of abnormal click responses of types II to V are that the latency has about the normal value, and that the amplitude at the saturation level is normal (types II and III) or larger than normal (types IV and V). Accordingly, at high intensities where these abnormal fibres are excited, the N_1 latency and amplitude are normal or border-line normal in most abnormal ears. Hence, even if one does not choose the correct actual types of abnormal response (II to V), simulation results generally should be better than with the M1 model (single-fibre response type I) as suggested by the scores in Table IIA. In this view the model assumptions of Elberling and Salomon (1976) that above threshold PSTHs of abnormal fibres are normal (when referred to sound level) appear reasonable. However, Table IIA also suggests that details in single-fibre responses are relevant: the best CAP simulation is achieved with response types which most likely were present in the studied ear. This modelling result and those for other ears (Figs. 6,7; Table IIB, C) demonstrate that specific response properties of abnormal fibres play a significant role in the deviations of CAPs to high-intensity clicks. Experimental results with a similar audiogram and different CAP deviations underline this conclusion. For instance, for audiograms with a high-frequency loss a larger polarity dependence of N_1 latencies was found for a larger percentage of fibres with response type III.

Beside the general CAP behaviour in noise-damaged ears, there are specific CAP deviations that can be well interpreted on the basis of the aberrant single-fibre responses. A nice example is animal GP123 which had a severe hearing loss with thresholds shifts of 40 dB in the high- and medium-frequency range and, paradoxically, short rarefaction-click latencies for levels more than 40 dB above normal click threshold (Fig. 3C). In this animal we found a large percentage of FTCs with a hypersensitive tail. The model simulations strongly indicated that the short single-fibre latencies associated to these FTC types caused the short N_1 latencies to rarefaction clicks. The same simulations made clear that the polarity dependence of the N_1 latency at high intensity is caused by the abnormal fibre responses, and not by dominant normal (and polarity variant) low-CF fibre responses, which at low intensities are responsible for the large N_1 -latency differences with polarity.

Our findings and model analysis clarify phenomena reported in pathological ears. It is demonstrated that normal N_1 latencies at high intensities as found by Wang and Dallos (1972), Eggermont (1976), Elberling and Salomon (1976), Salvi et al. (1979) and Pettigrew et al. (1984) are a consequence of the normal latencies for most abnormal single-fibre responses. Normal N_1 amplitudes to clicks as reported by Eggermont (1976) and Elberling and Salomon (1976) occur because of steeper single-fibre input/output curves and normal or larger than normal single-fibre response amplitudes. Eggermont (1979) observed in humans with a severe flat hearing loss abnormally short narrow-band derived CAP latencies to clicks. This might have been caused by hypersensitivity to low frequencies of fibres with a high CF and, thus, short latency. Finally, differences in

CAPs or ABRs to clicks between subjects with similar hearing loss as reported by Coats and Martin (1977) and Møller and Jho (1991) can be ascribed to the difference in types of single-fibre responses for similar audiograms.

From click CAPs to local cochlear dysfunctioning

Deviations in the CAP to high-intensity clicks are for one part caused by the threshold shifts and frequency range of hearing-loss areas, and for the other part by abnormalities in suprathreshold behaviour of single fibres from hearing-loss areas. On the basis of an audiogram and specific abnormal single-fibre response properties one can predict the click CAPs for pathological ears. Hence, given an audiogram and click CAPs, one might try to derive the underlying abnormal single-fibre responses. Accordingly, in view of the systematic relation between PSTHs and the type of abnormal FTC (Versnel et al., *), the changed frequency tuning might be derived. Furthermore, since the FTC shape is associated with a type of morphological cochlear damage (Lieberman and Dodds, 1984), one may also be able to assess cochlear damage on the basis of the CAP. Clicks should be presented at high intensities, where abnormal fibres respond, and it is important to record click CAPs for separate polarities, because potential deviations occur in the difference between responses. The latter suggestion has also been done by Coats and Martin (1977).

The application of click CAPs as here described for analysis of abnormal hearing will apply to guinea pigs in animal research. The merits for ECoG in humans are not as clear. It seems that with respect to polarity effects, larger variations between individuals exist in humans than in animals (Schoonhoven, 1990; data in our clinic). The additional application of narrow-band analysis of click responses would be useful here. See, e.g., in case of response types III and V: for low-frequency narrow bands an influence of hypersensitivity might be observed by short latencies or large amplitudes, for high-frequency bands a cancelling of polarity effects might occur (compared to broad-band click CAPs). Finally, the clinical application of the method of click CAPs, especially the possibility to obtain information on tuning characteristics, might be examined by recording both click CAPs and CAP tuning curves (cf. Rutten, 1986) in the same human ears. The opportunity to assess abnormal tuning characteristics would be very helpful in understanding specific problems with speech perception.

Appendix

The various components of the CAP model will be described here. Those that have been modified compared to the previous model version (Versnel et al., 1992a) are marked with an asterisk. New elements in the model are extensively described, for details on unchanged elements we refer to Versnel et al. (1992a). The quantities described are: 1) the model PSTH derived from the P-parameters, 2) the fibre population, and 3) the model UR. For abnormal cochlear threshold shifts for particular CF areas are inserted and parameters in the model PSTH are adapted as indicated in Table IA.

Model for click PSTHs

The model PSTHs $P(t)$ are simulated according to the following series of assumptions. The values of the parameters, listed in Table IA, are all derived from single-fibre data.

- i)* The PSTH is generally formulated as $P(t) = f(t; t_p, A_p, S_p) + f(t; t_{ps}, A_{ps}, S_{ps})$ where the symbols with subindex P represent the parameters of the dominant peak and those with subindices Ps represent the parameters for the secondary peak. All parameters depend on the fibre variables CF (f_c) and SR (r_c), and on the stimulus variables intensity (L_0) and polarity (m ; $m=1$ for condensation, and $m=-1$ for rarefaction click).
- ii)* The PSTH peaks (i.e. the dominant and the secondary) of a high-CF fibre ($f_c > 3$ kHz) are represented by a function $g(t)$ associated with the gamma distribution.

$$f(t; t_p, A_p, S_p) = g(t; \alpha, \beta, \gamma, \kappa) = \begin{cases} \kappa \{(t-\alpha)/\beta\}^{\gamma-1} \exp\{-(t-\alpha)/\beta\} & \text{for } t \geq \alpha \\ 0 & \text{for } t < \alpha \end{cases}$$

The relation of P-parameters with parameters of function $g(t)$ is as follows:

$$t_p = \alpha + \beta(\gamma-1), A_p = \kappa h, \text{ and } S_p = h/(2\beta) \text{ with } h = (\gamma-1)^{(\gamma-1)} \exp(1-\gamma).$$

The parameter γ was set at a constant value, we chose $\gamma=3$ (Versnel et al., 1992c).

The function $g(t; \alpha, \beta, \gamma, \kappa)$ could then be expressed as a function of the P-parameters:

$$f(t; t_p, A_p, S_p) = g(t; t_p - h/S_p, h/2S_p, 3, A_p/h) \text{ for } f_c > 3 \text{ kHz} \\ \text{with } h = 4\exp(-2) = 0.54.$$

- iii) The PSTH peaks of a low-CF fibre are represented by half a period of a sinusoid with a frequency of S_p/π (see step vii) on parameter S_p).
- $$f(t; t_p, A_p, S_p) = A_p \cos\{2S_p(t-t_p)\} \text{ with } |t-t_p| \leq \pi/(4S_p) \text{ for } f_c \leq 3 \text{ kHz}$$
- iv) The SR dependence is incorporated in the intensity dependence, the effective intensity L is taken different for the three SR groups: $L = L_0 - \delta L(r_c)$, with L_0 the actual intensity and $\delta L(r_c)$ the threshold difference of low- or medium-SR fibres with high-SR fibres.
- v)* The description of latencies of low-CF fibres is modified in view of their polarity dependent behaviour. The condensation-click latencies are directly derived from the data, but the rarefaction-click latencies of the low-CF fibres are now taken a half cycle ($1/2f_c$) longer or shorter than the condensation-click latencies, for low intensities longer and for high intensities shorter. The transition intensity increases with CF according to the data (Versnel et al., 1992a). The rarefaction-click latencies of high-CF fibres (where the difference between rarefaction and condensation clicks deviates from $1/(2f_c)$, see Versnel et al., 1990) are directly derived from the data. The CF dependent latency term t_1 has now been made to vary with the effective level L instead of L_0 , which introduces a simplification

without resulting in significant changes since the level dependence of the latency is mainly expressed by the second term t_2 .

$$t_p = t_1(f_c; L, m) + t_2(L) \text{ in which} \\ t_1(f_c; L, m) = \begin{cases} c_1(L)f_c^{-c_2} + 0.5(1-m)j(f_c, L)/(2f_c) & \text{for } f_c \leq 3 \text{ kHz} \\ c_1(L)3^{-c_2} + 0.5(1-m)c_1(L) & \text{for } f_c > 3 \text{ kHz (independent of } f_c) \end{cases} \\ \text{and } t_2(L) = t_2(0)\exp(-c_3L) \\ \text{with } j=1 \text{ or } j=-1, \text{ and } c_r \text{ accounts for a rarefaction- minus condensation-click difference.}$$

Figure 1 illustrates the gradual decrease of latency with intensity.

For low CFs the latency of the second peak, t_{ps} , is longer or shorter than the dominant peak by one period of $1/f_c$. For condensation clicks t_{ps} is longer for all conditions, for rarefaction clicks it is shorter if t_p is longer for rarefaction than for condensation clicks, which occurs at low intensities as described above, and vice versa for high intensities. If the period $1/f_c$ is less than the absolute refractory period (1.0 ms) and the sum of the two peaks reflects an integral discharge probability greater than 1, then the interpeak period is set at two or three periods of $1/f_c$ such that it is larger than 1.0 ms. The second peak for high-CF PSTHs is set at the experimentally observed interpeak time of 1.0 ms.

$$t_{ps} = t_p + t_{ip}(f_c; L, m) \text{ with the interpeak interval } t_{ip} \text{ described as} \\ t_{ip} = \begin{cases} c_4 & \text{for } f_c > 3 \text{ kHz} \\ 0.5\{(m+1) + (m-1)j(f_c, L)\} n/f_c & \text{with } n=1,2,3 \text{ for } f_c \leq 3 \text{ kHz.} \end{cases}$$

Note in Fig. 1A the interpeak intervals of 1.0 ms (c_4 value), and note in Fig. 1B in the rarefaction-click histograms the shift of the peak dominance between 21 and 31 dB nSL induced by a sign change of $j(f_c, L)$.

- vi)* The amplitudes A_p and A_{ps} are assumed to increase linearly with the effective intensity (in dB) up to a saturation value:

$$A_p(f_c; L) = \begin{cases} 0 & \text{for } L \leq 0 \\ a(f_c)L & \text{for } 0 \leq L \leq L_s \\ a(f_c)L_s(f_c) & \text{for } L > L_s \end{cases}$$

with $a(f_c)$ the rate of increase, and $L_s(f_c)$ the saturation intensity.

$$A_{ps} = r(f_c)A_p \text{ with ratio factor } r(f_c) \leq 1.$$

Figure 1 illustrates that the saturation levels are 40 and 30 dB for the high-CF (A) and low-CF (B) fibres, respectively.

We took into account not only the sharp increase of click threshold with CF for CFs above 12 kHz (see Versnel et al., 1992a), but also the threshold increase with decreasing CF for very low CFs. For CFs above 12 kHz we made important refinements. The increase of click threshold with CF (related to increase of CF-

tone threshold and decrease in click spectrum) was limited to a level that corresponds to an FTC-tail threshold, Θ_{ii} ; this threshold being hyper- or hyposensitive varies with a type of FTC (Versnel et al., *). Furthermore, for high click thresholds ($30 + \delta L(r_s)$ dB nSL), which are reached for CFs above 18 kHz, the increase rate a was enlarged and L_s was reduced by a factor 2.

$$\begin{aligned} L &= L_0 - \delta L(r_s) - d_i^2 \log(0.5/f_c) && \text{for } f_c < 0.5 \text{ kHz} \\ L &= L_0 - \delta L(r_s) - d_h^2 \log(f_c/12) && \text{if } d_h^2 \log(f_c/12) < \Theta_{ii} \text{ or} \\ L &= L_0 - \delta L(r_s) - \Theta_{ii} && \text{if } d_h^2 \log(f_c/12) \geq \Theta_{ii} \text{ for } f_c > 12 \text{ kHz} \end{aligned}$$

with d_h and d_i rates of threshold increase (dB/octave).

- vii)* The CF dependence of the peak synchronization S_p and S_{ps} is modified. For CFs below 1 kHz S_p is set to make the peak duration be half a period of $1/f_c$, for CFs between 1 and 3 kHz S_p slightly increases with CF, above 3 kHz S_p is invariant with CF. The synchronization in the secondary peak is taken equal to that of the dominant peak.

$$\begin{aligned} S_p &= \pi f_c && \text{for } f_c \leq 1 \text{ kHz} \\ S_p &= \pi f_c^{0.25} && \text{for } 1 < f_c \leq 3 \text{ kHz} \\ S_p &= b && \text{for } f_c > 3 \text{ kHz with } b \text{ a constant.} \\ S_{ps} &= S_p. \end{aligned}$$

S_p is enlarged by making it equal to A_p in those cases that S_p would be smaller than A_p , because the firing probability that is represented in the PSTH peak, A_p/S_p , cannot be larger than 1.

PSTHs in cochlear regions of hearing-loss

In model M1 the parameters for hearing loss regions are described as normal but for a reduced effective intensity, in the analogy of the SR dependence (step iv). Parameter values are found in Table IA for normal/type I.

$$\begin{aligned} L &= L_0 - \delta L(r_s) - L_{TS} && \text{for } 0.5 \leq f_c \leq 12 \text{ kHz} \quad (1) \\ L &= L_0 - \delta L(r_s) - d_i^2 \log(0.5/f_c) - L_{TS} && \text{for } f_c < 0.5 \text{ kHz} \\ L &= L_0 - \delta L(r_s) - d_h^2 \log(f_c/12) - L_{TS} && \text{if } d_h^2 \log(f_c/12) < \Theta_{ii} \text{ or} \\ L &= L_0 - \delta L(r_s) - \Theta_{ii} - L_{TS} && \text{if } d_h^2 \log(f_c/12) \geq \Theta_{ii} \text{ for } f_c > 12 \text{ kHz} \end{aligned}$$

with L_{TS} the threshold shift that corresponds to the hearing loss.

For model M1 Eqn. (1) is applied in all steps i)-vii) of the PSTH model.

In model version M2 the specific PSTHs which correspond to different abnormal FTC types are explicitly incorporated. Parameters adapted according to M2 are: for t_p ; c_1 and c_r (see step v)); for A_p ; a and L_s (step vi)); for S_p ; b (step vii)); for t_{ps} ; c_4 (step v)); for A_{ps} (step vi)); r ; furthermore the tail level Θ_{ii} (step vi)) is dependent on the response type. The values of the parameters for the types II-V are listed in Table IA. For

M2 synthesized abnormal PSTHs Eqn. (1) is only applied to compute the amplitude (step vi)).

Model compound discharge latency distribution

A compound discharge latency distribution is computed by summation of the fibre's discharge probabilities $P(t)$ over a fibre population which is generated as follows.

- viii)* The CF range was extended from 0.5-24 kHz to 0.25-34 kHz. One hundred CF points are logarithmically distributed over an octave. For each discrete CF point the responses of 40 fibres are computed, which are subdivided into high-, medium- and low-SR fibres according to the ratio 25:9:6 (Versnel et al., 1990).
- ix) The spread of latencies of different fibres of similar CF and SR was simulated by convolution with a Gaussian distribution function $n(t) = \exp\{-(t-t_p)^2/2\sigma_t^2\}$. Particularly, Fig. 1B illustrates the effect of the latency spread in that the originally sinusoidal shaped PSTH has now become bell-shaped.

Model CAP

- x) For each audiogram the sum of $P(t)$'s of contributing fibres was convolved with the same standard UR according to Goldstein and Kiang (1958):

$$C(t) = \int_{-\infty}^t S(\tau) U(t-\tau) d\tau \quad (2)$$

in which $C(t)$ is the CAP, $S(t)$ is the sum of $P(t)$'s, and $U(t)$ the UR.

The model UR was chosen as follows (Versnel et al., 1992b):

$$\begin{aligned} U(t) &= (U_N/\sigma_N) (t-t_0) \exp\{1/2 - (t-t_0)^2/2\sigma_N^2\} && \text{for } t < t_0 \\ U(t) &= (U_P/\sigma_P) (t-t_0) \exp\{1/2 - (t-t_0)^2/2\sigma_P^2\} && \text{for } t \geq t_0 \end{aligned}$$

with the parameter values: $t_0 = -0.06$ ms, $U_N = 0.12$ μ V, $\sigma_N = 0.12$ ms, $U_P = 0.09$ μ V and $\sigma_P = 0.16$ ms.

Acknowledgements

This study was supported by the Netherlands organization for scientific research (NWO) and by the Heinsius Houbolt Fund. Technical assistance to the experiments was given by V. Gerritsma, A. van Wijngaarden, and P. Schotel. We thank E. de Boer (ENT dept., University of Amsterdam) and G. Hunt for their support and constructive comments on the manuscript.

References

- Aran, J.-M. and Cazals, Y. (1978) Electrocochleography: animal studies. In: R.F. Naunton and C. Fernandez (Eds.), *Evoked electrical activity in the auditory nervous system*, Academic Press, New York, pp. 239-257.
- Bappert, E., Hoke, M., Lütkenhöner, B. and Niestroj, B. (1980) Intensity dependence of the compound action potential and the deconvolution technique. In: M. Hoke, G. Kaufmann and E. Bappert (Eds.), *Scand. Audiol. Suppl.* 11, 45-58.
- de Boer, E. (1975) Synthetic whole-nerve action potentials for the cat. *J. Acoust. Soc. Am.* 58, 1030-1045.
- Coats, A.C. and Martin, J.L. (1977) Human auditory nerve action potentials and brain stem responses. *Arch. Otolaryngol.* 103, 305-310.
- Dolan, D.F., Teas, D.C. and Walton, J.P. (1983) Relation between discharges in auditory nerve fibres and the whole-nerve response shown by forward masking: an empirical model for the AP. *J. Acoust. Soc. Am.* 73, 580-591.
- Dolan, T.G. and Mills, J.H. (1989) Recoveries of whole-nerve AP thresholds, amplitudes and tuning curves in gerbils following noise exposure. *Hear. Res.* 37, 193-202.
- Eggermont, J.J. (1976) Electrocochleography. In: W. D. Keidel and W. D. Neff (Eds.), *Handbook of sensory physiology*, Springer Verlag, Berlin, Heidelberg, New York, Vol. V, pp. 626-705.
- Eggermont, J.J. (1979) Narrow-band AP latencies in normal and recruiting human ears. *J. Acoust. Soc. Am.* 65, 463-470.
- Elberling, C. (1976) Simulation of cochlear action potentials recorded from the ear canal in man. In: R. Ruben, C. Elberling and G. Salomon (Eds.), *Electrocochleography*, University Park Press, Baltimore, pp. 151-168.
- Elberling, C. and Salomon, G. (1976) Action potentials from pathological ears compared to potentials generated by a computer model. In: R. Ruben, C. Elberling and G. Salomon (Eds.), *Electrocochleography*. University Park Press, Baltimore, pp. 439-455.
- Goldstein, M.H. and Kiang, N.Y.S. (1958) Synchrony of neural activity in electric responses evoked by transient acoustic stimuli. *J. Acoust. Soc. Am.* 30, 107-114.
- Grashuis, J.L. (1974) The pre-event stimulus ensemble; an analysis of the stimulus-response relation for complex stimuli applied to auditory neurons. Ph.D. thesis, University of Nijmegen.
- van Heusden, E. and Smoorenburg, G.F. (1981) Eighth-nerve action potentials evoked by tone bursts in cats before and after inducement of an acute noise trauma. *Hear. Res.* 5, 1-23.
- Kiang, N.Y.S., Watanabe, T., Thomas, E.C. and Clark, L.F. (1965) Discharge patterns of single fibers in the cat's auditory nerve. M.I.T. Research Monograph No 35., M.I.T. Press, Cambridge Massachusetts.
- Lieberman, M.C. and Kiang, N.Y.S. (1978) Acoustic trauma in cats. *Acta Otolaryngol. Suppl.* 358, 1-63.
- Lieberman, M.C. and Dodds, L.W. (1984) Single-neuron labeling and chronic cochlear pathology. III. Stereocilia damage and alterations of threshold tuning curves. *Hear. Res.* 16, 55-74.
- Møller, A.R. and Jho, H.D. (1991) Effect of high-frequency hearing loss on compound action potentials recorded from the intracranial portion of the human eighth nerve. *Hear. Res.* 55, 9-23.
- Özdamar, Ö. and Dallos, P. (1978) Synchronous responses of the primary auditory fibers to the onset of tone burst and their relation to compound action potentials. *Brain Res.* 155, 169-175.
- Pettigrew, A.M., Lieberman, M.C. and Kiang, N.Y.S. (1984) Click-evoked gross potentials and single-unit thresholds in acoustically traumatized cats. In: J. B. Nadol and W. R. Wilson (Eds.), *Ann. Otol. Rhinol. Laryngol.* 93, Suppl. 112, 83-96.
- Popelář, J., Syka, J. and Berndt, H. (1987) Effect of noise on auditory evoked responses in awake guinea pigs. *Hear. Res.* 26, 239-247.
- Prijs, V.F. (1986) Single-unit response at the round window of the guinea pig. *Hear. Res.* 21, 127-133.
- Prijs, V.F. and Eggermont, J.J. (1981) Narrow-band analysis of compound action potentials for several stimulus conditions in the guinea pig. *Hear. Res.* 4, 23-41.
- Rutten, W.L.C. (1986) The influence of cochlear hearing loss and probe tone level on compound action potential tuning curves in humans. *Hear. Res.* 21, 195-204.
- Salvi, R.J., Hamernik, R.P. and Henderson, D. (1983) Response patterns of auditory nerve fibers during temporary threshold shift. *Hear. Res.* 10, 37-67.
- Salvi, R.J., Henderson, D. and Hamernik, R.P. (1979) Single auditory nerve fiber and action potential latencies in normal and noise-treated chinchillas. *Hear. Res.* 1, 237-251.
- Schoonhoven, R. (1990) Stimulus polarity dependence of click-evoked compound action potentials from the auditory nerve in man. 13th A.R.O. Midwinter Research Meeting, St. Petersburg Beach, Florida, abstract 162.
- Shivapuja, B.G. and Gu, Z.P. (1992) The effect of cocaine addiction on the cochlea. A.R.O. midwinter meeting, St Petersburg Beach, Florida, abstract 333.
- Versnel, H., Prijs, V.F. and Schoonhoven, R. (1990) Single-fibre responses to clicks in relationship to the compound action potential in the guinea pig. *Hear. Res.* 46, 147-160.
- Versnel, H., Schoonhoven, R. and Prijs, V.F. (1992a) Single-fibre and whole-nerve responses to clicks as a function of sound intensity in the guinea pig. *Hear. Res.* 59, 138-156.
- Versnel, H., Prijs, V.F. and Schoonhoven, R. (1992b) Round-window recorded potential of single-fibre discharge (unit response) in normal and noise-damaged cochleas. *Hear. Res.* 59, 157-170.
- Versnel, H., Schoonhoven, R. and Prijs, V.F. (1992c) Aberrant temporal discharge patterns in noise-damaged guinea-pig cochleas. In: Y. Cazals, L. Demany and K.C. Horner (Eds.), *Auditory Physiology and Perception, Advances in the Biosciences*, Pergamon Press, Oxford, Vol. 83, pp. 607-615.
- Versnel, H., Prijs, V.F. and Schoonhoven, R. (*) Click responses in noise-damaged guinea-pig cochleas. I. Abnormal single-fibre responses. *Hear. Res.* --,
- Wang, B. (1979) The relation between the compound action potential and unit discharges of the auditory nerve. Doctoral dissertation, Dept. of Electrical Engineering and Computer Science, M.I.T.
- Wang, C.-Y. and Dallos, P. (1972) Latency of whole-nerve action potentials: influence of hair-cell normalcy. *J. Acoust. Soc. Am.* 52, 1678-1686.

Chapter VIII

Summary and conclusions

The previous chapters of this thesis discussed auditory physiological experiments performed in the guinea pig. Whole-nerve and single-fibre responses to click stimuli were simultaneously recorded in both normal and noise-damaged cochleas. Also, the unit response at the round window was measured. The results of these experiments are summarized in this chapter, first for normal cochleas, then for abnormal cochleas. Subsequently, conclusions with respect to the electrocochleography are given. We refer regularly to the previous chapters and their figures, so that the reader can look up the details. For a complete summary of this research project both the General introduction (Chapter I) and this chapter should be read.

Normal cochleas

Single-fibre responses to clicks

We divide the auditory-nerve single fibres in three groups with respect to the spontaneous discharge rate (SR), with boundaries at 5 and 30 spikes/s. High-SR fibres are more sensitive than low-SR fibres, and medium-SR fibres have intermediate thresholds (*Ch. II, Fig. 1*). This agrees with findings of other investigators (Lieberman, 1978; Winter et al., 1990; Schmiedt, 1989). We distinguish fibres with low and high characteristic frequency (CF) on the basis of two distinct patterns in the click responses (*Ch. II, Fig. 5; Ch. III, Fig. 3*). The high-CF fibres (CF above 3 kHz) respond similarly to condensation and rarefaction clicks, the poststimulus time histograms (PSTHs) show one or two peaks, and the response latency is short. On the contrary, the responses of the low-CF fibres (CF below 3 kHz) are dependent on click polarity: the PSTHs have several peaks that alternate with polarity, and the click latency is long and increases with decreasing CF (cf. Kiang et al., 1965; Pfeiffer and Kim, 1972; Salvi et al., 1979).

The single-fibre data of click responses are applied in an empirical CAP model. In this model, discharge probabilities of click responses of single fibres are computed on the basis of the experimentally derived parameters of latency, amplitude, and synchronization of the dominant PSTH peak (*Ch. III, VII*). These PSTH parameters depend on the fibre variables CF and SR, and on the stimulus variables level (L_0) and click polarity (m). The SR dependence of the PSTH parameters is incorporated as a shift of effective intensity, $L = L_0 - \delta L(r_s)$, this describes reasonably well that with lower SR (lower L) latencies are longer and amplitudes are smaller.

Unit response

The unit response (UR) is derived with the method of spike-triggered averaging. Typically at least 5,000 averages were needed for a sufficient signal-to-noise ratio. In most recordings (usually in high-SR fibres since these provide a sufficient number of averages) the UR had a diphasic waveform and the amplitude of its first negative peak was $0.12 \pm 0.06 \mu\text{V}$ (*Ch. IV*). This confirms earlier reports on the UR, where the same method was applied (Kiang et al., 1976; Wang, 1979; Prijs, 1986). The spike-triggered averages of most low- and medium-SR fibres are found to be larger than $0.3 \mu\text{V}$ which is interpreted as resulting from synchrony of spontaneous activity of several fibres having each a UR of about $0.12 \mu\text{V}$ (cf. Evans, 1987). A model UR is described as follows:

$$\begin{aligned} U(t) &= U_N/\sigma_N(t-t_0)\exp\{1/2-(t-t_0)^2/2\sigma_N^2\} & \text{for } t < t_0 \\ U(t) &= U_P/\sigma_P(t-t_0)\exp\{1/2-(t-t_0)^2/2\sigma_P^2\} & \text{for } t \geq t_0 \end{aligned} \quad (1)$$

with $U_{N(P)}$ the amplitude and $\sigma_{N(P)}$ the width of the negative (N) and positive (P) UR peak, and t_0 the zerocrossing of the diphasic waveform, and with parameter values: $U_N = 0.12 \mu\text{V}$, $\sigma_N = 0.12 \text{ ms}$, $U_P = 0.09 \mu\text{V}$ and $\sigma_P = 0.16 \text{ ms}$, $t_0 = -0.06 \text{ ms}$.

Compound action potential

Simultaneously with single-fibre PSTHs we recorded compound action potentials (CAPs) to clicks of various levels and both polarities. These CAPs are simulated according to the convolution theorem of Goldstein and Kiang (1958). Model PSTHs (estimates of the discharge probability density) are summed over the whole-nerve population of single fibres each characterized by variables CF and SR. Subsequently, the sums (estimates of the whole-nerve discharge latency distribution) are convolved with the model UR (see Eqn. (1)) resulting in a model CAP. This CAP is expressed as follows:

$$C(L_0, m; t) = \int_{-\infty}^t \left\{ \sum_{f_c, r_s} P(f_c, r_s, L_0, m; \tau) \right\} U(t-\tau) dt \quad (2)$$

where $C(L_0, m; t)$ is the CAP as a function of stimulus level L_0 and click polarity m , and $P(f_c, r_s, L, m; \tau)$ the model PSTH with f_c and r_s representing fibre variables CF and SR. Note that the model unit response $U(t)$ is considered independent of fibre.

The synthesized CAPs agree with the experimental CAPs with respect to the latency and amplitude of the N_1 component (i.e. first negative peak) of the CAP, the polarity dependence in the N_1 parameters, and the basic waveform including the N_2 peak (*Ch. VII, Fig. 2*). Only the intensity increase of amplitudes at high intensities (above 50 dB normal sensation level, nSL) is not simulated accurately.

Abnormal cochleas

In the general introduction, we raised several questions addressing the core of our research project. How are click PSTHs of single fibres from hearing loss regions related to abnormal FTCs? Does the UR significantly change as a result of cochlear damage? To what extent are abnormal single-fibre responses responsible for deviations in CAPs? And, is it possible to derive from click CAPs the response properties at the single-fibre level? These questions are discussed in following sections.

Frequency threshold curves and click PSTHs

In 89 fibres with elevated thresholds we distinguished 5 types of abnormal tuning curves, classified by both the identification of the CF and the threshold of the low-frequency tail (*Ch. V*). Three out of the five correspond very closely to the tuning curves schematized by Liberman and Dodds (1984). Two types include the intriguing phenomenon of hypersensitivity of the FTC tail.

The click PSTHs of abnormal fibres correspond to the various types of FTCs. Main features (*Ch. V, Figs. 4, 5*) are as follows. A fibre with a broad tuning around CF (type II) shows a relatively short response duration. The PSTHs of a fibre with a double tuning (type III), around a (high) CF and a low frequency of an abnormally sensitive FTC tail, represent a high-CF character in that they have a short latency, and a low-CF character in that they show multiple peaks and a strong polarity dependence. The click responses of fibres in which a CF cannot be identified (type IV or V) and found in cochleas with a severe high-frequency loss, often have a short latency and a very large peak amplitude. These response patterns can be understood on the basis of the abnormal tuning, e.g., aberrant PSTHs of type III are caused by hypersensitivity of the tail as demonstrated by a close correspondence between the tail and the Fourier power spectrum of the click PSTHs (*Ch. V, Figs. 8, 9*). Moreover, the cochlear model simulated the PSTHs fairly well for different types of FTCs (*Ch. VI*), e.g., a simulation of type-III responses shows the multiple-peak pattern and the dominant-peak latency that is shorter for rarefaction than for condensation polarity.

Unit response

The UR in fibres with elevated thresholds is not significantly changed from normal, apart from a trend to shortening of the waveform duration and a small increase in amplitude of the positive peaks (*Ch. IV*). These minor deviations, which are not related to the amount of threshold shift, have not been considered in our modelling.

Compound action potential

Deviations of the click CAPs in pathological cochleas are significant (*Ch. VII*). Examples of such deviations are steep amplitude-versus-intensity curves with relatively large N_1 amplitude values for high intensities, an abnormally short N_1 latency and a large polarity dependence of the waveform including the N_1 latency. Most deviations are systematically related to the type of audiogram. Two types of CAP model computations

are applied in order to simulate the abnormal CAPs. These are:

- M1. Only threshold shifts in the tone audiogram are considered, suprathreshold responses of abnormal fibres are represented by parameters which are normal with respect to the elevated fibre's threshold: I/O curves of P-parameters shifted with intensity.
- M2. Deviations in PSTHs of fibres with threshold shifts are incorporated. Response types found in the corresponding animal are included. At low levels (where abnormal fibres do not respond) M2 is identical to M1.

Simulations were done for four ears with different audiograms. At low intensities most features can be predicted from the audiogram. However, according to our M1 model simulations, at high levels CAP deviations cannot be explained only on the basis of the audiogram. The model simulations with M2 demonstrate that specific abnormal single-fibre response patterns significantly contribute to deviations in the CAP to high-intensity clicks. If the types of abnormal single-fibre responses that were dominant in a certain cochlea were incorporated in the computation, the recorded CAPs could be better simulated than with other types or the M1 model (*Ch. VII, Table II*). Moreover, in absolute sense synthesized waveforms often well reproduced the abnormal CAP features (*Ch. VII, e.g., Figs. 3, 5*).

What do deviations in click CAPs tell us?

The choice of type of abnormal single-fibre response is critical for the model simulations of abnormal CAPs. Therefore, given an audiogram and click CAPs, one might derive the underlying abnormal single-fibre responses. To obtain from abnormal CAPs any information on cochlear dysfunctioning, it is crucial to present clicks at high intensities, where abnormal fibres respond, and it is important to record CAPs for separate click polarities, because potential deviations occur in the difference between responses. Information might be derived about the changed frequency selectivity in the hearing-loss regions since there is a consistent relation between PSTHs and the type of abnormal FTC. In the case of electrocochleography in humans, this method of estimating tuning properties would help to understand specific problems with speech perception. Furthermore, Liberman and Dodds (1984) related the various tuning manifestations to different stages of damage to IHCs and OHCs, thus it may even be possible to assess cochlear damage on the basis of click CAPs.

References

- Evans, E. F. (1987) On the nature of the round window recorded "unit response": the contribution of single unit responses to the gross cochlea action potential. *Brit. J. Audiol.* 21, 103-104.
- Goldstein, M.H. and Kiang N.Y.S. (1958) Synchrony of neural activity in electric responses evoked by transient acoustic stimuli. *J. Acoust. Soc. Am.* 30, 107-114.
- Kiang, N. Y. S., Moxon, E. C. and Kahn, A. R. (1976) The relationship of gross potentials recorded from the cochlea to single unit activity in the auditory nerve. In: R. J. Ruben, C. Elberling and G. Salomon (Eds.), *Electrocochleography*, University Park Press, Baltimore, pp. 95-115.

- Kiang, N. Y. S., Watanabe, T., Thomas, E. C. and Clark, L. F. (1965) Discharge patterns of single fibers in the cat's auditory nerve. M.I.T. Research Monograph No 35., M.I.T. Press, Cambridge Massachusetts.
- Liberman, M. C. (1978) Auditory-nerve response from cats raised in a low-noise chamber. *J. Acoust. Soc. Am.* 63, 442-455.
- Liberman, M.C. and Dodds, L.W. (1984) Single-neuron labeling and chronic cochlear pathology. III. Stereocilia damage and alterations of threshold tuning curves. *Hear. Res.* 16, 55-74.
- Pfeiffer, R. R. and Kim, D. O. (1972) Response patterns of single cochlear nerve fibers to click stimuli: descriptions for cat. *J. Acoust. Soc. Am.* 52, 1669-1677.
- Prijs, V. F. (1986) Single-unit response at the round window of the guinea pig. *Hear. Res.* 21, 127-133.
- Salvi, R. J., Henderson, D. and Hamernik, R. P. (1979) Single auditory nerve fiber and action potential latencies in normal and noise-treated chinchillas. *Hear. Res.* 1, 237-251.
- Schmiedt, R. A. (1989) Spontaneous rates, thresholds and tuning of auditory-nerve fibers in the gerbil: Comparisons to cat data. *Hear. Res.* 42, 23-36.
- Wang, B. (1979) The relation between the compound action potential and unit discharges of the auditory nerve. Doctoral dissertation, Dept. of Electrical Engineering and computer science, M.I.T.
- Winter, I. A., Robertson, D. and Yates, G. K. (1990) Diversity of characteristic frequency rate-intensity functions in guinea pig auditory nerve fibres. *Hear. Res.* 45, 191-202.

Samenvatting

Om gehoor te geven aan een verzoek van de Leidse universiteit volgt hier een samenvatting van het proefschrift in de Nederlandse taal. Voor een groot deel is dit stuk een vertaling van hoofdstuk I, *General introduction*, en van hoofdstuk VIII, *Summary and conclusions*. Dit proefschrift is getiteld "Effekten van abnormale responsies van afzonderlijke vezels op de samengestelde aktiepotentialen in beschadigde cochlea's", en beschrijft dierexperimenteel onderzoek in de electrocochleografie (ECoG). De ECoG is een audiometrische techniek waarmee een diagnose kan worden gesteld van de (pathologische) toestand van de cochlea. Deze techniek waarbij met geluidsstimuli elektrische zenuwpotentialen worden opgewekt en gemeten met behulp van een electrode dicht bij de cochlea of gehoorzenuw, is eind '60-er jaren ontwikkeld met het oog op klinische toepassing. Al spoedig is de ECoG toegepast aan de Keel-, Neus-, en Oorheelkunde afdeling van het Academisch Ziekenhuis te Leiden onder impulsen van J.J. Eggermont en P.H. Schmidt. Een deel van het experimenteel onderzoek in de Leidse audiologie is sindsdien gericht op verbetering van interpretatie van de ECoG signalen en ontwikkeling van nieuwe stimulusparadigma's. Het recente onderzoek is geïnitieerd door V.F. Prijs en heeft ondermeer geleid tot dit proefschrift.

De hoofdkomponent van de opgewekte ECoG signalen is de samengestelde aktiepotentialen (verder aangeduid met CAP, afkorting van de Engelse term *Compound action potential*), een signaal dat is samengesteld uit aktiepotentialen van gehoorzenuwvezels. De interpretatie van de CAP is voornamelijk gebaseerd op statistiek over een grote kollektie van experimentele CAP gegevens in mens en dier, zowel voor goede als slechte oren. Om tevens een mathematische onderbouwing van de CAP analyse te verkrijgen zijn modelstudies verricht waarbij gebruik gemaakt wordt van responseeigenschappen van afzonderlijke neuronen van de gehoorzenuw. Opvallend genoeg is slechts weinig gedaan aan modellering van CAPs voor beschadigde cochlea's. In dit proefschrift zijn experimenten beschreven waarbij CAPs en responsies van afzonderlijke zenuwvezels zijn gemeten in cavia's met gebruik van kliks als geluidsstimuli. Met behulp van een empirisch model is onderzocht welke veranderingen in vezelresponsies ten grondslag liggen aan afwijkingen in de CAP in beschadigde cochlea's. Alvorens in te gaan op de resultaten van dit onderzoek, volgen inleidingen over het oor, en over de ECoG.

Inleiding

Cochlea en gehoorzenuw

Voor visuele ondersteuning bij de uitleg over de cochlea in deze paragraaf zijn figuren 1, 2 en 4 van Hoofdstuk I aanbevolen. De cochlea is het deel van het

gehoororgaan waar de transductie van akoestische trillingen naar elektrische signalen van de gehoorzenuw plaatsvindt. De cochlea bestaat uit drie compartimenten die gevuld zijn met vloeistof en die van elkaar worden gescheiden door het membraan van Reissner en door het basilaire membraan. De cochlea is spiraalvormig gewonden, en heeft 2½ (mens) tot 4 (cavia) windingen. Vanwege de vorm wordt de cochlea ook wel slakkehuis genoemd.

De geluidstrillingen worden via de gehoorgang, het trommelvlies en de gehoorbeentjes (hamer, aambeeld en stijgbeugel) overgebracht op bewegingen van de vloeistof in de cochlea en op bewegingen van het basilaire membraan. Het basilaire membraan is tonotopisch georganiseerd: de frequenties waarvoor het membraan meest gevoelig is, variëren langs het membraan, en dit is aldus bij de stapes afgestemd op hoge tonen en bij de apex (top van de cochlea) op lage. Op het basilaire membraan bevinden zich de zintuigcellen, de haarcellen, te onderscheiden, zowel qua plaats, qua vorm als qua functie, in binnenste en buitenste haarcellen (*inner, outer hair cells*, IHCs, OHCs). Ten gevolge van de beweging van het basilaire en het tectoriële membraan gaan de haartjes, de cilia, van de haarcellen heen en weer. Er ontstaan daardoor ionenstromen in de haarcellen met als gevolg dat biochemicalïen, neurotransmitters, uit de haarcel naar de zenuwuiteinden bewegen, waar vervolgens aktiepotentialen gegenereerd worden. Langs de zenuwvezel wordt de aktiepotentiaal (vanwege de vorm ook *spike* genoemd) voortgeleid naar volgende zenuwkernen en uiteindelijk naar de hersenen leidend tot een gehoorsensatie. De informatie van het geluid (frequentieinhoud, volume) is gecodeerd door een specifiek tijds patroon waarin de aktiepotentialen gegenereerd worden, en in een specifieke groep van vezels die geactiveerd worden. De informatiestroom naar de hersenen loopt primair langs de binnenste haarcellen (IHCs), die fungeren als mechano-elektrische transducers. Per octaaf langs het basilaire membraan bevinden zich ongeveer 200 IHCs, en ongeveer 20 zenuwvezels zijn gekoppeld aan één IHC. Per binnenste zijn er drie buitenste haarcellen. Over de rol van die buitenste haarcellen is veel beweging in gehooronderzoekersland, de algemene opvatting is dat ze fungeren als electromotoren die een positieve terugkoppeling verzorgen naar het basilaire membraan om zo de detectie-gevoeligheid te vergroten en de frequentieafstemming te verbeteren.

Bij het gehooronderzoek kan informatie verkregen worden over het functioneren van de cochlea ondermeer door de responsies van de gehoorzenuwvezels te meten. Met behulp van zeer fijne micro-electroden kunnen metingen worden verricht aan de gehoorzenuwvezels in proefdieren. Lokale frequentiekaracteristieken in de cochlea worden weerspiegeld door de frequentieafstemming in een vezel, welke wordt bepaald uit frequentie-drempelkurven (*frequency threshold curves*, FTCs). Van een FTC wordt de karakteristieke frequentie (*characteristic frequency*, CF) en de responsdrempel afgeleid. Een andere responseigenschap die de vezel typeert, is de spontane vuurfrequentie (*spontaneous discharge rate*, SR). Het gedrag van de neurale respons als functie van tijd wordt afgeleid uit post-stimulus-tijd-histogrammen (*poststimulus time histograms*, PSTHs).

Electrocochleografie

De aktiviteit van de gehoorzenuw kan globaal bepaald worden door bij de cochlea een macro-electrode te plaatsen. Indien in respons op een geluidsstimulus in een voldoende aantal zenuwvezels gelijktijdig een aktiepotentiaal gegenereerd wordt, tellen die aktiepotentialen dusdanig op dat op de plaats van de macro-electrode een elektrische potentiaal meetbaar is. Deze samengestelde aktiepotentiaal geeft een indicatie van de (eventueel verslechterde) toestand van de cochlea. De methode waarbij de CAP wordt gemeten, is de ElectroCochleoGrafie (ECoG). De ECoG kan enerzijds dienen voor diagnose van gehoorstoornissen van een patiënt, anderzijds kan kennis worden verkregen over de werking van de cochlea (in een proefdier of specifiek in de mens).

De opbouw van de CAP uit de responsbijdragen van de verschillende zenuwvezels (totaal aantal vezels in gehoorzenuw is ongeveer 40.000) wordt mathematisch weergegeven als een convolutie van de som van de neurale vuurkansen met de eenheidsbijdrage. Deze eenheidsbijdrage (*unit response*, UR) is de potentiaalverandering ter plaatse van de macro-electrode die het gevolg is van een enkele aktiepotentiaal van een zenuwvezel. De vuurkans van de vezel wordt geschat uit het PSTH. De UR is in goede benadering gelijk voor alle vezels en is onafhankelijk van de geluidsstimulus. Het PSTH is vezelspecifiek en hangt af van de stimulus. De convolutievergelijking is uitgangspunt in modellering van CAPs, en in geval van dit proefschrift wordt die als volgt weergegeven:

$$C(L_0, m; t) = \int_{-\infty}^t \left\{ \sum_{f_c, r_s} P(f_c, r_s, L_0, m; \tau) \right\} U(t-\tau) d\tau \quad (1)$$

waar $C(L_0, m; t)$ de CAP voorstelt als functie van stimulus nivo (*level*) L_0 , klik polariteit m en tijd t , en waar $P(f_c, r_s, L_0, m; \tau)$ het model-PSTH is met f_c en r_s de vezelvariabelen CF en SR. Voorbeelden van een CAP, PSTH en UR zijn afgebeeld in figuur 5 van Hoofdstuk I.

De ECoG kan worden toegepast ten behoeve van de diagnostiek, omdat de CAPs afgeleid van slechte oren significante afwijkingen vertonen. Afwijkingen in de CAP kunnen op verschillende wijzen tot stand komen. Bij een aandoening aan de gehoorzenuw kan de UR veranderen, en aldus, zoals we eenvoudig begrijpen uit bovenstaande vergelijking, de CAP. Meer voorkomend (bij voorbeeld als gevolg van ouderdom of te veel lawaai) zijn cochleaire aandoeningen, die gewoonlijk bestaan uit schade aan de haarcellen. In een vroeg stadium van een haarcelkwetsuur zijn de cilia, de haartjes, aangedaan. Een functioneel gevolg van schade aan binnenste haarcellen varieert van een verhoging van de responsdrempel (onafhankelijk van de stimulusfrequentie) tot een complete uitschakeling. Een gevolg van kapotte buitenste haarcellen is een verandering van frequentieafstemming en van gevoeligheid (meestal uiteraard een verslechtering). Een preciezer verband tussen morfologische afwijkingen en dysfuncties is voorgesteld door Liberman, die verschillende beschadigingen aan IHCs en/of OHCs relateerde aan abnormale typen van FTCs (*Hfdst. I, figuur 6*). Een

verandering in een haarcel betekent een verandering in de transduktieketen buitenwereld-gehoorzenuw, en leidt tot veranderingen in de responsies van de zenuwvezels. Als gevolg van een verhoging van responsdrempels zullen bij lage geluidsnivo's minder vezels bijdragen tot de CAP. Bij hoge geluidsnivo's kunnen de vezelresponsies ($P(f_c, r_s, L_0, m; \tau)$) in vergelijking (1)) gewijzigd zijn en aldus de CAP.

Onderzoeksvragen

Het doel van het onderzoek is een betere basis te verschaffen voor interpretatie van CAPs in beschadigde cochlea's. Daartoe zijn experimenten uitgevoerd in cavia's met normale en met lawaai-beschadigde cochlea's. CAPs en PSTHs zijn simultaan gemeten op klikstimuli. In deze korte geluidspulsen (duur 0.1 ms) zijn alle frequenties vertegenwoordigd, zodat vrijwel alle vezels reageren. De kliks zijn gevarieerd in intensiteit en in polariteit (verdichting of verdunning, analoog aan blazen versus zuigen). In dezelfde vezels waarbij PSTHs zijn gemeten, zijn de FTC en SR gemeten en is, indien de micro-electrode nog in contact was met de vezel, de UR afgeleid. De volgende vragen zijn onderzocht. Ten eerste, zijn de klik-PSTHs van vezels die beschadigde cochleaire gebieden innervieren, veranderd, en hoe zijn veranderingen gerelateerd aan veranderingen in FTCs. Ten tweede, verandert de UR ten gevolge van een cochleaire aandoening? Ten derde, zijn naast een afname in bijdragen volgend uit drempelverhogingen van vezels, ook abnormale vezelresponsies verantwoordelijk voor afwijkingen in de CAP, en zo ja, in welke mate? Ten slotte, is het mogelijk om uit abnormale klik-CAPs afwijkingen in responsies van afzonderlijke vezels af te leiden en zo informatie te verkrijgen over lokale dysfuncties in de cochlea?

Resultaten voor de normale cochlea

Responsies van afzonderlijke vezels

De gehoorzenuwvezels van de cavia kunnen op grond van de spontane activiteit (weergegeven in SR) worden onderverdeeld in drie groepen. Vezels met een hoge SR (groter dan 30 spikes/s) hebben een lagere responsdrempel dan vezels met een lage SR (kleiner dan 5 spikes/s), en middel-SR vezels hebben een drempel daartussenin (Hfdst. II, figuur 1). Een verdere onderverdeling is aangebracht tussen vezels met hoge en die met lage CF en is gestoeld op twee verschillende temporele patronen in de klikresponsies (Hfdst. II, figuur 5; Hfdst. III, figuur 3). Vezels met hoge CF (boven 3 kHz) vertonen nagenoeg identieke responsies op verdichtings- en verdunnings-klikstimuli, en de PSTHs tonen een of twee pieken met een korte latentie. Daarentegen zijn de klikresponsies van vezels met lage CF sterk afhankelijk van klikpolariteit: de PSTHs hebben verscheidene pieken die in tegengestelde fase verschijnen als de klikpolariteit wordt omgewisseld, de latentie is relatief lang en neemt af als functie van CF. Deze resultaten komen overeen met bevindingen in zoogdieren van andere gehooronderzoekers.

Ten behoeve van het empirisch CAP model (Hfdst. III, VII) zijn de klikresponsies van de afzonderlijke zenuwvezels (de vuurkansen) geschat op grond van de experimenteel gevonden waarden van specifieke parameters van het PSTH: de latentie, amplitude en synchronisatie van de grootste piek. Deze parameters zijn afhankelijk van vezelvariabelen CF en SR, en van stimulusvariabelen intensiteit (L_0) en klikpolariteit (m). De SR-afhankelijkheid van de PSTH-parameters is gemodelleerd met behulp van een effectieve intensiteit L die varieert met SR: $L = L_0 - \delta L(r_s)$. Zo wordt zeer redelijk beschreven, dat vezels met een lagere SR (dus lagere L , hogere drempel) een langere latentie en een kleinere amplitude hebben.

Eenheidsbijdrage

De eenheidsbijdrage van afzonderlijke vezels is experimenteel bepaald met behulp van vuring-volgend middelen (*spike-triggered averaging*). In deze methode is het spontane elektrische signaal aan het ronde venster (waar gewoonlijk de CAP wordt afgeleid) in tijdsintervallen voor en na het optreden van een actiepotentiaal opgenomen en gemiddeld per optreden. Na minimaal 5000 middelingen wordt een potentiaal-golfvorm verkregen met redelijke signaal-ruis verhouding. De meest gevonden UR-golfvorm (meestal in vezels met hoge SR) is bifasisch en de amplitude van de eerste, negatieve piek is $0.12 \mu\text{V}$ (Hfdst. IV). Dit bevestigt spaarzame eerdere bevindingen verkregen met dezelfde methode. De UR-amplitude schattingen die gedaan konden worden in vezels met lage en middelhoge SR, bleken meestal groter uit te komen dan $0.3 \mu\text{V}$. Een verklaring van E.F. Evans (1987, Brit. J. Audiol. 21:103-104) dat zulke grote golfvormen het resultaat zijn van synchronie van spontane vuringen van verscheidene vezels (elk met een UR van ongeveer $0.12 \mu\text{V}$), is aannemelijk. Een model-UR, gelijk voor alle vezels van de gehoorzenuw, is beschreven als volgt:

$$\begin{aligned} U(t) &= U_N/\sigma_N(t-t_0)\exp\{1/2-(t-t_0)^2/2\sigma_N^2\} & \text{als } t < t_0 \\ U(t) &= U_P/\sigma_P(t-t_0)\exp\{1/2-(t-t_0)^2/2\sigma_P^2\} & \text{als } t \geq t_0 \end{aligned} \quad (2)$$

met $U_{N(P)}$ de amplitude en $\sigma_{N(P)}$ de breedte van de negatieve (N) en positieve (P) UR piek, en t_0 de nuldoorgang van de bifasische golfvorm, en met parameter waarden als volgt: $U_N = 0.12 \mu\text{V}$, $\sigma_N = 0.12 \text{ ms}$, $U_P = 0.09 \mu\text{V}$ en $\sigma_P = 0.16 \text{ ms}$, $t_0 = -0.06 \text{ ms}$.

Samengestelde actiepotentiaal

Gelijktijd met de responsies van afzonderlijke vezels op klikstimuli is de samengestelde respons aan het ronde venster afgeleid. Deze CAPs zijn gesimuleerd met een empirisch model dat gebaseerd is op de convolutie vergelijking (zie vergelijking (1)). De model-PSTHs ($P(f_c, r_s, L_0, m; \tau)$) in (1) zijn berekend voor een hypothetische populatie van gehoorzenuwvezels (voor CFs tussen 250 Hz en 34 kHz), waarbij elke vezel gerepresenteerd is met een CF en een SR-kategorie. De model-PSTHs zijn bij elkaar opgeteld, en vervolgens is de som geconvolveerd met de model-UR met als resultaat een CAP. Volgens dit concept zijn CAPs voor beide klikpolariteiten en voor verschillende intensiteiten gesimuleerd.

Voor normale oren komen de gesimuleerde klik-CAPs goed overeen met de experimenteel bepaalde CAPs (*Hfdst. VII, figuur 2*). De overeenkomst geldt de latentie en amplitude van de eerste CAP piek (N_1), het gedrag van deze parameters als functie van klikpolariteit, en de golfvorm van de CAP met inbegrip van de tweede piek (N_2). Het enige aspect dat niet naar tevredenheid is gesimuleerd, betreft de toename van de N_1 -amplitude als functie van intensiteit bij hoge intensiteiten.

Beschadigde cochlea's

Om cochleaire beschadigingen te bewerkstelligen zijn een aantal cavia-oren blootgesteld aan een langdurige, luide toon (2 uur, ongeveer 120 dB SPL). Drempelverhogingen in de orde van 20 tot 40 dB werden gevonden over een bepaald frequentiegebied. Ook de enkele gevallen waar al voor aanbidding van het lawaai drempelverhogingen aanwezig waren, zijn gebruikt voor de metingen.

Responsies van afzonderlijke vezels

In een totaal van 89 gehoorzenuwvezels in beschadigde cochlea's vonden we diverse afwijkende drempelkurven (FTCs) die konden worden ingedeeld in 5 klassen. De typering van de FTCs was gedefinieerd op grond van de identifikatie van een CF tip in de kurve en op grond van de drempel van de zogenoemde staart welke de FTC heeft bij frequenties kleiner dan de CF (*Hfdst. V*). Drie van de vijf typen abnormale FTCs vertonen nauwe gelijkenis met de kurven zoals door Liberman geschetst in relatie met bepaalde haarcelbeschadigingen (*Hfdst. I, figuur 6*). Twee typen FTCs vertonen het intrigerende verschijnsel van vergrote gevoeligheid voor lage frequenties, ook wel geduid als de hypersensitieve staart.

De klikresponsies van abnormale vezels vertonen een éénduidige relatie met de typen FTCs. Laten we enkele voorbeelden noemen (*Hfdst. V, figuren 4, 5*). Een vezel met brede frequentieafstemming rond de CF (type II) toont een korte responsduur. Een vezel met dubbele frequentieafstemming (W-vormige FTC, type III), namelijk op CF en op overgevoelige staart, toont zowel een hoogfrequent karakter met een korte responslatentie, als een laagfrequent karakter met een veelheid aan pieken en een sterke variatie met klikpolariteit. Klikresponsies van vezels waar een afstemming rondom CF praktisch verdwenen is (type IV of V), hebben vaak een korte latentie en een zeer grote piekamplitude. Dergelijke afwijkende responspatronen kunnen in grote lijn worden verklaard op grond van de abnormale frequentiekarakteristieken. Dit is bijvoorbeeld evident in de nauwe overeenkomst tussen de FTC staart en het Fourier amplitude-spectrum van de klik-PSTHs voor vezels met FTC type III of V (*Hfdst. V, figuren 8, 9*). Andere evidentie blijkt uit de simulatieresultaten van een cochleair model. Gegeven een willekeurige FTC produceert dit computermodel neurale klikresponsies. De klik-PSTHs die berekend zijn op grond van type II en type III FTCs, toonden vele aspecten van gelijkenis met de experimentele PSTHs (*Hfdst. VI*).

Eenheidsbijdrage

De eenheidsbijdrage in abnormale vezels is niet in belangrijke mate veranderd ten opzichte van normaal, zij het, dat er een trend tot versmalling van de golfvorm en tot toename in de amplitude van de positieve piek was waar te nemen. Deze minimale veranderingen, die overigens geen korrelatie met de drempelverhoging vertoonden, zijn verwaarloosd in de modelsimulaties.

Samengestelde aktiepotentiaal

De klik-CAPs in lawaaigetraumatiseerde cochlea's vertonen significante afwijkingen van normaal (*Hfdst. VII*). Voorbeelden zijn steile N_1 -amplitude/intensiteitskurven met relatief grote N_1 -amplitudes voor hoge intensiteiten, een abnormaal korte N_1 -latentie, en een grote polariteitafhankelijkheid van de totale golfvorm. De meeste afwijkingen komen systematisch voor bij bepaalde toonaudiogrammen.

Twee variaties van het empirisch CAP model hebben we uitgevoerd om klik-CAPs te simuleren. Variant M1: als pathologische veranderingen zijn alleen drempelverschuivingen in het toonaudiogram meegenomen in berekening, en de responsies van vezels met verhoogde drempels zijn berekend alsof de klikintensiteit overeenkomstig de drempelverhoging verlaagd was, ofwel de I/O kurven van de PSTH parameters zijn verschoven langs de intensiteitsas; variant M2: ook de specifieke afwijkende responspatronen van vezels met verhoogde drempels zijn verdiskonteerd. Nota bene: M1 en M2 zijn identiek voor lage intensiteiten waar abnormale vezels niet responderen.

Samengestelde aktiepotentialen zijn nagebootst voor vier oren met verschillende toonaudiogrammen. Uit de modelexercities blijkt dat voor lage intensiteiten de meeste verschijnselen voorspeld kunnen worden op grond van het audiogram. Daarentegen kunnen voor hoge kliknivo's, waar het M1 model namelijk faalt, CAP-afwijkingen niet verklaard worden uit het audiogram. De simulaties met het M2 model waren aanzienlijk beter dan met de M1 variant. Indien juist die typen van abnormale FTCs in het model verdiskonteerd werden die voorkwamen in de cochlea waarvoor CAPs werden nagebootst, waren de simulaties optimaal (*Hfdst. VII, tabel II*). Daarenboven toonden in enkele gevallen de berekende golfvormen op zich een treffende gelijkenis met de fysiologische werkelijkheid (*Hfdst. VII, figuren 3, 5*). De konklusie luidt, dat abnormale responsies van afzonderlijke vezels significant bijdragen aan afwijkingen in CAPs op luide klikstimuli.

Slotkonklusies

Abnormale klikresponsies van afzonderlijke gehoorzenuwvezels zijn bepalend voor een simulatie van de gemeten klik-CAP. Dit betekent, dat men op grond van een toonaudiogram en van klik-CAPs zou kunnen afleiden welke typen van abnormale vezelresponsies voorkomen. Om op deze wijze informatie te onttrekken over cochleair dysfunctioneren, is het van belang klikstimuli te gebruiken van hoge intensiteit, omdat daar abnormale vezels responderen. Ook dienen de CAPs voor beide klikpolariteiten

Curriculum vitae

Huib Versnel is geboren op 20 maart 1962 in het Brabantse dorp Waalre. Het voorbereidend wetenschappelijk onderwijs (V.W.O.) genoot hij aan het Eindhoven's Protestants Lyceum, alwaar hij in 1980 eindexamen deed in de exacte vakken en in de drie talen die op dit blad voorkomen. In dat jaar ging hij natuurkunde studeren aan de Rijksuniversiteit van Leiden. Het kandidaats natuurkunde met bijvak scheikunde (richting N2) werd in 1983 behaald, waarna een stage volgde in de experimentele vakgroep quantumvloeistoffen van Prof. dr. R. de Bruyn Ouboter onder studiebegeleiding van Dr. H. van Beelen. In deze groep in het Kamerlingh Onnes Laboratorium vervolgde Huib in samenwerking met Henk-Pieter Sierat een reeds lopend onderzoek aan het vierde geluid in vloeibaar helium bij temperaturen rond 1 Kelvin. Het onderzoek aan het superfluïde akoestische fenomeen kon worden besloten met een publikatie, en in 1986 werd het doctoraal examen in de experimentele natuurkunde gevierd. Op 1 oktober van dat jaar werd een promotieonderzoek aangevangen, in Leiden en met geluid. Edoch, een significante verschuiving naar het interdisciplinaire onderzoek in de audiologie was gemaakt. In de vakgroep Keel-, Neus-, en Oorheelkunde van Prof. dr. P.H. Schmidt en Prof. dr. J.J. Grote aan de medische faculteit deed hij gehooronderzoek bij Dr. Vera Prijs en Dr. Ruurd Schoonhoven. Hierbij kreeg hij regelmatig advies van *de* fysicus van het oor, Prof. dr. E. de Boer van de Universiteit van Amsterdam. Behalve in de vorm van artikelen, die als hoofdstukken zijn opgenomen in dit proefschrift, zijn resultaten van het onderzoek frequent gepresenteerd op gehooronderzoekersbijeenkomsten in binnen- en buitenland. In de zomer van 1991 vervolgde het leven zijn loop in de Verenigde Staten van Amerika, en de onderzoeks aandacht verplaatste zich van het perifeer naar het centraal auditief systeem. Sindsdien werkt Huib als onderzoeksmedewerker in het Neural Systems Lab van Dr. Shihab A. Shamma in het Institute for Systems Research aan de University of Maryland in College Park. In een interdisciplinaire context van de studie van spraakherkenning onderzoekt hij de responseïenschappen van de auditieve cortex.

Stellingen

Stelling 1

Het meten van de samengestelde aktiepotentiaal (CAP) in respons op klikstimuli van hoge intensiteit en van verdunnings- en verdichtings polariteit afzonderlijk lijkt een geschikte methode om een afwijkende frequentieselektiviteit in de cochlea te kwalificeren (dit proefschrift).

Stelling 2

De klik-CAP-methode als gesteld onder 1, dient getest te worden in slechthorenden in combinatie met de methode van CAP tuning curves, voordat tot toepassing in de klinische electrocochleografie kan worden overgegaan.

Stelling 3

Dankzij het fenomeen van de *walkman* is er een toenemende voorraad van potentiële proefpersonen te verwachten met lawaaigetraumatiseerde cochleas voor een test van de klik-CAP-methode.

Stelling 4

De bijdrage van intrinsieke mechanismen aan demping van het vierde geluid in superfluide helium wordt, zelfs voor temperaturen beneden 1 Kelvin, overschaduwed door bijdragen die met het niet-ideaal zijn van het vierde geluid geassocieerd kunnen worden (Sierat, Versnel en Van Beelen, *Physica B* 153:159-165, 1988).

Stelling 5

De verbreding van de CAP tuning curve en toename van CAP amplitude op lage intensiteits tonen na toediening van cocaïne (Shivapuja, ARO meeting, 1992) zou kunnen duiden op een uniek verschijnsel van verslechtering van frequentieselektiviteit zonder drempelverhoging.

Stelling 6

De aanzienlijke vergroting van het electrocochleografisch signaal op 1 kHz tonen in een Lermoyez oor in slechte toestand vergeleken met goede toestand (Schoonhoven, Schmidt en Eggermont, *Eur. Arch. Otorhinolaryngol.* 247:333-339, 1990), zou niet alleen veroorzaakt kunnen zijn door een vergroting van de sommatiepotentiaal, maar ook door vergroting van de CAP als het gevolg van hypersensitiviteit voor lage tonen van basale neuronen.

Stelling 7

De wijsvinger die de Nederlander zo menigmaal opheft naar de buitenlandse, verraadt zendingsdrang en vaderlandsliefde.

Stelling 8

Het ontbreken van hypersensitiviteit in alle basilaire membraan experimenten tot nu toe, kan niet worden aangevoerd om de mechanische oorzaak van hypersensitiviteit in twijfel te trekken, laat staan het verschijnsel op zich.

Stelling 9

Volgens het lateraal-inhibitie-model van Shamma (*JASA* 78: 1622-1632, 1985) is bij elk geluidsnivo het *temporele* gedrag van auditieve zenuwvezels met hoge spontane aktiviteit van belang voor codering van klinkers, en is een specifieke *plaatscoderingsrol* van laag-spontane vezels voor hoge nivo's niet noodzakelijk (Winslow en Sachs, in: *Auditory processing of complex sounds*, Lawrence Erlbaum Associates, 1987).

Stelling 10

Voor fysiologische verklaringen van psychoacoustische verschijnselen wordt traditioneel naar het perifeer auditief systeem gekeken, maar het zou beter zijn modellen te hanteren op basis van het centraal auditief systeem.

Stelling 11

De term *abstract* is ontleend aan de visuele kunsten en kan niet worden gebruikt in de muziek.

Stelling 12

De auditief corticale neuronen functioneren als filters van het spectrale profiel, zoals corticale neuronen in het visuele zintuigstelsel functioneren als filters van het ruimtelijke profiel.

Stelling 13

De *walkman* zou voorzien moeten zijn van een waarschuwing tegen beschadiging van het gehoor.

Stelling 14

Indien sprake is van een gelijke toonhoogte waarneming voor beide oren kan de slechthorende zonder klachten naar muziek luisteren (*Muziek en (slecht) gehoor*, red. Lamoré en De Laat, N.V.A., 1993).

Stelling 15

De fundamentele sociale verschillen tussen vrouw en man kunnen zeer goed beschreven en begrepen worden op basis van de gedragsrollen van de prehistorische voorouders zijnde de rol van de verzamelaar (vrouw) en die van de jager (man) (naar Rob Becker, *Defending the Caveman*, 1993).